Vol. 58 FEBRUARY, 1954 No. 2

THE JOURNAL OF PHYSICAL CHEMISTRY

(Registered in U. S. Patent Office)

SYMPOSIUM ON PROTEIN DENATURATION, LOS ANGELES, CALIF., MARCH, 1953

* * * * * * *

THE JOURNAL OF PHYSICAL CHEMISTRY will appear monthly in 1954
After January 1, 1954, Notes and Communications to the Editor
will be accepted for publication.

THE JOURNAL OF PHYSICAL CHEMISTRY

(Registered in U. S. Patent Office)

Published monthly by the American Chemical Society at 20th and Northampton Sts., Easton, Pa.

Entered as second-class matter at the Post Office at Easton, Pennsylvania.

The *Journal of Physical Chemistry* is devoted to the publication of selected symposia in the broad field of physical chemistry and to other contributed papers.

Manuscripts originating in the British Isles, Europe and Africa should be sent to F. C. Tompkins, The Faraday Society, 6 Gray's Inn Square, London W. C. 1, England.

Manuscripts originating elsewhere should be sent to W. Albert Noyes, Jr., Department of Chemistry, University of Rochester, Rochester 3, N. Y.

Correspondence regarding accepted copy, proofs and reprints should be directed to Assistant Editor, Allen D. Bliss, Department of Chemistry, Simmons College, 300 The Fenway, Boston 15, Mass.

Business Office: American Chemical Society, 1155 Sixteenth St. N. W., Washington 6, D. C.

Advertising Office: American Chemical Society, 332 West 42nd St., New York 36, N. Y.

Articles must be submitted in duplicate, typed and double spaced. They should have at the beginning a brief Abstract, in no case exceeding 300 words. Original drawings should accompany the manuscript. Lettering at the sides of graphs (black on white or blue) may be pencilled in, and will be typeset. Figures and tables should be held to a minimum consistent with adequate presentation of information. Photographs will not be printed on glossy paper except by special arrangement. All footnotes and references to the literature should be numbered consecutively and placed on the manuscript at the proper places. Initials of authors referred to in citations should be given. Nomenclature should conform to that used in *Chemical Abstracts*, mathematical characters marked for italic, Greek letters carefully made or annotated, and subscripts and superscripts clearly shown. Articles should be written as briefly as possible consistent with clarity and should avoid historical background unnecessary for specialists.

Symposium papers should be sent in all cases to Secretaries of Divisions sponsoring the symposium, who will be responsible for their transmittal to the Editor. The Secretary of the Division by agreement with the Editor will specify a time after which symposium papers cannot be accepted. The Editor reserves the right to refuse to publish symposium articles, for valid scientific reasons. Each symposium paper may not exceed four printed pages (about sixteen double spaced typewritten pages) in length except by prior arrangement with the Editor.

Remittances and orders for subscriptions and for single copies, notices of changes of address and new professional connections, and claims for missing numbers should be sent to the American Chemical Society, 1155 Sixteenth St., N. W., Washington 6, D. C. Changes of address for the *Journal of Physical Chemistry* must be received on or before the 30th of the preceding month.

Claims for missing numbers will not be allowed (1) if received more than sixty days from date of issue (because of delivery hazards, no claims can be honored from subscribers in Central Europe, Asia, or Pacific Islands other than Hawaii), (2) if loss was due to failure of notice of change of address to be received before the date specified in the preceding paragraph, or (3) if the reason for the claim is "missing from files."

Subscription Rates: to members of the American Chemical Society, $8.00 for 1 year, $15.00 for 2 years, $22.00 for 3 years; to nonmembers, $10.00 for 1 year, $18.00 for 2 years, $26.00 for 3 years. Postage free to countries in the Pan American Union; Canada, $0.40; all other countries, $1.20. Single copies, $1.25; foreign postage, $0.15; Canadian postage $0.05.

The American Chemical Society and the Editors of the *Journal of Physical Chemistry* assume no responsibility for the statements and opinions advanced by contributors to THIS JOURNAL.

The American Chemical Society also publishes *Journal of the American Chemical Society, Chemical Abstracts, Industrial and Engineering Chemistry, Chemical and Engineering News, Analytical Chemistry*, and *Journal of Agricultural and Food Chemistry*. Rates on request.

THE JOURNAL OF PHYSICAL CHEMISTRY

(Registered in U. S. Patent Office) (Copyright, 1954, by the American Chemical Society)

VOLUME 58 FEBRUARY 27, 1954 NUMBER 2

THE CHANGE IN HEAT CONTENT ACCOMPANYING DENATURATION*

BY JULIAN M. STURTEVANT

Sterling Chemistry Laboratory, Yale University, New Haven, Connecticut

Received July 24, 1953

The available data on the enthalpy change accompanying protein denaturation are summarized. In the two cases where measurements have been made over a range of *p*H values, it has been found that the ΔH of denaturation is strongly dependent on *p*H. The maximum in the ΔH *vs.* *p*H curve for pepsin is so sharp that ordinary ionization equilibria cannot be invoked to explain it. The data for pepsin can, however, be reasonably well accounted for on the basis of a triggered ionization similar to that recently proposed by Steinhardt and Zaiser in the case of ferrihemoglobin

Introduction

The change in heat content accompanying a chemical reaction is devoid of fundamental significance unless the initial and final states of the system are accurately defined. In discussing the enthalpy changes accompanying the denaturation of proteins, we are faced with the difficulty that there is no adequate way of defining the state of a denatured protein. Indeed, there is no unanimity as to what is meant by the term denaturation. In a situation beset by such ambiguities, it is hardly to be expected that thermochemical data will advance very markedly our understanding of denaturation. On the other hand, it is particularly important, in the case of a very complex problem, to bring to bear on it evidence obtained by as wide a variety of experimentation as possible. Thus, even though enthalpy data concerning denaturation cannot be assigned as much reliability as one usually wishes for thermodynamic data, it is reasonable to assume that such data are of sufficient importance to justify the considerable efforts required to obtain them.

In this paper we review briefly the available enthalpy data pertaining to denaturation. Data recently obtained for the denaturation of pepsin are discussed in some detail, and are shown to be of significance in connection with the mechanism of denaturation.

* Based on a paper presented before the Division of Physical and Inorganic Chemistry of the American Chemical Society, Los Angeles, California, March, 1953. Contribution No. 1169 from the Sterling Chemistry Laboratory of Yale University.

Equilibrium Data.—The first quantitative estimate of the heat content change in a denaturation reaction was obtained by Anson and Mirsky[1] in 1934. They measured the equilibrium in the denaturation of trypsin, as estimated by proteolytic activity, in 0.01 *N* hydrochloric acid over the temperature range 42–50°, and calculated equilibrium constants on the assumption that the reaction is first order in protein in both directions. Application of the van't Hoff equation gave the value 67,600 cal. per mole for the ΔH of denaturation.

A consideration of some importance is frequently overlooked in connection with free energy and enthalpy data based on equilibrium measurements. In attaching any meaning to such data, one is necessarily making an assumption concerning molecular weight. Particularly in the case of complicated substances such as proteins, one has no *a priori* justification for asserting that the molecular weight pertaining to some reversible reaction is the same as the molecular weight determined, for example, from sedimentation and diffusion experiments. (The same consideration applies to the calculation from rate data of heats and free energies of activation.)

It should also be remembered that the ΔH value obtained from equilibrium measurements pertains to the reaction with reactants and products in their standard states. In the case of trypsin, although the equilibrium constant is presumably independent of concentration units, the standard

(1) M. L. Anson and A. E. Mirsky, *J. Gen. Physiol.*, **17**, 393 (1934).

states are by implication specified, though in an unknown way in the absence of activity data, in the assumption of unit activity coefficients under the conditions of the experiments. Enthalpy values usually do not change very rapidly with concentration, and it is probably frequently permissible to neglect the differences between standard and non-standard ΔH values, at least for reactions involving no change in mole number.

Equilibrium measurements have been used to obtain ΔH values in other denaturation reactions. Anson and Mirsky[2] found that the extent of the apparently reversible denaturation of methemoglobin by salicylate is independent of temperature, so that ΔH for this reaction appears to be small; and Herriott[3] estimated 31 kcal. per mole for the enthalpy change in the reversible heat inactivation of pepsinogen. Kunitz[4] studied the reversible heat denaturation of the soybean trypsin inhibitor at *p*H 3, employing loss of solubility at the isoelectric point as the criterion of denaturation. He found ΔH = 57.3 kcal. per mole for this reaction.

Recently Eisenberg and Schwert[5] have carried out a very thorough investigation of the reversible denaturation of chymotrypsinogen. They demonstrated quite convincingly that the reversed protein is identical with the native protein with respect to several properties. As Kunitz had done in the case of the soybean trypsin inhibitor, Eisenberg and Schwert measured the rates of the denaturation and renaturation reactions, and showed that the thermodynamic quantities for activation in the two directions are consistent with those for the overall process. Of particular interest is the fact that Eisenberg and Schwert carried out complete sets of measurements at two different *p*H values; they found for ΔH at *p*H 2.0 the value 99.6 kcal. per mole, and at *p*H 3.0, 143 kcal. per mole.

Calorimetric Data.—Three calorimetric determinations of the heat of denaturation have been carried out by Kistiakowsky and his colleagues. Denaturations of methemoglobin[6] and pepsin[7] by alkali were investigated by observing the heats of reaction of the native protein and of the denatured protein with alkali, the heat of denaturation being taken as the difference between these. Thus, in the case of pepsin, a typical experiment consisted of (1) mixing the native protein at a low *p*H where it is indefinitely stable with sufficient sodium hydroxide to raise the *p*H to a value where the denaturation is rapid; (2) returning the solution to the original *p*H with acid; and (3) treating the solution again with alkali to give the same final *p*H. The ΔH for step 1 less that for step 3 was taken as the heat of denaturation at the initial *p*H. A procedure of this sort of course involves the assumption that the heat content of the denatured protein at low *p*H is independent of whether the protein has or has not been exposed to a high *p*H.

By this sort of measurement, the value ΔH = 138 kcal. per mole was found for the denaturation of methemoglobin. The apparent ΔH value for the pepsin denaturation was found to decrease from 85 kcal. per mole at *p*H 4.3 to nearly zero at *p*H 6.8 (at 31°), this decrease not following the same course as the decrease in the proteolytic activity of the enzyme observed over this *p*H range.

The calorimetric data of Roberts[8] on the denaturation of methemoglobin by salicylate appear to be in disagreement with equilibrium observations of Anson and Mirsky. Roberts found the heat of reaction to increase steadily as the salicylate concentration was increased, and concluded that the reaction is not stoichiometric.

The Denaturation of Pepsin.—Buzzell and the present author[9] studied the denaturation of pepsin. The calorimetric method[10] used in their work permitted measuring the heat of the denaturation reaction carried out at constant *p*H, and also gave values for the rate of absorption of heat during the denaturation. Measurements were made in phosphate buffers over a *p*H range at 15 and 35°.

A summary of the enthalpy changes observed is given in Fig. 1, in which the heat of reaction in joules per pepsin unit (hemoglobin substrate) is plotted against the *p*H. The various types of points refer to experiments using pepsin from different sources.[11] The crossed circles are data obtained with an earlier calorimeter,[12] using *p*-nitrophenol buffers and a different pepsin assay method. The thermal data may be converted to kcal. per mole, taking the activity of pepsin to be 0.39 pepsin units per milligram of protein nitrogen,[9] and assuming the protein to contain 14.6% nitrogen,[13] and to have a molecular weight of 35,000. On this basis, 0.05 joule per pepsin unit becomes 24 kcal. per mole.

Buzzell and Sturtevant found that the heat absorption during denaturation followed accurately a first-order law, the logarithm of the apparent rate constant increasing linearly with *p*H with a slope of 1.40. However, they found the loss of proteolytic activity under similar conditions to follow entirely different kinetics of non-integral order, with the half-times for inactivation increasing approximately as the inverse fourth power of hydrogen ion concentration. It appears that, just as different reagents and experimental conditions produce different reactions classed as denaturation, so the same experimental conditions can produce different kinetic results depending on the method of observation.

The situation concerning the kinetics of the loss of peptic activity is rather confused. Steinhardt[14]

(2) M. L. Anson and A. E. Mirsky, *J. Gen. Physiol.*, **17**, 399 (1934).
(3) R. M. Herriott, *ibid.*, **21**, 501 (1938).
(4) M. Kunitz, *ibid.*, **32**, 241 (1948).
(5) M. A. Eisenberg and G. W. Schwert, *ibid.*, **34**, 583 (1951).
(6) J. B. Conn, G. B. Kistiakowsky and R. M. Roberts, *J. Am. Chem. Soc.*, **62**, 1895 (1940).
(7) J. B. Conn, D. C. Gregg, G. B. Kistiakowsky and R. M. Roberts, *ibid.*, **63**, 2080 (1941).
(8) R. M. Roberts, *ibid.*, **64**, 1472 (1942).
(9) A. Buzzell and J. M. Sturtevant, *ibid.*, **74**, 1983 (1952).
(10) A. Buzzell and J. M. Sturtevant, *ibid.*, **73**, 2454 (1951).
(11) All of the pepsin preparations for which data are given in Fig. 1 contained approximately 20% of non-protein nitrogen (determined by trichloroacetic acid precipitation).
(12) M. Bender and J. M. Sturtevant, *J. Am. Chem. Soc.*, **69**, 607 (1947).
(13) J. H. Northrop, M. Kunitz and R. M. Herriott, "Crystalline Enzymes," Columbia University Press, New York, N. Y., 1948, p. 74.
(14) J. Steinhardt, *Kgl. Danske Videnskab. Selskab. Math.-Fys. Medd.*, **14**, No. 11 (1937).

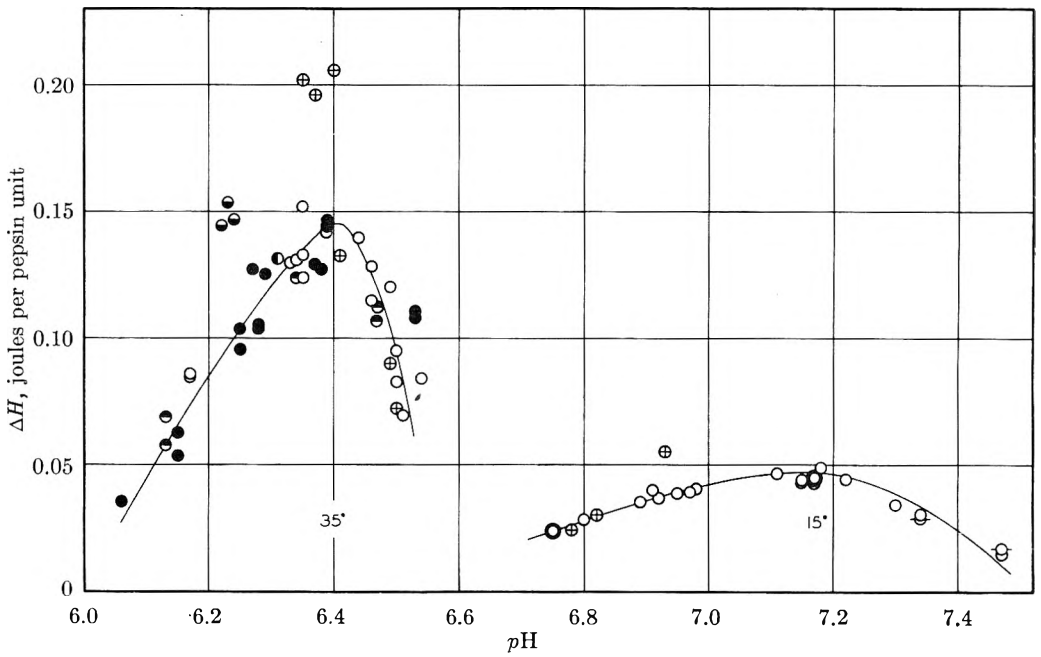

Fig. 1.—Heat content change in the denaturation of pepsin as a function of pH.[9]

has reported good first-order kinetics for the inactivation in p-nitrophenol buffers, the rate increasing as the inverse fifth power of the hydrogen ion concentration. He was able to obtain pepsin free from non-protein nitrogen in the dilute solutions used in his kinetic experiments. Casey and Laidler[15] found the order of the reaction to vary between one and five, depending on the initial concentration of the protein, in pH 4.8 acetate buffer at 50 to 60°.

The variation of ΔH with pH recorded in Fig. 1 is most unusual. It is perhaps significant that the maxima in the ΔH curves for 15 and 35° both occur at a pH corresponding to a specific rate of heat absorption of 0.0021 sec.$^{-1}$. It is interesting that the only other ΔH values for denaturation which have been reported over a pH range, those of Eisenberg and Schwert and of Conn, Gregg, Kistiakowsky and Roberts, have also indicated unusual pH dependence.

Buzzell and Sturtevant were unable to determine whether the ΔH of denaturation becomes negative at low and high pH because the rates of reaction become respectively too low and too high to permit measurements to be made. It seems reasonable to assume that the heat of reaction is close to zero except in the pH range where measurements were made, which means that the heat contents of native and denatured pepsin are nearly equal at low and high pH. The observed heats of reaction would then be consistent with the schematic enthalpy diagram given in Fig. 2. The type of result observed by Kistiakowsky, *et al.*,[7] can be qualitatively accounted for by the assumption that the heat content of pepsin denatured at a high pH is not reversible with respect to pH changes. According to this view, Kistiakowsky, *et al.*, measured the quantity denoted by ΔH_{app} which bears no direct relation to the heat of denaturation. It is planned to explore calorimetrically the variation with pH

(15) E. J. Casey and K. J. Laidler, *J. Am. Chem. Soc.*, **73**, 1455 (1951).

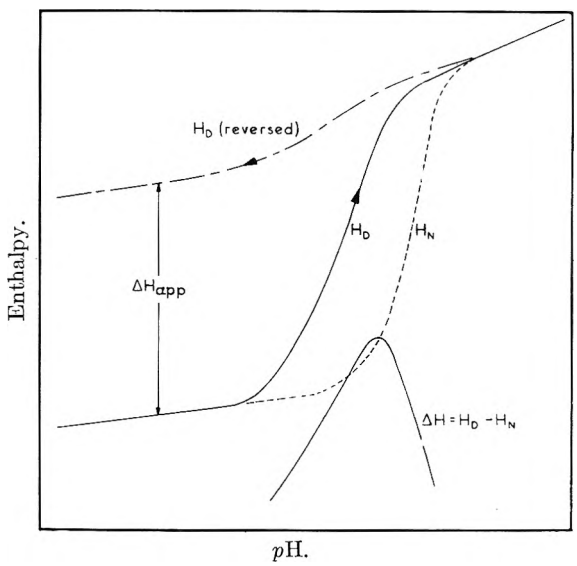

Fig. 2—Schematic representation of proposed variation with pH of the heat contents of native and denatured pepsin.

of the heat content of denatured pepsin, to throw further light on its peculiar thermal behavior.

Following the treatments proposed by Steinhardt[14] and Levy and Benaglia[16] to explain the variation of the rate of denaturation with pH, we may investigate the possibility of accounting for the variation of ΔH in terms of ionization equilibria. We assume that in the pH range of interest native pepsin exists in $m + 1$ ionized forms and denatured pepsin in $n + 1$ ionized forms, related by the equilibria

$$N_{i-1} = N_i + H^+; \quad K_{N,i}; \quad i = 1, \ldots, m \qquad (1)$$

$$D_{i-1} = D_i + H^+; \quad K_{D,i}; \quad i = 1, \ldots, n \qquad (2)$$

Since the denaturation of pepsin appears to be irreversible, it is unnecessary to include equilibria

(16) M. Levy and A. E. Benaglia, *J. Biol. Chem.* **186**, 829 (1950).

involving both native and denatured forms. The concentration of N_i is given by

$$[N_i] = [P] \frac{K_{N,0}K_{N,1}\ldots K_{N,i}[H^+]^{m-i}}{[H^+]^m + K_{N,1}[H^+]^{m-1} + \ldots + K_{N,1}\ldots K_{N,m}} \quad (3)$$

where $[P] = \Sigma[N_i] = \Sigma[D_i]$ is the total protein concentration. $K_{N,0}$ is defined as being equal to unity. A similar expression holds for $[D_i]$. If we represent by $H_{N,i}$ and $H_{D,i}$ the apparent molar heat contents, referred to any convenient origin, of N_i and D_i, respectively, and if concentrations are expressed in moles per liter, then the change in heat content, ΔH, per mole of protein is given by

$$[P]\ \Delta H = \sum_0^n H_{D,i}[D_i] - \sum_0^m H_{N,i}[Ni] \quad (4)$$

The simplest assumptions one can make to obtain equation (4) in manageable form are as follows: (a) $H_{D,i}$ and $H_{N,i}$ are independent of concentration; (b) the number of ionized forms is the same in both native and denatured forms; (c) all ionizing sites have the same intrinsic dissociation constants, $K_D \neq K_N$ and there is no interaction between sites, so that

$$K_{N,i} = \frac{n - (i-1)}{i} K_N \quad (5)$$

This leads to the closest spacing of dissociation constants, and the largest dependence on pH, which can be obtained with ordinary ionizations. It then follows that

$$[N_i] = [P] \frac{\binom{n}{i} K_N^i [H^+]^{n-i}}{\sum_{j=0}^{n} \binom{n}{j} K_N^j [H^+]^{n-j}} \quad (6)$$

A similar expression holds for $[D_i]$. We may assume further that, (d) the heat contents of the various forms are given by

$$H_{N,i} = H_{N,0} + ih_N \quad (7)$$

$$H_{D,i} = H_{D,0} + ih_D \quad (8)$$

However, since $\Delta H \to 0$ at both low and high pH

$$H_{N,0} = H_{D,0} = H_0 \text{ and } h_N = h_D = h \quad (9)$$

Equation (4) then becomes

$$\frac{\Delta H}{nh} = \frac{K_D - K_N}{K_D + K_N + (x + 1/x)\sqrt{K_D K_N}} \quad (10)$$

where $x = [H^+]/\sqrt{K_D K_N}$ has the value unity at the maximum of the ΔH curve. Of course, a symmetrical set of assumptions such as we have chosen here will give a symmetrical ΔH *vs.* pH curve, while the observed curve appears to be unsymmetrical at both 15 and 35°. However, this model fails for a more serious reason. If $x_{1/2}$ is the value of x at which $\Delta H = {}^1/_2\,\Delta H_{max}$

$$x_{1/2} + \frac{1}{x_{1/2}} = \frac{K_D/K_N + 4\sqrt{K_D/K_N} + 1}{\sqrt{K_D/K_N}} \quad (11)$$

Since the right side of this equation is greater than 6 for $K_N \neq K_D$, it follows that

$$|pH_{max} - pH_{1/2}| > 0.765 \quad (12)$$

whereas, at 35°, the observed pH differences are 0.23 and 0.12 on the low and high pH sides, respectively.

A sufficiently sharp, though still symmetrical, ΔH maximum can be obtained by replacing the equilibria of equations 1 and 2 by

$$N_0 = N_n + nH^+; \quad K_N \quad (13)$$

$$D_0 = D_n + nH^+; \quad K_D \quad (14)$$

$$[N_i] = [D_i] = 0; \quad i = 1, \ldots, n-1 \quad (15)$$

These equilibria are of an unorthodox type, and require some sort of a structural change accompanying the ionizations which causes the liberation of the n protons to be an all-or-none process. Equilibria similar to these have recently been postulated by Steinhardt and Zaiser[17] to account for their observation of the liberation of acid-binding groups in the denaturation of ferrihemoglobin. If $H_{N,n} - H_{N,0} = H_{D,N} - H_{D,0} = \Delta$, these equilibria lead to an equation of the form of equation (10), with $nh = \Delta$ and $x = [H^+]^n/\sqrt{K_D K_N}$. Taking the mean value of $|pH_{max} - pH_{1/2}|$ to be 0.18 (at 35°), the smallest integral value of n which can be used turns out to be 5. Equation 11 then gives $\sqrt{K_D/K_N} = 3.81$. The expression

$$\frac{\Delta H_{max}}{\Delta} = \frac{\sqrt{K_D/K_N} - 1}{\sqrt{K_D/K_N} + 1} \quad (16)$$

with $\Delta H_{max} = 69$ kcal. per mole, gives the value $\Delta = 118$ kcal. per mole. This value is not unreasonably large since it may well be that a number of hydrogen bonds[18] are broken in the process in addition to the dissociation of five protons. As a necessary result of the calculations, $K_D = (6.3)^5$ and $K_N = (6.5)^5$.

Asymmetry of the type observed in the ΔH *vs.* pH curve could be introduced by assuming fewer than 5 ionizable protons in the denatured protein. However, in view of the unsubstantiated nature of the assumed mechanism and the scatter of the experimental data, detailed calculations are not warranted.

The mechanism considered here is certainly not unique, though it is the most reasonable one based on ionization equilibria we have been able to devise. Two obvious weaknesses should be emphasized. (1) the ΔH maximum at 15° is considerably broader than at 35°, so that a smaller n can be used. In any case, a much smaller Δ is necessary at 15°. (2) Although a consideration of the heat data at 35° leads to an ionization involving approximately five protons (the same number as indicated by Steinhardt's kinetic data), the variation with pH of the rate of heat absorption points toward an ionization of an average of 1.4 protons. We are thus faced with the problem of accounting for an essentially instantaneous establishment (after initiating the reaction by raising the pH of the native pepsin solution) of an equilibrium mixture of N_0 and N_n, followed by conversion of this to an equilibrium mixture of D_0 and D_n at a rate controlled by the concentration of native protein which has lost only an average of 1.4 protons relative to N_0.

(17) J. Steinhardt and E. Zaiser, *J. Am. Chem. Soc.*, **75**, 1599 (1953).

(18) A. E. Mirsky and L. Pauling, *Proc. Nat. Acad. Sci.*, **22**, 439 (1936).

THERMAL AND ELASTIC PROPERTIES OF α-KERATIN

BY HENRY B. BULL

Biochemistry Department, State University of Iowa, Iowa City, Iowa

Received July 24, 1953

The elastic coefficient of hair fibers indicates the existence of structural changes occurring at about 5% and at about 25% extension. The volume of the hair fiber exhibits a minimum at about 5% and a maximum at about 30% stretch. There are conspicuous and sharp maxima in the energies of activation for the decay of the stress of a hair fiber at about 5% and at about 20% stretch. Typical protein denaturants have no large effects on the elastic properties of hair which indicates that hydrogen bonds are not primarily responsible for the elastic properties of hair; emphasis is placed on the disulfide bonds. It is suggested that whatever molecular folding of the peptide chains as may have been originally present in the hair follicle has been extensively deformed by the formation of inter-chain disulfide bonds.

Since the work of Astbury and Street,[1] it has been known that hair and wool are converted from what is called α-keratin into another molecular structure known as β-keratin as a fiber is progressively stretched beyond about a 20% extension.

The elastic properties of keratin fibers have been extensively studied by a number of workers and much detailed information on this subject is available. The present paper reports additional information along these lines and attempts an interpretation in terms of protein denaturation and in terms of the recent ideas of Pauling and Corey.

A simple stress–strain apparatus for the stretching of human hair immersed in water at desired temperatures was constructed; this apparatus permitted a study of the stress as a function of the stretch or of the stretch as a function of the stress applied to the hair. The human hair used was described as virgin hair by the commercial dealer. It was exhaustively extracted with alcohol, with ether and finally washed with water and electrodialyzed. It was dried and stored.

Shown in Fig. 1 is the coefficient of elasticity of the hair expressed in dynes per square centimeter as a function of the stretch at 25° and at 85°. Clearly evident at 25° are two sharp maxima in the coefficient of elasticity. The stretch up to the first maxima corresponds to the stretch in the so-called Hook's law region. The position of the first maxima is insensitive to temperature and to the previous history of the hair. On the other hand, the position and magnitude of the second maxima is very sensitive in regard to temperature and to the treatment the hair has received. As shown, the second maxima has very greatly decreased at 85° and furthermore has shifted to a position of greater extension. Not shown in Fig. 1 are the elastic coefficients at 45° and at 65°. These exhibited the expected behavior which was intermediate between 25 and 85°.

As is well known hair is a complex biological structure. It is composed of two main parts, the cuticle and the cortex. The cuticle forms a sheath around the shank or cortex of the hair fiber and makes up to 10 to 20% of the cross-sectional area of the hair fiber. We have found that when a hair fiber is extended to between 40 and 60% of its original length, the cuticle ordinarily tears in a circular direction around the hair forming sleeve-like sections of irregular lengths. If such a hair is

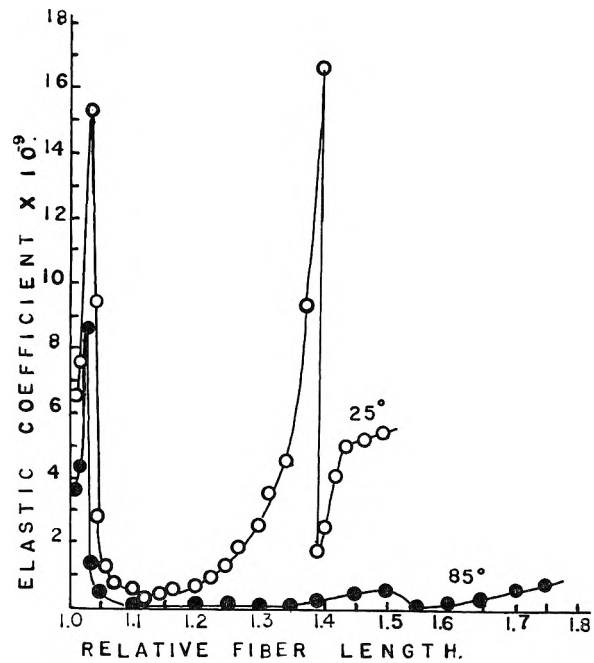

Fig. 1.—Coefficient of elasticity of human fibers at 25° and at 85° as a function of stretch, the original length of the hair being taken at unity.

relaxed and restretched, the cuticle disintegrates completely and the hair fiber is obtained free from cuticle. We cannot be absolutely certain that the second maxima shown in Fig. 1 is not in fact due either in part or entirely to the onset of the rupture of the cuticle before such a rupture is microscopically visible. The second maxima is greatly diminished upon restretching a relaxed hair whether the cuticle has been visibly ruptured by the first stretch or not.

The diameters of the hair fibers have been measured as a function of the extention. This has been accomplished by direct microscopic observation using a filar micrometer. The hair fibers are not perfect cylinders and have elliptical cross sections. The variation of the apparent diameters of 5 hairs have been measured as a function of stretch and these values averaged and the average volume of the hairs calculated from the averaged diameters on the assumption of cylindrical shapes. The volume of the hair fibers so calculated as a function of the extension of the hair at 25° is shown in Fig. 2. The original length and volume of hair was taken as unity. All the hairs showed the same qualitative

(1) W. B. Astbury and A. Street, *Phil. Trans. Roy. Soc. (London)*, **A230**, 75 (1930).

volume changes with stretch although there were quantitative differences between the hairs. Notable is the decrease in volume associated with stretch in the Hook's law region and the maximum in the volume at about 30% stretch.

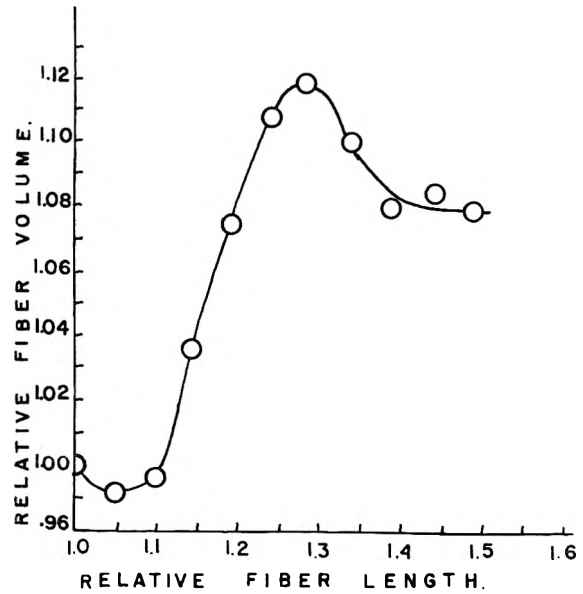

Fig. 2.—Relative volume of hair fibers as a function of extension at 25°. The original length of hair was assumed to be unity.

The $^{9}/_{10}$-times for the decay of the stress at selected extensions have been determined at 25° and at 45° for 5 different hairs. If we assumed that the $^{9}/_{10}$-times are an inverse measure of the rate of decay of the stress, we can estimate the energies of activation for the decay of the stress as a function of the extension. The hairs were first stretched to 50% extension and the loads were removed and the hairs allowed to recover. The $^{9}/_{10}$-times up to about 40% stretch were then measured at 25° for various intermediate extensions. The hair fibers were unloaded and allowed to relax. The temperature of the bath was raised to 45° and the $^{9}/_{10}$-times determined at this temperature. The $^{9}/_{10}$-times varied, depending on the extent of stretch, from over 2,000 seconds down to 30 seconds. Shown plotted in Fig. 3 are the estimated energies of activation expressed in kilocalories per mole as a function of the extent of stretch; the original length of the fiber being taken as unity. Clearly evident are two pronounced maxima, one at the end of the Hook's law region and another at about 20% stretch.

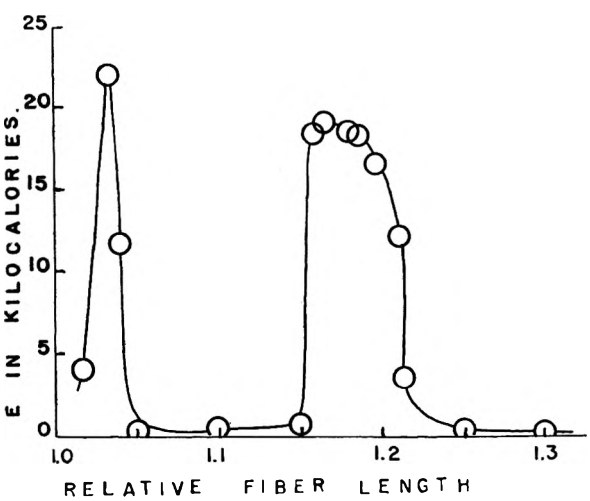

Fig. 3.—Energies of activation in kilocalories for the decay of stress for the average of 5 hair fibers.

Discussion

This research was undertaken with hopes that it might shed light on two important problems and these are: (1) protein denaturation and (2) to see if any information could be gathered which would be relevant to the polypeptide structures proposed by Pauling and Corey.[2]

The stretching of a hair fiber can be regarded in a sense as a kind of mechanical protein denaturation; the peptide chains are moved relative to each other in the stretching process and the molecular configuration in the "native" unstretched state is certainly different from what it is in the stretched state. This "denaturation" is to a large extent reversible, the unloaded hair returning to very nearly its original length after stretch. The change from the "native," unstretched state to the stretched, denatured state involves two energy humps (see Fig. 3) and these humps are not very much less than the energies of activation associated with the thermal denaturation of globular proteins in solution. The stretching of the fiber beyond the Hook's law region also shows a volume increase. Such a volume increase is characteristic of protein denaturation.[3]

The denaturing influence of concentrated urea on globular proteins is well known. Six molar urea decreases the work of extending a hair fiber about 30%. A 0.2% solution of sodium lauryl sulfate decreased the work of extension about 10%. It is known that *p*H has only a moderate effect upon the work of extension of keratin fibers except at sufficiently high *p*H to initiate the hydrolysis of disulfide bonds where the work of extension falls very drastically. The reduction of the disulfide bonds if sufficiently extensive, causes the hair to lose its elastic properties and become a plastic solid and the work of extension drops to almost zero.

It is not clear how the elastic properties of hair can be interpreted in terms of the Pauling–Corey helical structure. This structure provides for about 117% stretch in the transformation of α-keratin to β-keratin. In reality the on-set of the conversion of α- to β-keratin does not begin until the hair has been stretched about 20% and the X-ray picture is entirely of the β-keratin type at 70% extension.[1] Thus the actual stretch for the conversion of α- to β-keratin is about 45%.

Furthermore, there is no provision in the Pauling–Corey structure for two structural changes observed as hair is stretched as indicated in Fig. 3, and less certainly in Fig. 1.

It is undoubtedly true that in most proteins, the stabilizing energy arises principally from hydrogen

(2) L. Pauling and R. B. Corey, *Proc. Natl. Acad. Sci.*, **37**, 261 (1951).

(3) F. H. Johnson and D. H. Campbell, *J. Cell. Comp. Physiol.*, **26**, 43 (1945).

bond formation between the oxygen and the nitrogen atoms in the peptide chain. There are two such bonds per residue and Pauling and Corey estimate their energy of formation to be about 8 kcal. per bond. Hydrogen bonds also arise from the polar R-groups. In hair there are about 0.4 such hydrogen bonds per residue.[4] There is also van der Waals interaction leading to close packing of the R-groups. The energy contributed by the van der Waals interaction can be estimated to be about 2 kcal. per residue.[5] It therefore appears that the stabilizing energy arising from the hydrogen bond formation on the oxygen and nitrogen atoms in the peptide chain is by far the more important of the stabilizing factors. We have seen, however, that agents capable of denaturing globular proteins by hydrogen bond rupture have no pronounced influence on the work of extending a hair fiber. We feel that the reason for the failure of typical protein denaturants to influence the work of extension in any dramatic way resides in the very high cystine content of hair which provides disulfide links between adjacent peptide chains. It is principally to the inter-chain disulfide bonds that unstretched hair owes its structure and only secondarily to hydrogen bond formation.

It is probable that a large fraction of the α-helical forms of hair have suffered extensive deformations due to the formation of disulfide bonds as the hair fiber leaves the hair follicle and the sulfhydryl groups are oxidized to disulfide.

The structural change initiated at the end of the Hook's law region probably arises from a straightening of the partly folded peptide chains and the second structural change occurring in the 20 to 30% stretch region probably involves the start of the conversion of the partly folded chains to the α-keratin structure.

(4) H. B. Bull, *J. Am. Chem. Soc.*, **66**, 1499 (1944).

(5) W. D. Harkins, "Surface Chemistry," Pub. No. 21, Am. Assoc. Adv. Sci., 1943.

DENATURATION OF HEMOGLOBINS BY ALKALI[1]

BY FELIX HAUROWITZ, RICHARD LYNN HARDIN[2] AND MARTHA DICKS

Department of Chemistry, Indiana University, Bloomington, Indiana

Received July 24, 1953

The decomposition of hemoglobin and oxyhemoglobin from man, rabbit and beef blood, at *p*H 11.9 and at temperatures between 2 and 30° proceeds according to first-order kinetics. The first-order velocity constants for human, rabbit and beef oxyhemoglobin at 2° are 2.3×10^{-2}, 2.8×10^{-4}, and 9.3×10^{-6}, respectively. The presence of two or more hemoglobins in rat blood is indicated by a break in the denaturation velocity. The alkali denaturation of hemoglobins differs from that of oxyhemoglobins by the lower values for $\Delta H^{\ddagger}$, and by more negative values for $\Delta S^{\ddagger}$. This is ascribed to configurational changes accompanying oxygenation. The denaturation velocity of human, rabbit and beef globin at *p*H 11.9 and 11.0 is much higher than that of the corresponding hemoglobins and is similar for all three types of globin. The differences in the resistance of various hemoglobins against alkali are attributed to different degrees of complementariness of a non-polar "anti-heme" pattern in the globin surface, high resistance against alkali indicating a high degree of spatial adjustment of globin to the rigid planar porphin structure of the heme molecule.

In contrast to most proteins the hemoglobins of different species of animals differ from each other considerably in their resistance to the action of alkali. Thus, human oxyhemoglobin is changed by 0.05 *N* NaOH within less than one minute to a brown product, whereas bovine oxyhemoglobin remains bright red for many hours under the same conditions.[3,4] The change in color and absorption spectrum is due to denaturation as shown by the parallel loss of solubility at *p*H 7–8.[4] The extent of denaturation can, therefore, be measured spectrophotometrically. When the per cent. of denatured oxyhemoglobin is plotted against reaction time, continuous curves are obtained in most cases. Breaks in the curves reveal the presence of two or more hemoglobins in the investigated blood. In this manner multiple hemoglobins were detected in the blood of new-born children[5] and adult persons.[6,7] In spite of the frequent use of the alkali denaturation method in biochemical and clinical work,[8–13] not much is known about the mechanism of the reaction. We investigated, therefore, the rate of alkali denaturation at different temperatures and also compared the denaturation rate of oxyhemoglobin with that of hemoglobin and globin.

Methods.—In order to prevent the denaturation of oxyhemoglobin during its preparation, organic solvents and lengthy manipulations were avoided. The red cells from oxalated blood were washed rapidly three times with 0.9% NaCl solution, hemolyzed by water, and centrifuged to obtain a clear solution. The hemolysate was then diluted to give an absorbancy of 0.5–0.8 on the Beckman spectrophotometer. The freshly prepared solution was placed in a 10-mm. absorption cell, mixed with one-fifth of its volume of 0.25 *N* NaOH, and the reaction followed photometrically at 576 mμ. The denaturation of reduced hemoglobin was

(1) Support of this work by research grants from the U. S. Public Health Service, National Institutes of Health, and from the American Cancer Society upon recommendation of the Committee on Growth of the National Research Council, is gratefully acknowledged. The authors are indebted to Mrs. Margaret Kennedy for assistance in some of the experiments.

(2) U. S. Public Health Service predoctorate fellow, 1951–1952.

(3) F. v. Krüger, *Z. vergleich. Physiol.*, **2**, 254 (1925).

(4) F. Haurowitz, *Z. physiol. Chem.*, **183**, 78 (1929).

(5) F. Haurowitz, *ibid.*, **186**, 141 (1930).

(6) R. Brinkman and J. H. P. Jonxis, *J. Physiol. (London)*, **88**, 162 (1937).

(7) K. Betke, *Biochem. Z.*, **322**, 186 (1951).

(8) R. Brinkman, A. Wildschut and A. Wittermans, *J. Physiol. (London)*, **80**, 377 (1934).

(9) F. D. White, G. E. Delory and L. G. Israels, *Can. J. Research* **28E**, 231 (1951).

(10) H. S. Baar and T. W. Lloyd, *Arch. Diseas. Childhood*, **18**, 1 (1943).

(11) E. Ponder and P. Levine, *Blood*, **4**, 1264 (1949).

(12) A. Rossi-Fanelli, *Bull. soc. chim. biol.*, **31**, 457 (1949).

(13) H. J. Ramsay, *J. Cell Comp. Physiol.*, **18**, 369 (1941).

examined in solutions containing 0.2% sodium dithionite $Na_2S_2O_4$, wave length 558 mμ being used. In those experiments which lasted more than one hour, the reduced hemoglobin solution was kept in a stoppered cylinder under nitrogen, to prevent reoxidation by the air. At various times, samples from the bottom layer were carefully pipetted into the absorption vessels and immediately measured. The addition of dithionite caused a decrease in *p*H from 11.9 to 11.8, and a negligible increase in the ionic strength. All solutions were brought to the desired temperature before mixing; the temperature was maintained constant within ±0.5° by means of a Beckman thermospacer.

The extinction, E_n, of the native oxyhemoglobin or hemoglobin anions was determined by mixing their solutions with one-fifth volume of 1% sodium carbonate solution. This did not cause measurable denaturation but cleared up slightly turbid hemolysates. The extinction, E_D, of the fully denatured product is the final value after prolonged exposure to *p*H 11.9. The per cent. of native oxyhemoglobin or hemoglobin at time t (sec.) is $n = 100(E_t - E_D)/(E_N - E_D)$, where E_t is the extinction of the partially denatured solution at the time t. In Figs. 1 and 2, log (n) is plotted *versus* t; the straight lines are drawn according to the method of least squares.

Globin was prepared from the hemoglobins of man, rabbit and beef according to Anson and Mirsky.[14] The alkaline denaturation of globin was examined at *p*H 11.0 and 11.9; at 5 and 25°; 10 ml. of a solution containing 50–150 mg. of globin were adjusted to the desired *p*H by adding 1.0 ml. of an alkaline phosphate solution or 2 ml. of 0.25 *M* NaOH. After 2 minutes, the *p*H was brought to 7.5 by adding 0.25 *M* HCl. The denatured globin was centrifuged off, and the concentration of the soluble native globin determined by Kjeldahl analysis. Control experiments were run, simultaneously, with the oxyhemoglobin of the same blood. The results are shown in Table II.

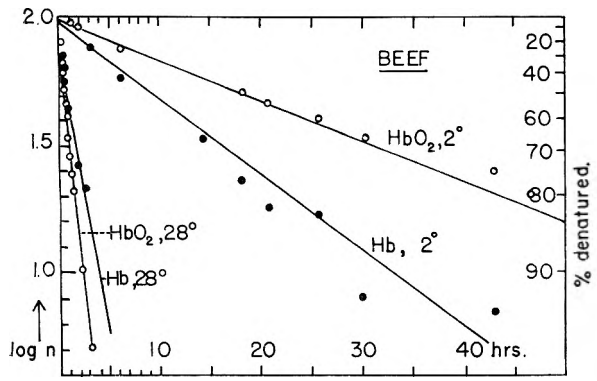

Fig. 1.—Denaturation of beef hemoglobin (Hb) and oxyhemoglobin (HbO_2) at *p*H 11.9 (n = per cent. of native pigment).

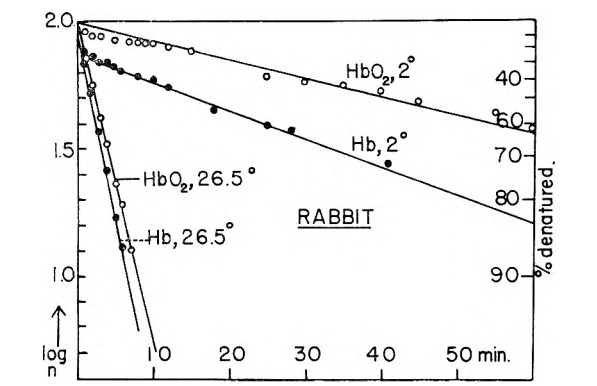

Fig. 2.—Denaturation of rabbit hemoglobin (Hb) and oxyhemoglobin (HbO_2) at *p*H 11.9 (n = per cent. of native pigment).

(14) M. L. Anson and A. E. Mirsky, *J. Gen. Physiol.*, **13**, 469 (1930).

Results

The Figs. 1 and 2 confirm previous reports on the enormous differences in the alkali resistance of oxyhemoglobins from different animals. The time required for 50% denaturation is approximately 7 seconds for human, but 2100 seconds for beef oxyhemoglobin at 28–30°. The linear decrease in log (n) in Figs. 1 and 2 is in agreement with first-order kinetics. Oxyhemoglobin from the rat showed noticeable deviation from the straight course of the reaction indicating the presence of two or more oxyhemoglobins.

The slope of the straight lines drawn in the figures is proportional to the first-order velocity constants of denaturation; it is clear from the figures that the velocity constants increase considerably when the temperature is raised. The activation energy, E_a, was calculated from the ratio k_2/k_1 at two temperatures T_2 and T_1 by means of the equation $E_a = R(T_1T_2/(T_2 - T_1))\ln(k_2/k_1)$. According to the theory of absolute reaction rates,[15] the heat of activation is $\Delta H^\ddagger = E_a - RT$, and the free energy of activation, $\Delta F^\ddagger = 2.3R \log (kh/KT)$, where h and K are Planck's and Boltzmann's constants, respectively. The entropy of activation is $\Delta S^\ddagger = (\Delta H^\ddagger - \Delta F^\ddagger)/T$. Values for $\Delta H^\ddagger$, and $\Delta S^\ddagger$, are recorded in Table I.

TABLE I

DENATURATION OF HEMOGLOBIN (Hb) AND OXYHEMOGLOBIN (OxyHb) AT *p*H 11.9

Protein	T°	k,[a] sec.$^{-1}$	$\Delta H^\ddagger$, kcal./mole	$\Delta S^\ddagger$ e.u.
Human OxyHb	275	2.3×10^{-2}	7.6	−39
	303	9.3×10^{-2}		
Rat OxyHb [b]	285	2.1×10^{-3}	15.1	−17
	301	9.2×10^{-3}		
Hb[b]	285	2.4×10^{-3}	12.2	−27
	301	8.1×10^{-3}		
Rabbit OxyHb	275	2.8×10^{-4}	18.5	− 8
	299.5	4.8×10^{-3}		
Hb	275	4.2×10^{-4}	16.9	−13
	299.5	5.7×10^{-3}		
Beef OxyHb	275	9.3×10^{-6}	21.0	− 6
	301	2.8×10^{-4}		
Hb	275	2.0×10^{-5}	12.0	−37
	301	1.5×10^{-4}		

[a] k is the first-order velocity constant $(1/t)\ln(n_1/n_2)$ calculated according to the method of least squares. [b] Since rat hemoglobin is a mixture, the values in Table I are "apparent values" only. They refer to the more stable of the two hemoglobins because the experimental data obtained after longer periods of time have more weight in calculating k than those obtained after short periods.

Since globin, in contrast to hemoglobin, is colorless, the denaturation rate cannot be measured spectrophotometrically; it was determined by separating the insoluble, denatured globin from the soluble native globin. This method is not very accurate because some of the soluble protein may be adsorbed to the insoluble denatured material, and denatured protein may be kept in solution by native protein. It is clear, however, from Table II that the investigated globins are more rapidly denatured by alkali than the corresponding hemo-

(15) H. Eyring and A. Stearn, *Chem. Revs.*, **25**, 253 (1939).

globins. Denaturation takes place not only at *p*H 11.9, but also at *p*H 11.0, where none of the oxyhemoglobins is denatured. Table II also shows that the denaturation velocity of all globins is of the same order of magnitude, although that of the corresponding hemoglobins varies enormously.

TABLE II

DENATURATION OF GLOBIN (Gb) AND OXYHEMOGLOBIN (OxyHb) OF VARIOUS ORIGINS

The figures indicate the per cent. of denatured protein after exposure for 2 minutes to alkaline reaction.

Protein	*p*H 11.0 5°	*p*H 11.9 5°	*p*H 11.0 25°
Human OxyHb	0	53	9
Human Gb	0	58	74
Rabbit OxyHb	0	Trace	..
Rabbit Gb	0	40	..
Beef OxyHb	0	0	Trace
Beef Gb	0	30	35

Discussion

A satisfactory theory of the denaturation of hemoglobin and oxyhemoglobin by alkali has to account for the following facts substantiated by the preceding sections of this paper and by previous experimental work: (1) denaturation of hemoglobin by alkali takes place according to first-order kinetics provided that the investigated hemoglobin is homogeneous, (2) the denaturation velocity varies from species to species and is typical for the hemoglobin of each animal species, (3) the denaturation velocities of oxyhemoglobin and hemoglobin are of the same order of magnitude, that of hemoglobin requiring a lower activation energy, (4) the entropy of denaturation is negative, and (5) the denaturation velocities of globins are much higher than those of the corresponding hemoglobins and are similar for the globins of all investigated animal species.

The last mentioned result leads to the conclusion that the enormous differences in the alkali resistance of hemoglobins of different origin are not caused by analogous differences in the alkali resistance of the corresponding globins. Evidently, the high stability of certain hemoglobins against alkali denaturation is brought about by the combination of their protein component with heme.

The almost identical absorption spectrum of all mammalian hemoglobins indicates that the coordinate bond between heme iron and globin is the same in all of them; hence, it cannot be responsible for differences in the alkali resistance. It is more probable that these differences are due to different degrees of complementariness of an "anti-heme" pattern in the surface of the globin molecules. Interaction between the porphin ring system and native globin has been first suggested by Hill and Holden[16] and is made highly probable by the reaction taking place between globin and heme in the water/*p*-xylene interface.[17] While other proteins reduce the interfacial tension between water and *p*-xylene by 10–12 dynes/cm., globin causes a drop by approximately 20 dynes/cm. indicating the presence of a non-polar hydrophobic area in the surface of its molecule. When hemin is added, the high interfacial activity of globin is lost; evidently, heme combines with the non-polar portion of the globin molecule. One can reasonably assume that the stability of the heme–globin complex and its resistance against alkali denaturation will increase considerably by a close fit between globin and the rigid planar heme structure.

According to Table I, the activation process involves a decrease in entropy. The negative $\Delta S^{\ddagger}$ values may be due to the immobilization of water molecules by the activated complex. Table I also shows that the velocity of denaturation is of the same order of magnitude for hemoglobin and oxyhemoglobin, but that the heat of activation is lower for hemoglobin than for oxyhemoglobin. This is, probably, caused by configurational changes in the globin portion of the heme–globin complex which accompany the oxygenation of hemoglobin; the occurrence of such a structural rearrangement in the molecule is proved by changes in the crystalline shape,[18] in the solubility,[19] and in the dichroism[20] of hemoglobin crystals when they combine with molecular oxygen.

(16) R. Hill and F. Holden, *Biochem. J.*, **20**, 1326 (1926).

(17) F. Haurowitz, P. Boucher and M. Dicks, *Federation Proc.*, **12**, 215 (1953).

(18) F. Haurowitz, *Hoppe-Seyler Z. Physiol. Chem.*, **254**, 266 (1938).

(19) J. Roche, Y. Derrien and M. Moutte, *Compt. rend. Soc. Biol.* **132**, 531 (1938).

(20) M. F. Perutz, in J. Raoul, Symposium sur la Biochimie de l'Hematopoiese, Paris, 1952, p. 101.

DENATURATION OF BOVINE PLASMA ALBUMIN[1]

BY MILTON LEVY AND ROBERT C. WARNER

Department of Chemistry, New York University College of Medicine, New York 16, N. Y. and Marine Biological Laboratory, Woods Hole, Mass.

Received July 24, 1953

The kinetics of denaturation of bovine plasma albumin is first order from *p*H 0.8 to about 4 when suitable solubility conditions are used as a test for denaturation. Criteria for the selection of suitable conditions are discussed. The variation of rate of denaturation with *p*H is accommodated by an equation based on the postulate that four prototropic groups are involved importantly in the stability of the protein in the *p*H region covered. Thermodynamic analogs for the activation processes involving the postulated groups are derived from the temperature variation of the parameters of the rate equations. Evidence is adduced for the hypothesis that the chemical groups are not those ordinarily thought of as proton donors in this *p*H region.

The rate of denaturation of a protein in solution is simultaneously a function of temperature and *p*H.[2,3] The nature of the function may give clues to the specific chemical structures which are essential to the native configuration of proteins.[3-5] A rational interpretation of the rate of denaturation as affected by *p*H and temperature was developed to fit the results on ricin, a protein of castor beans, over a wide range of *p*H and temperature and shown to be applicable to more limited data on other proteins.[3] It is our intent to study other proteins from the point of view outlined in the paper on ricin. The present paper describes some of our experiences with bovine plasma albumin.

Solubility as Criterion of Denaturation.—We have followed the change in solubility of the protein as evidence of denaturation. The technique consists of maintaining a solution of protein in a buffer of known composition, at a constant temperature and sampling at measured time intervals into a cool "stopping" solution to "freeze" the situation. The stopping solution has the function of establishing conditions in which no further reaction occurs, in which the native protein is soluble and the denatured protein is insoluble. Its composition is a matter of choice with respect to final salt concentration and *p*H, but once fixed, these conditions are maintained for all experimental runs. The chosen conditions are critical for the result of the experiments as will be detailed below. The insoluble material is removed by centrifuge and the amount of soluble protein determined through its light absorption at 278 mμ.

In our first experiments with bovine plasma albumin the same stopping solution applied to ricin was used. When mixed with the experimental solutions this established a *p*H of 4.6 and 0.5 *M* concentrations of sodium acetate and acetic acid. Runs made with this stopping solution are typified by curve A, Fig. 1. There is a latent period during which nothing becomes insoluble in the stopper followed by a more or less rapid development of insoluble material. Complete conversion to insolubility did not occur in most of the experiments but often more than 90% conversion was reached. Curves of this type can be kinetically interpreted as resulting from a first-order isomerization of the native albumin followed by a second or higher order polymerization. The stopper left both the native and isomeric protein in solution but precipitated a polymerized fraction. This has been confirmed by ultracentrifuge studies of the experimental solutions.[6] It was established that removal of the heated solution to a lower temperature (25 or 4°) for 18–24 hours did not restore the native character. The lag period was essentially of the same length and the subsequent course of reaction unchanged whether it was interrupted or not. The processes occurring in the lag period thus appeared to be irreversible. The residue which never became insoluble may be an impurity or may be the consequence of our operational definition of "never" which was about a week.

The equations applicable to the kind of kinetics postulated require considerable refinement of the data to produce well defined constants. It became evident that the test of denaturation by solubility required refinement for practical reasons. To guide us in the selection of a suitable stopping solution we set up the following requirements for a solubility test for denaturation.

1. The native protein must not be precipitated or coprecipitated with the denatured. A test for this can be made with artificial mixtures of native and denatured protein.
2. The greater the observed rate of denaturation the more suitable is the stopping condition.
3. The amount of material precipitated should be independent of small variations in actual stopping conditions as to salt concentration and *p*H.
4. The rate observed should be kinetically first order since it is difficult to escape the logic that the essential step in denaturation is a change in structure (unfolding) or isomerization. If the essential step is of this kind the reaction must be unimolecular with respect to protein. The over-all reaction must then be first order if the stopping conditions precipitate the initial product or a material so rapidly formed from it that the first step is rate controlling. However, this condition is a necessary result if the essential step is being measured, but is not sufficient to establish that it is being measured.

By adding ammonium sulfate to the stopping solution in sufficient amounts the rates observed at all *p*H values were much faster than with a "low salt" stopper. This result is illustrated by curve

(1) This work was supported in part by a grant from the office of Naval Research.

(2) J. Steinhardt, *K. Danske Videnskab. Selsk. Math-fys. Medd.*, **14**, 11 (1937).

(3) M. Levy and A. E. Benaglia, *J. Biol. Chem.*, **186**, 829 (1950).

(4) V. K. LaMer, *Science*, **86**, 614 (1937).

(5) H. Eyring and A. E. Stearn, *Chem. Revs.*, **24**, 253 (1939).

(6) M. Levy and R. C. Warner, *Federation Proc.*, **12**, 239 (1953).

B, Fig. 1. The observed rate did not follow the first-order law at experimental *p*H values above about 4.0 but between *p*H 0.8 and 4.0 first-order reaction rates were obtained when the final solution contained 2.16 *M* ammonium sulfate, 0.67 *M* sodium acetate and 0.13 *M* acetic acid. The final *p*H in the precipitating mixture was 5.4–5.5. The lag period disappeared under all conditions with this stopper but in solutions alkaline to *p*H 4.0 (at 65.7°) the rate constant diminished with time. We expect to discuss this region in detail at another time.

Using the high salt buffer the course of reaction was unaffected by a fourfold change in protein concentration whether it was first order kinetically or not. The reaction measured is therefore monomolecular in protein from *p*H 0.8 to *p*H 12 which was the region explored.

Relationship of Rate to *p*H.—The logarithms of the first-order rate constants observed in buffers at ionic strength 0.2 are shown in Fig. 2 at four temperatures plotted against *p*H. The buffers used were HCl, KCl; glycine, KCl, HCl; formic acid, KCl, KOH; and acetic acid, KCl, KOH. Overlapping between buffers did not produce irregularities in the curves. The *p*H of the mixture of protein and buffer was measured at room temperature at the end of the run and corrected to the experimental temperature as indicated in the paper by Levy and Benaglia.[3] The solid lines drawn on the graph are calculated (see below) and cover the *p*H range in which the first-order law applied. The additional points connected by dashed lines at each temperature are for initial velocity "constants" and are given for orientation only. A second and pronounced minimum on the *p*H–log rate function occurs at *p*H 5.5 on the basis of initial rates. This is followed by a rise in the rate above *p*H 7 to a value higher than that at the peak at *p*H 4.

To account for the relationship of rate to *p*H it is necessary to assume four proton donor groups in the protein which are associated with its activation for denaturation. One of these has a $pK < 0.8$ and the other three average to $pK > 4$. The K's for the groups are designated successively K_1, K_2, K_3, K_4 in the conventional manner. Each acid and base form associated with this succession has a characteristic rate constant of denaturation designated k_1 for the most acid to k_5 for the most alkaline type. Application of these postulates and nomenclature to the general equation developed previously[3] shows the rate constant (j) at constant hydrogen ion activity (h) to be

$$= \frac{k_1h^4 + k_2K_1h^3 + k_3K_1K_2h^2 + k_4K_1K_2K_3h + k_5K_1K_2K_3K_4}{h^4 + K_1h^3 + K_1K_2h^2 + K_1K_2K_3h + K_1K_2K_3K_4} \quad (1)$$

In the region *p*H 0.8 to 4.0 the denominator is equal practically to K_1h^3 since $K_1 > h > K_2, K_3, K_4$. Equation 1 then becomes the approximation

$$j = \frac{k_1h}{K_1} + k_2 + \frac{k_3K_2}{h} + \frac{k_4K_2K_3}{h^2} + \frac{k_5K_2K_3K_4}{h^3} \quad (2)$$

The lines drawn in Fig. 2 are those fitted to this equation by successive approximation leading to the numerical constants listed in Table I for the various temperatures. The value 0 entered in the table for $k_4K_2K_3$ indicates that the fourth term on

TABLE I

PARAMETERS FOR DENATURATION OF BOVINE PLASMA ALBUMIN AT VARIOUS TEMPERATURES

Dimensions, k's in reciprocal seconds, K's in moles per liter

Parameter	Temperature, °C. 46.2	56.1	65.7	75.0
k_1/K_1	5×10^{-5}	1.2×10^{-4}	4×10^{-4}	8×10^{-4}
k_2	5×10^{-6}	7×10^{-6}	2×10^{-5}	6×10^{-5}
k_3K_2	5×10^{-9}	2×10^{-8}	4.3×10^{-8}	8×10^{-8}
$k_4K_2K_3$	0	0	0	0
$k_5K_2K_3K_4$	4×10^{-14}	4×10^{-14}	4×10^{-14}	4×10^{-14}

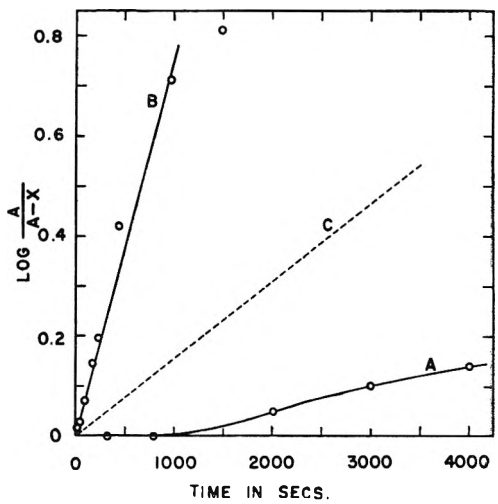

Fig. 1.—Time course of denaturation at 65.7° as shown by the use of low (A) and high (B) salt concentration in the buffer in which the denatured product was precipitated. Experiments A and B were carried out at *p*H 3.28 and *p*H 3.48, respectively. Curve C shows the slope of the first-order reaction at *p*H 3.28 derived from the constant interpolated on Fig. 2. Curve C therefore refers to the rate indicated by the use of the high salt precipitating buffer on the same reaction mixture run under the same conditions as used for curve A.

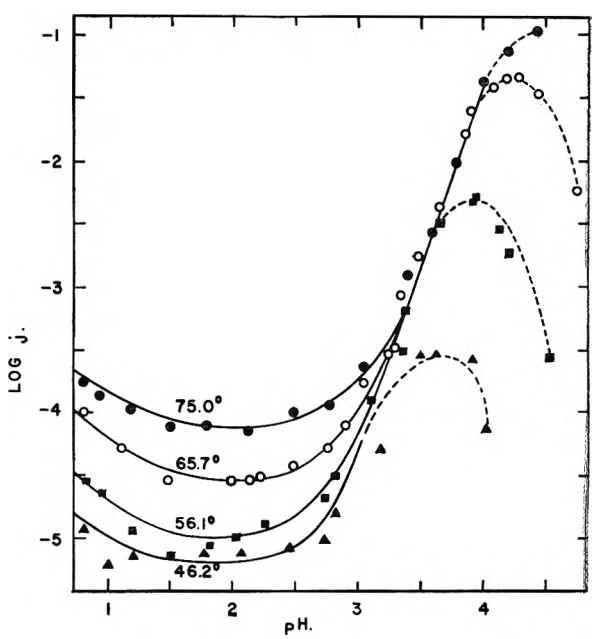

Fig. 2.—Effect of *p*H on the first-order constant of denaturation of bovine plasma albumin at four temperatures. The solid lines were calculated as described in the text. The broken lines are for orientation only. Points on the broken lines refer to the initial velocity

the right in equation 2 is not significant at any temperature compared to the other terms. This indicates that the proton donating step it represents does not of itself produce any greater instability than is present in the donor ion. It does however enter into the activation represented by the fifth term as indicated by the presence of K_3 in that term and the fact that it is cubic in h.

It is recognized that the protein loses more than four protons in passing from pH 0.8 to pH 4. We believe that the fitting of the data by four groups indicates that the influence of the majority of prototropic groups on the stability of the protein is insignificant. The changes of purely electrostatic forces such as may arise between positive and negative sites on the protein cannot be very important factors in the stabilization of their native structure.[7]

To give a special character to the prototropic groups evident in Fig. 2 and postulated in the equations we have assumed that they are prototropic hydrogen bonds (or prototropic chelations of other sorts). This is supported for the case of bovine plasma albumin by the small number involved and the fact that the pK of at least one (pK_1) is obviously less than 0.8 and outside the range suggested for any known carboxyl group in protein.[8]

The postulates[3] on which equation 1 is developed do not exclude its accommodation of any number of prototropic groups. It is true of course that the approximation and logarithmic fitting used will tend to minimize any but those terms which effect large contributions to the stability or instability of the protein. For example we may picture as belonging to the species P^{3+} a number of charge subspecies P^{3+}_{1+} P^{3+}_{2+} $P^{3+}_{3+}\cdots P^{3+}_{n+}$ and P^{3+}_{1-} P^{3+}_{2-} $P^{3+}_{3-}\cdots$ P^{3+}_{n-}. These subspecies may have cumulative effects as large as 50% (0.3 log units) without being evident as significant departures on the diagrams. Conversely fitting to this extent indicates that the subspecies do not differ greatly from one another in their susceptibility to denaturation compared, for instance, to the difference between P^{4+} and P^{3+} as groups of subspecies.

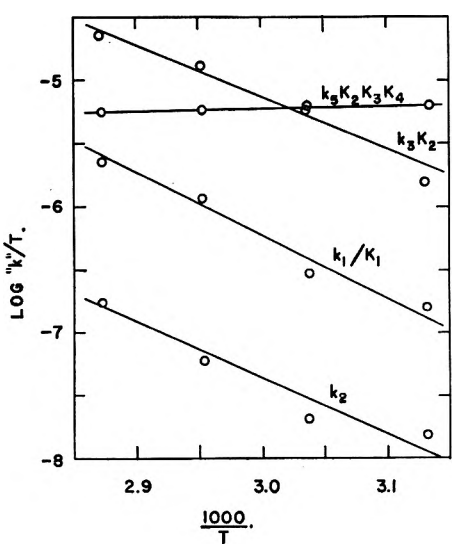

Fig. 3.—Relation to temperature of parameters describing the effect of pH on denaturation. To bring the lines into the field, 5 has been added to each value of log k_3K_2 and 11 to each value of log $k_5K_2K_3K_4$.

An additional factor inherent in the nature of the fitting used is that K_2 in the third and fifth terms is not necessarily referable to the same group. Since the constants enter the equations in mixed form one cannot from the data prove the identity or lack of it for any constant in the sets. The total number of prototropic groups postulated (in this case four) to affect the stability is the minimum number required to account for the relation of rate to pH. The maximum number could be five since K_2 appears in two significant terms of the equation.

Temperature Coefficients.—The set of constants in equation 2 for the four temperatures are plotted in Fig. 3 according to a form for the theory of absolute reaction rates[9]

$$\log \frac{"k"}{T} = -\frac{\Delta H^*}{2.3RT} + \frac{\Delta S^*}{2.3R} + \log \kappa \frac{k}{\mathbf{h}}$$

"k" is the rate parameter observed at the absolute temperature T. ΔH^* is the heat of activation obtained from the slope of the plot of log "k"/T against $1/T$. ΔS^* is the entropy of activation obtained from the intercept after subtracting the last term which has the numerical value 10.32 for a transmission coefficient κ arbitrarily set as 1, the Boltzmann constant k is 1.37×10^{-16} and the Planck constant $\mathbf{h}$ is 6.55×10^{-27}.

For the theory of absolute reaction rates the kinetic constants k are converted to activation equilibrium constants. Our data and interpretation yields mixed constants involving both proton donation and activation. The thermodynamic analogs obtained refer to the following reactions.

Reaction	Constant of eq. 2	Activation reaction	Activation constant
1	k_1/K_1	$P^{3+} + H^+ \rightleftarrows P^{4+*}$	K_1^*/K_1
2	k_2	$P^{3+} \rightleftarrows P^{3+*}$	K_2^*
3	k_3K_2	$P^{3+} \rightleftarrows P^{2+*} + H^+$	$K_3^*K_2$
4	$k_5K_2K_3K_4$	$P^{3+} \rightleftarrows P^{0*} + 3H^+$	$K_5^*K_2K_3K_4$

The values of ΔH^* ΔS^* and ΔF^*_{298} are entered in Table II.

TABLE II

THERMODYNAMIC ANALOGS OF ACTIVATION REACTIONS FOR BOVINE PLASMA ALBUMIN

Activation constant	ΔH^*, kcal.	ΔS^*, e.u.	ΔF^*_{298}, kcal.
K_1^*/K_1	23.2	− 6.2	25
K_2^*	24.3	− 8.6	26.8
$K_3^*K_2$	17.1	− 42.4	29.7
$K_5^*K_2K_3K_4$	0.6	−124	36.3

Discussion

The small heat of activation in reaction 4 Table II reflects the very low temperature coefficient of denaturation shown in Fig. 1 around pH 3.5. This fact contradicts the generally held opinion that denaturation always has a high temperature coefficient.

(7) C. F. Jacobsen and K. Linderstrøm-Lang, *Nature*, **164**, 411 (1949).

(8) R. K. Cannan, *Chem. Revs.*, **30**, 395 (1942).

(9) S. Glasstone, K. J. Laidler and H. Eyring, "The Theory of Rate Processes," John Wiley and Sons, Inc., New York, N. Y., 1941.

The separation of the composite equilibrium constants into a thermal activation step and proton donating or accepting steps is not possible except for K_2^* which is purely a thermal activation. As an example of a number of hypotheses that can be built on these data we may observe that the ΔH^* for reaction 4 is practically zero. This might suggest that the sole free energy factor in the activation is the proton donation to the solvent. Formally this amounts to the hypothesis that K_5^* is near 1. The average free energy for the three protons donated may then be given the value 36.3/3 = 12.1 corresponding to a pK of 8.8 for the average group. This value suggests amino group dissociations, but amino group dissociations are usually given ΔH values of about 10 kcal. per mole.[10] An imidazole group requires ΔH of about 6 kcal. and in addition its pK value is about 2 units less than the average pK for the three groups suggested by ΔF^*. The low ΔH^* of itself is compatible with carboxyl groups, but the ΔF^* suggests that their dissociation constants would be profoundly modified if they are the active groups. If we assume that the three groups are not identical or equal we are left with no way of assigning the individual pK's or their thermodynamic descriptions. Another possibility is that the low value of ΔH^* is a balance between a positive ΔH^* of activation and a negative ΔH for proton donation which makes the situation worse as far as assigning the prototropic changes to known groups. The other situation of a negative ΔH^* for activation is rather implausible.

In reaction 1 the pK of the proton group is below 0.8 because there is no sign of leveling off in the rate even at pH 0.8. In reaction 3 the large ΔH^* is greater than is compatible with either carboxyl, imidazole or amino groups as is ΔF^*. The position of the group concerned on the pH scale could be at about 3, but if any significant part of the ΔH^* and ΔF^* comes from it, the suggestion that it is a carboxyl group must be associated with the assumption of a profound modification due to its environment. In other words this group is bound to something else in the protein. The fourth step has been discussed above.

The discussion is intended to emphasize the plausibility of the conclusion that the proton donating or accepting groups in protein shown through the relationship of rate of denaturation to pH are not the ordinary prototropic groups of proteins such as carboxyl, imidazole or amino except as they may be greatly modified by hydrogen bonding or other reaction within the protein molecule.

(10) J. Wyman, Jr., *J. Biol. Chem.*, **127**, 1 (1939).

Experimental

Crystalline bovine plasma albumin obtained from Armour and Co. was used. A 1.2% solution in water was prepared with addition of sufficient HCl to bring the pH to about 3 if the experimental pH was less than 4.5 or enough KOH to bring the pH to 6 if the experimental pH was greater than 4.5. This avoids having the protein pass through the region of maximal denaturation rate during the mixing process. Eighteen ml. of a buffer mixture was preheated in a 25 × 200 ml. test-tube and placed in the constant temperature bath (oil, regulated to ±0.1°). When the temperature of this solution had dropped to a definite point above that of the bath 2 ml. of the protein solution at room temperature was added and mixed by a stream of air bubbles. The mixture was practically at bath temperature at zero time. The remaining techniques are as described by Levy and Benaglia[3] except that the residual protein was measured by ultraviolet absorption at 278 mμ at pH 5.4 in a Beckman DU spectrophotometer. The pH of the protein–buffer mixture was taken on the residual experimental solution on a glass electrode pH meter.

If very long experimental periods were involved the solutions were sealed in glass tubes before immersing in the oil-bath.

The high salt stopping buffer was prepared from a solution containing 38.3 g. of ammonium sulfate and 13.9 g. of sodium acetate hydrate dissolved to make 100 ml. of solution. To this was added an amount of glacial acetic acid calculated to give a ratio of acetate to acetic acid of 7 in the final mixture with the experimental buffer. Additional water was added to the stopping solution to make 2 ml. of added liquid. Three ml. of stopping solution was used for each ml. of experimental solution.

CONFORMATION CHANGES OF PROTEINS[1]

BY RUFUS LUMRY AND HENRY EYRING

Department of Chemistry, University of Utah, Salt Lake City, Utah

Received July 24, 1953

Recent developments in protein structure make one model for globular proteins especially attractive. This model consists of polypeptide chains folded on themselves to give hydrogen-bonded secondary structures which are in turn folded in a rigid tertiary arrangement through the interaction of amino acid side chains. The implications of the model are examined in terms of possible energy states available to proteins and possible denaturation reactions. Denaturation is defined as change in conformation. The folding process is considered to be spontaneous and directed by the composition and order of peptide amino acid residues. Reversible thermal denaturation processes are presented as changes in tertiary structure, irreversible processes as changes in secondary structure. The activated complex for denaturation and for enzymic function is discussed and the possibility presented that enzymic activity, reversible denaturation and ion-binding are all aspects of the same protein property.

Introduction

The term protein denaturation even in its original meaning included all those reactions destroying the solubility of native proteins and has since acquired so many other meanings as to become virtually useless. It is now generally realized that peptide and other primary bonds are not destroyed under the mild conditions of most denaturation reactions unless specific reagents or catalysts for these bonds are available. Hess and Sullivan[2] were able to preserve intact sulfhydryl and primary sulfur–sulfur groups during careful hydrolysis of several proteins but sulfur–sulfur bonds are easily destroyed catalytically and their exact state in any given denaturation reaction may be uncertain. In any event the bulk of denaturation changes consist of changes in secondary bonds: ion–dipole, hydrogen and van der Waals; and in the rotational positions about single bonds which are controlled by the secondary bond structure. Such rearrangements of the secondary-bonded structure are defined as changes in conformation[3] and are exemplified by the conversion of cyclohexane from "chair" to "boat" form or the melting of a crystal. We shall thus speak of transconformation reactions rather than denaturation reactions. Certain transconformation reactions involve only a few secondary bonds; others are extensive and similar to second and higher order phase changes in solids. These last are of particular interest and we shall designate them cooperative transconformations. Numerous attempts have been made to describe such reactions in terms of changes in ionization, hydration or degree of folding of polypeptide chains.[4,5] In this paper we shall examine conformation changes in terms of the newer pictures of protein structure.

The Structure of Globular Proteins

1. Primary Structure.—Proteins will be destroyed by breaking a single primary bond in the skeleton of a constituent polypeptide chain if the broken bond can be rearranged before the break is healed. Cathode ray,[6] ultrasonic,[7] ultraviolet[8] and ionizing radiation in general breaks or weakens primary bonds but the structure of the molecule in native form, especially when held in the solid, does not allow reorganization and subsequent reaction at the broken ends. At low temperatures which favor the recombination process of low activation energy or in the absence of oxygen which is frequently able to cauterize the stumps or to react with strained bonds, the break may recover or persist in high-energy state.[9] At normal temperatures in solution unfolding rapidly permits destructive rearrangement. Rubber and other large polymeric substances behave in a similar fashion following breakage or strain of primary bonds.[10] Enzyme attack on peptide linkages will also introduce fatal weaknesses[11] though in the conversion of proenzymes to active enzymes simple conversion from one native protein to another occurs.

Recently Elliott[12] has established another important source of weakness in the primary structure previously suggested by Bergmann, *et al.*[13] Where serine and threonine residues exist in the chain, "acyl shifts" may occur in acid media, about *p*H 3 in model compounds

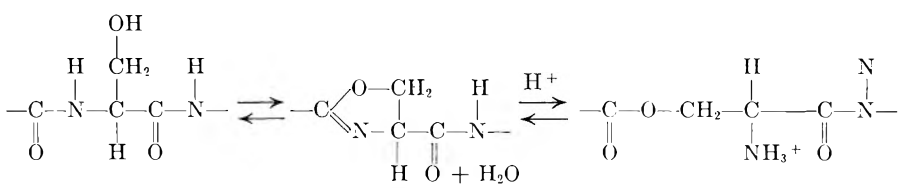

The reaction is in effect an internal hydrolysis to increase the chain by one bond length and to introduce an easily hydrolyzed ester bond. Du Vigneaud[14] actually observed the formation of N-methyl groups in insulin in a reversible reaction

(1) This work was supported by the National Science Foundation. The paper was originally presented at a Symposium on Protein Denaturation held during the Spring meeting of the American Chemical Society at Los Angeles, 1953.

(2) W. C. Hess and M. X. Sullivan, *J. Biol. Chem.*, **151**, 635 (1943).

(3) W. J. Kauzmann, J. E. Walter and H. Eyring, *Chem. Revs.*, **26**, 339 (1940).

(4) H. Neurath, J. P. Greenstein, F. W. Putnam and J. O. Erickson, *ibid.*, **34**, 157 (1944).

(5) M. L. Anson, *Advances in Protein Chem.*, **2**, 361 (1945).

(6) H. Smetana, *J. Exptl. Med.*, **73**, 223 (1941).

(7) P. Grabar and R. Prudhomme, *J. chim. phys.*, **44**, 145 (1948); *Bull. soc. chim. Biol.*, **29**, 122 (1947).

(8) A. D. McLaren and S. Pearson, *J. Polymer. Sci.*, **4**, 45 (1949).

(9) S. Fiala, *Biochem. Z.*, **318**, 67 (1947).

(10) W. Kauzmann and H. Eyring, *J. Am. Chem. Soc.*, **62**, 3113 (1940).

(11) K. V. Linderstrøm-Lang, Lane Medical Lectures: "Proteins and Enzymes," Stanford University Press, Stanford, California, 1952.

(12) D. F. Elliott, *Biochem. J.*, **50**, 542 (1952).

(13) M. Bergmann and J. S. Fruton, *J. Biol. Chem.*, **118**, 405 (1937).

(14) V. du Vigneaud, *Cold Spring Harbor Symposia Quant. Biol.*, **6**, 275 (1938).

and Elliott has observed their occurrence in silk fibroin. The reaction is normally slow and its pH of occurrence will undoubtedly vary with the type of bonds the hydroxy or amino forms can make. The well-known lability of peptide chains at serine and threonine residues[15,16] is thus explained and we shall see indications of acyl shift involvement in several transconformation reactions. Acid titration experiments will almost universally need re-evaluation in light of this finding.

A somewhat similar set of reactions leading to thiazolidine formation between cysteine, sulfhydryl and aldehyde groups has been suggested by Linderstrøm-Lang and Jacobsen.[17] Sulfhydryl groups of proteins frequently become available to external attack only after extreme treatment of the protein and well after the exposure of disulfide groups. In view of the demonstration of N to O rearrangement in the acyl shift, a similar N to S shift may possibly be an important reaction of —SH groups though it is probably not energetically favored. At present only the serine and threonine reaction is established as a source of alternation in primary structure during denaturation. We shall thus be primarily concerned with secondary bonds to the exclusion of the hydrolyzed states of proteins. Complete peptide hydrolysate is probably the ultimate state of lowest free energy for proteins though some question as to this conclusion exists in view of the high stabilization energies available from the secondary bonds of the folded structure.[11] The free energy difference between native (folded) protein and hydrolyzed protein (amino acids) is probably small and, in any event, the peptide chain is protected by high free energies of activation from hydrolysis.

Structural Features Due to Secondary Bonds.—Physical and immunological studies demonstrate unequivocally that globular proteins are rigid bodies undoubtedly a result of cross linking between peptide chains. X-Ray diffraction studies show considerably more internal order than is consistent with random cross linking. Pauling and coworkers[18-20] have pointed out that the key to protein structure lies in the considerable strength (8 kcal.) of hydrogen bonds which can exist between the carbonyl of one peptide link and the amino group of another. Only this type of bond can be made in quantity and in a way to produce extensive regularity. It would be favored in competition with other secondary bonds even though a considerable entropy decrease was concomitant. Fibrous rods have been reported to exist in insulin,[21] hemoglobin,[22] myoglobin,[23] ribonuclease,[24] and a few other proteins studied by X-ray methods. The rods of hemoglobin are believed to possess the α-keratin structure of fibrous proteins[25] and these are thought to consist of single peptides folded on themselves.[26] The final structure of fibers of the α-keratin type probably consists of aggregates of these single-peptide structures arranged to form larger patterns characteristic of a given fiber type. Pauling, Corey and Branson[20] have suggested a helical folding with hydrogen bonds between any peptide link and its third neighboring peptide link on either side. While this proposed "α-helix" is not yet fully established in globular proteins, there is considerable agreement that poly-α-amino acids such as poly-γ-methyl-L-glutamate spontaneously adopt that structure.[27,28] Considerations of stability and certain observations on transconformation reactions to be presented further support the assumption that some, if not all, globular proteins consist of peptide chains folded on themselves into secondary structures of great stability. Pauling and Corey have presented the case for the occurrence of their "α-helix" in globular proteins.[20]

Just as α-keratin may be stretched to form sheets of parallel extended polypeptide called β-keratin, extremely denatured proteins assume a more or less perfect sheet structure giving the β-keratin X-ray diagram.[29] This must occur in a polymolecular reaction of peptide chains since folded stability results from hydrogen bonds between parallel chains and thus depends on an arrangement of a number of chains.[20,21,30] The sheet structure is apparently less stable in water than the α-arrangement as judged from fiber studies, though many globular proteins are easily converted to stable β-keratin forms.[29] Conceivably, when protein concentration is high, the β-structure may be the more stable or limited by a high activation energy requirement from regaining the separate α-keratin structures. The β-keratin structure would be expected to be less stable when only one or a few peptide chains are available in a single protein molecule. Though we are prejudiced in favor of single peptide structures such as the α-form, present evidence is certainly insufficient to select any secondary structure for any protein other than hemoglobin. What seems important is the existence of relatively stable cooperative secondary structures. Whatever their detailed form, they must depend on hydrogen bonds between peptide linkages.

In addition to primary and secondary structural features the evidence from protein properties and inactivation reactions requires a tertiary structure of secondary tubes held together in loops by the interaction of R groups of amino acids: hydroxyl, sulfhydryl, phenolic, indole, carboxyl, carboxylate, amino, ammonium, benzoic, aliphatic and others. Thus we distinguish three types of structure, primary, secondary and tertiary, using names given by Linderstrøm-Lang in a similar suggestion he

(15) Ovalbumin, for example, has a total of 59 serine and threonine residues, 56 of which are very susceptible to acid hydrolysis. Lysozyme shows a similar susceptibility to hydrolysis in acid solution.

(16) Reviewed by H. L. Fevold, *Advances Protein Chem.*, **6**, 205 (1951).

(17) K. V. Linderstrøm-Lang and C. F. Jacobsen, *Compt. rend. trav. lab. Carlsberg*, **23**, 289 (1940).

(18) A. E. Mirsky and L. Pauling, *Proc. Nat. Acad. Sci. (U. S.)*, **22**, 439 (1933).

(19) L. Pauling and R. B. Corey, *ibid.*, **37**, 205, 235, 241, 251, 261, 272, 282, 729 (1951).

(20) L. Pauling and R. B. Corey, *Nature*, **171**, 59 (1953).

(21) B. Low, *ibid.*, **169**, 955 (1952).

(22) W. L. Bragg, E. R. Howells and M. F. Perutz, *Acta Cryst.*, **5**, 136 (1952).

(23) J. C. Kendrew, *Proc. Roy. Soc. (London)*, **A201**, 62 (1950).

(24) C. H. Carlisle and H. Scouloudi, *ibid.*, **A207**, 496 (1951).

(25) M. F. Perutz, *ibid.*, **195**, 474 (1949).

(26) A. Elliott and B. A. Toms, *Nature*, **169**, (1952).

(27) J. T. Edsall, *Disc. Faraday Soc.*, **13**, 9 (1953).

(28) E. Katchalski, *Advances Protein Chem.*, **6**, 123 (1951).

(29) F. R. Senti, M. J. Copley and G. C. Nutting, THIS JOURNAL, **49**, 192 (1945).

(30) E. J. Ambrose, A. Elliott and R. B. Temple, *Nature*, **163**, 859 (1949).

has made recently.[11] Neurath, *et al.*, have made similar proposals[4] as have Johnson, Eyring and Polissar in their discussion of the sol–gel equilibrium for gelatin.[31]

There is little reason to expect perfect secondary conformations. Proline residues, acyl shifts to the free amino form, or a better tertiary structure formed at the expense of imperfect bonding in the secondary arrangement will introduce imperfections. Similarly the existence of sulfur–sulfur cross-links between peptides will prescribe the orders of tertiary and to a lesser extent secondary structure. Thus serum albumin has sixteen such bridges[4] which must play the most important role in determining the conformation of this protein. These also seem to allow a very flexible structure without denaturation since this protein swells markedly as the net negative charge is increased. The protein cannot be completely unfolded until primary bonds are broken.[32]

Holes, Hydration and Folding.—A further structural requirement lies in the absence of holes. Holes the size of half a water molecule can be formed in a molecule or crystal only at the expense of about 5 kcal. of energy if such holes do not provide an entropic advantage to the structure. Thus the α-helix, to exist, must be completely filled by its atoms or water molecules. Removal of water molecules from the helix can only result in its collapse. Hence favorable sites for water molecules may be expected as a consequence of any rigid secondary or tertiary structure. Proteins are highly hydrated, an average value being about two water molecules per amino acid residue.[33] Other sites for binding are provided by carboxylate and ammonium groups, many of which exist in free ionic form possibly being selectively concentrated at the protein "surface." Binding energies at these sites are probably large, perhaps greater than the 6 kcal. magnitude found by Benson, *et al.*,[34] for much of the bound water. However, even an extremely polar protein like serum albumin possesses under maximum conditions only about 200 ionized groups, and it is unlikely that the 1400 water molecules can be distributed about even this large number of ions. Other and weaker interactions may be expected at the residual hydrogen-bonding valences of the peptide amino groups both within and without any coiled secondary structures. Some of the water must be simple solvation water which fills unavoidable holes in the total structure and increases its flexibility. Obviously, while a major requirement exists that the holes be filled, different types of molecules will have differing efficiencies in the process depending on the material forming the walls of the holes. Thus while water is the usual solvent for proteins and water molecules form an integral part of the protein structure, organic molecules will be able to fill holes near hydrophobic R-groups more satisfactorily than water as will be demonstrated shortly.

It is precisely the lack of attraction between water and aliphatic or aromatic R-groups which appears to provide the tertiary structure of proteins since in the absence of large numbers of lipophilic solvent molecules, the best bonds such R-groups can make is with each other. Though cross linkages involving ionized groups and other polar groups are undoubtedly important in the tertiary structure, van der Waals interactions appear to be much involved. This fact is emphasized by the large surface activity of proteins at air–water interfaces[35] where the molecules become completely unfolded into disordered β-keratin sheets at little advantage to the polar side chains but at great advantage to the non-polar R-groups of which there are usually a great many. Denaturation by detergents can be interpreted in the same manner. Detergents solubilize proteins with extensive unfolding even at very low concentrations of the reagent. Presumably their effect is soap-like with van der Waals interactions between organic portions of detergent and lipophilic R-groups, though charge effects are also important.[36] Thus the detergent acts as a non-polar "medium" for such R-groups. The effectiveness of low concentrations testifies to the unsatisfactory state of the aliphatic and aromatic groups in native proteins.

Much of the bound water must have little freedom of motion since its density is greater than that of bulk water.[33] This situation plus the extensive secondary cross linking produces the over-all rigidity in tertiary structure which is necessary for enzymic function and, at least in part, for the antigenic properties of serum gamma globulin.[37] In addition, as Schellman[38] has proposed, the internal rigidity of globular proteins must result in a decreased effective dielectric constant both at the protein surface and within so that electrostatic interactions, frequently involved in enzyme reactions, may be exaggerated. Perhaps it is also this effect which makes ammonium and carboxylate groups strongly electrolytic in proteins with an apparent preference for hydration rather than salt formation. Jacobsen and Linderstrøm-Lang[39] have reviewed the case against salt bonds between pairs of such ionized groups and it appears unlikely that they are common. Hence these groups must exist as ions, and where they participate in cross linking, do so by ion–dipole interactions. In general these groups appear to be readily available to hydrogen or hydroxyl ions though the intricacies of interpreting titration experiments of polyelectrolytes do not allow exclusion of weak bonds involving these groups.[40] Bonds involving tyrosine phenolic groups and carboxyl groups have been suggested as being most important in determining ovalbumin tertiary folding by Crammer and Neuberger.[41] Tyrosine

(31) F. H. Johnson, H. Eyring and M. Polissar, "The Kinetic Basis of Molecular Biology," John Wiley and Sons, Inc., New York, N. Y., in press.

(32) E. Barbu and M. Joly, *Bull. soc. chim. Biol.*, **32**, 123 (1950).

(33) F. Haurowitz, "Chemistry and Biology of Proteins," Academic Press, Inc., New York, N. Y., 1950.

(34) S. W. Benson, D. A. Ellis and R. W. Zwanzig, *J. Am. Chem. Soc.*, **72**, 2102 (1950).

(35) H. Bull, *Advances Protein Chem.*, **3**, 95 (1947).

(36) F. W. Putnam, *ibid.*, **4**, 79 (1948).

(37) F. Haurowitz, *Biol. Revs.*, **27**, 247 (1952).

(38) J. Schellman, THIS JOURNAL, **57**, 472 (1953).

(39) C. F. Jacobsen and K. Linderstrøm-Lang, *Nature*, **164**, 411 (1949).

(40) C. Tanford and G. L. Roberts, Jr., *J. Am. Chem. Soc.*, **74**, 2509 (1952).

(41) J. L. Crammer and A. Neuberger, *Biochem. J.*, **37**, 302 (1943).

TABLE I

THERMODYNAMIC (ΔF) AND RATE PARAMETERS FOR FORWARD ($\Delta F^{\ddagger}_{1}$) AND BACKWARD ($\Delta F^{\ddagger}_{-1}$) REACTIONS IN REVERSIBLE TRANSCONFORMATION

	Soybean trypsin inhibitor,[43]	Chymotrypsinogen[14]		Luciferase[31,42] (*Cypridina*)	Pepsinogen[58]	Trypsin[59,61]
ΔF,[a] kcal.	1	−0.91	+0.16	+1.6	+1.3	0
ΔH,[a] kcal.	57.3	99.6	143	60.0	31	67.6
ΔS.[a] e.u.	180	316	432	196	93	213
$\Delta F^{\ddagger}_{1}$,[a] kcal.	25.4	20.4	21.5	(19.5)[b]		(25.7)[c]
$\Delta H^{\ddagger}_{1}$,[a] kcal.	55.3	84.6	80.2	57.0		(40.2)
$\Delta S^{\ddagger}_{1}$,[a] e.u.	95.5	202	178	(+118)		(45)
$\Delta F^{\ddagger}_{-1}$,[a] kcal.	24.4	21.4	21.6	(+21.1)		
$\Delta H^{\ddagger}_{-1}$,[a] kcal.	− 1.9	− 15.7	− 63.7	(3.0)		
$\Delta S^{\ddagger}_{-1}$,[a] e.u.	−85	−116	−258	(−76)		
*p*H	3.0	2.0	3.0	(6.8)	7	6.5
Temp., °C.	40	45.5	45.5	45	45	44(50–60)
Method	Solub.	Solub.	Solub.	Enzymic activity	Solub.	Solub.
Mol. wt.	25,000	36,000		...	~37,000	36,500

[a] Per mole of protein. [b] Rough estimates from Chase's data.[31] [c] Calculated from data of Pace,[60] of limited reliability.

groups are tied up internally but the data appear to allow ammonium-group involvement as well as carboxyl. An alkaline shift is frequently observed in transconformation reactions[4] and suggests that bound positive groups are liberated in the process. Generally speaking tyrosine, imidazole and similar groups appear to be much less available in the native protein than carboxylate and ammonium groups. We shall consider this matter further in the section on reaction segment.

The Energy States of Proteins

Available Conformations.—Excluding states involving hydrolysis of peptide bonds, the folded native conformation in its stable range of *p*H values appears to be the form of lowest free energy for the isolated protein molecule in water solution. The ease with which many proteins regain this native form following thermal transconformation, and the ease with which conformations change in native or reversibly unfolded states on varying *p*H allow no other interpretation.[31,42-44] Thus the conformation of a protein is determined by the type and sequence of amino acids in its peptide chains which fold in such a way as to minimize free energy. Considerable leeway in composition is possible. The small insulin molecule can exist as a stable protein with hormonal properties despite a slightly varying amino acid composition.[45] Proteins with similar functions but secured from different organisms frequently have large differences in composition. These observations perhaps suggest that most polypeptide chains greater than some minimum size and with proper proportion of polar to non-polar R-groups can fold in stable tertiary arrangement. Some further enzymic control may be available to the organism through its control of the sulfur–sulfur bonds.

The tertiary structure affords protection against enzymic attack of peptide bonds as has been well demonstrated by Linderstrøm-Lang and coworkers.[11] Hence a further requirement for most globular proteins is the possession of a stable tertiary structure. Incomplete proteins or experimental polypeptides unable to form such a structure will be rapidly hydrolyzed in the organism. The process of aggregation, common to many proteins such as hemoglobin, and insulin[46] is superimposed on tertiary folding.

We have mentioned the possibility that tertiary and secondary folding will partially stabilize globular proteins against hydrolysis, though probably not sufficiently to make the former state favored in a free-energy balance. Similarly the various conformations available to the protein as demonstrated in reversible transconformation reactions of Table I are not separated by large free energy differences nor indeed by large free energies of activation though the entropy and heat changes are very large. Thus there exists a remarkable balance between the latter thermodynamic quantities. This balance is probably preserved to a considerable degree in minor conformation changes so that the positive energy required to break a few secondary bonds in the tertiary structure is partially balanced by parallel positive entropy changes resulting from local relaxation. The net free energy will usually be small. Similarly charge isomers and hydration isomers will not differ much in free energy nor will occasional aggregations of molecules so that the protein has available a large number of easily accessible states in a small range of free energy. At any given solution condition, temperature and pressure there will usually be one most stable state represented by the largest number of molecules. However, many altered states may also be well represented, considerably more so, in fact, than in solutions of simpler molecules where different states are usually secured with a larger expenditure of free energy.

Multiple Reaction Paths.—Any large change in solvent composition, temperature or pressure will produce large alterations in the distribution of conformation isomers, most thoroughly demonstrated for the luciferase system.[31] For this reason proteins will not show the simple behavior of simple molecules under *p*H, ionic strength, dielectric constant or other alterations and their reactions can be ex-

(42) F. H. Johnson, H. Eyring, R. Steblay, H. Chaplin, C. Huber and G. Gherardi, *J. Gen. Physiol.*, **28**, 463 (1945).

(43) M. Kunitz, *ibid.*, **32**, 241 (1948).

(44) M. A. Eisenberg and G. W. Schwert, *ibid.*, **34**, 583 (1951).

(45) E. J. Harfenist and L. Craig, *J. Am. Chem. Soc.*, **74**, 4219 (1952).

(46) R. F. Steiner, *Arch. Biochem. Biophys.*, **39**, 333 (1952).

pected to give complicated kinetics. Thus any of these reactions whether they be transconformations, catalytic function or immunological reactions, start not from one major species but from many. Certain reaction paths of lower free energy will be available from certain conformations and will emphasize the participation of one or a few forms. The general reaction however is the sum of processes which begin at a number of closely related states and end at another group of closely related states. This situation must be taken into consideration by summing the rate of reactant loss $-dRi/dt$ over all reaction paths i and thus over all activated complexes of concentration $C_i^{\ddagger}$, a detail usually unnecessary for systems of simpler molecules

$$-\frac{dR}{dt} = -\sum_i \frac{dRi}{dt} = \frac{kT}{h}\sum_i K_i C_i^{*}$$

K_i = transmission coefficient for ith path
k = Boltzmann's constant
h = Planck's constant
T = absolute temperature

Arrhenius plots for protein transconformations and for enzymic reactions are frequently non-linear, as would be expected when several simultaneous processes evolve the same product,[47,48] either as the result of different activation energies or changing distribution of species with temperature. Four simultaneous processes have been proposed to account for the destruction of edestan[49] and other examples of this interpretation have been reported.[31] When subsequent reactions such as irreversible transconformation take place from the initially unfolded states, the kinetics and products of these reactions must depend on the speed of the initial reaction and whether the intermediate product is formed in equilibrium or as a steady-state intermediate.

Coöperative Transconformation Reactions

Types of Conformation Change.—Alterations in solvent or addition of small molecules can produce major as well as minor conformation changes. Thus the *p*H–activity relationship for enzymes may express the concentration of a reactive form which differs by simple change in ionization at the catalytic site[50] or by a major change in the structure of the molecules.[51] Similarly three molecules of ethanol per molecule of luciferase produces a cooperative transconformation.[42] Heat frequently is employed to produce such changes which can, within reasonable upper temperature limits, be reversed by the application of moderate pressures (a few hundred atmospheres). High pressures produce irreversible changes in structure as do high temperatures, extreme acid or base conditions, and certain small molecules.[4,31] The reversible processes are nevertheless very common and we suggest that they consist in the simple breaking and remaking of the tertiary structure. This hypothesis is somewhat more specific than that originally proposed by Wu[52] who emphasized only the rearrangement of peptide chains. At the present state of protein study it represents no great novelty.

Irreversible processes invariably produce β-keratin forms. On the basis of the evidence previously cited, we believe that an α-keratin structure usually exists in globular proteins and that this type of secondary structure is preserved in preliminary reversible transconformation to be rearranged in subsequent processes usually found to be irreversible. Thus we distinguish transconformation reactions of the tertiary and of the secondary structure, the latter usually appearing in irreversible processes. Let us designate these simply as tertiary and secondary transconformation reactions, respectively.

Coöperative Tertiary Transconformations.—In Table I are listed a selection of the better data available on reversible transconformation reactions which involve large entropy changes. These phase-like changes decrease solubility, increase viscosity and are frequently accompanied by large changes in molecule symmetry.[4] The state of hydration of higher-temperature species is an open question. No direct studies of either the structure or the hydration of these forms has been reported. The amount of hydration of irreversibly denatured proteins is also in question. Evidence is available to show that irreversibly destroyed proteins are either less[53] or about equally[54] as hydrated as native forms. Molecular weight studies of irreversibly denatured proteins which do not change their state of aggregation indicate only a small decrease. The changes in physical properties, molecular asymmetry and availability of R-groups and peptide bonds for enzymic attack cannot readily be explained by changes in hydration or in state of ionization. They are undoubtedly the result of a destruction of the tertiary structure, complete destruction in small proteins of the type listed in Table I, and perhaps only partial destruction for some larger proteins.[55] The characteristic decrease in solubility is thus attributed to the extrusion of hydrophobic R-groups into the water solvent and the increase in viscosity to an increase in molecular asymmetry and R-group availability for intermolecular attraction. There is little doubt that large changes occur in the symmetry of thermal transconformed proteins[5] though Barbu and Joly have presented evidence for the existence of aggregation reactions of globular proteins which also alter symmetry.[56]

Complications due to separation of component peptide chains not held together by disulfide primary links may appear in the tertiary transconformation of larger proteins but it is probable that the appropriate conditions can be found to produce reversibility for most, if not all, proteins. Neurath and co-workers have seriously questioned the existence of total reversibility in any transconformation reaction.[4] In view of the number of states accessible to the native protein and the ease with which

(47) R. Ege, *Z. physiol. Chem.*, **224**, 129 (1934).
(48) T. Winnick, A. R. Davis and D. M. Greenberg, *J. Gen. Physiol.*, **23**, 301 (1940).
(49) K. Bailey, *Biochem. J.*, **36**, 140 (1942).
(50) L. Michaelis and Davidsohn, *Biochem. Z.*, **36**, 280 (1911).
(51) M. Kunitz and J. Northrup, *J. Gen. Physiol.*, **17**, 59 (1934).
(52) H. Wu, *Chinese J. Physiol.*, **5**, 321 (1931).
(53) E. Heymann, *Biochem. J.*, **30**, 126 (1936).
(54) F. Haurowitz, *Kolloid-Z.*, **71**, 198 (1935).
(55) We are excluding simple disaggregation and association reactions of separately folded components unless these involve concomitant conformation changes.
(56) E. Barbu and M. Joly, *Disc. Faraday Soc.*, **13**, 77 (1953).

the distribution of these states is altered, complete reversal may be achieved only with great care. One might expect a rearrangement or breaking of disulfide bonds or that the conditions for regeneration may not favor the easy production of certain groups forming cross links in the original protein. Thus it may be necessary to introduce an acyl shift at acid *p*H before an important cross link can be formed. The proteins of Table I were carefully investigated for reversibility and passed all tests. Trypsin[57] maintained its enzymic activity though not completely and pepsinogen could be converted to pepsin.[58] The re-establishment of enzymic activity is a delicate test but subsequent investigations of specific primary bond reactions will probably demonstrate that a very narrow range of experimental conditions must be maintained to re-establish all the original properties.

Neurath, *et al.*,[4] have also suggested the need for "contractility" in the unfolded protein so as to cause it to refold.[59] As has been stated, this property is probably the unrestricted ability to assume the state of lowest free energy compatible with the normal environment of the native protein. Reversibly connected states thus far observed are very little different in free energy and since labile equilibria have been shown to exist between them, there will be some significant population of unfolded forms even at low temperatures. It is probable that proteolytic enzymes must find such forms or maintain contact with folded forms sufficiently long to take advantage of the spontaneous occurrence of the unfolded form. Linderstrøm-Lang[11] has, however, presented evidence that a preliminary enzymic attack may in some cases accelerate subsequent unfolding.

The existence of a reversible secondary transconformation is suggested by du Vigneaud's[14] success in regenerating acid-denatured insulin which has undergone the acyl rearrangement (see also ref. 71). If several serine or threonine residues undergo the rearrangement, the secondary structure may experience a large alteration. There is no information as to the normal coexistence of secondary and tertiary transconformation processes but the magnitudes of the entropies involved in the examples of Table I, though large, are smaller per residue than would be expected in processes in which both types of change occur.

It will be noted that the reversible transconformation reaction appears to be triggered by partial secondary bond destruction in which increasing enthalpy outruns increasing entropy with the activated complex lying between initial and final states. Most of the over-all heat change occurs in forming the activated complex with small proteins but a smaller percentage with the larger protein trypsin if the rate data taken from Pace[60] may be compared with the equilibrium measurements of Anson and Mirsky.[61] The free energy of activation is so small that the activated complex must resemble one of the stable states there being inadequate free energy to produce appreciable alteration in structure. We have called this the *Principle of Similitude*[62] and it has general application. It is especially pertinent for the various reactions of proteins which normally demonstrate remarkably small free energies of activation.

An unusual feature of protein transconformations is the existence of negative energies and heats of activation (see Table I). Eyring and Stearn[63] in particular, have emphasized this characteristic. Arrhenius was familiar with the large positive activation energies for the forward process but had he studied the reverse reaction, he might have been driven to the concept of the essential importance of free energy rather than heat in dynamic processes. The Arrhenius formulation for kinetic processes is generally applicable to the reactions of small molecules. A reaction to be observable must have an activation free energy of the order of 5 to 45 kcal. depending on the available methods for observation. These high values can be achieved in small molecules only by requiring that their energy be high with respect to that of the average population. In systems of very large molecules it is possible to observe either negative or very large positive energies of activation since entropies of activation may acquire large values of either sign thus balancing very small or very large activation energies. Thus the forward process of reversible coöperative transconformation is accelerated by the gain in entropy of the activated complex as bonds are broken; while the reverse process is measurable, despite its negative activation energy, because of the great loss in freedom as the secondary coils are grouped to resemble the native conformation. Similar behavior is to be expected in many large molecules such as nucleic acids and polysaccharides. It is also noteworthy that these reactions can be very fast despite large activation energies so that it is impossible to draw conclusions as to type of reaction from free energies of activation alone. On the other hand the all-or-none behavior of these cooperative transconformation reactions makes them readily distinguishable *in vivo* and indeed the luciferase system has been extensively studied in extracts of *Cypridina* and in live luminescent bacteria.[31] The sensitivity of these reactions to conditions of the medium may make their quantitative interpretation doubtful.[64]

Irreversible Transconformation Reaction.—The reversible processes just discussed are uniformly first order as are many irreversible reactions of proteins.[4] For many proteins the first-order behavior is the result of the over-all process being limited by a preliminary reversible step. The proteins of Table I proceed to irreversible products on continued maintenance of the reversibly unfolded forms at high temperatures. Their over-all irreversible process consists of at least two steps. This type of behavior, first noticed by Hardy,[65] has

(57) J. H. Northrup, *J. Gen. Physiol.*, **16**, 323 (1932).
(58) R. M. Herriott, *ibid.*, **21**, 501 (1938).
(59) A. S. Stearn, *Ergeb. Enzymforsch.*, **7**, 1 (1938).
(60) J. Pace, *Biochem. J.*, **24**, 606 (1930).
(61) M. L. Anson and A. E. Mirsky, *J. Gen. Physiol.*, **17**, 393 (1934).
(62) H. Eyring, R. Lumry and J. Spikes, "Symposium on Enzyme Reactions," McCollum-Pratt Institute, in press, 1953.
(63) H. Eyring and A. E. Stearn, *Chem. Revs.*, **24**, 253 (1939).
(64) J. R. Bronk, E. N. Harvey and F. H. Johnson, *J. Cell. Comp. Physiol.*, **40**, 347 (1952).
(65) W. B. Hardy, *J. Physiol.*, **24**, 158 (1899).

since been well substantiated in many examples of irreversible aggregation.[4] Measurements of some over-all change, such as the heat produced in the reaction, are thus likely to be a difficult method for studying the slow step in the over-all process.

At normal *p*H values in the absence of denaturing substances, aggregation is the usual fatal step in the over-all irreversible process. The proteins listed in Table I are destroyed by prolonged heating or heating at higher temperatures. The reaction is second order for chymotrypsinogen[44] and soybean trypsin inhibitor[43] to produce what is probably simple aggregation of the intact secondary structures of the native form. The ultimate product, at least in the case of chymotrypsinogen, is a polymolecular gel and not a dimer. The gel presumably is of a β-keratin or other type of secondary structure not present originally in the globular protein[66] thus suggesting the existence of a secondary transconformation reaction in the process as in other irreversible denaturations which yield the β-keratin structure. It will be remembered that an extended polypeptide chain is unstable, being able to make only inferior hydrogen bonds with water, and that it gains stability in the β-keratin sheet by hydrogen bonding to neighbors similarly oriented. The formation of such sheets must therefore involve the coöperation of several polypeptides and thus usually several molecules. Either the α- or β-keratin type of native secondary conformation may be expected to undergo rearrangement. The α- to β-process produced by stretching keratin is spontaneously reversible.[67] Thermally destroyed proteins give imperfect β-keratin diffraction patterns but are usually stable in this form.[29] The patterns are frequently of the "supercontracted" type which suggests regions of imperfect hydrogen bonding.[33] Several instances of partial restoration from extreme denaturation have been reported[68,69] though the completeness of reversal has been questioned.[4] The common irreversible aspect of the imperfect arrays and of perfect arrays obtained from them by stretching is unknown. The polymolecular structure may possess actual thermodynamic advantage over isolated native molecules at low temperatures as it does at high, but the possibility also exists that the return reaction is limited by too high an activation energy to allow significant back reaction at the stable temperatures of the native form.

Casey and Laidler[70] observed in the thermal destruction of insulin a fifth-order dependence on protein concentration at low concentrations going over to a first-order process with increasing concentration. They interpreted these observations to be the result of repulsion interactions between protein molecules which force the molecules into higher potential energy states. An alternate picture appears if we suppose the final product to consist of the usual β-keratin form, for then it may be assumed that five molecules are required to form the activated complex for the secondary transconformation process which will thus be rate-limiting at low concentrations. At higher concentrations the rate would then be limited by an ordinary reversible tertiary transconformation, the reversible product of which is apparently not stable with respect to the native form at available temperatures. This mechanism, if applicable, may be particularly simple. In other cases a number of complications can be introduced by the variety of imperfect β-structures available and by simultaneous tertiary and secondary transconformations, the latter in some instances triggered by acyl shifts. Thus carbonyl hemoglobin in acid denaturation develops 36 basic groups in an all or none reaction probably due to the 36 acyl rearrangements possible when the secondary structure of the peptide is broken open.[71] While this process appears to occur following tertiary transconformation, the tertiary structure of any protein is unlikely to be sufficiently strong to prevent extensive acyl rearrangement and will thus be automatically destroyed in a preliminary step.

Mechanism of Denaturing Agents.—Detergent effects have been briefly discussed. Detergents are the most effective denaturing substances known. Guanidine hydrochloride, urea and other substances making strong hydrogen bonds denature proteins but only at very high concentrations. Presumably they are able to break the hydrogen bonds between peptide links, thus destroying secondary structures.[72] Evidence is quite clear that completely unfolded and extended peptide chains as allowed by sulfur–sulfur bonds are ultimately produced. Thus the dissymmetry of ovalbumin is increased to 90:1, the dissymmetry of the extended chain.[73] Hydrogen bonds between urea molecules and peptide linkages appear to isolate individual unfolded polypeptides to prevent, at least under mild conditions of time and temperature, the polymolecular aggregation which frequently establishes irreversibility in thermal transconformation of secondary structures. Thus urea replaces other polypeptides so that as the urea is removed, the original secondary structure can reform.[4]

A necessary consequence of secondary unfolding is the initial destruction of any tertiary structure, The all or none characteristics of the latter reaction, which are apparent in thermal transconformation, disappear in urea and similar reagents probably because the reagent molecules in destroying polar and non-polar cross-links can form a successive series of stable intermediate compounds. Thus progressive increase in availability of cysteine and cystine groups of ovalbumin follows progressive increase of urea concentration.[74] It is not clear which conformation change is rate-limiting but it is reasonable to suspect that tertiary unfolding will be important only when the tertiary structure is tight. However, the careful studies of Kauzmann and co-workers on urea denaturation of ovalbumin and serum albumin may lead to the converse con-

(66) J. D. Ferry, *Advances Protein Chem.*, **4**, 1 (1948).
(67) A. C. Chibnall, *Proc. Roy. Soc.* (*London*), **B131**, 136 (1942).
(68) L. Michaelis and P. Rona, *Biochem. Z.*, **27**, 38 (1910).
(69) M. L. Anson and A. E. Mirsky, *J. Gen. Physiol.*, **13**, 121 (1929).
(70) E. J. Casey and K. J. Laidler, *Science*, **111**, 110 (1950).
(71) E. M. Zaiser and J. Steinhardt, *J. Am. Chem. Soc.*, **73**, 5568 (1951); **75**, 1599 (1953). We are indebted to Dr. E. L. Smith for pointing out the possible involvement of acyl rearrangements in this reaction.
(72) R. B. Simpson, M. T. Watson, B. Levedahl, J. Schellman, H. K. Frensdorff and W. Kauzmann, personal communication, 1951.
(73) A. Rothen, *Ann. N. Y. Acad. Sci.*, **43**, 229 (1942).
(74) J. P. Greenstein, *J. Biol. Chem.*, **125**, 501 (1938).

clusion.[72,75] In the initial period of denaturation both proteins underwent parallel changes in viscosity and optical rotation equivalent to opening the primary chain to the full extent allowed by disulfide linkages. Had secondary unfolding been slow, a period of increased viscosity but slight optical rotation change would be the expected result of initial tertiary transconformation. Major changes in optical rotation would be expected only in secondary transconformation for it is only in the latter that large changes in the local conformation about the individual amino-acids is to be expected according to our hypothesis and optical rotation is dependent only on local conformation. Furthermore the fact that urea denaturation is more rapid for serum albumin than the other proteins studied is compatible with the idea that this protein has a very weak tertiary structure just as would be anticipated for any protein which has to satisfy the structural limitations of many disulfide bonds.[72]

In addition to the complications to be expected as a result of the reactant existing in several quite different conformation states of similar population, the further complication of irreversible urea denaturation does occur especially on long standing or exposure to elevated temperatures.[4,72] Thus diphtheria antitoxin,[76] serum albumin[77] and some other proteins[31] simultaneously participate in a reversible (at least in several sensitive properties) and an irreversible reaction. Presumably irreversibility is again due to aggregation of chains or to rearrangement of sulfur–sulfur bonds.

Other Conformation States.—Just as many crystals demonstrate several phase changes, so it may be expected that several quite different conformations may exist for some protein molecules, transitions from one to the other being phase-like. β-Lactoglobulin,[31] for instance, undergoes such a change on cooling. Lipase, trypsin and pepsin at temperatures near 0° appear to undergo phase transconformations as indicated by sharp breaks in the Arrhenius plots of enzymic rate constants.[78] Such breaks are possible only with large entropy changes.[79] The situation is similar to conformation change under *p*H variation, as previously discussed. On the other hand, proteins like pepsin according to the present interpretation of the work of Casey and Laidler do not manifest any stable unfolded states in the available temperature range. It is only possible to infer the transient existence of such states from the occurrence of irreversible reactions from these states. The common occurrence of rapid irreversible processes coupled with the high freezing point of water allow only a very narrow range of experimental conditions in which to find new states in solution and very few have been reported. Crystalline hemoglobin demonstrates a series of coöperative changes in the solid state, but these are produced by changing the water content[80] of the crystal and may involve no change in tertiary structure.

Reaction Segments

Composition of the Reaction Segment.—In rough analogy with the term "diffusion segment" employed in polymer literature we will define the reaction segment of a protein as those parts of the protein which participate in forming the activated complex for a given reaction. There will be reaction segments for transconformation, catalytic function, immunological activity and the like. The term has utility in that present day studies of the above reactions are largely concerned with determining the composition and size of the reaction segment.

In general the size of the reaction segment must be determined by heats, volumes and entropies of activation. For transconformation reactions the data of Table I demonstrate large entropies and heats of activation and there is abundant evidence that positive volume changes occur in these reactions.[31] All such changes would be expected to accompany the loosening of tertiary structure to form the activated complex. A little information about the reaction segments involved is available from studies of reversible transconformation but most has been obtained from irreversible reactions on the assumption that the limiting process is the same in the two cases. Such comparisons may be uncertain as in the case of pepsin to be discussed. Rate studies of some property changed in the first step of the reaction, like the spectral change of hemoglobin and the loss of enzymic activity in luciferase systems, give less ambiguous information than studies of solubility or other means for detecting the final product.

Ionized Groups in the Reaction Segment.—The general importance of ionization or proton-association processes in transconformation reactions has been disputed since 1938. Most ionized groups are undoubtedly present in simple hydrated state[81] though some may have the dipolar end of some R-group insinuated into their hydration sphere so as to make a cross link. Thus the tertiary structure of ovalbumin appears to depend on such bonds between tyrosine and either carboxyl or amino groups.[41] Ionization of tyrosine groups immediately destroys the native conformation so that the reaction segment for ovalbumin at high *p*H values includes some fraction of the tyrosine bonds. Increased temperature favors dissociation of protons from carboxyl and ammonium groups and would be expected to break bonds involving these groups. Rates of transconformation reactions are frequently sensitive to *p*H and since the usual *p*H values are very large with respect to the conventional standard state of zero *p*H, appreciable fractions of the apparent entropy change may be due to the entropy of

(75) J. Schellman, personal communication. ADDED IN PROOF. The details of these studies are now available in R. B. Simpson and W. Kauzmann, *J. Am. Chem. Soc.* **75**, 5139 (1953); J. Schellman, R. B. Simpson and W. Kauzmann, *ibid.*, **75**, 5152 (1953); W. Kauzmann and R. B. Simpson, *ibid.*, **75**, 5154 (1953); H. K. Frensdorff, M. T. Watson and W. Kauzmann, *ibid.*, **75**, 5157, 5167 (1953). Minor revisions have been made in the text at this point as necessitated by the published version of the experiments.

(76) G. G. Wright and V. Schomaker, *J. Am. Chem. Soc.*, **70**, 356 (1948).

(77) H. Neurath, G. R. Cooper and J. O. Erickson, *J. Biol. Chem.*, **142**, 249 (1942).

(78) I. W. Sizer and E. S. Josephson, *Food Research*, **7**, 201 (1942).

(79) G. B. Kistiakowsky and R. Lumry, *J. Am. Chem. Soc.*, **71**, 2006 (1949); J. L. Kavanau, *J. Gen. Physiol.*, **34**, 193 (1950).

(80) H. E. Huxley and J. C. Kendrew, *Acta Cryst.*, **6**, 76 (1953).

(81) H. H. Weber and D. Naehmansohn, *Biochem. Z.*, **204**, 215 (1929); H. H. Weber, *ibid.*, **218**, 1 (1930).

dilution of hydrogen ions.[41] It is unfortunate that pepsin was the first example for consideration of the role of ionization, since changes in ionization are unusually important in the irreversible denaturation of this protein. Steinhardt[82] and LaMer[83] offered a proposal that in the alkaline region for pepsin 45 kcal. of an activation energy of 63.5 kcal. was due to dissociation of five protons[41] (possibly from imidazole nitrogens). The parallel entropy calculation reduced the entropy of activation from 135.9 to 8.8 e.u. per mole. There can be little doubt that the reaction segment for irreversible denaturation of pepsin in the region studied largely consists of five groups able to lose protons but Eyring and Stearn[41] showed that a large entropy change must occur in the protein as it achieves the activated state. Thus cross links are broken on dissociation and the general picture of a triggered unfolding reaction is preserved. More recently Johnson, Eyring and Polissar[31] have shown that the five protons are probably lost one from each of five protein molecules forming the fivefold association complex leading to irreversible transconformation. If their interpretation is correct, the reaction studied in pepsin systems was not the usual reversible tertiary transconformation. At lower *p*H values the denaturation of pepsin is quite different not only in hydrogen-ion dependence and reversibility but probably in the states of both reactants and products.[58]

Variations in solution properties and composition generally alter the distribution and make up of reaction segments. Other processes in which positive heat change may more advantageously outrun positive entropy change become possible. There is furthermore no general rule relating ionization processes and reaction segments. Soybean trypsin inhibiter shows no marked *p*H effect either on the rate or equilibrium in its reversible transconformation over a range from about *p*H 3 to 10 except that in the region near the isoelectric point irreversible aggregation is accelerated by the neutral state of the protein.[43] Chymotrypsinogen actually gains rather than loses three protons in its reversible conformation change.[44] The average pK for the processes is 2.5 indicating either carboxyl formation or acyl shift. We have recalculated the data of Eisenberg and Schwert[44] to the usual standard state of unit hydrogen ion activity. ΔS and $\Delta S_1{}^{\ddagger}$ are found to increase by 27 e.u. per mole of protein at *p*H 2 and by 42 e.u. at *p*H 3. If carboxyl groups are formed, an additional heat increment of 4.5 kcal. must be added to the heat of activation to secure the true value of the positive heat required to break bonds in forming the activated state. Thus only minor participation of proton association processes in the reaction segment is indicated.

We find, using the same data, that bimolecular irreversible aggregation of chymotrypsinogen from the reversibly achieved state is accelerated by the removal of one proton with a pK of about 4.8, typical of a gamma glutamyl carboxyl group.[44] Thermodynamic data are not available to determine whether this dissociation is part of a triggering process of coöperative transconformation or simply a preliminary to simple association.

Weak *p*H dependences of a secondary nature not associated with actual change in degree of ionization may be greatly magnified by the fact that the free energy requirement for activated complexes enters exponentially in reaction velocities. Thus hemoglobin (Table II) varied over the *p*H range 5.7 to 8 shows very little change in reaction segment for transconformation as witnessed by the constancy of $\Delta H^{\ddagger}_1$ and $\Delta S^{\ddagger}_1$. Ionizing groups do not appear in the reaction segment. The minor change in $\Delta F^{\ddagger}_1$ is magnified in rate measurements leading to some theoretical if not practical overemphasis on *p*H effects. It seems probable that the small variation in $\Delta F^{\ddagger}_1$ is due merely to increased internal electrostatic repulsion as the *p*H is varied about the value for maximum stability.

TABLE II

KINETICS OF HEMOGLOBIN THERMAL DENATURATION CONVERTED TO 60°[a]

Solvent	*p*H	$\Delta H^{\ddagger}_1$, kcal./mole	$\Delta S^{\ddagger}_1$, e.u./mole	$\Delta F^{\ddagger}_1$, kcal./mole
Water	5.7	75.6	152.7	24.8
	6.8	76.3	152.0	25.5
	8.0	77.3	157.3	24.9
0.001 M $(NH_4)_2SO_4$	6.76	76.5	152.5	25.7
1.14 M $(NH_4)_2SO_4$	6.76	87.0	184.6	25.5
2.27 M $(NH_4)_2SO_4$	6.76	103.8	230.9	26.9
3.03 M $(NH_4)_2SO_4$	6.76	119.8	275.8	28.1
20% Ethanol	6.0	107.4	263.9	19.6
	6.5	102.6	248.8	19.7
	7.0	98.2	236.1	19.6
30% Ethanol	6.0	117.0	308.9	14.1
	6.5	120.1	319.5	13.8

[a] Values calculated from original data by Stearn and Eyring.[41]

At the *p*H of maximum stability for hemoglobin, 6.76, interesting changes in reaction segment occur with salt or ethanol addition.[84] $\Delta H^{\ddagger}_1$ and $\Delta S^{\ddagger}_1$ are progressively increased without any indication of change in the particular reaction segments involved (Table II). These values may indicate more extensive bond breaking in forming the activated complex or greater internal integration of the protein molecules. The latter explanation is the more attractive since both ions and polar organic solvents might be expected preferentially to replace water molecules to produce a more compact and better bound native conformation. The alcohol effect is very large amounting to a decrease in entropy for the folded protein of 171 e.u. in 30% alcohol. The free energy of activation is reduced in alcohol solution probably because the activated complex has improved stability in the strongly organic solution. The progressive increase in size of reaction segment with added substances supports the present hypothesis that the observed coöperative conformation changes involve the tertiary structure. It is unlikely that the added substances can alter secondary conformations in an important way.

The free energy values of Table II have been

(82) J. Steinhardt, *Kgl. Danske Videnskab. Selskab. Math-Fys. Medd.*, **14**, No. 11 (1937).

(83) V. K. LaMer *Science*, **86**, 614 (1937).

(84) P. S. Lewis, *Biochem. J.*, **20**, 984 (1926).

adjusted to the same temperature to emphasize the extraordinary balance which exists between entropy and heat changes relative to free energy changes. It is this property of proteins which appears to be their most novel feature and to provide the most promising source of mechanism for protein reactions. A coöperative secondary transconformation is now indicated as the source of muscle function.[85] Changes in the permeability of neural membranes which are involved in nerve function may similarly consist in coöperative transconformations produced by changes in electrical potential gradient across the membrane.[86]

The range of protein molecular weights for comparable proteins which have been carefully studied in denaturation is not large (Table I and Table II). Nevertheless, the size of the reaction segment for tertiary transconformation does not seem to increase with molecular weight on the basis of the present assumption that tertiary transconformation is the slow step in most irreversible processes. This conclusion suggests either that only partial changes in tertiary structure occur or that a preliminary destruction of the cross links between limited sections of secondary tubes is necessary to trigger the remainder of the process. Some comparative data are available for a series of hydrolytic enzymes (Table III) which show a remarkable similarity in both activation parameters and *p*H region of maximum stability. The preliminary conclusion must be drawn that these proteins in the solvents employed are very similar in their reaction segments despite the differences in molecular weight. Thus we may infer that tertiary transconformation reactions are zipper-like. Preliminary unfolding, perhaps of a terminal loop of secondary structure triggers the remainder of the tertiary unfolding.

TABLE III

THERMAL INACTIVATION OF ENZYMES[a]

Protein	Solvent	*p*H	*T*, °C.	$\Delta H^{\ddagger}_{1}$, kcal./mole	$\Delta S^{\ddagger}_{1}$, e.u./mole	$\Delta F^{\ddagger}_{1}$, kcal./mole
Pancreatic lipase	50% Glycerol	6.0	40–50	45.4	68.2	24.0
Trypsin	24% Glycerol	6.51	50–60	40.2	44.7	25.7
Enterokinase	Water	6.50	50–60	42.2	52.8	25.1
Trypsinkinase	24% Glycerol	6.5	50–60	44.3	57.6	26.2
Pancreatic proteinase	Water	6.9	50–60	37.9	40.6	24.7

[a] Taken from Neurath, *et al.*[4]

The Mechanism of Enzymic Catalysis

Small molecules such as phenobarbital, amytal or even ethanol appear to be able to stabilize new conformation changes in some proteins. Even a single molecule is able to produce conformation changes by which the native conformation is altered by 100 entropy units or more. The new state is intermediate in degree of folding between native and reversible transconformed states. As usual the free energy changes in producing the new states are very small. This ability of small molecules to relax major regions of proteins suggests a mechanism for the binding of organic dye molecules and some uncharged organic molecules to proteins. The serum albumins are the only efficient proteins for multiple binding thus far found.[87] The driving force in their reactions is largely entropic there being small heat changes.[88,89] Schellman, Lumry and Samuels have proposed the possibility that the small molecules can bridge or break cross links in the tertiary structure of serum albumin. Klotz and co-workers[90] have found ammonium and tyrosine groups of the protein to be involved in the binding at most of the sites and Karush[91] has suggested that serum albumin possesses "configurational adaptability" which allows it to assume conformations more suitable for binding small molecules. If the two protein groups form a cross link, a small molecule with sufficient separation of two polar or one polar and one hydrocarbon end could break such a link forming new bonds with the groups to produce a long bridge between secondary tubes. The hydrocarbon or one polar end would be attached to the tyrosine group and the other polar end to the ammonium group. A small heat change might be expected with a large increase in entropy resulting from relaxation of the tertiary structure. Such changes would explain Karush's configuration adaptability as a consequence rather than a preliminary of binding. Increasing *p*H increases binding as it should since net negative charge and hence net internal repulsion increases with *p*H to provide a greater entropy increase when a cross link is extended. The unique ability of serum albumin to bind a wide variety of such small molecules we may attribute with Kauzmann and co-workers[72] to the looseness of tertiary structure in this protein in turn apparently related to its large number of disulfide bonds. Presumably the cross links are more available than in other proteins.

A somewhat similar situation may be involved in enzymic catalysis if substrates can act as narcotic substances to produce large changes in conformation. The well-known ability of substrates to protect their enzymes against thermal denaturation[92] speaks in favor of a mechanism in which the reaction segment for transconformation and that for enzymic function contain some of the same groups if not all. A further indication that there may be a connection between reversible transconformation and enzymic function may be provided by the work of Massey and Weber recently discussed by Edsall.[27] These investigators observed a large change in the depolarization of fluorescence of dye molecules attached to the enzyme fumarase when the substrate was added. Depolarization is a measure of the rate of rotation of the protein in solution so that these experiments suggest a large change in factors affecting rotation and thus perhaps a large change in protein conformation. Laidler[93–95] has inter-

(85) M. Morales and J. Botts, *Disc. Faraday Soc.*, **13**, 125 (1953).

(86) H. Eyring, R. Lumry and W. Woodbury, *Record Chem. Progress, Summer*, 100 (1949).

(87) I. M. Klotz and J. M. Urquhart, *J. Am. Chem. Soc.*, **71**, 1597 (1949).

(88) I. M. Klotz and J. M. Urquhart, *ibid.*, **71**, 847 (1949).

(89) J. Schellman, R. Lumry and L. T. Samuels, *ibid.*, in process.

(90) I. M. Klotz and J. Ayers, *ibid.*, **74**, 6178 (1952).

(91) F. Karush, *ibid.*, **72**, 2705 (1950).

(92) J. B. S. Haldane, "Enzymes," Longmans Green and Co., London, 1930.

(93) K. J. Laidler, *Arch. Biochem.*, **30**, 226 (1951).

(94) E. J. Casey and K. J. Laidler, *J. Am. Chem. Soc.*, **72**, 2159 (1950).

(95) K. J. Laidler, paper presented at the Symposium on Biochemical Kinetics at the Diamond Jubilee Meeting of the American Chemical Society, New York, September, 1951.

preted existing pressure and temperature studies on a number of enzymes in terms of the two slow steps of the Michaelis–Menten–Briggs–Haldane reaction mechanism which applies to most enzymic reactions.[95]

$$\text{enzyme} + \text{substrate} \xrightarrow{k_1} \text{intermediate compound}$$
$$\text{intermediate compound} \xrightarrow{k_0} \text{enzyme} + \text{product}$$

Typical volume and entropy changes in the first process (k_1) are 10 to 20 cc. and 0 to 10 e.u. The sign is opposite to that expected in bimolecular reactions. For the second step (k_0) the volume and entropy changes in forming the activated complex are all negative; 0 to 30 cc. for $\Delta V^{\ddagger}_0$ and 10 to 30 e.u. for $\Delta S^{\ddagger}_0$ being typical. Negative values are not usually observed in unimolecular reactions. Laidler has proposed that all these changes indicate rearrangements in the protein and we agree that this is undoubtedly the case. However, the values are not sufficiently large to be in accord with major conformation changes as occur in coöperative transconformation (Table I). Such changes, if they are involved in enzymic mechanisms, must take place in some reaction steps not usually rate-limiting.

Eyring, Lumry and Spikes[62] have explored certain general aspects of the analogy between crystallite and native protein as a source of catalytic mechanism. Contact catalysis is generally believed to take place at surface atoms of the cracked grain which have been left with unsaturated valences. Similar sites may be available in proteins as a result of the stretching or bending of primary bonds produced in improving a number of the secondary bonds. Such a situation might, for instance, be expected when polypeptide tubes are forced back on themselves or when a single cross link plays a major role in tertiary folding. On the other hand it is possible that the reaction segment for catalysis involves nearby tubes of secondary structure between which the bound substrate molecule may be stretched. Such an activated complex has been called a "rack." The atoms of a stretched bond partially resemble free radicals in their reactivity allowing ready attack by cosubstrate molecules. The substrate would have to be held to the protein at both ends of the susceptible bond, a situation found necessary in some hydrolytic enzymes and proposed as general by Smith.[96] A very similar picture to that given here has been proposed by Smith[96] in his theory for the mechanism of enzymes requiring metal–ion coenzymes but with a very important additional feature. Smith assumes that polydentate chelation to the metal ion held by the protein causes strain in the susceptible bond but at the same time the metal–protein combination acts as a generalized base to facilitate electron rearrangement in the substrate. Further strain appears to be required in reactions of this last class of enzymes since another substrate–protein bond is indicated. Nevertheless the ability of linkage points at the catalytic site to act as generalized acids and bases may be very important.[95]

Oxidative enzymes such as peroxidase and catalase appear to act by facilitating electron changes in the substrate which makes but a single bond to the enzyme.[97] Thus H_2O_2, a substrate of peroxidase, is held at the iron atom of its heme prosthetic group. This arrangement does not allow stretching the substrate. However, the sensitivity of globin structure and denaturation properties to the chemical state of the heme iron of hemoglobin[4] suggests that conformation changes influence the electronic properties of the prosthetic group in a reciprocal fashion. For instance, changes in conformation may distort the normally planar heme group out of the plane, or the coördination bond between the metal atom of the heme and the protein may itself be held on a rack as the result of conformation change in the protein. Such changes could be expected to alter the oxidation–reduction potential of the iron atom in peroxidase as well as in hemoglobin. The coupling which exists among the heme groups of hemoglobin could be explained in this way. Pauling and St. George[98] and Wyman[99] have suggested involvement of changes in conformation in the coupling of hemes. It seems further possible that conformation changes provide a principle mechanism for enhancement of catalysis by enzymes functioning through prosthetic groups.

The first author is very grateful for the discussions afforded him by Drs. Emil Smith and John Schellman.

(96) E. L. Smith, *Proc. Nat. Acad. Sci. U. S.*, **35**, 80 (1949).
(97) P. George, *Advances Catalysis*, **4**, 367 (1952).
(98) L. Pauling and R. C. C. St. George, Jr., *Science*, **114**, 629 (1951).
(99) J. Wyman and D. W. Allen, *J. Polymer Sci.*, **7**, 499 (1951).

THE STABILITY OF COMPLEX IONS WITH SPECIAL REFERENCE TO HYDRATION

By R. J. P. Williams

Merton College, Oxford, England

Received December 18, 1952

The principal factors controlling the stability of complex ions in aqueous solution are discussed. These factors are the charges and sizes of the reacting species and their electronegativities but they cannot be directly related to complex stability without consideration of the heats and entropies of hydration of the reactants and products. Mention is also made of the less important influence of orbital contributions.

The stability of a complex ion in solution is measured by the equilibrium constant, K, for the reaction

$$M(H_2O)_a + L(H_2O)_b \rightleftharpoons ML(H_2O)_c + (a + b - c)H_2O \quad (1)$$

where M is any metal ion and L is any ligand. (Charges are omitted for convenience.) Many authors have attempted to correlate such experimentally found equilibrium constants with properties of the metal ion involved. In particular it has been pointed out that there is an empirical relationship between the ionic potential of the cation, z/r, (where r is the radius of the cation and z its charge) and log K for a limited number of simple complexes of the alkaline earth metals[1]; and that there is also a relationship between the ionization potential, I_{02},[2] of the cation and log K for a large number of complexes of the divalent cations of the first transition series of the elements in the periodic table.[3] Other more extensive correlations have been suggested also but they are of limited applicability.[7,8] In order to further clarify the factors affecting the values of K a search of the literature has been made for the corresponding heats and entropies of complex formation. The values found are listed in Table I.

The Entropy Changes upon Complex Formation

The equilibrium constant for the formation of a complex, K, can be expressed in the form

$$-2.303\,RT \log K = \Delta F^0 = \Delta H^0 - T\Delta S^0 \quad (1)$$

where ΔF^0, ΔH^0 and ΔS^0 are the standard molar free energy, heat, entropy of formation of the

(1) R. J. P. Williams, *J. Chem. Soc.*, 3770 (1952).

(2) The ionization potential for the stage $M \rightarrow M^{++} + 2e$, I_{02}, will be used in this paper as a rough measure of the electronegativity of a cation.[3] Other authors have used the ionization potential for the stage $M \rightarrow M^{-} + e$, I_0,[4] and that for the stage $M^{+} \rightarrow M^{++} + e$, I_{12},[5] as measures of the electron affinity of a divalent ion. It is possible to defend the choice of I_{12} on the ground that the charge on the central ion never falls below unity. The choice of I_{01} would appear to be indefensible. I_{02} represents the total electron affinity of the divalent ion and is therefore the maximum interaction with a ligand by electron exchange—in keeping with Pauling's theory of the essential neutrality of the central ion in complexes.[6] The fact that the heat of hydration increases much more slowly than the ionization potential, I_{02}, for a series of cations would suggest however that the Pauling theory is incorrect. The use of either I_{02} or I_{12} would appear to be equally admissible at the present time.

(3) H. Irving and R. J. P. Williams, *Nature*, **172**, 746 (1948); *Analyst*, **77**, 813 (1952); *J. Chem. Soc.* 3192 (1953).

(4) W. S. Fyfe, *ibid.*, 2018, 2023 (1952).

(5) M. Calvin and N. C. Melchior, *J. Am. Chem. Soc.*, **70**, 3270 (1948).

(6) L. Pauling, "Victor Henri Memorial Volume," Liege, 1948, p. 1.

(7) T. O. Denny and C. B. Monk, *Trans. Faraday Soc.*, **47**, 992 (1951); C. B. Monk, *ibid.*, **47**, 297 (1951).

(8) D. P. Mellor and L. Maley, *Nature*, **161**, 436 (1948).

Table I[a]

Molar Heats and Entropies of the Formation of Complex Ions in Aqueous Solution

	Reaction	$\Delta F°$, kcal.	$\Delta H°$, kcal.	$\Delta S°$, cal./°C.	Ref.
Cu^{I}	$2Cl^-$	−11.3			9
Cu^{I}	CN^-		−26.3		9
Ag^{I}	Cl^-	− 4.5	− 2.7	+ 6.0	10
Ag^{I}	$3I^-$		−29.2		9
Ag^{I}	$2S_2O_3^{--}$	−11.5	−19.3	−26.0	9
Ag^{I}	$2CN^-$	−40.5	−33.0	+25.1	9
Au^{I}	$2CN^-$	−60.5	−55.4	+17.0	9
Mg^{II}	SO_4^{--}	− 3.6	+ 5.7	+31.0	11
Mg^{II}	$CH_2(CO_2)_2^{--}$	− 4.0	+ 3.2	+24.0	11
Ba^{II}	$S_2O_3^{--}$	− 3.1	+ 2.6	+19.0	11
Zn^{II}	$CH_2(CO_2)_2^{--}$	− 5.0	+ 3.1	+27.0	11
Zn^{II}	$4CN^-$	−23.8	−26.0	− 7.3	9
Cd^{II}	$2CN^-$	−14.3	−24.6	+30.0	9
Hg^{II}	$2Cl^-$	−18.2	−13.4	+16.0	9
Hg^{II}	$3Cl^-$	−19.4	−15.3	+13.7	9
Hg^{II}	$2Br^-$	−23.9	−20.9	+10.0	9
Hg^{II}	$4Br^-$	−29.0	−25.9	+10.3	9
Hg^{II}	$4I^-$	−38.9	−43.0	−13.7	9
Hg^{II}	$2CN^-$		−46.9		9
Hg^{II}	$4CN^-$	−40.5	−59.6	−15.3	9
La^{III}	SO_4^{--}	− 5.3	+ 2.5	+26.0	11
Cr^{III}	OH^-	−14.0	− 1.0	+43.3	9
Cr^{III}	$2OH^-$		+ 4.5		9
Cr^{III}	Cl^-	− 2.0	+ 5.0	+23.3	9
Cr^{III}	$2Cl^-$	− 2.6	+10.0	+40.2	9
Cr^{III}	$2Br^-$		+11.6		9
U^{IV}	OH^-	−17.2	− 2.1	+50.5	9
Fe^{III}	O_2H^-	−12.5	+ 1.8	+49.0	12
Fe^{III}	OH^-	−16.0	− 1.2	+50.0	12
Fe^{III}	F^-	− 6.9	+ 7.5	+49.0	12
Fe^{III}	Cl^-	− 2.0	+ 8.5	+35.0	12
Fe^{III}	Br^-	− 0.8	+ 6.1	+23.0	12
Fe^{III}	N_3^-	− 5.7	− 4.3	+ 5.0	12
Fe^{III}	$C_2O_4^{--}$	−13.2	− 0.3	+43.0	12
Ni^{II}	$4CN^-$		−42.0		9
Sn^{II}	OH^-	−17.0	−10.0	+23.0	13
Sn^{II}	Cl^-	− 1.6	+ 2.6	+14.0	13
Sn^{II}	Br^-	− 1.0	+ 1.4	+ 8.0	13
Cd^{II}	Cl^-	− 1.9	+ 0.6	+ 8.0	14
Mg^{II}	$2NH_3$	− 0.3	− 1.2	− 3.0	9
Zn^{II}	$4NH_3$	−12.0	−14.0	− 6.7	15
Cu^{II}	$4NH_3$	−16.6	−19.7	−10.0	15
Ni^{II}	$6NH_3$	−11.3	−19.0	−25.7	15
Co^{II}	$6NH_3$	− 7.9	−13.0	−17.0	15
Cd^{II}	$4NH_3$	− 9.1	−13.0	−13.0	16
Hg^{II}	$4NH_3$	−26.2	−28.5	− 7.7	16
Cu^{I}	$2NH_3$	−15.2	−16.0	− 2.7	16
Ag^{I}	$2NH_3$	−10.0	−13.3	−11.0	16
Co^{III}	$5NH_3$	−42.4	−49.4	−23.3	9

TABLE I (*Continued*)

Reaction	$\Delta F°$, kcal.	$\Delta H°$ kcal.	$\Delta S°$ cal./°C.	Ref.
Co^{III} $4NH_3$ $2Cl^-$ (*cis*)		−33.3		9
Co^{III} 2En $2Cl^-$ (*cis*)		−40.6		9
Cu^{II} En	−14.2	−18.9	−15.0	17
Cu^{II} 2En	−27.1	−26.1	+ 3.3	18
Ni^{II} En	− 9.9	−12.6	−12.0	17
Co^{II} En	− 6.3	− 8.4	− 7.0	17
Zn^{II} En	− 7.7	− 9.8	− 7.0	17
Cu^{II} Trien	−28.7	−22.0	+22.0	19
Ni^{II} Trien	−19.9	−13.0	+23.0	19
Co^{II} Trien	−15.6	− 9.0	+22.0	19
Fe^{II} Trien	−11.5	− 9.0	+ 8.0	19
Mn^{II} Trien	− 7.5	− 4.0	+12.0	19
Fe^{II} Dipy	− 7.5	− 7.5	0.0	20
Fe^{II} 3Dipy	−24.5	−24.5	0.0	20
Ag^{I} Pyridine	− 2.8	− 4.7	− 6.3	21
Ag^{I} α-Picoline	− 3.1	− 4.2	− 3.7	21
Ag^{I} γ-Picoline	− 3.1	− 4.2	− 3.7	21
Ag^{I} Butylamine	− 4.7	− 6.2	− 5.3	21
Ag^{I} Ethylamine	− 4.7	− 6.2	− 5.3	21
Ag^{I} Tolylamine	− 4.5	− 6.2	− 5.8	21
H^{I} $CH_3CO_2^-$	− 6.5	− 0.1	+22.1	22
H^{I} OH^-	−19.0	−13.4	+19.2	22
H^{I} SO_4^{--}	− 2.6	+ 5.2	+26.3	22
H^{I} $C_2O_4^{--}$	− 5.8	+ 1.7	+25.0	22
H^{I} NH_3	−12.6	−12.1	+ 1.0	23
H^{I} CH_3NH_2	−14.5	−13.1	+ 4.5	23
H^{I} Pyridine	− 7.2	− 4.7	+ 8.4	21

[a] The symbol "En" in the table refers to a molecule of ethylenediamine while the symbol "Trien" refers to the molecule $NH_2CH_2CH_2NH{\cdot}CH_2CH_2NH{\cdot}CH_2CH_2NH_2$. It should be noted that whereas the data for the formation of complexes with anions are often available for the first stage of complex formation only, the data for the complexes with neutral molecules more frequently refer to the reaction between a metal ion and several molecules or combining groups. The entropy and the heat changes in the latter reactions are therefore disproportionately large. The heats and entropies of formation of undissociated acid molecules are included so as to show the similarity between the formation of hydrogen ion complexes and complexes of other cations. All the free energies and heats are given in kilocalories.

complex from its components in aqueous solution at 25°. The values of ΔS^0 given in Table I will be discussed first. The table consists of two groups of reactions. In the first group the reactions are between cations and anions with a resulting reduction in the total number of ions in solution and a concomitant neutralization of charge. In the second group the complex is formed from a cation and a neutral molecule and there is no net reduction of the sum of the positive and negative charges in the solution. In all but four of the thirty-one examples in the first group ΔS^0 favors complex formation. In all but six of the twenty-eight reactions in the second group the entropy change does not favor the formation of the complex. Five of the unusual examples in the latter group are taken from one reference and it would appear to be advisable to check these data. A reasonable explanation of the difference between the entropy changes in the two groups of reactions suggests itself.

Frank and Evans[24] have suggested that ions in aqueous solution order the water molecules around them so as to form an "iceberg," the process being similar to a partial freezing of the liquid. On this picture the removal of ions from solution, as in the process of complex formation between oppositely charged ions, will lead to the break-down of the "icebergs" and a resulting entropy change favoring complex formation. Qualitatively the data in Table I agree with this picture. A quantitative approach can also be made as Evans and Uri[12] have shown. If the entropy change upon the formation of a complex is due to the loss of hydration of the components of the complex, then for a series of anion complexes with one cation the entropy change of complex formation should be proportional to the entropy of hydration of anions. Table II lists some of the molar entropies of hydration of gas ions as given by Latimer and Powell.[25] A simple comparison between the entropies of hydration of the anions fluoride, hydroxyl, chloride, bromide and oxalate and the entropies of formation of the ferric, chromic and stannous complexes of these anions which have been measured, will show that the two quantities are roughly proportional. A similar comparison should be possible for the formation of complexes of different cations with the same anion and in this case the entropy of formation of the complex should be proportional to the entropy of hydration of the cation. Although there are some exceptions to this generalization the following comparisons do confirm this suggestion for the most part. For the hydroxides the entropy change on complex formation follows the order, U^{IV} (50.5), Fe^{III} (50.0), Cr^{III} (43.3), Sn^{II} (23.0); for the chlorides the order is Fe^{III} (35.0), Cr^{III} (23.3), Sn^{II} (14.0), Cd^{II} (8.0), Ag^{I} (6.0); for the formation of the chlorides of formula MCl_2, Cr^{III} (40.2), Hg^{II} (16.0); for the monobromides, Fe^{III} (23.0), Sn^{II} (8.0); for the formation of cyanides of formula $M(CN)_2$, Cd^{II} (30.0), Ag^{I} (25.1), Au^{I} (17.0); and for the tetracyanide complexes Zn^{II} (−7.3) and Hg^{II} (−15.3). The order of the molar entropies of hydration of the cations is $U^{IV} > Cr^{III} > Fe^{III} > Zn^{II} > Cd^{II} > Sn^{II} > Hg^{II} > Ag^{I} > Au^{I}$.[5] In their paper Latimer and

(9) "Selected Values of Chemical Thermodynamic Properties," National Bureau of Standards, Circular 500, Washington, 1952.

(10) J. N. Jonte and D. S. Martin, *J. Am. Chem. Soc.*, **74**, 2052 (1952).

(11) I. J. Evans and C. B. Monk, *Trans. Faraday Soc.*, **48**, 934 (1952).

(12) M. G. Evans and N. Uri, S.E.B. Symposium, No. 5, Cambridge, 1951.

(13) C. E. Vanderzee, *J. Am. Chem. Soc.*, **74**, 3552, 4806 (1952).

(14) E. L. King, *ibid.*, **71**, 319 (1949).

(15) J. Bjerrum, "Metal Ammine Formation in Aqueous Solution," P. Haase and Sons, Copenhagen, 1941.

(16) W. S. Fyfe, *J. Chem. Soc.*, 2318, 2323 (1952).

(17) H. Irving and R. J. P. Williams (unpub.); R. J. P. Williams, D.Phil. Thesis, Oxford, 1950.

(18) J. Bjerrum and E. J. Nielsen, *Acta Chem. Scand.*, **2**, 297 (1948).

(19) H. B. Jonassen, G. G. Hurst, R. B. LeBlanc and A. W. Meibohm, THIS JOURNAL, **56**, 16 (1952).

(20) J. H. Baxendale and P. George, *Trans. Faraday Soc.*, **46**, 736 (1950).

(21) G. A. Carlson, J. P. McReynolds and F. H. Verhoek, *J. Am. Chem. Soc.*, **67**, 1334 (1945).

(22) W. M. Latimer, *Chem. Revs.*, **18**, 349 (1936).

(23) D. H. Everett and W. F. K. Wynne-Jones, *Proc. Roy. Soc. (London)*, **177A**, 506 (1941).

(24) H. S. Frank and M. W. Evans, *J. Chem. Phys.*, **13**, 507 (1945).

(25) W. M. Latimer and R. T. Powell, *ibid.*, **19**, 1139 (1951).

TABLE II

Metal ion	Radius, Å.	Ion. pot., I_{02}, kcal.	Entropy of hydration,[25] cal./°C.	Heat of hydration,[a] kcal.	$\Delta H'$ calcd. from equation 4, kcal.
Mg^{II}	0.66	523	−28.2	464	471
Ca^{II}	0.99	414	−13.2	382	382
Sr^{II}	1.15	385	− 9.4	350	350
Ba^{II}	1.37	350	3.0	316	316
Mn^{II}	0.78	532	−20.0	445	460
Fe^{II}	.76	555	−27.1	468	467
Co^{II}	.74	583		496	483
Ni^{II}	.73	596		507	490
Cu^{II}	(.72)	646	−23.6	507	507
Zn^{II}	.72	631	−25.5	491	491
Ti^{II}	.85	471		426	434
V^{II}	.82	483		453	441
Cr^{II}	.80	541		460	468
Cd^{II}	.96	597	−14.6	436	444
Hg^{II}	1.10	673	− 5.4	441	444
Sn^{II}	1.10	506	− 5.9	373	389
Pb^{II}	1.27	517	5.1	359	369
Pd^{II}	(0.96)	651		505	488
Fe^{III}			−70.1		
Cr^{III}			−73.5		
U^{IV}			−78.0		
OH^-			− 2.5		
F^-			− 2.3		
Cl^-			13.2		
Br^-			19.2		
Ox^{--}			12.2		

[a] L. L. Quill, "Chemistry and Metallurgy of Misc. Materials," Nat. Nuclear Energy Series, IV-19V, McGraw-Hill Book Co., Inc., New York, N. Y., 1950.

Powell also showed that the entropy of hydration of all ions was given by

$$S^0 = \frac{3}{2} R \ln M + 37 - 270 \frac{z}{r_e^2}$$

where M is the atomic weight of the ion, z its charge and r_e its effective radius. It will be interesting to see if experimental evidence will show that the above examples of the orders of the entropies of complex formation can be generalized to a relationship between this entropy and the entropy of hydration of the ions. The limited data so far available do indicate that the entropy of complex formation in reactions in which there is a neutralization of charge is directly proportional to the charge on the reacting ions and inversely proportional to their radii.

The Heat Changes upon Complex Formation

The heat changes in a displacement reaction such as (1) must depend both upon the nature of the final complex and upon the nature of the hydration of the ions and molecules involved in the reaction. Relevant heats of hydration of the gas ions are included in Table II. Figure 1 is a plot of these heats against z/r for a number of divalent cations and it shows clearly that there is no simple relationship between the heat of hydration and electrostatic interaction with the possible exception of the group IIA cations. An alternative plot of these heats against the ionization potential of the divalent cations, I_{02}, (see footnote 2) which can be used as an approximate measure of the electron

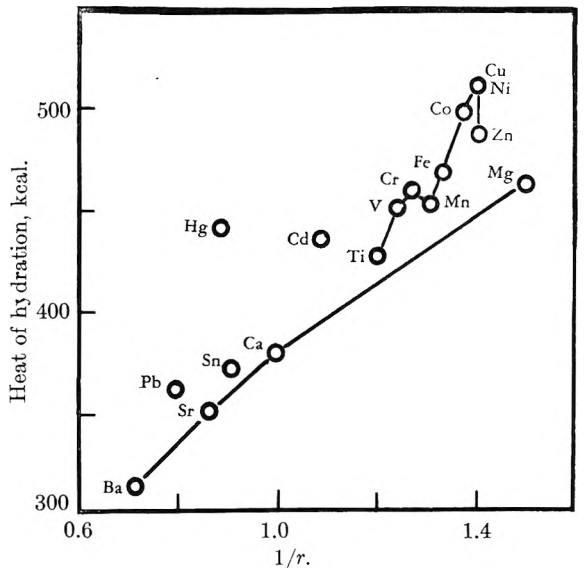

FIG. 1.—Heats of hydration of divalent ions plotted against the inverse of their ionic radii, $1/r$.

affinity of these ions, shows that the donation of electrons to the central metal ion from the water molecules is not the only factor controlling the heat of hydration. Clearly however heats of hydration must be linked to a combination of electrostatic and covalent interactions, together with additional stabilization due to the different available bonding orbitals of the cations. As no treatment of this problem has been forthcoming as yet it would appear to be reasonable to approach the problem on an empirical basis. A formula of the kind

$$\Delta H' = A(z/r) + B'I_{02} - C'(1/r^3) \qquad (2)$$

where $\Delta H'$ is the heat of hydration and A, B and C are constants can be made to give all the heats of hydration of the divalent cations by putting $A' = 150$, $B' = 0.3$, $C' = 40$, with a maximum error of $\pm 5\%$, Table II. This equation can only have descriptive value as A, B and C will not be real constants, but it does contain terms which represent electrostatic, covalent and repulsion forces. The use of equation 2 is that it can be treated so that it sufficiently represents the controlling factors in complex formation for it to be used to illustrate the nature of the heat terms involved on the exchange of a water molecule for another ligand. Let the heat of formation of a complex ML (in aqueous solution) from a gas cation and a hydrated ligand (in aqueous solution) be represented by equation 3.

$$\Delta H'' = A''(z/r) + B''I_{02} - C''(1/r^3) \qquad (3)$$

The heat of formation of the complex in aqueous solution is now given by $\Delta H = \Delta H'' - \Delta H'$.

$$\Delta H = (A'' - A')(z/r) + (B'' - B')I_{02} - C'' - C')(1/r^3) \qquad (4)$$

Equation 4 would suggest that for divalent ions of very similar radius the heat of formation of a complex would be dependent on I_{02}. If the entropy of formation of these complexes is small or constant then the dependence on I_{02} should appear in the stabilities of the complexes of such cations. Both

Irving and Williams[3] and Calvin and Melchior[26] have observed such a relationship and it has been confirmed since by many other authors.[27,28] The correlation is particularly striking in the series of divalent ions Mn < Fe < Co < Ni < Cu > Zn, the ions being listed in increasing order of their ionization potentials, and in the order of the stability of their complexes. The changes in stability along the series is most marked for the formation of complexes with neutral ligands where the entropy changes are not so important, see for example the data in Table I for the ammines and ethylenediammines. However, the same order of stabilities is found for the formation of oxalate and acetate complexes suggesting that even in these cases the heat terms control the stability order although in the one case where the heat of such a reaction has been measured it has been shown that the heat of formation is opposed to the reaction, see zinc malonate in Table I.

Equation 4 would also suggest that when steric factors are unimportant and the ionization potentials of the cations small the heat of formation of a complex would depend upon z/r. Such a correlation between complex stability and z/r has been found among A sub-group cations in the case of the hydroxides[1,29] and with a number of simple organic anions.[1] Without further experimental data however no conclusion can be drawn from this evidence as it has already been indicated, in previous paragraphs, that a very similar relationship could arise from the entropy changes in these reactions,[1] as well as from the heats of complex formation.

There remains to be discussed the effect upon the stability of complexes of a simultaneous change in both the radius and the ionization potential of the cation. When water is replaced by ammonia, a larger molecule, around a cation there must be an increase in the repulsion between the ligands and also a decrease in the electrostatic interaction as ammonia has a lower dipole moment than water. These two terms must be more opposed to the formation of a complex the smaller the cation. Ammonia however is a better electron donor than water so that the BI_{02} term in equation 4 would favor complex formation. Now therefore for ions of the same charge and very similar ionization potentials the stability of their ammines should be directly proportional to their size. A similar argument should apply to the formation of halides and cyanides as these ions are considerably larger than the water molecule but in this case as the entropy of formation of the complex may well be acting so as to stabilize the complexes of the smaller ions to the greatest extent the heats of formation and not the free energies, must be compared. The following examples illustrate the way in which the loss of electrostatic interaction and the increase in repulsion forces are balanced against the increase in covalency in different complexes.

Ammines.—The ammine of plumbous (r = 1.27, I_{02} = 517) is more stable than that of magnesium (r = 0.66, I_{02} = 523). The ammine of mercuric, $Hg(NH_3)_2$, for which log K = 17.5 is much more stable than that of cupric, $Cu(NH_3)_2$, for which log K = 7.65. Mercuric has a slightly larger ionization potential but a considerably larger radius. Cadmium can form a hexammine but the stability of the hexammine of zinc is very small.[30] The entropy change upon complex formation, where known, is not large in these cases, see Table I.

Chlorides, Bromides and Iodides.—In Table I the heats of formation of these halides are much greater for mercuric than for any other ion. Cadmium forms more stable halide complexes than zinc yet its ionization potential is smaller. The ionization potentials of stannous (r = 1.10, I_{02} = 506) and plumbous are less than that of magnesium; the former ions form stable halide complexes and are the larger ions. The ions in the first transition series form very weak halide complexes; the halide complexes of the larger ions of the next two transition series are stable. The ionization potentials in the three series are not very different but the ions are of very different size.

Cyanides.—Plumbous forms a stable cyanide, magnesium does not. The most stable cyanide is that of mercuric, a large ion of large ionization potential.

It is interesting to observe, Table I, that for those cations which react strongly exothermically with halides the order of the stability of the halides is $I^- > Br^- > Cl^-$, for example, Ag^I and Hg^{II}, while for those ions where the differences in stability along the series of halides are small the reaction would seem to be generally slightly endothermic, *e.g.*, Cd^{II} and Sn^{II}, and finally, for those ions which react with halides with a larger heat uptake the order of stability reverses to $Cl^- > Br^- > I^-$, *e.g.*, Cr^{III} and Fe^{III} due to entropy changes. The orders of these heat changes and their relation to the different orders of halide complex stabilities is paralleled by the orders of the heat changes of formation of anhydrous halides from aqueous solutions of the corresponding ions, Table III.

The data given in Table I have been compiled from two sets of measurements: (1) studies of the formation of complexes over a range of temperature, and (2) from the heat of formation of the aqueous solution of the complex as compared with the heats of solution of the component ions and molecules in their standard states. There is however another source of qualitative data. The heats of solution of many salts have been measured at different dilutions. Whereas in the very dilute solutions of the salts complete dissociation of the salts occurs, in more concentrated solutions many salts can be shown to be more than 90% associated.[31] The difference of the heat of solution under the latter circumstances and the theoretical heat of solution of the component ions at infinite dilution will always give a rough guide to the value of the heat of formation of the complex and where detailed information is available about the state of the ion in solution over a range of concentrations it

(26) M. Calvin and N. C. Melchior, *J. Am. Chem. Soc.*, **70**, 3270 (1948).
(27) H. Freiser, *Analyst*, **77**, 830 (1952).
(28) G. Schwarzenbach and J. E. Prue, *Nature*, **163**, 723 (1949).
(29) C. W. Davies, *J. Chem. Soc.*, 1257 (1951).
(30) J. Bjerrum, *Chem. Revs.*, **46**, 381 (1950).
(31) T. F. Young and A. C. Jones, *Ann. Rev. Phys. Chem.*, **3**, 281 (1952).

TABLE III[a]

THE HEATS OF SOLUTION OF SOME ANHYDROUS SALTS, KILOCALORIES

Anion	Divalent cation								
	Mg	Ba	Mn	Ni	Zn	Cd	Hg	Pb	Sn
Chloride	−37.1	−3.2	−17.5	−19.9	−17.1	− 4.4	+ 3.2	+ 6.2	−1.6
					(− 0.5)	(− 1.0)		(+13.0)	(−2.0)
Bromide	−44.5	−6.0	−16.1	−18.9	−16.1	− 0.7	+12.4	+ 8.8	+1.6
					(− 0.2)	(+ 0.1)		(+20.0)	(−2.0)
Iodide	−51.5	−9.4	−13.2	−21.5	−13.2	+ 4.0	+30.0	+15.5	+5.8
					(− 1.6)	(+ 2.8)			(−0.2)
Sulfate	−21.8	+5.4	−15.0	−19.2	−19.5	−12.2			
	(− 1.0)			(− 1.8)	(− 1.0)	(− 1.5)			

[a] The values in parentheses are differences between the heat of solution in 0.1 *M* solution and an infinitely dilute solution. Values are given where complex formation is known to account for more than 80% of the total salt. A positive value represents a heat favoring complex formation. A negative heat of solution represents a heat opposed to the formation of the anhydrous salt. All data are from reference 9.

may well be possible to determine this heat quite accurately. For example, both conductivity measurements and spectrophotometric studies have shown that cupric sulfate is at least 80% associated at a concentration of 0.1 *M*.[31] The difference between the heat of solution at this concentration and that at infinite dilution is some 1.8 kcal.—opposed to the formation of the complex. Approximately the same value can be obtained[9] for a large number of 2.2 sulfates such as Mg^{II}, Zn^{II}, Mn^{II}, Ca^{II}, Ni^{II} and Co^{II}. The study of the stability constants of these sulfates by conductometric means has shown that all these cations form sulfate complexes with a stability constant of about 10^2. Moreover a positive heat of complex formation of some 2 kcal. compares favorably with the determination of the heat of formation of the magnesium sulfate complex as found by conductivity methods.[11] This kind of examination can be extended to halide complexes but in these cases the heats of solution can only be used to indicate the direction of the heat changes upon complex formation as it is not easy to assess the degree of formation of these complexes readily. Even so the numerical values that can be compared between Table I and III are not widely discrepant.

Chelation Free Energy.—Recently Schwarzenbach has discussed the stability of chelate complexes and has concluded that the important contribution of chelate stability arises from an entropy change.[32] There are many reasons for rejecting this argument in favor of one that places greater stress on the favorable heat of chelate formation which is thought to arise from the reduction of repulsion forces between neighboring ligands in a chelate as compared with these forces in a complex formed with monodentate ligands.[3,17] Three points in favor of the latter theory can be made. (1) The heat of formation of cupric and cobaltic complexes with ethylenediamine are considerably greater than those with ammonia, Table I. In collaboration with Dr. Irving the author has confirmed this in the cases of the zinc and cobaltous complexes.[33] (2) The explanation of the stability of chelates put forward by Schwarzenbach suggests that the free energy of chelation is independent of the central cation. In fact this is not the case as will be shown in a forthcoming paper.[3] (3) The entropy of stabilization of the oxalate complex of ferric is in no way anomalous. Using the data of Evans and Uri, see Fig. 1 of their paper,[12] (a plot of the entropy of formation of a number of ferric complexes against the entropy of hydration of the anion involved in the complex) the expected value of the entropy change for the formation of ferric oxalate is 40 cal./°C. The value found was 43 cal./°C. The greater stability of the oxalate complex as compared with the halides arises from a larger heat of formation.

Other Factors Affecting the Stability of Complexes. (1). The Detailed Nature of Hydration.—Recently Orgel[34] has suggested an explanation of the heats of hydration of some transition metal ions which are larger than would be expected on either a simple electrostatic picture of hydration or even from the values of the ionization potentials of the ions concerned. The heat of hydration of the nickel ion is as large as that of cupric for instance and although equation 4 fits the heats of hydration of all divalent ions quite well it is noticeable that the deviation from it rises steadily through the series Mn^{II}, Fe^{II}, Co^{II}, Ni^{II}, and then falls to Cu^{II} and further to Zn^{II}, see Table II. This deviation would appear to follow the amount of stabilization which might be expected from the influence of "3d" orbitals.[34] It should be noticed that this idea is a modification of the Pauling theory of the introduction of 3d orbital stabilization in complexes. In the latter the orbital stabilization could not arise without a change of magnetism, the stability gain is of the "all or nothing" kind. In the former however orbital stabilization occurs continuously, the change in paramagnetism representing only a change in ease of availability of this additional stabilization on increasing the electrostatic field strength. The latter is more nearly in accord with observations on the stability of complexes of the transition metal ions. For example if the stability of a nickel complex is dependent upon an octahedral disposition of ligands, as Orgel would suggest, its tetrahedral complexes must be somewhat more unstable than would be expected. This has been observed in the following cases.

The differences between the stability constants for the formation of the bis-ethylenediammine complexes, $M(En)_2$, and the complexes of trien, $N(CH_2CH_2NH_2)_3$, M(Tren): and between the constants for the formation of the bis-glycine complexes $M(Glyc)_2$ and the complexes of triac

(32) G. Schwarzenbach, *Helv. Chim. Acta*, **35**, 2844 (1952).

(33) H. Irving and R. J. P. Williams, unpublished observation.

(34) L. E. Orgel, *J. Chem. Soc.*, 4756 (1952).

$N(CH_2COOH)_3$, M(Triac), show that not only is the stabilization of the cupric complex, relatable to the use of planar dsp^2 orbitals, but also that of nickel is affected adversely by being forced into a tetrahedral complex, Table IV.[28]

TABLE IV[24]

DIFFERENCES OF STABILITY, $\log_{10} K$ UNITS, ON THE EXCHANGE OF LIGANDS

	Mn	Fe	Co	Ni	Cu	Zn
Tren for 2En	+1.0	+1.3	+2.1	+1.0	−0.8	+4.2
Triac for 2Glyc	+0.8	+0.8	+1.7	+0.2	−2.7	+0.7

As was observed in the heats of hydration these data reflect additional stabilization of the nickel complexes, when octahedral, over those of either cobalt or ferrous.[34]

In the above complexes the stability order $Ni^{II} > Co^{II}$ holds although the differences between the stabilities of the complexes with triac are small. In the unsubstituted oxine complexes the increment in stability on passing from cobalt to nickel is already small, approximately 1.5 logarithmic units, and therefore it might have been anticipated that substitution in the oxine molecule such as to increase its interference volume around the central cation would lead to a repulsion of the residual water molecules attached to the cation and thus invert the order of the stabilities of the two cation complexes. Aluminum 2-methyl oxinate is not precipitated from aqueous solution, nor does 2-methyloxine form 3:1 complexes readily with either gallium or ferric[17] which suggests that the interference volume occupied by the ligand is preventing the easy formation of octahedral complexes. Now although the zinc complex of 2-methyloxine forms as readily as the oxinate, presumably both complexes are tetrahedral, the cupric complex is considerably less stable than the oxinate and the nickel complex is so reduced in stability that it is no longer more stable than the cobaltous complex.[27] This would suggest that when the increments in stability between the cobaltous and nickel complexes are small then substitution in the ligand close to the coördinating groups would invert the order of stability $Ni^{II} > Co^{II}$. In general however the differences in stability of the complexes along the series $Mn^{II} < Fe^{II} < Co^{II} < Ni^{II} < Cu^{II}$ must be sufficiently great to mask the effect of the hydration energies.

Orbital Changes.—A discussion of the effect of orbital changes upon the stability of complexes has been presented elsewhere.[3] There it was pointed out that although one case was known in which the stabilization of a complex, ferrous tris-phenanthroline, amounted to some 10 kcal., stability measurements had shown little other evidence of large changes of free energy of complex formation which could be certainly ascribed to orbital changes. In the case of the ferrous complexes as in that of the nickel complexes, there would appear to be good grounds for thinking that the 3d orbital stabilization is partially available before a rearrangement of the atomic electrons takes place. The stability of the ferrous complexes is more dependent on the nature of the ligand, and particularly on its aromatic character, than is the stability of either the zinc or cadmium complexes.[3] Another indication of the gradual introduction of orbital stabilization through a group of complexes is obtained from the recent work of Brandt and Gullstrom on the substituted *o*-phenanthroline complexes of ferrous and ferric iron. Their measurements show that as the stability of the ferrous complex falls its stability relative to the ferric complex rises, so that the stabilization due to 3d orbital interaction falls off continuously but at different rates for the two valency states. There is no sudden change in the spectrum of the ferric complex but the position of the absorption maximum moves to shorter wave lengths as the stability of the complex diminishes.[35] It should be of great interest to see if this effect can be produced in a series of nickel complexes of substituted dioximes.

ADDED IN PROOF.—In two recent papers [W. M. Latimer and W. L. Jolly, *J. Am. Chem. Soc.*, **75**, 1548 (1953); J. W. Cobble, *J. Chem. Phys.* **21**, 1446, 1451 (1953)] the same method as that employed in this paper has been used independently to calculate certain entropies of hydration of complex ions. In the paper of Latimer and Jolly and in this paper the calculations have been restricted to reactions of the type

$$ML_n(H_2O)_a + L(H_2O)_b \longrightarrow ML_{n+1}(H_2O)_c + (a+b-c)H_2O$$

where n is five and the number of water molecules displaced from the coördination sphere is one. In such cases the entropy of hydration of the complex ion is found from the equation

$$\Delta S_{\text{reaction}} = S^\circ_L - S^\circ_{H_2O} + S^\circ_{ML_nH_2O} - S^\circ_{ML_{n+1}}$$

Cobble has extended the method to complex ions where n is any number and the number of water molecules displaced is assumed equal to the number of ligands added. This extension is likely to be of limited application as the last assumption is very uncertain. In many other particulars the discussion of entropy of complex formation in aqueous solution made by Cobble is similar to the one given above.

(35) W. W. Brandt and D. K. Gullstrom, *J. Am. Chem. Soc.*, **74**, 3532 (1952).

HEATS OF COMBUSTION OF THE FIVE-CARBON FATTY ACIDS AND THEIR METHYL AND ETHYL ESTERS[1]

BY C. KINNEY HANCOCK, GEORGE M. WATSON AND RALPH F. GILBY

Contribution from the Department of Chemistry of The A. and M. College of Texas, College Station, Texas

Received March 17, 1953

The heats of combustion, heats of formation and resonance energies of the isomeric five-carbon fatty acids and of their methyl and ethyl esters have been determined. Based on previously reported isomerization energies of six-carbon alkanes, resonance energies of the acids and esters have been corrected for the chain-branching effect to obtain values which do not differ significantly among a group of isomers.

Originally, it was hoped that resonance energies of isomeric acids, calculated from heats of combustion, might be correlated with the relative strengths of the acids. A literature search failed to disclose combustion data on a representative group of isomers. For these reasons, it was decided to determine the heats of combustion of the isomeric five-carbon fatty acids, this being the simplest group of isomers which exhibit all degrees of α-branching. Also, in order to check further the effect of chain-branching, the heats of combustion of the methyl and ethyl esters of these acids were determined.

Experimental

The apparatus included a Parr Series 1300 plain jacket type calorimeter, a Parr No. 1102 self-sealing oxygen bomb, and a Beckmann differential thermometer with 0.01° subdivisions which could be estimated to ±0.001° by using a reading lens. Following the procedure outlined in the manual[2] obtained with the calorimeter, the sample was weighed into a small metal crucible which was supported in a holder attached to the bomb head. A measured length of iron fuse wire was attached to the holder so as to hang just above the sample. One ml. of water was delivered from a transfer pipet into the bomb (capacity, 360 ml.). The bomb was then assembled and filled with oxygen to a pressure of 25 atmospheres. Two kilograms of water, weighed on a large analytical balance, was always used in the calorimeter bucket.

Runs were made when the room temperature was about 25°. The water in the calorimeter bucket was cooled to about 24°. Under these conditions, the calorimeter reached steady state in about five minutes. The rate of temperature rise during the next five minutes was noted (about 0.003° per minute). The sample was ignited and the temperature was noted at intervals (in seconds) of: 60, 15, 15, 15, 15, 60, 60, etc., until the maximum temperature was reached; then, the temperature was noted at one-minute intervals for an additional five minutes. The inflection point of the curve of temperature rise *versus* time occurred during the second minute after ignition. The maximum temperature rise usually occurred about seven minutes after ignition and amounted to about 2.5°. Correction for heat leakage was made by the method of Dickinson.[3] Also, corrections were made for the heat evolved in the formation of nitric acid and for the heat given off by the combustion of the iron wire.

The energy equivalent of the calorimeter was determined by the combustion of benzoic acid Standard Sample No. 39g from the U. S. National Bureau of Standards (heat of combustion of 26.4338 abs. kj. per g. mass, weighed *in vacuo*) and found, from seven runs, to be 2457 cal. deg.$^{-1}$ with a standard deviation of 3 cal. deg.$^{-1}$ Using this value, the heat of combustion at constant volume at 25° of carefully purified propionic acid was found to be 4923 cal./g. which compares favorably with the value of 4927 cal./g. (corrected to 25°) given by Schjånberg,[4] and the heat of combustion at constant pressure at 25° of carefully purified salicylic acid was found to be 5236 cal./g. which compares satisfactorily with the average of six values at 20°, 5236 cal./g., given by Timmermans.[5]

The calorie used in this study is defined as 4.1840 absolute joules. The precision obtainable with this apparatus is 0.1–0.2%.

The heats of combustion, $-\Delta U_B$, of the isomeric five-carbon fatty acids and of their methyl and ethyl esters, determined in the same way as in the determination of the energy equivalent of the calorimeter, are shown in Table II.

Materials.—The acids used in this study were prepared by the following classical methods: valeric acid from butyl bromide by the nitrile synthesis, isovaleric and α-methyl butyric acids from isobutyl and sec-butyl bromides by the Grignard synthesis, pivalic acid by the bromoform degradation of pinacolone obtained from acetone through pinacol hydrate. Esters of these acids were prepared by the following well-known methods: the methyl and ethyl esters of α-methylbutyric and of pivalic acids by treating the acid chloride (prepared with $SOCl_2$) with the appropriate alcohol; methyl valerate, methyl isovalerate and ethyl isovalerate, by acid-catalyzed esterification with the corresponding alcohol; ethyl valerate, by the acid-catalyzed reaction between valeronitrile and ethyl alcohol. The esters were fractionated under a 25:1 reflux ratio in a 90 cm. × 12 mm. Todd[6] column packed with 1/8-in. glass helices. Portions of the fractionated esters were used directly for the determination of heats of combustion. Other portions of the fractionated esters were converted to acids in the usual manner. The resulting acids were dried by azeotropic distillation with benzene and then used in the determination of heats of combustion. Physical constants of the acids and esters are shown in Table I.

Calculations.—Buoyancy corrections were made on all weights. Referring data to a standard temperature of 25°, the Washburn[7] correction was applied to obtain $-\Delta U_R$, the heat of combustion at constant volume. Assuming the perfect gas law to apply, $-\Delta H_c$, the heat of combustion at constant pressure, was calculated. The standard heat of formation at 25° and one atmosphere, $-\Delta H_f°$, was calculated from $-\Delta H_c$ and the heat of combustion of graphite, 94.052 kcal./g. atom,[8] and of hydrogen, 68.317 kcal./mole.[9]

Results and Discussion

Values of $-\Delta U_R$, $-\Delta H_c$, and $-\Delta H_f°$ are given in Table II. In order to calculate the resonance energies of the compounds by Wheland's method,[10] it was first necessary to correct the $-\Delta H_c$ values to the monomeric vapor state at 25° and one atmosphere.

All of the compounds used are liquids at 25°, ex-

(1) Abstracted from the M.S. thesis of Ralph F. Gilby, The A. & M. College of Texas, 1952.

(2) "Oxygen Bomb Calorimetry and Oxygen Bomb Combustion Methods," Parr Manual No. 120, Parr Instrument Co., Moline, Ill., 1948.

(3) H. C. Dickinson, *Natl. Bur. Standards (U.S.), Bull.* **11**, 189 (1915).

(4) E. Schjånberg, *Z. physik. Chem.*, **A172**, 197 (1935).

(5) J. Timmermans, "Physico-Chemical Constants of Pure Organic Compounds," Elsevier Publishing Co., Inc., New York, N. Y., 1950, p. 482.

(6) F. Todd, *Ind. Eng. Chem., Anal. Ed.*, **17**, 175 (1945).

(7) E. W. Washburn, *Bur. Standards J. Research*, **10**, 525 (1933).

(8) E. J. Prosen, R. S. Jessup and F. D. Rossini, *J. Research Natl. Bur. Standards*, **33**, 447 (1944).

(9) D. D. Wagman, *et al.*, *ibid.*, **34**, 143 (1945).

(10) G. W. Wheland, "The Theory of Resonance," John Wiley and Sons, Inc., New York, N. Y., 1944, pp. 62–75.

TABLE I

PHYSICAL CONSTANTS OF ACIDS AND ESTERS

Compound	B.p., °C.[a,b]	$n^{25}D$[b]
Valeric acid	186.7	1.4069
α-Methylbutyric acid	176.5	1.4040
Isovaleric acid	176.7	1.4022
Pivalic acid	164.4	solid
Methyl valerate	127.9	1.3953
Methyl α-methylbutyrate	115.9	1.3922
Methyl isovalerate	117.4	1.3910
Methyl pivalate	101.9	1.3876
Ethyl valerate	144.4	1.3986
Ethyl α-methylbutyrate	132.9	1.3949
Ethyl isovalerate	135.4	1.3944
Ethyl pivalate	118.4	1.3887

[a] Boiling points corrected to 760 mm. [b] The values of boiling point and of refractive index are in good accord with the values reported in E. H. Huntress and S. P. Mulliken, "Identification of Pure Organic Compounds, Order I," John Wiley and Sons, Inc., New York, N. Y., 1941; F. K. Beilstein, "Handbuch der Organischen Chemie," 4th ed., J. Springer, Berlin, 1929.

cept pivalic acid. The heat of fusion of this acid was not found, but it was noted that the heats of fusion of several normal acids were in the range of 30–40 cal./g. It was evident that the use of a value of this magnitude would yield anomalous results for the acids when compared with the relations noted among the esters. It was found that, although the heat of fusion of hexane is 3.114 kcal./mole, the heat of fusion of 2,2-dimethylbutane is only 0.1385 kcal./mole.[11] The latter value was used to calculate a heat of combustion for pivalic acid in the liquid state which compared favorably with the value to be expected from a study of the pivalate esters.

Of the four acids used, the heats of vaporization of only two, valeric and isovaleric acids, were found.[12] Using the entropy of vaporization of these two acids, 23.0 cal. mole^{-1} °K.$^{-1}$, the heats of vaporization of the other two acids were estimated. Using the entropies of vaporization calculated from heats of vaporization of methyl isovalerate[12] and of isomeric $C_7H_{14}O_2$ esters,[13] 21.6 and 21.7 cal. mole^{-1} °K.$^{-1}$, the heats of vaporization of the other seven esters were estimated. The heats of vaporization of all twelve compounds at 25° were estimated by assuming the same difference in heat capacities between liquid and vapor as that between liquid[12] and gaseous[11] hexane.

Corrections to the monomeric vapor state were made by using a value of 7.0 kcal. mole^{-1} of monomer for the heats of dimerization of the acids.[14] The resulting heats of combustion in the monomeric vapor state, $-\Delta H_M$, are given in Table III. The uncertainties in the values of $-\Delta H_M$ are related to the following factors: (1) an observed variation of 0.5 entropy unit in the entropy of vaporization of the hexanes, (2) a variation of 0.6 kcal. mole^{-1} in the correction of the heats of vaporization of the

(11) "Selected Values of Properties of Hydrocarbons," Circular C461, National Bureau of Standards, U. S. Government Printing Office, Washington 25, D. C., 1947.

(12) N. A. Lange, "Handbook of Chemistry," 7th ed., Handbook Publishers, Inc., Sandusky, Ohio, 1949.

(13) E. Schjånberg, *Z. physik. Chem.*, **A178**, 274 (1937).

(14) E. W. Johnson and L. K Nash, *J. Am. Chem. Soc.*, **72**, 547 (1950).

TABLE II

THERMOCHEMICAL DATA

Compound	$-\Delta U_B/M$,[a,b] cal./g.	$-\Delta U_R$,[c] kcal./mole	$-\Delta H_c$, kcal./mole	$-\Delta H_f°$, kcal./mole
Valeric acid	6664 ± 7	680	681	131
α-Methylbutyric acid	6645 ± 12	678	679	133
Isovaleric acid	6629 ± 8	677	678	134
Pivalic acid	6622 ± 5[d]	676[d]	677[d]	135[d]
Methyl valerate	7293 ± 15	847	848	126
Methyl α-methylbutyrate	7280 ± 5	845	846	128
Methyl isovalerate	7271 ± 5	844	845	129
Methyl pivalate	7243 ± 15	841	842	132
Ethyl valerate	7706 ± 9	1003	1004	132
Ethyl α-methylbutyrate	7682 ± 4	1000	1001	135
Ethyl isovalerate	7674 ± 5	999	1000	136
Ethyl pivalate	7663 ± 6	997	999	138

[a] Average of five determinations on each compound. [b] Uncertainties expressed as average deviation. [c] Washburn correction added. [d] Solid state, other compounds in liquid state.

compounds at the boiling points to the heats of vaporization at 25°, (3) an observed variation of 0.5 kcal. mole^{-1} of monomer in the reported heats of dimerization of the acids, and (4) an estimated uncertainty of 0.15 kcal. mole^{-1} in the approximation of the heat of fusion of pivalic acid. Considering these related factors, all taken in the same direction, an average uncertainty of 1.2 kcal. mole^{-1} for corrections of heats of combustion to the monomeric vapor state appeared reasonable. Combining this value with the calibration and experimental uncertainties, the over-all uncertainties shown in Table III were estimated.

TABLE III

RESONANCE ENERGIES

Compound	$-\Delta H_M$, kcal./mole	$-\Delta H_T$,[a] kcal./mole	Resonance energy, kcal./mole	Cor.[b] resonance energy, kcal./mole
Valeric acid	700 ± 2	719	19	19
α-Methylbutyric acid	698 ± 2	719	21	20
Isovaleric acid	696 ± 2	719	23	21
Pivalic acid	695 ± 2	719	24	19
Methyl valerate	858 ± 3	888	30	30
Methyl α-methylbutyrate	856 ± 2	888	32	31
Methyl isovalerate	855 ± 2	888	33	31
Methyl pivalate	851 ± 3	888	37	32
Ethyl valerate	1014 ± 2	1045	31	31
Ethyl α-methylbutyrate	1011 ± 2	1045	34	33
Ethyl isovalerate	1010 ± 2	1045	35	34
Ethyl pivalate	1008 ± 2	1045	37	33

[a] 16.5 kcal./mole used for carbonyl group. [b] Corrected for chain-branching effect calculated from corresponding isomeric hexanes.

Using Wheland's values for bond combustion energies, the theoretical heats of combustion, $-\Delta H_T$, of $C_4H_9CO_2H$, $C_4H_9CO_2CH_3$ and $C_4H_9CO_2C_2H_5$ were calculated. Resonance energies were obtained by subtracting from these theoretical values the corrected heats of combustion in the

monomeric vapor state. The values are also shown in Table III.

The energies of isomerization from hexane, in kcal./mole, of gaseous six-carbon alkanes have been reported[15] as follows: 3-methylpentane, −1.1; 2-methylpentane, −1.7; 2,2-dimethylbutane, −4.4. Close inspection indicates that these isomerization energies are about the same as the differences among the resonance energies found for the analogous isomeric five-carbon fatty acids or their methyl or ethyl esters. Using the isomerization energies of analogous hexanes, the resonance energies of the acids and esters were corrected for the chain-branching effect to obtain the values given in the last column of Table III. Inspection of these corrected resonance energies and consideration of the estimated uncertainties associated with them leads to the conclusion that there is no significant difference among them. Consequently, it is concluded that the differences found in the resonance energies of five-carbon fatty acids or of their methyl or ethyl esters are due to the chain-branching effect. It is recognized that in some cases the difference between values for two isomers is about the same as the uncertainty involved; however, it is believed that a closer determination of the values would bear out the reported findings.

(15) F. D. Rossini and E. J. R. Prosen, *J. Am. Chem. Soc.*, **62**, 2250 (1940).

Acknowledgment.—The authors acknowledge the assistance of Dr. John D. Christian in the preparation of the acids and esters used in this study.

THE ADSORPTION AND REACTIONS OF ENZYMES AND PROTEINS ON KAOLINITE. I[1]

By A. Douglas McLaren

Department of Soils, University of California, Berkeley, Calif.

Received April 21, 1953

Enzymes and other proteins are readily adsorbed by silicate minerals under proper conditions of *p*H and solvent composition. Adsorption leads to a reduction or loss of enzyme activity. The adsorption of proteins on kaolinite seems to involve partly an ion exchange with adsorbed metal cations and partly simple adsorption on the external surfaces of particles. Adsorption isotherms are presented. The amount of a protein (lysozyme) adsorbed at a given total protein concentration and *p*H depends upon the concentration of buffer, the chemical composition of the buffer (acetate, phosphate, ethylammonium) and the concentration of neutral salts, *e.g.*, sodium chloride (0–0.1 *M*) present. The maximum amount of lysozyme adsorbed corresponds roughly to the surface area of an unfractionated kaolinite; the number of cationic groups involved in the lysozyme is nearly equal to the exchange capacity of the kaolinite. Less than a stoichiometric amount of cation is released to the solvent medium during the adsorption of lysozyme on sodium-saturated kaolinite, which is consistent with the amphoteric nature of proteins. The adsorption of a protein (ovalbumin, pepsin, trypsin inhibitor, chymotrypsin, lactoglobulin, lysozyme, etc.) to kaolinite above the isoelectric point of the protein is relatively low or nil compared with the amounts adsorbed below the isoelectric point.

Introduction

The adsorption of macromolecules, both natural[2] and synthetic,[3–6] at solid–liquid interfaces, has not been investigated extensively and only a few systematic studies have been reported. In view of the existence of adsorbed proteins and polysaccharides in soil[7] and the influence of adsorption on the metabolism of proteins and amino acids by soil microbes[7,8] and on enzymatic activity,[9,10] it is worthwhile to investigate the extent and nature of binding of typical proteins and related substances by soil minerals. Some observations have appeared on this topic and are summarized in recent reviews[10,11] and elsewhere.[12,13]

In connection with soil biochemistry, two questions are obvious: namely, how much protein is adsorbed on a clay and how does sorption influence the kinetics of enzyme reactions and microbial nutrition involving the adsorbed proteins. This paper is concerned with an exploratory study of the first question. As a simple clay mineral, kaolinite was chosen for study since the adsorption of proteins is expected to be only external to kaolinite particles.[10] With bentonite, *e.g.*, adsorption on internal surfaces is possible, thereby adding a greater degree of complexity to the problem. Since kaolinite behaves as a weak acid above *p*H *ca.* 4,[14,15] it is desirable to study the binding to kaolinite of proteins having isoelectric points (I.P.) both above and below this *p*H. As will be illustrated, charge plays an important role in kaolinite to protein binding.

Experimental

The Proteins.—Most of the crystalline enzymes and proteins were obtained from Worthington Biochemical Labora-

(1) Presented at the Division of Colloid Chemistry, 123rd Meeting, American Chemical Society, Los Angeles, California, March 15–19, 1953.

(2) (a) B. Ingelman and M. S. Halling, *Arkiv Kemi*, **1**, No. 10, 61 (1949); (b) C. A. I. Goring and W. V. Bartholomew, *Soil Sci.*, **74**, 149 (1952).

(3) (a) S. Claesson, *Disc. Faraday Soc.*, No. 7, 321 (1949); (b) I. Claesson and S. Claesson, *Arkiv Kemi, Mineral. Geol.*, **19A**, No. 4 (1945).

(4) H. Mark and G. Saito, *Monatsh.*, **68**, 237 (1936).

(5) E. Jenckel and B. Rumbach, *Z. Elektrochem.*, **55**, 612 (1951).

(6) R. A. Ruehrwein and D. W. Ward, *Soil Sci.*, **73**, 485 (1952).

(7) S. A. Waksman "Humus," Second Ed., Williams and Wilkins Co., Baltimore, Md., 1938.

(8) L. A. Pinck and F. E. Allison, *Science*, **114**, 130 (1951).

(9) (a) L. E. Ensminger and J. E. Gieseking, *Soil Sci.*, **53**, 205 (1942); (b) A. E. Erickson, Ph.D. Thesis, University of Illinois, 1948.

(10) J. E. Gieseking, *Advances in Agron.*, **1**, 159 (1949).

(11) C. A. Zittle, *Advances in Enzymol.*, **14**, 319 (1953).

(12) O. Talibudeen, *Nature*, **166**, 236 (1950).

(13) I. Barshad, *Proc. Soil Sci. Soc. Am.*, **16**, 176 (1952).

(14) C. E. Marshall, "The Colloid Chemistry of the Silicate Minerals," Academic Press, Inc., New York, N. Y., 1949.

(15) R. P. Mitra and K. S. Rajagopalan, *Soil Sci.*, **73**, 349 (1952).

tory and the Armour Laboratories. (Pepsin and chymotrypsinogen (recrystallized 8 times by Dr. H. Goldenberg) were from the Plaut Research Laboratory; soy bean trypsin inhibitor was prepared by Dr. E. Sheppard.) Pure crystalline proteins which have been investigated are lysozyme (I.P. 11–11.2)[16a] and to a lesser extent, ovalbumin (I.P. 4.7),[16b] chymotrypsinogen (I.P. 9.5),[16a] chymotrypsin (I.P. 8.6),[16a] trypsin (I.P. 7, 8.4, 10.2–10.8),[16c] trypsin inhibitor (I.P. 4.5) [16d] pepsin (I.P. 3.4–3.8),[16e] edestin (I.P. 5.5–6),[16f] and β-lactoglobulin (I.P. 5.2).[16g]

The Adsorbents.—Several samples of kaolinite were used. One sample (L) of Merck kaolin (colloidal N. F. No. 781603) was prepared by suspension, 2% in water containing 3 meq. of sodium hydroxide per 100 g. of kaolin. The suspension was fractionated by sedimentation according to Stokes' law to give an equivalent spherical diameter of 1 to 2 μ (supplied by Dr. R. Laird). A second sample (M) was fractionated by sedimenting at *p*H *ca.* 7.8–8.4 (25–26°) in sodium hydroxide solution to give a fractionated sodium clay of 1 to 5 μ. The fractionated material was then resedimented several times in 0.001 *M* potassium phosphate buffer of *p*H 7.6 in order to replace sodium ions by potassium. The completeness of substitution is not considered significant here since the adsorption surface areas of various alkali metal kaolinites are not markedly different.[17]

A third Merck sample was prepared by sedimentation at *p*H 8.5–9 in KOH only to give a 1 to 5 μ fraction (sample K).

A 1 to 2 μ fraction from Merck kaolin N. F. No. 781601 was also prepared.[18a] A natural gradation of Peerless No. 2 grade kaolin[18b] was prepared as described by Keenan, *et al.*[17] The electrodialyzed kaolin was titrated to *p*H *ca.* 8 with KOH.

Kaolinite concentrations were determined[17] by pipetting 1-ml. quantities into weighing bottles and then drying the suspensions to constant weight at 105–110°.

Adsorption of Proteins on Kaolinite.—Generally, to 1 ml. of clay suspension in screw cap vials (1.5 × 8.2 cm.) was added first, a buffer solution, and then various volumes of protein solution (*ca.* 1 mg. per ml. in *M*/1000 HCl or in a buffer) to bring the total volume to 8 ml. (lactoglobulin was first dissolved in *M*/100 HCl; it is stable at *p*H *ca.* 2[16g]). In any series of experiments the total amount of buffer used in the mixture was constant. The capped vials were then placed radially in copper fuse clamps mounted on a 10-inch diameter Leucite wheel and turned at 3.7 r.p.m. The speed chosen was rapid enough to prevent settling of the kaolinite suspension, yet slow enough to prevent foaming and rapid agitation, thereby keeping air–water interfacial denaturation of proteins to a minimum. After turning, the clay was sedimented in plastic tubes in a high speed centrifuge (International Reinforced centrifuge with a multispeed attachment giving up to 18,000 r.p.m.) and the concentration of the non-adsorbed protein in the supernatant liquid was determined by means of spectrophotometric readings at 2800 or 2810 Å. in a Beckman DU spectrophotometer.[19]

For most of the work a "universal buffer"[20] (UB), recommended by the originators "for biological and surface chemistry work," was utilized. It contained approximately 0.07 *M* Na^+, 0.01 *M* phosphate, 0.007 *M* citrate and 0.01 *M* borate with varying amounts of HCl. The universal buffer *per se* has a nearly constant ionic strength (0.08–0.1) over a wide *p*H range.[20]

In order to determine protein concentrations spectrophotometrically one needs to know the optical density for unit concentration (one mg. per ml.) and unit path length (one cm.), preferably at the protein absorption maximum near 2800 Å. These optical densities of the crystallized proteins were taken from the literature[19,21] or were determined on samples dried over phosphorus pentoxide in a vacuum to constant weight. The dry proteins were dissolved in 0.1–0.01 *M* HCl. These optical densities are nearly independent of *p*H from *p*H 1–8. Above *p*H 8 suitable corrections were of course applied.[19b,22] Table I summarizes the optical density data at 2800 Å. (D_{2800}) for solutions containing 1 mg. protein/ml.

TABLE I

OPTICAL DENSITIES OF PROTEINS PER MG. PER ML.

Protein	D_{2800}	Ref.
Ovalbumin	0.700	...
Edestin	0.780	...
Pepsin	1.35	16c
Chymotrypsinogen	2.07	21
Chymotrypsin	2.00	19a
Trypsin	1.79	19a
Lactoglobulin	0.965	...
Lysozyme	2.64	19b
Trypsin inhibitor	1.05	19a

It was found that in universal buffer solutions a small amount of light-scattering material was "leached" from the kaolinite and would not precipitate in the centrifuge. To correct the protein optical densities at 2800 Å., optical densities of the supernatant solutions from controls of kaolinite alone in buffer were measured as a function of wave length, particularly at 3400 and 2800 Å. By measuring the optical density of supernatant solutions containing protein at 3400 Å. (where absorption by protein is very small)[22] the density of light-scattering material was ascertained. The corresponding density of light-scattering material at 2800 Å. was then computed and subtracted from that of the mixture to give a correct value for the protein. This procedure was checked and found to be valid by mixing pure protein in buffer with buffer extract from kaolinite alone: the total density was the sum of protein and light-scattering material from 2500–3400 Å. This correction due to light scattering was most serious at high and low *p*H and precision of the uncorrected absorption data is only 5–10%. The correction is least serious near neutral *p*H; the precision was better, 2–5%. At high and low *p*H the ratio D_{2800}/D_{3400} due to light scattering by the extracted material from kaolinite was *ca.* 3, whereas at *p*H 6–9 the ratio was only *ca.* 2. The amount of scattering from this cause was at a maximum at *p*H 4–5. Incidentally, the amount of light scattering in experiments with ethylamine hydrochloride or sodium acetate buffers was virtually nil and no scattering corrections were necessary.

The following series of experiments will illustrate the overall procedure. To various amounts of kaolinite in one ml. of water in glass vials were added UB buffer and lysozyme in UB buffer to give a total volume of 8 ml. in each vial. The extremes in variation of protein and of kaolinite concentrations were *ca.* ten-fold each, in various combinations. After turning the vials *ca.* 48 hours the kaolinite from each was spun down in the centrifuge and the optical densities of the supernatant liquids were determined at 2800 and 3400 Å. The optical density for protein in the absence of kaolinite was D_i. The amount of protein bound per gram of clay is proportional to $(D_i - [D])$/g. kaolinite, where $[D]$ is the corrected density, proportional to unbound protein concentration at equilibrium.

The results from thirty such experiments are shown in Fig. 1. All points fall about a common isotherm regardless

(16) (a) E. A. Anderson and R. A. Alberty, THIS JOURNAL, **52**, 1345 (1948); (b) H. L. Fevold, *Advances in Protein Chem.*, **6**, 187 (1951); (c) M. Bier and F. F. Nord, *Arch. Biochem. Biophys.*, **33**, 320 (1951); J. H. Northrop, *J. Gen. Physiol.*, **6**, 337 (1924); J. H. Northrop and M. Kunitz, *ibid.*, **16**, 295 (1932); (d) M. Kunitz, *ibid.*, **30**, 291 (1947); (e) A. D. McLaren and C. Lewis, *J. Polymer Sci.*, **5**, 379 (1950); Y. Tazowa, *Symposia on Enzyme Chem. (Japan)*, **2**, 24 (1949); (f) C. L. A. Schmidt's "Chemistry of Amino Acids and Proteins," C. C. Thomas, Springfield, 1945, p. 618; (g) K. O. Pedersen, *Biochem. J.*, **30**, 961 (1936).

(17) A. G. Keenan, R. W. Mooney and L. A. Wood, THIS JOURNAL, **55**, 1462 (1951).

(18) (a) Gift of Merck and Co., Inc. This is stated by the manufacturer to be essentially the same as that used by O. J. Kelly and B. T. Shaw (*Proc. Soil Sci. Soc. Am.*, **7**, 58 (1942)); (b) gift of R. T. Vanderbilt Co., N. Y. This is the source from which the kaolinite used by Keenan, *et al.*,[17] was obtained.

(19) (a) *Cf.* M. Kunitz, *J. Gen. Physiol.*, **30**, 291 (1947); *ibid.*, **30**, 311 (1947); (b) C. Fromageot and G. Schnek, *Biochem. Biophys. Acta*, **6**, 113 (1950).

(20) S. Östling and P. Virtama, *Acta Phys. Scand.*, **11**, 289 (1946). The buffer consists of Na_2HPO_4 and citric, boric and hydrochloric acids.

(21) M. A. Eisenberg and G. W. Schwert, *J. Gen. Physiol.*, **34**, 583 (1951).

(22) G. H. Beaven and E. R. Holiday, *Advances in Protein Chem.*, **7**, 319 (1952).

of initial amounts of protein and kaolinite. In subsequent experiments it was found that the results had greater precision if one ml. of kaolinite suspension of fixed concentration was used (*ca.* 0.046–0.047 g. per ml.) together with varying initial concentrations of protein.

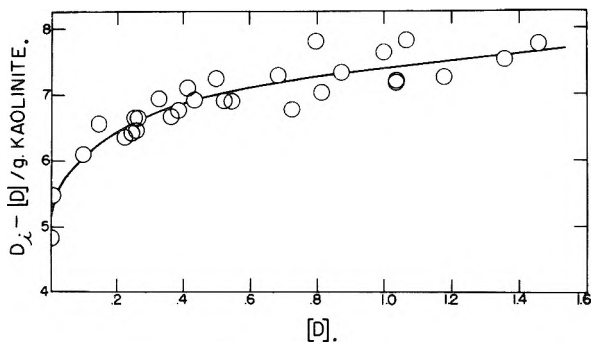

Fig. 1.—Adsorption isotherm of lysozyme on kaolinite (K) in 7/8 universal buffer concentration. Data below $D_i - [D]/g. = 4$ are essentially on the ordinate and are not shown; total volume 8 ml., *p*H 6.8–7.0; temp. 21.5–23°.

As a preliminary survey, to one ml. of kaolinite (K) suspension, *ca.* 0.047 g. per ml. of water, was added 5 ml. of universal buffer and 2 ml. of a protein solution (*ca.* 0.8–1.1 mg./ml. in *M*/100 or *M*/1000 HCl). The concentration of a given protein was constant for all experiments involving that protein. The times for turning on the wheel varied from 10–14 minutes for the enzymes and edestin, lactoglobulin and ovalbumin, to 2 hours for chymotrypsinogen and 2 days for STI. Controls of identical composition except for an absence of kaolinite were always observed to check for any loss of solubility of protein. The short times for the enzymes and three of the proteins were necessary to avoid either appreciable autolysis or denaturation attributable to the gentle agitation and/or extremes of *p*H. After mixing, the kaolinite was removed and the unbound protein was determined.

Results

The results of the preliminary survey of binding of some proteins to kaolinite are summarized in Figs. 2 and 3. The amounts of the various proteins bound to kaolinite are probably not equilibrium amounts and somewhat less than maximum amounts, as will be illustrated below by a detailed study with lysozyme. The survey does reveal qualitatively a pronounced relationship between adsorption and the isoelectric points, however. Below the isoelectric points, proteins tend to show an increase in binding with an increase in *p*H above *p*H 2 (*cf.* Fig. 8). Above the isoelectric points there is a marked decrease in amounts of protein adsorbed. (Isoelectric points are indicated by dotted lines in the figures.) This is quite clear for ovalbumin, STI, lactoglobulin, chymotrypsinogen and lysozyme.

Edestin is not sufficiently soluble between *p*H *ca.* 4.5–9.5 to be studied under these conditions, hence the points at high and low *p*H are connected by a dotted line, Fig. 3.

In general, above the isoelectric points of the proteins the kaolinite seemed to be dispersed as well in the presence of protein as in the absence of protein. Below the isoelectric point, in the presence of protein the kaolinite tends to be flocculated and to settle out of suspension much more quickly than in the absence of protein. Even in the presence of protein kaolinite was observed to be well dispersed at *p*H *ca.* 2 in some cases, however.

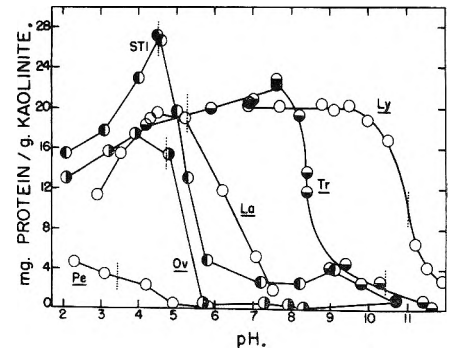

Fig. 2.—The adsorption of proteins on kaolinite as a function of *p*H: lactoglobulin (La), lysozyme (Ly), ovalbumin (Ov), pepsin (Pe), soy bean trypsin inhibitor (STI) and trypsin (Tr). The dotted vertical lines show the isoelectric points.

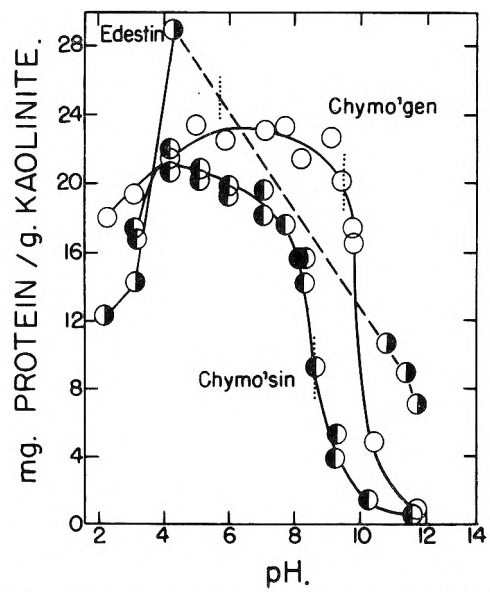

Fig. 3.—The adsorption of proteins on kaolinite as a function of *p*H: edestin, chymotrypsin (chymo'sin) and chymotrypsinogen (chymo'gen). The dotted vertical lines show the isoelectric points.

Binding of Lysozyme to Kaolinite as a Function of Time.—It was found that with a suspension of *ca.* 47 mg. of kaolinite and *ca.* 2 mg. of lysozyme in 8 ml. of buffer, nearly the maximum amount of protein which kaolinite could bind was adsorbed in about 24 hours at *p*H 7.6. Tubes of similar mixtures at several *p*H's were turned on the wheel for various times and then the contents were centrifuged to sediment completely the clay with bound protein. From the clear supernatant solutions the amounts of uncombined protein were determined by optical density measurements at 2800 Å. Figure 4 shows how the density of the supernatant liquids decreased with time. The *p*H's indicated were measured on the supernatant liquids.

In universal buffer at *p*H 3.1 or 3.2 the binding of lysozyme is complete in less than 10 minutes. At *p*H 5.5, 7.3 and 9.3 there is a rapid initial binding taking place in the first few minutes, amounting to *ca.* 90% of the ultimate binding (length of vertical lines), followed by a marked decrease in binding rate with no additional binding after 15–24 hours. The amount bound during the first ten minutes is

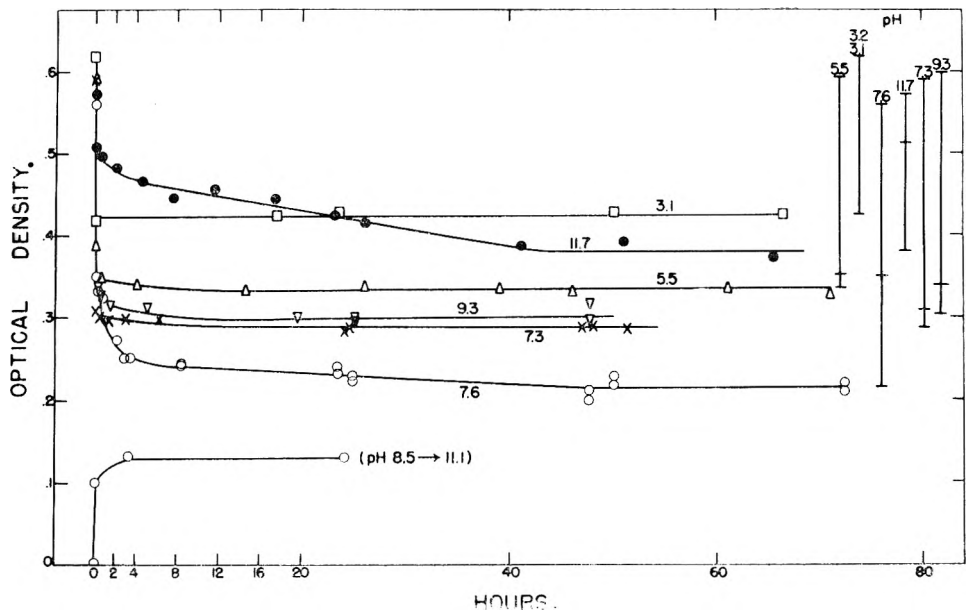

Fig. 4.—Optical density measurements, a measure of uncombined lysozyme, as a function of time of mixing with kaolinite. For an explanation of the vertical lines to the right of the figure, see text. Data at *p*H 3.2, 5.5, 7.3, 9.3 in universal buffer with kaolin (K). Data at *p*H 7.6 in *M*/500 phosphate buffer, at *p*H 11.7 in UB/2, at *p*H 3.1 in universal buffer, all with kaolin (M). Lowest curve shows rate of elution of lysozyme as a washed kaolinite–protein product at *p*H 8.5 is resuspended in buffer of *p*H 11.1.

indicated by a crossbar on the vertical lines to the right in Fig. 4.

In *M*/500 potassium phosphate of *p*H 7.6 the results are qualitatively similar to those in UB of *p*H 7.3 but quantitatively different. There is a very fast rate of binding during the first 2–3 minutes, giving rise to *ca.* 63% of the amount ultimately bound after 48 hours.[23] As will be shown in detail below, the total equilibrium binding of protein under these conditions, and for this total amount of protein in the system, is greater in dilute buffer than in universal buffer.

Results in universal buffer (UB) diluted with an equal volume of water (UB/2) at *p*H 11.7 are also shown in Fig. 4. Lysozyme undergoes denaturation at this *p*H and this may be reflected by the comparatively long time required to reach an apparent equilibrium. The comparatively long time for equilibrium to be reached is probably not due to any tendency for flocculation of the clay by protein since flocculation is least at higher *p*H.

In subsequent studies involving isotherms as a function of *p*H, more than 48 hours was allowed for equilibrium to be reached, unless otherwise noted.

Desorption of Lysozyme from Kaolinite.—A few observations were made on the elution of lysozyme. After equilibrium in the above described rate experiment at *p*H 7.6, the clay–protein mixtures were sedimented and drained. After agitation for 48 hours in *M*/500 phosphate buffer, no protein was found to have been eluted. To 0.046-g. quantities of clay, with adsorbed protein, .7 ml. of universal buffer, *p*H 11.1, or 7 ml. of 0.012 *N* KOH was added. The total final volume was 8 ml. in each case. After different times the suspensions were centrifuged and the supernatant liquids were tested for *p*H and eluted protein. The results at *p*H 11.1 are shown in the lower curve of Fig. 4. At *p*H 11.5, induced by KOH, the amount of protein eluted was greater than at *p*H 11.1. In fact, the amounts of protein remaining on the kaolinite after partial elution corresponded roughly to the equilibrium binding at these final *p*H's and total protein concentrations.

Similarly, with protein–kaolinite complex in 7 ml. of UB/10, *p*H 7.4, plus one ml. of 0.8 *M* NaCl or 5 *M* NaCl, elution was essentially complete after 24 hours of turning. In the solvent of 0.1 *M* NaCl, 11% of the bound protein had been eluted, and in the 0.63 *M* NaCl solvent 62% elution had taken place at a final *p*H of 6.8. The small *p*H drop was not responsible for the elution (see below).

Incidentally, after equilibrium in UB, *p*H 9.3, lysozyme–kaolinite suspensions were compared with a kaolinite (Merck colloidal N. F.) suspension under a microscope. Without protein present the particles were single, *i.e.*, completely dispersed and similar in appearance to pictures by Kelly and Shaw[24] as regards particle shape. With protein the particles occurred in one's, two's, etc., and in small clumps of a dozen or more particles. The absorption spectra were identical for eluted protein and the original protein prior to adsorption.

Amounts of Lysozyme Bound to Kaolinite.—On the basis of the rate curves as a guide, equilibrium adsorption isotherms were obtained. Even in UB buffer at full strength the *p*H after equilibrium tended to be *ca.* 0.1 *p*H unit from the initial *p*H of the buffer, hence UB was used full strength for a binding study of lysozyme as a function of concentration over a range of *p*H values.

(23) The faster rate of binding for the major fraction bound in more concentrated buffers may result from a diminution of repulsion between negative charges of the kaolinite and of protein by the ion cloud of high densitys.[6]

(24) O. J. Kelly and B. T. Shaw, *Proc. Soil Sci. Soc. Am.*, **7**, 58 (1942).

In Figs. 5 and 6 are shown some typical curves of amounts of lysozyme in mg./g. kaolinite, m, bound as functions of the equilibrium concentration of lysozyme $[C]$, expressed as mg. per ml. The results were checked for completion of binding, *i.e.*, for equilibrium, at several *p*H's. It may be noted that below *p*H *ca.* 10 the isotherms rise steeply at low values of $[C]$ and only begin to level off after 75–90% of the maximum binding has taken place.[25] The curves below *p*H 7.0 level off to nearly constant values of m at each *p*H above $[C]$ equal to 0.02–0.1 mg. per ml. of protein.

The adsorption of lysozyme on kaolinite in some additional buffer systems is illustrated by Fig. 7.

Discussion

Adsorption of Some Proteins.—The decrease in binding of proteins to kaolinite above the isoelectric point is expected since above the isoelectric points the proteins have a net negative charge as does the kaolinite; the repulsion leads to a reduction in adsorption. On the other hand, on the surface of protein molecules there are probably small surface regions bearing positive charges even above the I.P. of the protein and unless the net charge of the molecule is highly negative, some binding to the mineral surface would be anticipated.[26]

It is interesting to note that two widely different isoelectric points for trypsin and also for chymotrypsinogen (and chymotrypsin) have been reported. For chymotrypsinogen Kunitz and Northrop[27] found *ca.* *p*H 5 by microcataphoresis, Ingram found *ca.* 6.3 by Donnan equilibrium[23] and Anderson and Alberty found 9.5 by the electrophoresis–moving boundary method. An isoionic point (isoelectric point in the absence of adsorbed counterions) of 9.8 has been calculated from the amino acid composition of chymotrypsinogen by McLaren and Lewis.[16e] The variation of adsorption of chymotrypsinogen by kaolinite with *p*H indicates that the higher estimates of Anderson and Alberty are probably correct. Above *p*H 9.8 the adsorption falls very rapidly. Similar considerations apply to chymotrypsin. With trypsin, isoelectric points of *ca.* 7, 8.4, 10.2 and 10.8 have been reported (*cf.* 16c), based on four different methods. Results shown in Fig. 2 suggest an intermediate value.

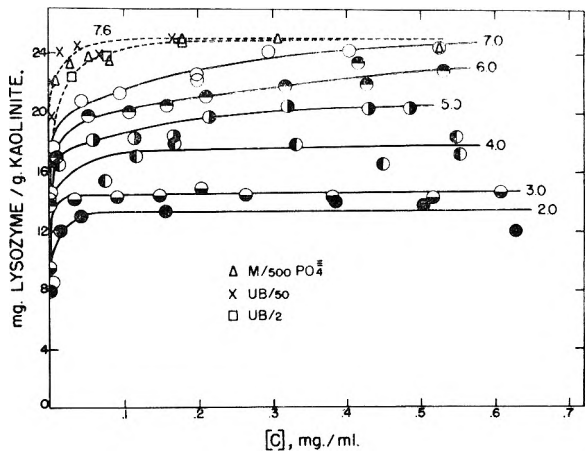

Fig. 5.—Amount of lysozyme bound in mg./g. of kaolinite (M) at various *p*H values (indicated at right of figure). Solid curves are for universal buffer; curves at *p*H 7.6 are broken.

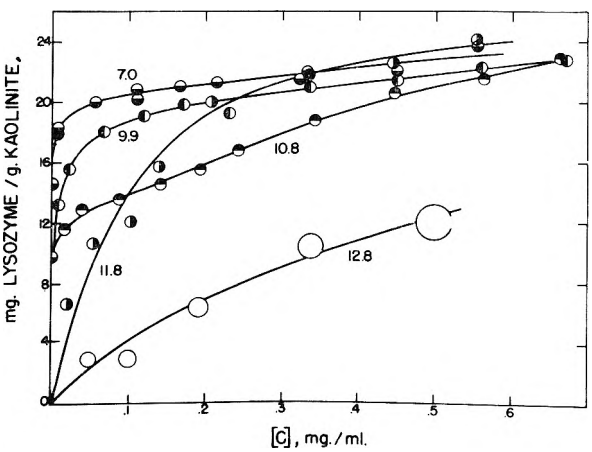

Fig. 6.—Amounts of lysozyme bound to kaolinite (K) in mg./g. at *p*H 7–12.8 (universal buffer).

Rates of Binding of Lysozyme.—The adsorption of lysozyme is very rapid at first and then is either complete, at low *p*H, or else the rate becomes much less, as at higher *p*H. Claesson and Claesson[3b] similarly found that the rate of adsorption of polyvinyl acetate on carbon was at first rapid and then fell as the remaining polymer was bound. They ascribed the course of their rate curves to different kinds of active spots or sites on carbon. This explanation is reasonable for kaolinite since, with an increase in *p*H from 3.1 to 9.3, additional, unlike, sorptive sites of negative charge appear.[15] Other phenomena could also be involved. For example, random adsorption at first may leave patches of residual active sites too small for other protein molecules. These could be covered by any tendency for a layer (mobile) of protein to pack more tightly or to "crystallize in two dimensions." The existence of this phenomenon in the Claessons' work is supported by the fact that more of the lower molecular weight polymer is adsorbed than a higher molecular weight fraction of the polymer. Low molecular weight materials would tend to leave less isolated area by random sticking to the surface,

(25) The data conform roughly to the Langmuir type isotherm

$$m = \alpha[C]/1 + \beta[C]$$

and to the so-called Freundlich equation

$$m = k[C]^n$$

However, the value of n, which is about $^1/_{10}$, is far from the value $^2/_3$ expected theoretically for small molecules (B. P. Gyani, THIS JOURNAL, **49**, 442 (1945)). It must be remembered that the derivations of both the Langmuir equation (A. R. Miller, "The Adsorption of Gases on Solids," Cambridge University Press, Cambridge, 1949, p. 20) and the Freundlich equation (Gyani) assume implicitly that there is no interaction between adjacent, adsorbed molecules. This is probably far from true with protein molecules which, even though adsorbed, would expectedly have side chain polar groups for protein–protein interaction. Since plots of the data according to these equations have not been instructive they have been omitted.

(26) It should be pointed out that this method of indicating the approximate isoelectric point of a protein does not depend on any change in the isoelectric point of the *bound* protein but is only dependent on the charge of the protein in solution. It differs therefore from the method of microscopic electrophoresis using coated particles of collodion, etc.; *e.g.*, C. W. N. Cumper and A. E. Alexander, *Australian J. Sci. Res.*, **4**, 372 (1951).

(27) J. H. Northrop, M. Kunitz and R. M. Herriott, "Crystalline Enzymes," Columbia University Press, New York, N. Y., 1948.

(28) V. M. Ingram, *Nature*, **170**, 250 (1952).

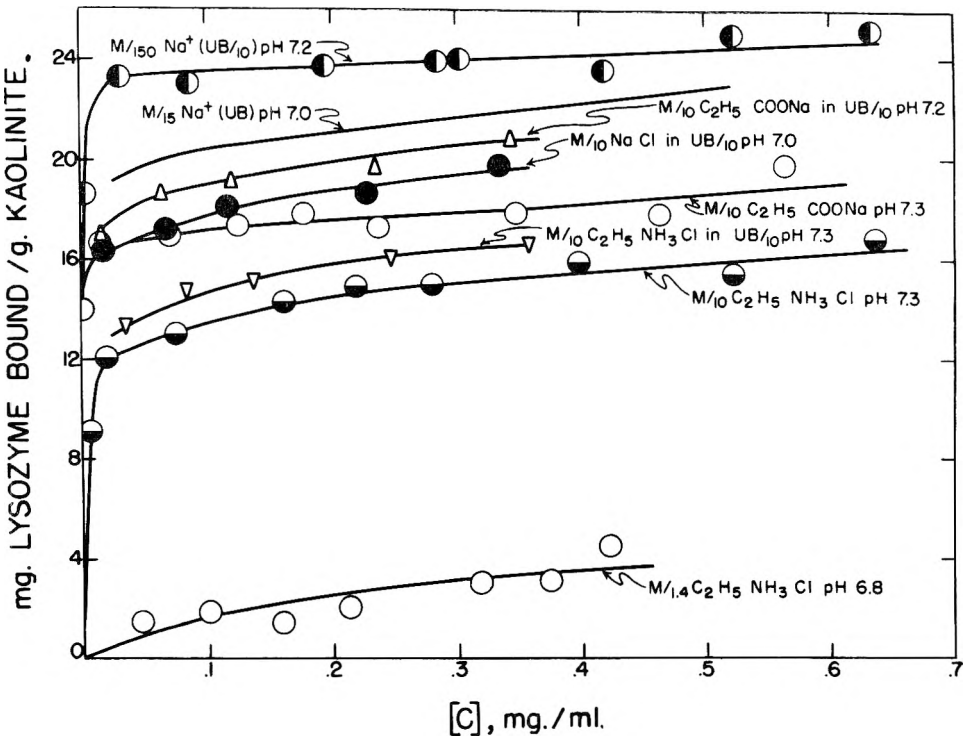

Fig 7.—Adsorption of lysozyme to kaolinite (K) in UB/10, $M/10$ ethylamine hydrochloride and $M/10$ sodium acetate and mixtures.

assuming that only a monolayer of molecules is possible.

Adsorption Isotherms of Lysozyme.—Generally the isotherms have two distinct regions. The initial rise in m probably reflects a binding to random sites on the clay surface. At higher values of $[C]$ it may be that protein–protein interaction, and perhaps a necessity for two-dimensional translational movement to cover up uncovered areas isolated by random adsorption, and too small to accommodate a protein molecule, prevents the isotherm from leveling off more sharply to parallel the $[C]$ axis (see below). There is some question as to the maximum value of m at higher pH. Although up to pH 11.8 the curves tend toward a maximum m comparable to that of pH 7, above pH 7 the adsorption at low $[C]$ falls off with increasing pH (Fig. 6).

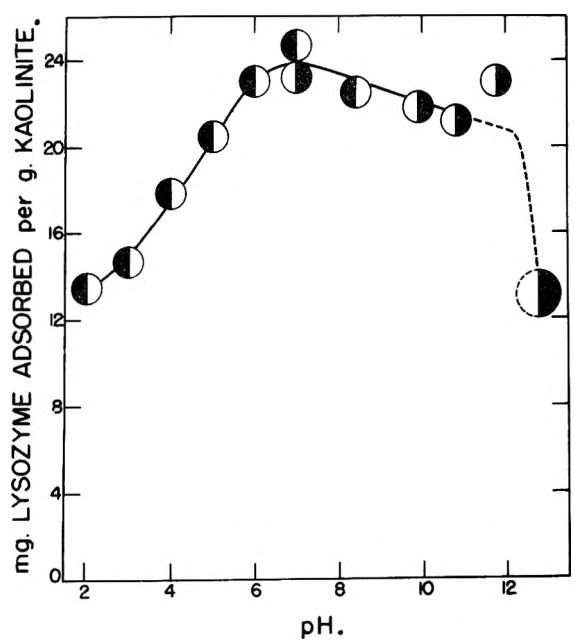

Fig. 8.—Plot of "maximum" amount of lysozyme bound to kaolinite as a function of pH in universal buffer. The shaded points are for the two different kaolinite samples, M and K.

We may assume that there is a "maximum" amount of protein bound, I, which would cover all available sorption sites on the clay particles. (The existence of a maximum binding is much more apparent in very dilute buffer: see below and compare Figs. 6 and 7.) We can then find I by plotting the data according to the equation $[D] = D_i - I$ and extrapolating a tangent to the nearly linear part of the curve to $[D] = 0$. Here $[D]$ is the equilibrium optical density (of the supernatant liquid after centrifuging the kaolinite down) and D_i is the initial density of protein solution prior to binding (equal to the optical density of protein alone in solvent). The extrapolation is carried out from the points which fall on, or nearly on, a line of slope equal to 1. These points were found to be those in the neighborhood of $[C] \geqq 0.5$. In Fig. 8 there is plotted the amount of protein bound at $[C] = 0.5$ as a function of pH taken from the isotherms in Figs. 5 and 6 and others. It will be seen that between pH *ca.* 6 and 11.8 the "maximum" amount of protein bound is about the same and is about twice that at pH 2–3.

An interpretation of these data is the following. Below pH *ca.* 3, COOH groups in lysozyme and OH groups on the clay are not ionized. Binding to the clay will be partly through hydrogen binding between these COOH groups, and perhaps NH_3^+

groups, and OH groups on the clay. This mechanism seems probable: the binding of COOH groups in polymers to OH groups on a cellulose surface has already been demonstrated.[29] If any phosphate is bound to the clay,[30] positive groups in the protein may also aid in binding. The amount of phosphate bound to kaolin is small, especially in the presence of citrate.[30] The indications are that only relatively small amounts of citrate and/or phosphate are bound to kaolin, perhaps 1 or 2 meq./100 g.[14,30] As the *p*H is increased from 4 to 7 the kaolinite acquires an increased negative charge[14] and more lysozyme is bound. It is of interest to examine the charge on lysozyme molecules also. We can calculate[16e] the numbers of negative and positive charges and the net charge on a lysozyme molecule as a function of *p*H from amino acid data tabulated by Fevold.[31] Between *p*H 2 and 8 the total positive charge is 17–18 per molecule (neglecting any phosphate binding by the protein)[31] for a molecular weight of 15,000. The isoionic point is calculated to be at *p*H 11.8, which is an agreement with the value of *p*H 11–11.2 for the isoelectric point.[16a] At *p*H 7–8 the net plus charge on lysozyme is about 17. The maximum amount of protein bound in this region is about 24 mg./g. kaolinite. Per 100 g. of kaolinite we therefore have

$$\frac{2.4 \times 17 \times 10^3}{15{,}000} = 2.7 \text{ meq. of positive charge}$$

This is in the range of the exchange capacity of kaolinite,[14] namely, 2–4 meq. per 100 g. Thus, in addition to hydrogen bonding, it seems probable that the protein is bound partly by coulombic attraction to charges on the clay surface.

It seemed that if the process of sorption of lysozyme on kaolinite involves some ion exchange as well as simple adsorption to the surface of the particles, a desorption of monovalent cations might be detectable. As a test the following observation was made. To 0.042 g. of Merck colloidal hydrogen saturated kaolinite (1–2 μ e.s.d.) was added enough sodium hydroxide to bring the *p*H of the suspension to 7.1; the total volume was 8 ml. The number of meq. of sodium hydroxide added was 2.4 per 100 g. kaolinite. A second tube contained 2 mg. of lysozyme in 8 ml. of water (*p*H 2.6). A third tube contained the same amounts of sodium hydroxide, kaolinite and lysozyme in 8 ml. of water (*p*H 7.0). The three tubes (in replicate) were turned on the wheel for 2.5 hours, then allowed to stand until the kaolinite had settled out of suspension. The amounts of sodium ion in the clear supernatant solutions were measured in a Beckman flame spectrophotometer. The results were as follows: The amount of lysozyme adsorbed was *ca.* 25 mg./g. kaolinite (2.8 meq. of cationic groups/100 g. kaolinite) at a final *p*H of 7.0. The number of meq. of sodium ion apparently released to the supernatant solution as a result of the binding of lysozyme was not more than *ca.* one-fourth of the sodium ion bound to the sedimented kaolinite in the absence of lysozyme, however. [The fact that so little bound sodium was released to the supernatant solution as protein was adsorbed was not altogether unexpected. As the kaolinite–protein complex precipitates, most of the exchangeable sodium must precipitate with the kaolinite–protein particles in order to maintain electrical neutrality.] This is illustrated by the following equation for a reaction which, for simplicity, involves only one of x exchangeable sodium ions. Here $(NH_3^+)_n$–P–$(CO_2^-)_h$ represents the lysozyme molecule with its positive and negative groups.

$$\text{Na}_x\text{Kaolinite} + (\text{NH}_3^+)_n\text{–P–}(\text{CO}_2^-)_h \longrightarrow \text{Na}_{x-1}\ \text{Kaolinite–}\underset{|\atop (\text{NH}_3^+)_{n-1}}{\text{NH}_3}\text{–P–}(\text{CO}_2^-)_h\text{–Na}$$

Strictly speaking, the n groups include guanidino residues, and at *p*H 7 n is greater than h. With n greater than h, the protein with a net positive charge, $n - h$, is accompanied by $n - h$ anions, *e.g.*, chloride. The anions are not shown in the equation. (The Armour crystalline lysozyme was not an isoelectric preparation but a salt, presumably the carbonate, which dissolved in water to give a *p*H of 6.5 at 2 mg. per 8 ml.) The fact that a little cationic sodium is released to the solvent during the adsorption of lysozyme indicates a small amount of hydrolysis of the kaolinite–protein complex and/or that there has been a small shift in the ion binding properties of the protein. That the apparent isoelectric point of a protein is sometimes changed by adsorption on solids is well known. It is also possible that not all n groups (2.8 meq./100 g. kaolinite) are actually involved in the adsorption.

Both cationic displacement and anionic displacement may play roles in the mechanism of protein binding. (Anionic displacement has been postulated[6] to account for the binding of polymethacrylate to kaolinite, which exhibits a maximum binding of *ca.* 2 meq. of polymeric COOH groups per 100 g. Cation binding may be considered roughly equal to the anion-exchange capacity of kaolinite clays,[32] and since proteins also have cationic groups these too may be involved in adsorption.) This picture is consistent with the following observations. In diluted universal buffer the adsorption of lysozyme is greater at low values of $[C]$ than in universal buffer itself, Figs. 5 and 7, whereas at high $[C]$ the maximum binding is less influenced by buffer concentration, showing a competition of protein with ions for the exchange sites on kaolinite. The curves at *p*H 7.2–7.6 in dilute buffer level off to a constant value of m at much smaller $[C]$ of protein than in universal buffer. The adsorption of lysozyme on kaolinite in $M/10$ sodium chloride in UB/10, or in $M/10$ sodium acetate in UB/10 is even less than in UB containing $M/15$ Na^+, again showing the competitive influence of the cation concentration on sorption. The binding of protein in dilute universal buffer, UB/10, containing $M/10$ sodium acetate is not much greater than in $M/10$ sodium acetate, showing that the presence of phosphate and citrate does not influence the binding greatly. This point is also brought out by a com-

(29) C. H. Hofrichter and A. D. McLaren, *Ind. Eng. Chem.*, **40**, 329 (1948).

(30) L. A. Dean and E. J. Rubins, *Soil Sci.*, **63**, 377 (1947).

(31) For a review, see H. L. Fevold, *Advances in Protein Chem.*, **6**, 187 (1951).

(32) Reference 14, p. 133.

TABLE II

COMPARISON OF MAXIMUM BINDING OF LYSOZYME WITH SURFACE AREA OF KAOLINITE

Kaolinite	Size, μ (eq. sph. diam.)	Meq./100 g.	Surface area, cm.²/g.	Lysozyme, mg./g. (maximum)	Lysozyme area, cm.² Spheres	Monolayer
K-Kaolinite (Peerless)	Natural	4.2	18.9×10^4	27.0–33		27×10^4
Na-Kaolinite (Merck colloidal N. F.)	1–2	2.4	As plates: 2.6×10^4 As spheres: 2×10^4	26.0	8.9×10^4	26×10^4
Na-Kaolinite (Merck N. F.)	1–2	3.8	As plates: 2.6×10^4	35		35×10^4

parison of binding of lysozyme in $M/10$ ethylamine hydrochloride and in $M/10$ ethylamine hydrochloride in UB/10, Fig. 7: the two isotherms are close together. The competition of amino groups in the protein with those in the amine buffer is pronounced. The molar concentration of cationic groups in the protein suspension is only *ca.* 10^{-4} to 5×10^{-4}, revealing a preferential binding of protein over ethylamine.[33] In $M/10$ ethylamine the adsorption of lysozyme is only about $^2/_3$ of that in dilute universal buffer (UB/10) or in $M/500$ potassium phosphate buffer (*cf.* Figs. 5 and 8), and in M 1.4 ethylamine the binding of protein is very greatly reduced. In neutral solution the binding of chloride ions to kaolinite is negligibly small, incidentally.[32]

Since the influence of added NaCl on the sorption of lysozyme is to decrease protein binding, and is opposite to that of the influence on the sorption of sodium polymethacrylate,[6] we may conclude that cation exchange is more important than anion exchange in the lysozyme–kaolinite system. At *p*H 3.8 in UB/10 with or without the presence of $M/10$ NaCl, the adsorption isotherms are identical (not shown). This indicates that ion exchange as a mode of binding is not involved at this low *p*H.

At *p*H greater than 9 the net charge on the protein molecule is becoming more negative, *i.e.*, less positive, and eventually at *p*H 12 the net charge is negative. This reflects itself in the shapes of the isotherms, Fig. 6. It takes a much greater driving force, $[C]$, to attain the amount of binding extant at *p*H 7. Probably the increasing influence of negative charges in the protein molecule exerts a local repulsive effect. This repulsion is not able to reduce the adsorption completely at *p*H 12.8, however. Although there is uncertainty about the maximum binding of lysozyme at *p*H 12.8, the significant point is that apparently the residual positively charged guanidino groups of the arginine residues existing even at *p*H 12.8 are able to anchor the protein molecules even though the net charge per molecule is -5. At this *p*H the kaolinite particles must be highly negative. It is interesting to remember, however, that adsorption may alter the apparent, *i.e.*, operational, isoelectric point of the protein.[34,35]

The crossing over of the isotherms of *p*H 10.8 and 11.8 probably reflects a denaturing action of the higher *p*H on the lysozyme, as mentioned above. It is known that such high alkalinity destroys the enzyme activity of lysozyme. Alderton, *et al.*, found a 60% loss in activity at *p*H 12 in 7 days[36] and in our experiments 2 days were allowed for equilibrium to be reached. The enzyme[31,36] is quite stable below *p*H 9.

TABLE III

ADSORPTION OF LYSOZYME ON KAOLINITE IN $M/500$ PHOSPHATE BUFFER

(8 ml. total volume, *p*H 7.6)

Kaolin	$[D]$	$D_{initial} - [D]$	*p*H	Kaolinite, g.
Merck, colloidal	0	0.271	7.4	0.0345
N. F. 1–2 μ	0.022	.290		
	.042	.297		
	.101	.306		
	.179	.296		
	.243	.294		
	.515	.298		
Peerless Natural	.319	.272	7.6	0.0304
	.615	.272		
	.620	.267		

In considering the total, maximum amounts of protein bound to kaolinite it is also instructive to compare the area of kaolinite particles with the area "covered" by protein. The surface area of Peerless kaolinite has been determined by nitrogen adsorption isotherms by Keenan, *et al.* This is tabulated in Table II. Kelly and Shaw[24] give electron microscopic and hydrodynamic data, from which the surface area of Merck kaolin N. F. (1–2μ) may be computed, Table II. Also, at 900 $\times$ magnification, Merck kaolin colloidal N. F. (1–2 μ) appears to have the same particle shapes as shown by their pictures for kaolin N. F. Further, the exchange capacity of the kaolin colloidal N. F. is low; hence, it has probably not been ground. We therefore compute the same areas for both Merck kaolins. (The exchange capacities of Peerless and Merck N. F. kaolins are quoted from the original papers.[24,37]) Because of particle irregularities, the actual adsorptive areas of the Merck kaolins are doubtless greater than the minimum values calculated. For a comparison with protein adsorption data, the area found by Keenan, *et al.* is most appropriate on a molecular basis. The maximum amount of lysozyme bound to kaolinite is nearly independent of $[C]$ in very dilute buffer, Tables II and III (*cf.* Fig. 7). From the molecular weight and density of lysozyme we compute a cross sectional area of 834 Å.². The sorption of 26–27 mg. per g. kaolinite amounts to an area of *ca.* 9

(33) For a given heat of binding of charged groups, coulombically to a charged surface, the protein will bind preferentially over small ions of equal molar concentration because of the smaller entropy change (a decrease) of binding of a chain segment of a macromolecule as compared to a free small ion. The chain segment has less randomness to lose than a small, free ion; hence the over-all free energy decrease of binding of the macromolecule–ion will be greater.

(34) S. Mattson, *Soil Sci.*, **33**, 41 (1932).

(35) *Cf.* E. A. Ancerson and R. A. Alberty, THIS JOURNAL, **52**, 1345 (1948); and M. Kunitz, *J. Gen. Physiol.*, **22**, 207 (1938).

(36) G. Alderton, H. L. Fevold and H. D. Lightbody, *Federation Proc.*, Part II, **5**, 119 (1946).

(37) R. T. Shaw, THIS JOURNAL, **46**, 1032 (1942).

$\times 10^4$ cm.^{2}. Hendricks has postulated that about 20% of the total surface of kaolinite is on the lattice edges,[38] which leads to a comparable value for a natural gradation of Peerless kaolinite, namely, 4×10^1 cm.^{2}/g. If the monovalent exchangeable ions are involved in protein adsorption, and if they are on the edges of the kaolinite particles, the area per ion[17] is 16 Å.^{2}. Thus a protein molecule may cover many surface exchange sites.

This comparison of figures rests on the assumption that the molecules of protein do not unfold during the adsorption process. Unfolding at air–liquid interfaces at least can lead to protein denaturation,[39] and we have found that eluted lysozyme is active. Hence, the globular state of the adsorbed molecule seems probable. The problem is not unambiguous. If we assume that the molecule unfolds on the mineral surface, and adopt[39] the area per mg. protein as *ca.* one m.^{2} (which is typical of proteins), 26 mg. of protein would cover 26×10^1 cm.^{2}, which is comparable to the total surface area of the kaolinite particles, namely, *ca.* 19×10^4 cm.^{2}. On this basis, the area per molecule is *ca.* 2,500 Å.^{2}. Keenan, *et al.*, find 80 Å.^{2} per exchangeable ion if averaged over the entire surface and the protein molecule in the unfolded state would still cover many exchange sites. Another reason for believing that the adsorbed molecules are still globular is that if they were elongated the actual surface area covered would expectedly be far less than that of the kaolinite particles for reasons of steric hindrance.[40] The data of Claesson and Claesson, showing a decrease in maximum adsorption of a linear polymer with increasing molecular weight, illustrates this point of view.

Elution of Lysozyme.—Others[41–43] have shown that lysozyme[32] is strongly adsorbed to kaolin, cellulose, charcoal, etc. As is seen from Fig. 4, it is possible to elute lysozyme with suitable change in *p*H or addition of salt, as demonstrated by ultraviolet absorption spectroscopy. Preliminary observations indicate that lysozyme may also be eluted with ethylamine hydrochloride and that the eluted enzyme is fully active.[44]

In the adsorbed state, lysozyme is inactive toward *Micrococcus lysodeicticus*.[43] Gieseking, *et al.*,[45] have shown that the addition of clays to enzymes in solution decreases the enzyme activity. It is possible that most of the residual enzyme activity in these systems is due to unbound enzyme.

Acknowledgments.—The author wishes to thank Dr. D. E. Williams for aid with the sodium analyses.

(38) S. B. Hendricks, *Ind. Eng. Chem.*, **37**, 625 (1945).
(39) H. B. Bull, *Advances in Protein Chem.*, **3**, 95 (1947).
(40) E. L. Mackor and J. H. van der Waals, *J. Colloid Sci.*, **7**, 535 (1952).
(41) L. K. Wolff, *Immunitatsforsch, u. exp. therapy*, **50**, 88 (1927).
(42) H. Fleming, *Proc. Roy. Soc. (London)*, **B93**, 306 (1922).
(43) I. Buyanovskaya and Z. W. Jermol'eva, *Acta med. U.R.S.S.*, **1**, 248 (1938).
(44) We are indebted to Dr. R. Feeney for the bio-assays.
(45) M. M. Mortland and J. E. Gieseking *Proc. Soil Sci. Soc. Am.* **16**, 10 (1952).

FILTRATION OF MONODISPERSE ELECTRICALLY CHARGED AEROSOLS[1]

By Guy G. Goyer,[2] Ruth Gruen and Victor K. LaMer

Department of Chemistry, Columbia University, New York 27, N. Y.

Received May 25, 1953

Uniform particle size liquid aerosols were charged electrically by passage through a wire to cylinder corona discharge. The unipolar droplets carried a positive charge ranging from 25 to 150 electronic charges depending on the intensity of the charging field (5–18 e.s.u.) and the radius of the aerosols droplets (0.25–0.55μ). Charge and radius were determined with a Millikan-type oil drop apparatus. The maximum theoretical charge was not obtained and a distribution of charge on uniform particle size particles was observed. Factors affecting the incompleteness and non-uniformity of charge in the present procedure are: electric winds, turbulent flow, non-uniform velocity of flow and charging times, inhomogeneity of the field gradient. Although a completely uniform charge was not obtained, a sufficiently well defined charge range was obtained for the particle radii studied, to yield reproducible filtration at a given size as a function of the average particle charge. Filtration of charged dioctyl phthalate monodisperse aerosol droplets through Chemical Corps No. 5 filters was studied at two linear velocities, 2.7 and 28 cm./sec. An appreciable decrease in penetration is observed upon charging. As would be expected, this decrease is larger at smaller linear velocities. The time of transit of the charged particles through the filter layer is an important factor. The effect of charges on filter penetration is larger the smaller the droplet size.

Introduction

The theory of electrical charging of conductive and dielectric spherical particles involves two distinct mechanisms: charging by diffusion, important at smaller sizes (<0.1 μ) and field charging, important at larger sizes.

In charging by diffusion, the gaseous ions as a result of thermal motion collide with the aerosol particles moving through the ion atmosphere, surrendering their charges to the particle. The charge acquired is then proportional to the radius of the particle as proven by Townsend[3] for conducting spheres, and established experimentally by Schweitzer[4] and Deutsch[5] for tobacco smoke and paraffin droplets.

In field charging, the important factor becomes the stream of ions along the lines of force of the field through which the aerosol flows. Pauthenier and Moreau-Hanot[6] have shown that the net force

(1) (a) This work was carried out under Atomic Energy Commission Contract AT(30-1)-651. (b) Presented at the 27th National Colloid Symposium, Ames, Iowa, June 25–27, 1953.
(2) Now at Cloud Physics Project, Department of Meteorology, University of Chicago, Chicago, Illinois.
(3) J. S. Townsend, "Electricity in Gases," Oxford University Press, New York, N. Y., 1915, pp. 214–215.
(4) H. Schweitzer, *Ann. Physik*, **4**, 33 (1930).
(5) W. Deutsch, *Z. tech. Physik*, **7**, 623 (1926).
(6) M. Pauthenier and M. Moreau-Hanot, *J. phys. Radium*, [7] **3**, 590 (1932).

between ions and charged particles is always attractive when the charge on the particle is smaller than pE_0r^2; the maximum charge is proportional to the square of the radius.

An experimental verification of this theory has been achieved[6] for conducting and dielectric spheres in a cylindrical field. Spheres of rose alloy (Pb, Bi, Su) 5 to 100 μ radius, and steel spheres 0.5 to 3.5 mm. radius were used as conductive particles. Dielectric particles were made from ebonite, paraffin and naphthalene spheres ranging from 80 to 125 μ radius.

In the present work a technique has been devised for conferring a high charge to aerosol droplets. Charging laws have been verified for particles of dielectric constant $D = 5.2$ in a size range below the one studied by most of the previous investigators. Moreover, for the first time, a *monodisperse* aerosol was used to investigate charging characteristics.

In good agreement with the work of Fuchs, Petrjanoff and Rotzeig[7] our experimental data lead to the conclusion that field charging is the dominant charging mechanism even in the low size range investigated. Calculation of the theoretical charges from the field charging equation lead to a better fit with the experimental data than charges estimated from the diffusion equation.

Apparatus.—Unipolar charging results from the passage of the aerosol through an atmosphere of ions of a given sign. A wire-to-cylinder corona discharge provides the necessary ion atmosphere.[8,9]

The aerosol flows through a channel at right angles to an electric discharge between the wire W and the brass cylinder wall C as shown in Fig. 1. A narrow slot in the cylinder above the grounded plate P permits the ion current to form a curtain perpendicular to the flow of aerosol. Precipitation of the charged particles is prevented by making the charging curtain thin; hence the time of charging is short.

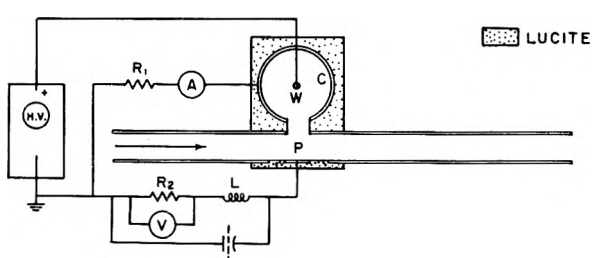

Fig. 1.—Charging device and electrical circuit.

The charging region in the channel is 0.6 cm. high, 1 cm. wide and 0.5 cm. long. The area of the channel is 0.78 cm.^{2} yielding a linear velocity of 42.3 cm./sec. for a flow of 2 l./min. The time of transit through the charging region is 0.012 sec. The cylinder perpendicular to the channel is 7.62 cm. long to prevent end effects from disturbing the uniformity of the charging region. The interior diameter is 1.92 cm. and a tungsten wire 0.005 cm. in diameter is stretched along the cylinder axis.

A Dumont High Voltage Power Supply is used as a source of potential. The positive potential varies from 4 to 12 kv. The cylinder wall C is grounded through a microammeter (A), in series with a 20-megohm resistor (R_1). The cylinder current (16–220 μa.) is read directly on the microammeter. The voltage difference between cylinder and collector plate P equals the product of R_1 times the cylinder current since the voltage drop in R_1, ranging from 320 to 4640 v., is large compared to that in R_2 ranging from 2 to 30 v.

The collector plate, insulated from the brass channel, is grounded through a 20-megohm resistor R_2. The plate current is calculated from the voltage drop across R_2 (2–30 v.), measured with a Vacuum Tube Electrometer. An auxiliary circuit for protecting this meter in case of sparking to the collector plate consists of a high inductance L in series with the resistor, with a low-voltage spark gap shunting both.

The aerosol prepared in the LaMer–Sinclair homogeneous generator[10] is passed through the charging device at a flow rate of 2 l./min. in a field varying from 5.16 to 18.3 e.s.u. A sample of the emerging aerosol is bypassed through a Millikan oil drop apparatus and the sizes and charges of approximately fifty different particles are measured and averaged for each charging current.

The apparatus used for the penetration measurements reported in this work has been described by Knudson and White[11] and consists of a light scattering cell and a photometer circuit.

Characteristic curves of the charging device appear in Fig. 2 where the number of charges per particle has been calculated as a function of the ion density from the equation for field charging.[12]

$$n = \frac{Q}{e} = \left[1 + \frac{2(D-1)}{(D+2)}\right] \times \frac{Er^2}{e} \times \frac{t}{t + (1/\pi NeK)} \qquad (1)$$

Here

Q is the charge per particle
D is the dielectric constant of the particle
E is the field in statvolts/cm.
r is the radius in cm.
t is the time of charging, sec.
N is the ion density, number per cc.
e is the electronic charge, 4.8×10^{-10} statcoulomb
K is the ion mobility in e.s.u.

The value of r was determined experimentally by the light scattering methods involving higher order tyndall spectra (H.O.T.S.),[13] and also by the time of settling in the Millikan oil drop apparatus.

The value of N in Fig. 2 was calculated from the equation

$$N = i_s/EeK \qquad (2)$$

where i_s is the plate current in statamp./cm.^{2}. The plate current i_s was measured in the absence of aerosol particles, and the assumption made that in the presence of aerosol particles the same ionic current was discharged from the wire. The effect of the space charge due to the presence of the aerosol particles was neglected.

Figure 2 shows that at large values of N, small fluctuations in N will cause a small change in the average charge per particle.

As the first approximation the value of the field in the charging region was assumed to be that at the cylinder[6]: it was calculated from

$$E = [2i/K]^{1/2} \times [1 + KC^2/2ib^2]^{1/2} \qquad (3)$$

where C is $V_{ab}/\ln(a/b)$, V_{ab}, is the difference of potential between the wire and the cylinder, and i the cylinder current per cm. length of wire.

Assuming laminar flow of the aerosol in the charging device, the charges acquired by the particles are a function of the height at which they travel

(7) N. Fuchs, I. Petrjanoff and B. Rotzeig, *Trans. Faraday Soc.*, **32**, 1131 (1936).
(8) C. A. Meek and R. W. Lunt, *ibid.*, **32**, 1273 (1936).
(9) G. Merdel and R. Seeliger, *ibid.*, **32**, 1284 (1936).
(10) V. K. LaMer and P. R. Gendron, *Chemistry in Can.*, **4**, 45 (1952).
(11) H. W. Knudson and I. White, NRL report No. P-2642, 18 (1945).
(12) H. J. White, *Elec. Eng.*, **70**, 682 (1951).
(13) D. Sinclair and V. K. LaMer, *Chem. Revs.*, **44**, 245 (1949).

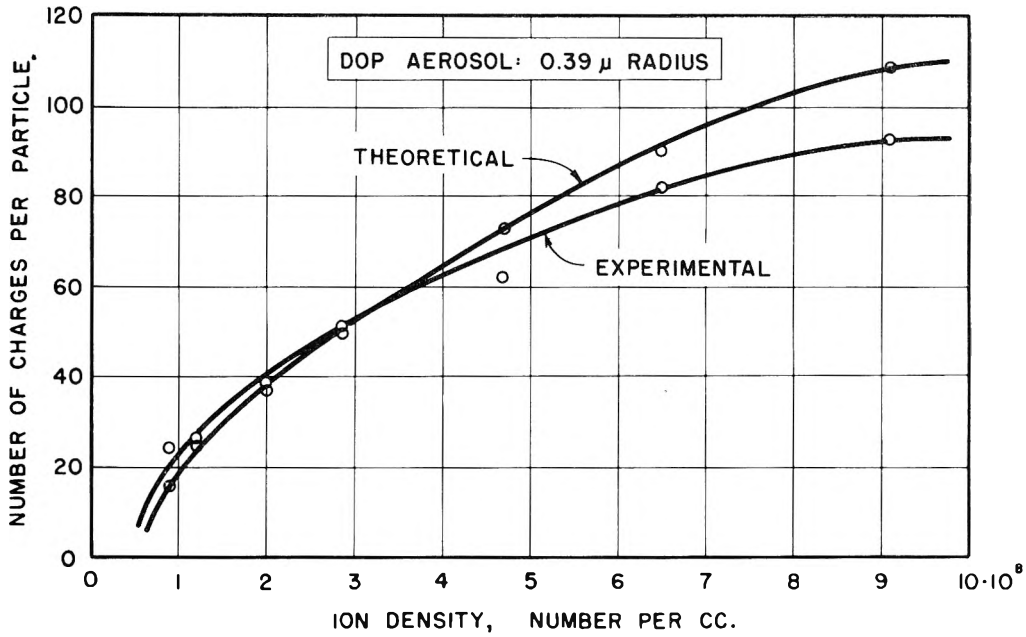

Fig. 2.—Field charging; DOP aerosol, 0.39 μ radius.

in the channel because of the parabolic distribution of velocities along its depth.

The velocity and time of charging distributions have been calculated from the equation reported by Brackett and Daniel.[14]

TABLE I

DISTRIBUTION OF PARTICLE VELOCITIES

Height	v, cm./sec.	t, sec.
Y/8	27.7	0.018
Y/4	47.6	.011
Y/2	63.4	.008

Particles traveling at the top of the channel will not only remain longer in the charging region, but will also pass through a region of higher ion density; hence they will pick up a higher charge.

Assuming a uniform particle radius of 0.385 μ, the calculations show that the limiting charges arising from variations in the time of charging at constant E, cover the range 13 to 21 electronic charges for a field of 5.62 e.s.u., and the range 134 to 151 for a field of 21.82 e.s.u.

The fraction of the maximum charge acquired was calculated for the limiting value of the charging fields employed and for several values of the time of charging, and showed that at $t = 0.012$ sec., which was the actual time of charging employed in the apparatus, only 45% of the maximum charge is acquired at $E = 5.16$, but 89% is acquired at $E = 18.29$. Unfortunately, an increase in the time of charging is impossible because of the precipitation losses. Moreover, N cannot be made larger because of the breakdown potential which sets an upper limit to the operating electrode potential.

The charges acquired by individual particles under various charging conditions were studied. The mean radius and charge ($\bar{r}$, $\bar{n}$) and the deviations (Δr, Δn) from the means were calculated.

Table II lists the per cent. average deviation of both the radius and the charge. As the spread of charge distribution (measured by $\Delta n/n$ 100) for a given aerosol does not vary appreciably with the charging voltage, the $\Delta n/n$ 100 listed is averaged over all charging voltages used.

TABLE II

$r_{\text{H.O.T.S.}}$	$\frac{\Delta r}{r}$ 100, %	$\frac{\Delta n}{n}$ 100, %	2. $\frac{\Delta r}{r}$ 100, %
0.300	12.6	25.4	25.2
.375	9.6	24.7	19.2
.400	9.0	19.9	18.2
.440	8.0	15.0	16.0

The agreement between the third and the fourth columns indicates that the dispersion of charge distribution is mainly due to that of the particle radii. As the generator produces an aerosol with a degree of polydispersity of approximately 10%, we can expect that the charges will have an average deviation of approximately 20% of the mean, since the charge varies as the radius squared.

From these considerations it can be concluded that the spread of particle charges caused by non-uniform charging conditions is of the same order of magnitude as that arising from the variation in the particle radius, *i.e.*, in the particle size distribution. Even under optimum conditions, a 20% charge distribution is still to be expected because of non-uniformity of size.

Figure 3 shows the average particle charge as a function of the cylinder current for several particle radii. The spread of these averaged values is shown by the scattering of the circles from the curve for 0.4 μ radius.

When the individually measured charges are plotted as a function of the particle radius, both measured in the Millikan apparatus, the plot exhibits, of course, a wider scattering of the points. The size distribution of the aerosol, the velocity distribution in the channel, and the electrical winds are some of the many possible factors producing the broad distribution of charge. For a given

(14) J. H. Daniel and F. S. Brackett, *J. Appl. Phys.*, **12**, 542 (1951).

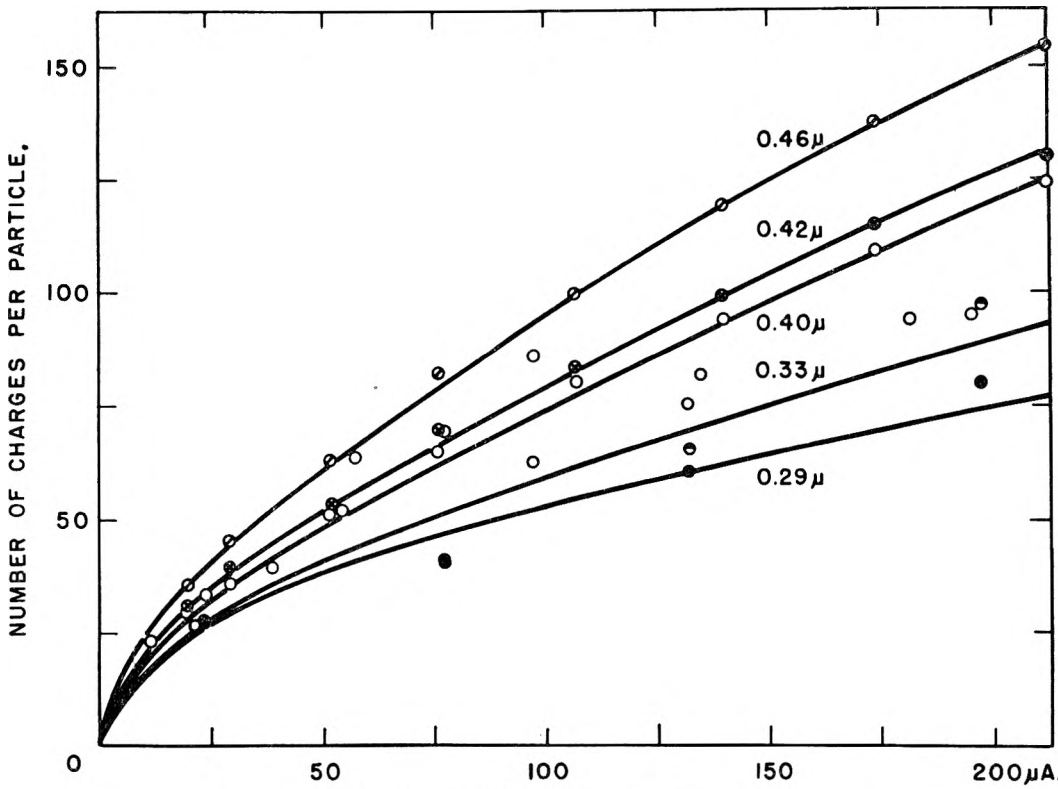

Fig. 3.—Average particle charge *vs.* cylinder current.

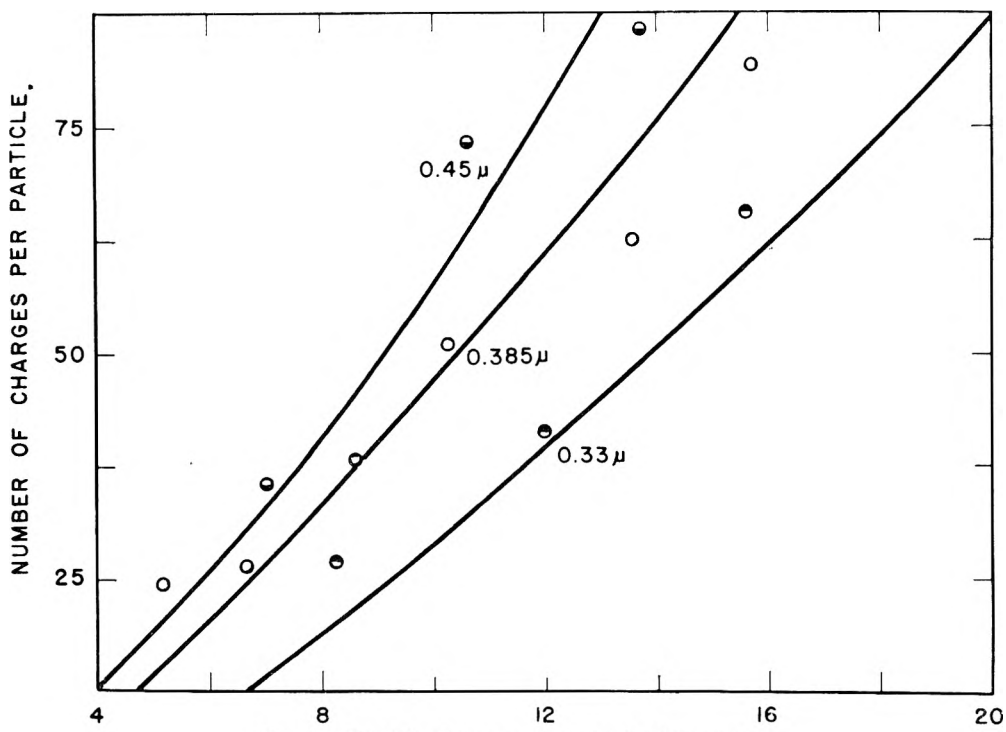

Fig. 4.—Particle charge *vs.* charging field in e.s.u.

charging field, the maximum charge is obviously not attained.

Nevertheless, the order of magnitude of the charge per particle shown on Fig. 3 is reliable. The theoretical charge was calculated from the experimental values of the fields for three particle radii. The results are plotted in Fig. 4. Neglecting the effects due to diffusion of ions, the experimental points agree fairly well with the calculated curve. The values of charge acquired from the diffusion mechanism are thus shown to be negligible compared with the ones reported in Fig. 4. The poorer agreement for large values of the field as compared to lower values can be explained by the

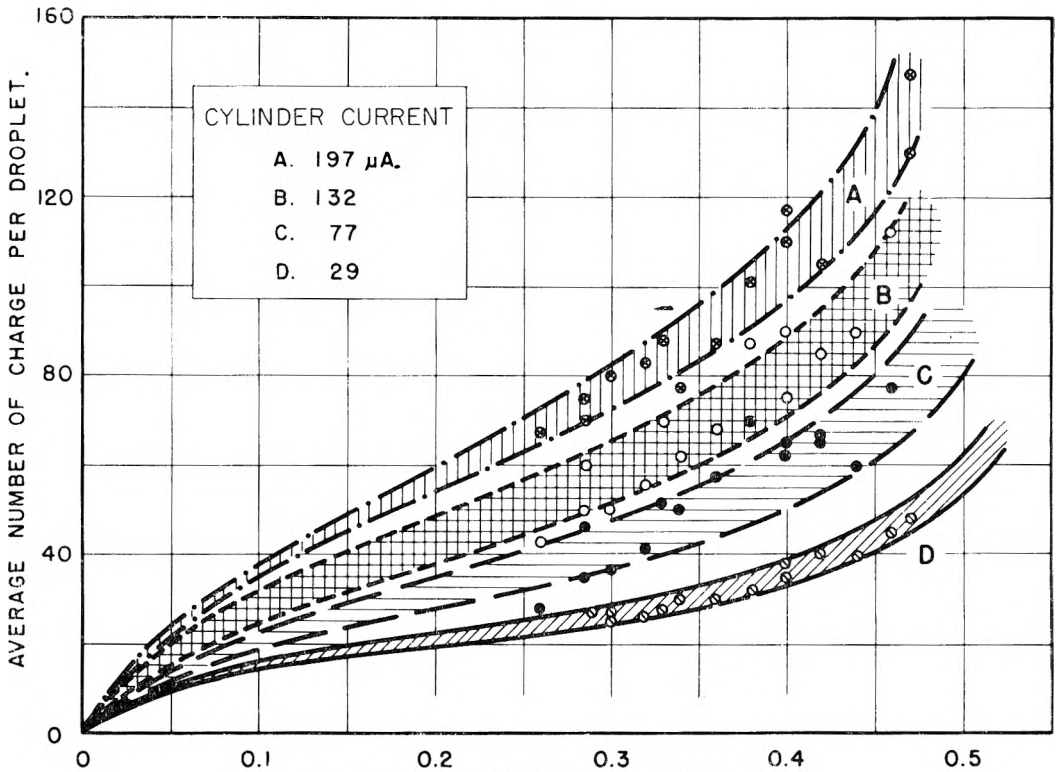

Fig. 5.—Range of droplet charge *vs.* droplet size in μ.

fact that the simple equation for field calculation in a wire-to-cylinder corona discharge does not apply to the modified conditions in the present apparatus, especially at higher voltages. Moreover, at such high voltages (> 8000 v.) electrical winds appear which disturb not only the field, but also the laminar flow of the aerosol. In any case, these curves show an average discrepancy of 14% between the theoretical and the experimental curves, easily accounted for by the theoretical considerations above.

Figure 5 shows the range of the average particle charge as a function of particle radius at different cylinder currents. The range of average charge is fairly well defined at each charging voltage.

Results

Penetrations were measured at four charging voltages corresponding to values of the cylinder current of 29, 77, 132 and 197 microamps. Corrections were introduced for the losses due to charging

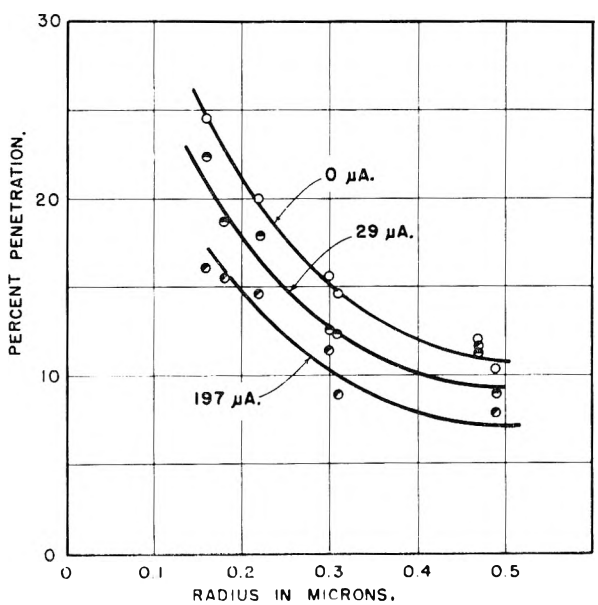

Fig. 6.—Filtration of charged DOP aerosol; CC-5 filter, linear velocity = 2.52 cm./sec.

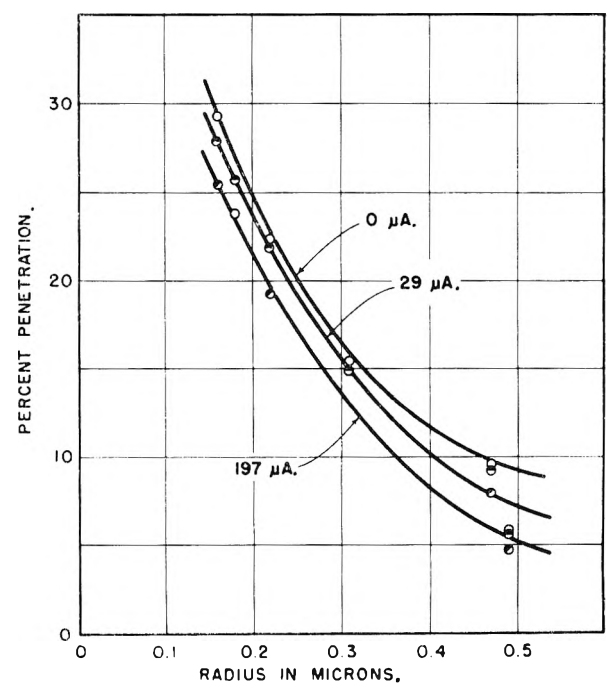

Fig. 7.—Filtration of charged DOP aerosol; CC-5 filter, linear velocity = 28.01 cm./sec.

at each voltage, in the filter holder and connecting tubes.

Penetration measurements have been performed on Chemical Corps No. 5 filters with charged dioctyl phthalate aerosol ranging in particle size from 0.15 to 0.50 μ radius at two linear velocities, 2.5 and 28.0 cm./sec. The penetration percentages averaged over several filter samples are plotted in Figs. 6 and 7. The linear velocity was varied by using filter holders of different area: (1.19 and 13.00 cm.^{2}) for a constant flow rate of 2 l./min.

For a given droplet radius, the results show that the penetration decreases as the average particle charge increases. The average decrease of penetration is 20.3% of the penetration of uncharged particles at 28 cm./sec. and 45.2% at 2.7 cm./sec.

At the slower velocities the effect of particle charges on filtration characteristics should, of course, be greater because of the longer time the particle is subjected to the attraction of the filter fibers. A general trend in every case of this series of experiments indicates that the larger percentage decrease in penetration values occurs for charges corresponding to the lower cylinder currents, 29 and 77 μa. The decreases at 132 and at 197 μa. are nearly equal. In other words, the percentage decrease in penetration is not a linear function of charges. The experimental data now on hand only suggest this trend which further data should clarify.

An absolute value of charge cannot be attributed to any of the penetration curves since the charge increases with particle size. At a cylinder current of 197 μa. the average charge varied in the particle size range indicated from 47 to 130 electronic charges, and at 29 μa. from 19 to 45 electronic charges. It should be noted that at larger sizes a threefold increase in charge produces the same percentage decrease in penetration as the 1.5-fold increase at smaller sizes.

Penetration of charged aerosol particles as a function of average particle charge shows that the effect of charges is larger the smaller the droplet size. This effect is explained as follows. Under our charging conditions, the number of charges per unit area (n/r^2) of the droplet is larger the smaller the size of the droplet. Consequently, the forces acting on the charged droplets due to polarization charges on the fibers will decrease with increasing size of droplet. The evaluation of the effect of the electrostatic charge on the various mechanisms of filtration as a function of droplet size will be simplified when n/r^2 is kept constant for all sizes.

The over-all average deviation for this series of experiments is of the order of 4.5% of the average penetration value. Hence the observed decrease in penetration upon charging is much larger than the experimental errors.

Acknowledgment.—We are indebted to Miss Joan Kruger of this Laboratory for the performance of the penetration measurements and to Mr. G. W. Hewitt of the Westinghouse Corporation for his advice and suggestions on the design of the aerosol charging device. We also thank the Protective Division of the Naval Research Laboratory for the continued loan of certain filtration equipment.

A ROTATING COMBUSTION BOMB FOR PRECISION CALORIMETRY. HEATS OF COMBUSTION OF SOME SULFUR-CONTAINING COMPOUNDS[1]

BY WARD N. HUBBARD, CHARLES KATZ AND GUY WADDINGTON

Contribution No. 37 from the Thermodynamics Laboratory, Petroleum Experiment Station, Bureau of Mines, Bartlesville, Okla.

Received June 6, 1953

To obtain accurate heat of formation data for organic sulfur compounds, a heat of combustion calorimeter has been developed in which it is possible to rotate the bomb after the combustion. Rotation of the bomb tends to produce a thermodynamically defined final state for the combustion process, because the stirring action hastens the attainment of (a) homogeneity of the bomb solution and (b) equilibrium with respect to solution of the bomb gases in the solution. Uncertainties inherent in the use of conventional calorimeters for heat of combustion studies of sulfur compounds are thereby minimized. Results, comparable in precision to those possible in similar studies of hydrocarbons, have been obtained. The indications are that the rotating bomb will have many other applications in combustion calorimetry, particularly in cases in which it is advisable to add a large amount of liquid to the bomb. The following values in kcal. mole^{-1} are reported for the standard heats of formation, $\Delta H_f°(25°)$, of some organic sulfur compounds from graphite, hydrogen gas and rhombic sulfur: 1-pentanethiol, (l) -36.1_2, (g) -26.2_3; 3-thiapentane, (l) -28.9_7, (g) -20.4_0; 2-methyl-2-propanethiol, (l) -33.7_6, (g) -26.3_7; thiacyclopentane, (l) -17.3_1, (g) -8.0_8; thiacyclobutane, (l) $+6.2_0$, (g) $+14.7_8$; and thianthrene, (s) $+43.6_8$.

Introduction

Procedures for accurate heat of combustion determinations for compounds of carbon, hydrogen and oxygen, and for compounds of carbon, hydrogen, oxygen and nitrogen, have been evolved during recent decades. However, reliable procedures have been lacking for compounds that contain either sulfur or the halogens, and the accumulation of thermochemical data for such compounds has consequently been slow. Because of the current importance of sulfur compounds in petroleum technology, this Laboratory, during the past several years, has developed methods for determining, with high accuracy, the heats of combustion and

(1) This investigation was part of American Petroleum Institute Research Project 48A on "The Production, Isolation and Purification of Sulfur Compounds and Measurement of their Properties," which the Bureau of Mines conducts at Bartlesville, Okla., and Laramie, Wyo.

formation of organic sulfur compounds by bomb calorimetry. The main problems were concerned with equipment and techniques that would yield a final state in the bomb that could be defined thermodynamically and could be referred thermochemically to accepted standard states.

When the combustion of an organic sulfur compound occurs in a bomb that is charged with pure oxygen, the sulfur appears in the products of combustion in both its +4 and +6 oxidation states. The mixture of products is not stable, and consequently the combustion reaction is not suitable for high-precision calorimetry. However, it is the usual practice to direct the oxidation so that the +6 oxidation state (sulfuric acid) alone is formed. The oxidation is so directed by deliberately contaminating the oxygen with nitrogen by not removing the air from the bomb before it is charged. Oxides of nitrogen are then formed in the combustion reaction, and these catalyze the oxidation of the sulfur to the +6 oxidation state.

Since 1934 several investigators have studied the combustion calorimetry of organic sulfur compounds and attempted to obtain results comparable in precision and accuracy with other modern thermochemical studies. Becker and Roth[2] carried out the combustions in a bomb to which 10 ml. of water had been added and then applied corrections for the difference in concentration of sulfuric acid that was formed in various parts of their bomb. However, it is probable that equilibrium with respect to the solution of the bomb gases in the final solution is not established in this method and that the results are therefore of doubtful accuracy. In 1935, Huffman and Ellis[3] developed a method in which no liquid water is added to the bomb. They assumed that the sulfuric acid is formed in the combustion process as a mist and condenses at a uniform concentration on the various parts of the bomb. However, experiments in this Laboratory have shown that the concentration of the sulfuric acid varies enough in different parts of the bomb to lead to significant errors. This circumstance, and other uncertainties connected with the Huffman–Ellis method, have made a more satisfactory method desirable.

At the University of Lund in Sweden, Sunner[4] studied the combustion calorimetry of organic sulfur compounds in moving-bomb[5] calorimetric systems. A relatively large amount of water was added to the bomb. After the combustion had occurred, the bomb was oscillated or rotated to promote equilibrium and homogeneity in the final state of the combustion process. This method appears to overcome the difficulties of non-equilibrium of the bomb contents in the Becker–Roth method and of inhomogeneity in the Huffman–Ellis method. For this reason, and because a moving-bomb calorimetric system has many possible applications to compounds other than those that contain sulfur, a rotating-bomb system was designed and built in this Laboratory. This paper describes the apparatus, discusses the method that was used for organic sulfur compounds and reports some of the results that were obtained.

(2) G. Becker and W. A. Roth, *Z. physik. Chem.*, **A169**, 287 (1934).

(3) H. M. Huffman and E. L. Ellis, *J. Am. Chem. Soc.*, **57**, 41 (1935).

(4) S. Sunner, (a) *Svensk Kem. Tid.*, **58**, 71 (1946); (b) Thesis, University of Lund (1950).

(5) The expression "moving-bomb" calorimetric system is used to describe a calorimetric system in which it is possible to agitate the contents of the bomb (after the combustion has occurred) by mechanical rotation or oscillation of the bomb, as distinguished from the conventional "stationary" or "static" systems.

Experimental

Apparatus.—A constant temperature jacket type calorimetric system is used. Figure 1 is a diagrammatic sectional view of this apparatus, which consists of the conventional parts (including calorimeter A, constant temperature jacket B and B′, and thermometer C) and a mechanism to rotate the bomb. The constant temperature jacket has two parts, tank B and lid B′ that cover the calorimeter "well" (the air space in which the calorimeter is suspended). The external parts of the jacket are brass and are nickel-plated and polished. The inner boundary of the jacket (the walls and top of the well) and the calorimeter can are 1-mm. copper sheet and are chromium-plated and brightly polished to minimize heat transfer by radiation. Water in the jacket is stirred by stirrers D and D′. A centrifugal pump at the base of stirrer D′ circulates water, first through one side of a hollow hinge into one side of the double-walled jacket lid, then around partition E in the lid into the other side of the jacket lid, and then back into the jacket tank through the other side of the hollow hinge. The jacket water is maintained at constant temperature to ±0.002° by balancing a small constant flow of cold water against an intermittent heat input supplied by a 100-watt tubular heater. Excess water overflows through tube F. The heater is actuated intermittently by a vibrating fixed-point mercury-in-glass thermoregulator in conjunction with an electronic relay.

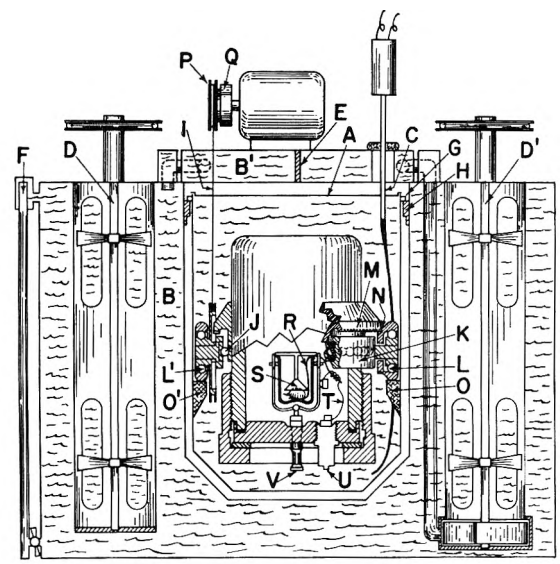

Fig. 1.—Sectional view of calorimetric system with bomb and rotating mechanism in place in calorimeter.

Calorimeter A is suspended in the jacket well. Three pegs G near the top of the calorimeter walls rest in V-grooves in corresponding plastic blocks H. The shape of the calorimeter and the walls of the well are such that a 10-mm. air gap separates them on all sides. The only objects in this space are the three supports H, part of thermometer C, drive wire I for the rotating mechanism, and four electrical leads which are not shown.

Figure 1 also shows the bomb and rotating mechanism in place in the calorimeter. The bomb is supported by ball bearing J mounted in yoke K, which may rotate in ball bearings L and L′. The yoke is rotated by the withdrawal of copper wire I, wound on a pulley on one axle of the yoke. Rotation of the yoke gives the bomb an end-over-end motion

perpendicular to the plane of Fig. 1. As the bomb rotates in this manner, gear M fastened to it walks around another gear N, fixed to the stationary outer race of bearing L, and the bomb spins about its longitudinal axis. The gear ratio is such that the bomb makes $4^3/_8$ end-over-end rotations to 1 spin on its axis. Consequently the path of the liquid in the bomb does not repeat itself until 35 complete end-over-end rotations have occurred.

A few details about the use of the mechanism follow. The mechanism (including bearings L and L′, which in construction are pressed upon the yoke axles) is assembled on the bomb outside the calorimeter. A fine copper wire (No. 28 B & S gage) is fastened to the yoke pulley (by a knot inserted in a keyhole slot) at such a point that tension on the wire when completely unwound will bring the bomb again to its initial position. The wire is then wound around the pulley 15 times, and the bomb and mechanism are placed in the calorimeter in such a way that bearings L and L′ rest in positioning grooves in copper blocks O and O′. Next, the bomb is inverted, and two spring clips, which serve as electrical leads and hold the bomb in a stationary position (one clip is shown in Fig. 3, item 6), are connected to the bomb. The wire is passed through a 0.5-mm. diameter sapphire orifice (Fig. 3, item 4) in the calorimeter lid, then through a hole in the jacket lid and is attached to pulley P driven by a small synchronous motor. Rotation may then be started at the appropriate time when the motor is turned on. As motion begins, the electrical circuit clips are disconnected and snap out of the way. Then a link that connects pulley P directly with drive plate Q is removed. After removal of the link, pulley P is driven only by friction against plate Q. The direct drive link is necessary initially, since the starting torque is large because of the clips. When the copper wire has been unwound from the yoke pulley, the drive pulley slips on plate Q, exerts tension on the wire and brings the bomb into its initial position.

Two combustion bombs are used. Bomb Pt-3, which was used for measurements on all of the compounds except thiacyclobutane, is made of stainless steel and is lined with platinum 0.01 inch thick. The electrodes, gimbal, crucible and other internal fittings are fabricated from pure platinum. The sealing gasket, $^1/_{16}$ inch thick, is fine gold. The internal volume is 0.3433 l. Bomb Pt-4, which was used for the measurements on thiacyclobutane, is similar except that the internal volume is 0.3471 l.

The bomb is used in the calorimeter in the inverted position shown in Fig. 1. With this arrangement, the combustion gases come into contact only with pure platinum and with the aqueous solution that covers the valve and gaskets. The crucible is supported in a gimbal. This arrangement permits various preparatory operations, such as the addition of water to the bomb *while it is in a normal upright position*, and allows the bomb to be inverted for combustion experiments without spilling the contents of the crucible. The gimbal is designed so that when the bomb is turned past the inverted position, when rotation is started after combustion has occurred, the crucible drops from its support and is washed by the aqueous solution.

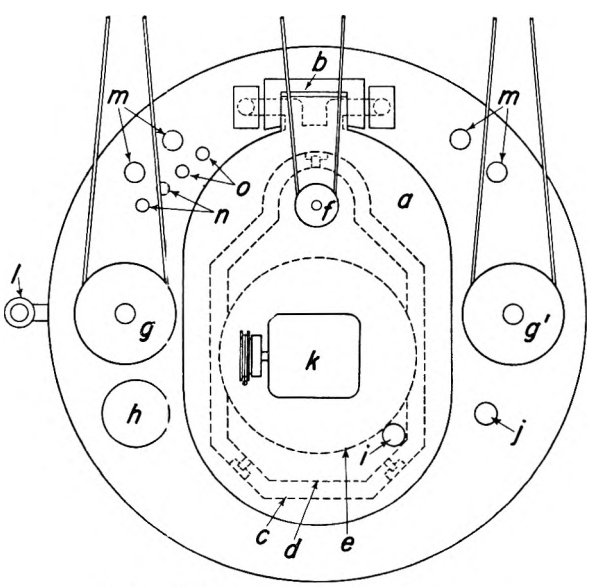

Fig. 2.—Top view of calorimetric system.

Figure 2 is a top view of the calorimetric system. It shows the cylindrical form of the outside of the jacket, the shape of the jacket lid a and its hinge b. Dashed lines show the openings in the hinge through which jacket water is pumped into and out of the lid. The other dashed lines, c, d and e, show the shape and position of the well, calorimeter and calorimeter lid, respectively. Pulley f, which is driven by a synchronous motor that operates from a constant-frequency power supply, is the end of a spring collet that drives a stirrer in the calorimeter. Pulleys g and g′ drive the jacket stirrers. Ports h, i and j are for the jacket thermoregulator, the calorimeter thermometer and the jacket thermometer, respectively. Fig. 2 also shows bomb-rotating motor k, overflow pipe l, jacket heater terminals m, calorimeter heater terminals n and terminals o for the electrical ignition circuit.

Figure 3 is a perspective view of the calorimeter can. To accommodate the rotating bomb, the calorimeter must be larger for this system than for a static system. The rather unusual shape of the calorimeter is the result of an effort to keep the volume as small as possible. Shown in Fig. 3 are: 1, the stirrer for circulating water in the calorimeter can; 1′, the oil seal through which the stirrer shaft passes; 2, the pegs for suspending the calorimeter in the jacket well; 3, the calorimeter heater to bring the temperature up to the desired starting value; 4, the sapphire orifice in the lid through which the drive wire passes; 5, the partition that separates the stirrer well from the rest of the calorimeter; 6, the spring clip that serves as an electrical lead and device for positioning the bomb; and 7, the opening for the calorimeter thermometer.

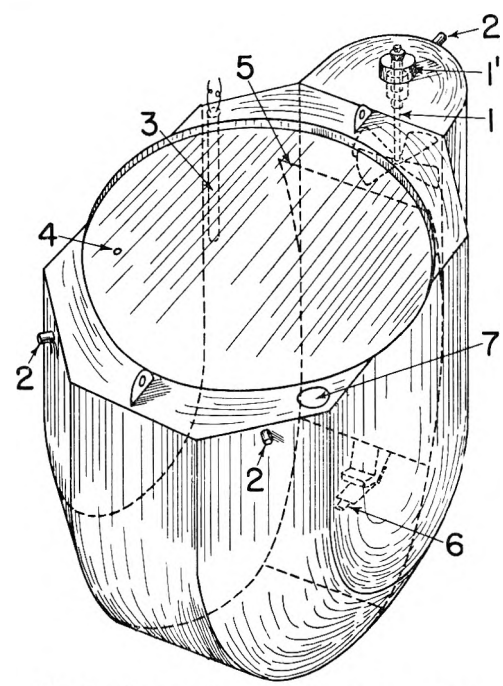

Fig. 3.—Perspective view of calorimeter can.

Temperature measurements are made with a 25-ohm calorimetric type platinum resistance thermometer (bent to fit along the wall of the calorimeter) the resistance of which is measured with a type G-2 Mueller bridge and a sensitive galvanometer. A rubber bushing on the shaft of the thermometer closes the opening in the calorimeter (Fig. 3, item 7) when the system is assembled.

Calibration.—The energy equivalent of the calorimeter, $C_{eff.}$ (calor.), is determined by combustion of benzoic acid (National Bureau of Standards standard sample 39 g.). The certificate value of 26.4338 abs. kj. $g.^{-1}$ (weight in vacuum) is taken for the quantity of heat evolved by combustion of the sample under the specified standard conditions. Corrections are applied for deviations of the experi-

mental conditions from standard. These deviations are kept as small as possible for reasons discussed later. Calibration experiments are interspersed with the heat of combustion experiments for each organic sulfur compound. The values that were obtained for $C_{eff.}$ (calor.) in each series of calibration experiments are included in Table I.

Experimental Procedures.—Each liquid sample was contained in a thin-walled soft glass (except as otherwise noted) ampoule filled by the method previously described.[6] A small amount (0.01 to 0.1 g.) of mineral oil (Nujol) was used to initiate combustion of the liquid samples. Solid thianthrene samples were pelleted, and no auxiliary oil was used. Samples of sulfur and oil mixtures were prepared by placing a few pieces of sulfur in the crucible and then adding oil.

After the sample has been weighed, one end of a weighed (0.004 ± 0.00025 g.) fuse of ashless filter paper (Fig. 1, item R) is placed under or in the sample in the crucible. A platinum baffle[7] (Fig. 1, item S) is hung over the charge and the crucible is placed in the gimbal. The other end of the fuse is placed in a double loop in the ignition wire (Fig. 1, item T). The loop is then collapsed on the fuse to hold it in place and give good contact. Ten grams of water is added to the bomb. The bomb, which initially contains air at atmospheric pressure, is assembled and charged with oxygen to a total pressure of 30 atm.

Water is added to the calorimeter can. The can and inside of the well are polished. The calorimeter (including the water) is placed on a balance, and the amount of water in it is adjusted against a tare weight to ±0.03 g. The calorimeter is then placed in the jacket well. The charged bomb, with the rotating mechanism attached, is lowered into the calorimeter, inverted and positioned by the clips. The drive wire is then fed through the orifices in the lids of the calorimeter and jacket, the calorimeter lid is pressed into place and the jacket lid is lowered over the well. The drive wire is connected to the pulley (Fig. 1, item P), the calorimeter stirrer (Fig. 3, item I) is coupled with the collet pulley (Fig. 2, item f) and the calorimeter thermometer (Fig. 1, item C) is placed in position.

After the system is assembled, the calorimeter is heated to a temperature about 0.07° lower than the temperature at which observations of the initial period are to be started. Then the temperature of the calorimeter is allowed to drift the remaining 0.07°, a matter of about 18 minutes duration. In the inital period, observations are made of time at selected values of the resistance of the thermometer (0.0005-ohm intervals over a 0.0040-ohm range). In the reaction period (about 780 seconds), the observations are continued. However, the intervals between resistance values are no longer constant. The values have been chosen such that a well-defined plot of resistance *vs.* time can be made. When the temperature is increasing most rapidly, the observations are made as often as every 5 to 7 seconds, but they are made less frequently later in the reaction period when the temperature is increasing more slowly. In the after period, observations are made of the resistance at 2-minute intervals for a 16-minute period during which the resistance changes about 0.0002 ohm.

In each standard combustion experiment, the calorimeter temperature at the beginning of the reaction period is 23.00°, and the corrected temperature rise is 2.00°. In special instances in which other values of the change of temperature are necessary, the reaction period is started at a temperature that is lower than 25.00° by the amount of the anticipated corrected increase in temperature. Combustion is initiated by a switch that automatically connects the ignition circuit[8] to a 6-volt battery for 0.6 second. When the increase in temperature of the calorimeter is 0.6 of the expected total increase (about 70 seconds after ignition), rotation of the bomb is started and continued for 15 complete end-over-end rotations at a speed of 10 r.p.m.

After the calorimetric observations have been made, the bomb gases are discharged through a scrubber that contains a known amount of sodium hydroxide solution. This solution is transferred to a volumetric flask and diluted to 200 ml. The bomb is opened, the inner parts and walls are washed with distilled water, the washings are collected and these are diluted to 250 ml. The following analyses are made on aliquots of these solutions. Nitrite ion is determined colorimetrically by the Griess method.[9] Total acid is determined by titration, either before carbon dioxide is removed (brom cresol green indicator) or after the solution has been boiled to remove carbon dioxide (brom phenol blue indicator). Usually no difference is found in cases in which the bomb washings are titrated by both methods. The titrated sample is next placed in a Kjeldahl bulb, and the nitrogen acids are reduced by Devarda's alloy to ammonia. The ammonia is distilled into standardized hydrochloric acid solution, which is then back-titrated with standardized sodium hydroxide solution. From the amounts of total nitrogen acids and nitrous acid found in these analyses, the amount of nitric acid is computed by difference.

Heats of Combustion

Materials.—The samples of liquid organic sulfur compounds were prepared and purified at the Laramie Station of the Bureau of Mines as part of A. P. I. Research Project 48A. The thianthrene sample was furnished by Dr. Stig Sunner of the University of Lund, Lund, Sweden. The purity of each sample is listed in Table II.

The sample of rhombic sulfur was prepared as follows: 350 g. of commercial "flowers of sulfur" was dissolved in 3 l. of toluene heated nearly to boiling. The solution was cooled rapidly to 5°, then filtered and the sulfur dried in vacuum for 2 days. The method described by Bacon and Fanelli[10] was then used to free the sulfur from organic material. Three 6-hour periods of boiling with magnesium oxide were required. The sulfur was then sublimed. Bacon and Fanelli's test for organic material in sulfur showed no black spots or discoloration when applied to the sublimed material.

Units of Measurement and Auxiliary Quantities.—The results of the combustion experiments are expressed in terms of the defined calorie equal to 4.1840 abs. joules and refer to the isothermal process at 25° and to the true mass. For the reduction of weights to vacuum, the density values used were (in g. ml.$^{-1}$ at 25°): for rhombic sulfur, 2.07; thianthrene,[11a] 1.44; 1-pentanethiol,[11b] 0.83763; 2-methyl-2-propanethiol,[11b] 0.79472; 3-thiapentane,[11b] 0.83120; thiacyclobutane,[11b] 1.01472; and thiacyclopentane,[11b] 0.99379. The molecular weights were computed from the 1951 table of international atomic weights.[11c] The observed values for the heat of the bomb process were corrected to obtain values for the energy of the idealized combustion reaction in which all the reactants and products are in their standard states at 25° and no external work is performed. The corrections, which included those for the formation of nitric and nitrous acids and for the dilution of sulfuric acid, were made as described by Hubbard, Scott and Waddington.[12] The heats of formation of water and carbon dioxide were taken to be 68,317.4[13] and 94,051.8[14] cal. mole^{-1}, respectively. The values of the energy of the idealized combustion reaction, $-\Delta U_c^\circ/M$, for the filter paper fuse and Nujol auxiliary oil were 3,923 and 10,544 cal. g.$^{-1}$. The electrical energy for the ignition of the fuse was 1.35 cal. per combustion.

Results.—The results of the individual combustion experiments are presented in Table I. The columns of the table list the series and number designation of each experiment; the mass of com-

(6) G. B. Guthrie, Jr., D. W. Scott, W. N. Hubbard, C. Katz, J. P. McCullough, M. E. Gross, K. D. Williamson and G. Waddington, *J. Am. Chem. Soc.*, **74**, 4662 (1952).

(7) The baffle is a modification of Sunner's "top"[4b] and is used to prevent mechanical loss of sample by spattering.

(8) The total resistance of the circuit, exclusive of the battery, is 1.44 ohm, and the resistance of the platinum ignition wire (0.006 inch diameter) alone is 0.40 ohm

(9) F. P. Treadwell and W. T. Hall, "Analytical Chemistry," Vol. II, 9th Eng. Ed., John Wiley and Sons, Inc., New York, N. Y., 1946, p. 306.

(10) R. F. Bacon and R. Fanelli, *Ind. Eng. Chem.*, **34**, 1043 (1942).

(11) (a) S. Sunner and B. Lundin, "Thermochemical Investigations on Organic Sulfur Compounds. III. On the Possible Use of Thianthrene as a Secondary Standard for Sulfur Compounds," to be published; (b) W. E. Haines, R. V. Helm and J. S. Ball, unpublished results A. P. I. Research Project 48A; (c) E. Wichers, *J. Am. Chem. Soc.*, **74**, 2447 (1952).

(12) W. N. Hubbard, D. W. Scott and G. Waddington, THIS JOURNAL, **58**, 152 (1954).

(13) D. D. Wagman, J. E. Kilpatrick, W. J. Taylor, K. S. Pitzer and F. D. Rossini, *J. Research Natl. Bur. Standards*, **34**, 143 (1945).

(14) E. J. Prosen, R. S. Jessup and F. D. Rossini, *ibid.*, **33**, 447 (1944).

TABLE I

RESULTS OF COMBUSTION EXPERIMENTS

Series and no.	m', g.	ΔT_c, deg.	q_{oil}, cal.	q_{fuse}, cal.	q_{CO_2}, cal.	q_N, cal.	$q_{diln.}$, cal.	$q_{corr.}$, cal.	$\Delta U_c^\circ/M$, cal. g.$^{-1}$
1-Pentanethiol									
M = 104.212, n = 115, $C_{eff.}$(calor.) = 3916.0 ± 0.22, $C_{eff.}$(cont.) = 13.2									
A1	0.63890	1.67684	− 517.38	−15.93	2.72	11.33	−0.31	−0.43	−9454.8
A2	.62964	1.68643	− 640.20	−15.85	2.73	10.64	− .29	− .42	−9459.9
A3	.63193	1.67848	− 591.59	−15.69	2.72	10.92	− .29	− .41	−9452.8
A4	.62900	1.67633	− 615.00	−15.93	2.73	6.50	− .28	− .41	−9452.8
A5	.61795	1.68544	− 745.06	−16.16	2.74	11.19	− .25	− .38	−9461.2
A6	.60463	1.68356	− 868.74	−15.57	2.77	10.78	− .23	− .35	−9454.5
A7	.60713	1.68432	− 847.20	−16.05	2.76	10.78	+ .01	− .35	−9454.8
A8	.52843	1.67716	−1560.71	−16.01	2.88	10.64	+ .01	− .17	−9459.1
A9	.56940	1.68300	−1200.54	−15.65	2.82	8.98	− .10	− .27	−9455.4
								Av.	−9456.2 ±1.09
3-Thiapentane									
M = 90.186, n = 80, $C_{eff.}$(calor.) = 3908.4 ± 0.17, $C_{eff.}$(cont.) = 13.5									
B1	0.68040	1.68154	− 304.54	−15.73	2.51	9.81	−0.04	−0.71	−9202.7
B2	.69027	1.68442	− 219.12	−16.20	2.48	10.09	− .05	− .70	−9210.2
B4	.68106	1.68185	− 294.21	−16.24	2.51	10.09	− .04	− .73	−9209.6
C1	.66784	1.68532	− 430.39	−15.77	2.84	12.85	− .02	− .70	−9204.4
C2	.68761	1.67857	− 221.32	−15.69	2.51	10.35	− .05	− .71	−9209.5
C3	.69704	1.77190	− 516.29	−16.08	2.66	11.33	− .07	− .69	(−9184.8)
								Av.	−9207.3 ±1.55
2-Methyl-2-propanethiol									
M = 90.186, n = 70, $C_{eff.}$(calor.) = 3908.6 ± 0.18, $C_{eff.}$(cont.) = 13.6									
A1	0.74963	1.99689	− 955.07	−16.32	3.01	9.40	+0.03	−0.76	(−9135.0)
A2	.74375	2.00245	−1015.21	−15.54	3.07	12.02	+ .06	− .72	−9152.9
A3	.81211	2.00531	− 400.63	−15.22	2.96	12.44	− .10	− .89	−9153.5
A4	.76691	2.00227	− 802.58	−15.69	3.04	11.61	+ .01	− .82	−9153.6
A5	.78915	1.99782	− 589.29	−16.32	2.99	10.23	− .04	− .84	(−9144.6)
B1	.76937	2.00140	− 775.10	−15.81	2.98	11.75	− .02	− .79	−9155.1
B2	.76615	2.00084	− 795.22	−16.12	2.98	11.35	− .01	− .79	(−9164.6)
B3	.75014	1.99981	− 945.95	−16.52	3.00	11.51	+ .03	− .77	−9152.8
B4	.74405	1.99980	−1002.35	−16.05	3.03	11.36	+ .04	− .77	−9152.8
								Av.	−9153.5 ±0.36
Thiacyclopentane									
M = 88.170, n = 60, $C_{eff.}$(calor.) = 3908.6 ± 0.16, $C_{eff.}$(cont.) = 13.5									
A1	0.80423	1.99797	− 744.96	−16.63	3.05	10.89	+0.14	−0.28	−8778.1
A2	.79321	1.99774	− 846.88	−16.01	3.06	11.06	+ .14	− .28	−8771.0
A3	.78145	1.99691	− 942.09	−16.12	3.08	9.99	+ .18	− .28	−8778.2
A5	.79774	1.99702	− 797.73	−16.32	3.06	10.27	+ .15	− .28	−8779.9
A6	.86022	1.99942	− 261.98	−16.24	2.96	10.53	+ .02	− .28	−8776.0
B1	.82739	2.00020	− 550.26	−16.52	3.02	10.60	+ .08	− .28	−8778.9
B2	.82478	1.99757	− 563.89	−15.26	3.02	10.79	+ .08	− .28	−8779.0
B3	.81262	1.99834	− 674.16	−15.61	3.03	9.95	+ .10	− .28	−8778.7
								Av.	−8777.4 ±1.03
Thiacyclobutane									
M = 74.144, n = 59, $C_{eff.}$(calor.) = 3909.6 ± 0.32, $C_{eff.}$(cont.) = 13.6									
A1	0.79388	2.00154	−1023.56	−15.38	2.79	8.98	+0.21	−0.58	(−8566.5)
A2	.80431	1.99948	− 924.38	−15.77	2.70	9.95	+ .16	− .60	−8567.2
A3	.82847	1.99842	− 713.82	−15.93	2.70	8.33	+ .10	− .62	(−8568.1)
A4	.83304	1.99774	− 673.75	−15.61	2.70	8.76	+ .09	− .62	−8566.2
A5	.84476	1.99809	− 570.39	−15.97	2.70	11.37	+ .05	− .63	−8567.9
A7	.85715	2.00021	− 472.43	−15.69	2.68	11.08	+ .02	− .64	−8568.8
								Av.	−8567.5 ±0.46

TABLE I (*Continued*)

Series and no.	m', g.	ΔT_c, deg.	q_{oil}, cal.	q_{fuse}, cal.	q_{CO_2}, cal.	q_N, cal.	$q_{diln.}$, cal.	$q_{corr.}$, cal.	$\Delta U_c^\circ/M$, cal. g.$^{-1}$
B1	0.83801	1.99894	− 635.44	−15.69	2.70	10.13	+0.07	−0.63	−8565.0
B4	.90287	2.02287	− 173.14	−15.69	2.63	10.13	− .12	− .68	−8566.1
B5	.90807	2.03244	− 167.09	−15.81	2.63	11.19	− .16	− .68	−8563.8
								Av.	−8565.0
				Thianthrene					
		M = 216.316, n = 60, $C_{eff.}$(calor.) = 3908.9 ± 0.32, $C_{eff.}^i$(cont.) = 13.5							
A1	0.97769	2.00166	...	−16.16	3.74	9.84	+0.07	+1.95	−7996.6*
A2	.97594	1.99778	...	−15.54	3.72	9.33	+ .07	+1.95	−7996.7
A3	.97540	1.99546	...	−15.34	3.73	7.44	+ .07	+1.95	−7993.8*
A4	.97680	1.99870	...	−16.28	3.72	6.23	+ .07	+1.95	−7995.6
A5	.97654	1.99873	...	−15.65	3.71	8.79	+ .07	+1.95	−7995.9
A6	.97677	1.99930	...	−16.08	3.73	8.04	+ .07	+1.95	−7996.6*
A7	.97657	1.99808	...	−15.57	3.73	6.62	+ .07	+1.95	−7995.3
A8	.97656	1.99951	...	−16.44	3.73	9.33	+ .07	+1.95	−7997.5
A9	.97501	1.99508	...	−15.30	3.72	6.80	+ .07	+1.95	−7996.6*
A10	.97682	1.99923	...	−15.69	3.72	8.02	+ .07	+1.95	−7996.7*
								Av.	−7996.2 ±0.44
				Sulfur (rhombic)					
		M = 32.066, n = 80, $C_{eff.}$(calor.) = 3909.0 ± 0.18, $C_{eff.}^i$(cont.) = 13.7							
A1	0.24279	1.53850	−4927.87	−15.69	2.47	5.91	−0.06	−0.13	−4457.0
A2	.24288	1.53974	−4933.14	−15.85	2.47	6.23	− .06	− .13	−4451.4
A3	.24286	1.53634	−4920.50	−15.61	2.46	6.25	− .07	− .13	−4450.0
A4	.24273	1.53618	−4922.10	−16.08	2.45	3.05	− .07	− .13	−4453.8
A5	.24279	1.53563	−4922.32	−15.57	2.46	2.74	− .07	− .13	−4446.6
A6	.24264	1.53529	−4920.78	−16.16	2.46	2.86	− .07	− .13	−4447.3
								Av.	−4451.0 ±1.65
				Sulfur (rhombic)					
		M = 32.066, n = 60, $C_{eff.}$(calor.) = 3908.6 ± 0.18, $C_{eff.}^i$(cont.) = 13.0							
B1	0.29016	2.45649	−8309.05	−15.97	3.80	10.09	+0.07	+0.29	−4455.1
B2	.29011	2.45450	−8307.29	−15.22	3.79	9.78	+ .07	+ .29	−4438.6
B4	.29016	2.45690	−8310.26	−16.08	3.81	10.54	+ .07	+ .29	−4454.5
B5	.29022	2.45651	−8309.27	−15.67	3.80	10.68	+ .07	+ .29	−4452.7
B6	.29030	2.45570	−8307.84	−14.87	3.80	11.46	+ .07	+ .29	−4445.7
B7	.29012	2.45635	−8309.60	−15.89	3.80	9.76	+ .07	+ .29	−4453.3
								Av.	−4450.0 ±2.68

pound that underwent combustion, m'; the increase in temperature of the calorimeter, corrected for heat transfer and stirring energy during the reaction period, ΔT_c; the correction for the combustion of the auxiliary oil, q_{oil}; the same for the fuse, q_{fuse}; the correction for the heat of solution of carbon dioxide, q_{CO_2}; the correction for the formation of nitric and nitrous acids, q_N; the correction for the difference in the concentration of the actual bomb solution from $H_2SO_4 \cdot nH_2O$ and 0.1 N HNO_3, $q_{diln.}$; the sum of all other corrections to standard states, $q_{corr.}$; and the energy, $\Delta U_c^\circ/M$, of the idealized combustion reaction

$$C_aH_bO_cS_d(s \text{ or } l) + (a + b/4 - c/2 + 3d/2)O_2(g) + (nd + d - b/2)H_2O(l) = aCO_2(g) + d(H_2SO_4 \cdot nH_2O)(l)^{15} \quad (I)$$

The headings for the experiments on each compound give the molecular weight, M; the value of n in eq. I to which the results are referred; the energy equivalent of the calorimeter in cal. deg.$^{-1}$, $C_{eff.}$ (calor.), as determined from a series of 5 to 8 calibration experiments; and the energy equivalent of the initial contents of the bomb in cal. deg.$^{-1}$, $C_{eff.}^i$ (cont.). The uncertainties assigned to C_{eff} (calor.) and $\Delta U_c^\circ/M$ are the standard deviations from the mean. It may not be possible to obtain an exact duplication of the results from the data given, mainly because $C_{eff.}^i$ (cont.) varies slightly from experiment to experiment and only the average value is given in Table I. The values of $\Delta U_c^\circ/M$ enclosed in parentheses are considered uncertain and are rejected in the computation of the average value.

All of the combustion experiments with 1-pentanethiol were satisfactory. The first two experiments with 3-thiapentane, A1 and A2, were made with a 6-gram crucible 13 mm. deep, and incomplete combustion occurred. Experiment B1 and all experiments listed after it in Table I were made with

(15) The terms listed in the various columns correspond to the item numbers in the computation form of Hubbard, Scott and Waddington[12] as follows: m', item 2; ΔT_c, item 79 minus item 78 minus item 80; q_{oil}, item 96; q_{fuse}, item 97; q_{CO_2}, item 87; q_N, item 92; $q_{diln.}$, items 90 and 91; $q_{corr.}$, sum of items 81, 82, 83, 84, 85, 88, 89, 93 and 94; and $\Delta U_c^\circ/M$, item 99.

TABLE II

DERIVED DATA AT 25°, KCAL. MOLE^{-1}. COMPARISON WITH RESULTS OF OTHER INVESTIGATORS

Compound and state	Investigators	Sample	Purity, mole %	$-\Delta U_c°$, reaction I (n = 115)	$-\Delta U_c°$, reaction II	$-\Delta H_c°$, reaction II	$\Delta H_f°$, liquid or solid	$\Delta H_f°$, gas
1-Pentanethiol (l)	This paper	NBS-906	99.92	985.05 ± 0.35	842.24	844.02	−36.12 ± 0.41	−26.29 ± 0.42
	Sunner	NBS-906	99.92	985.33 ± .15	842.15	843.93	−36.23 ± .19	
3-Thiapentane (l)	This paper	NBS-903	99.94	830.16 ± .34	687.35	688.83	−28.97 ± .40	−20.40 ± .41
2-Methyl-2-propanethiol (l)	This paper	NBS-905	99.92	825.37 ± .25	682.56	684.04	−33.76 ± .29	−26.37 ± .30
	Ref. 17	NBS-905	99.92				−34.6	
Thiacyclopentane (l)	This paper	API-USBM-9	99.95	773.80 ± .31	630.99	632.17	−17.31 ± .35	− 8.08 ± .36
	Sunner	SS	...	775.25 ± .10	632.07	633.25	−16.23 ± .16	
Thiacyclobutane (l)	This paper	API-USBM-10	99.95	635.23 ± .20	492.42	493.31	+ 6.20 ± .29	+14.78 ± .30
	Sunner	SS	...	635.30 ± .30	492.12	493.01	+ 5.90 ± .32	
Thianthrene (s)	This paper	SS	99.8	1730.01 ± .38	1444.39	1445.57	+43.68 ± .56	
	Sunner	SS	99.8	1729.30 ± .30	1443.32	1444.50	+42.61 ± .88	
Sulfur (s, rh.)	This paper	USBM-P1	...	142.83 ± .12[a]				
	This paper	USBM-P1	...	142.84 ± .25[a]				
	Sunner	USBM-P1	...	143.28 ± .20[a]				
	Sunner	SS	...	143.13 ± .10[a]				
	Sunner	SS	...	143.13 ± .10[a]				
	Sunner	SS	...	143.18 ± .20[a]				

[a] For reaction III with n = 115.

a 16-gram crucible 25 mm. deep. In five other experiments with 3-thiapentane, B3, B5, B6, B7 and B8, incomplete combustion also occurred. The low value of $\Delta U_c°/M$ in experiment C3 is attributed to incomplete combustion. Preliminary experiments with 2-methyl-2-propanethiol (not listed in Table I) gave erratic results for unexplained reasons. No definite explanations are known for the low value of $\Delta U_c°/M$ in experiment A1 and the high value in experiment B2. A slight deposit of carbon was observed in the bomb after experiment A5. Of all the experiments with thiacyclopentane, only A4 was unsatisfactory. In this experiment, the presence of carbon on the walls of the bomb and pieces of shattered glass indicated a violent bursting (hereafter called explosion) of the ampoule. Experiments A1 and A3 with thiacyclobutane were somewhat uncertain owing to slight calorimetric difficulties. The values of $\Delta U_c°/M$ are in good agreement with the rest of the series, but are not included in the average. Experiment A6 showed signs of explosion. In the B series of experiments, the sample was contained in ampoules made of Vycor (B1), quartz (B2 and B3) and Pyrex (B4 and B5). Both quartz ampoules exploded, probably because they were somewhat thicker walled and heavier (0.25 g.) than the usual ampoule (0.05 to 0.10 g.). The experiments with thianthrene were not entirely satisfactory. In experiments A1, A3, A6, A9 and A10, for which the values of $\Delta U_c°/M$ are starred in Table I, traces of carbon were left in the crucible. Approximately the same average value is obtained for all of the experiments as for the completely satisfactory experiments A2, A4, A5, A7 and A8. The only unsatisfactory experiment with mixtures of rhombic sulfur and oil was B3, in which the bomb smelled strongly of sulfur dioxide when it was opened. Apparently a leak when the bomb was being charged with oxygen allowed some of the air to be flushed out, and not enough nitrogen remained in the bomb to direct oxidation of the sulfur completely to sulfuric acid.

In Table II, the derived data are given and compared with the results of other investigators. The first four columns list the compound and the state (liquid or solid) to which the values of $-\Delta U_c°$ and $-\Delta H_c°$ refer, the investigators who made the determinations, the source of the sample and its reported purity. Designations NBS and API-USBM both denote A. P. I. Research Project 48A samples, the former distributed by the National Bureau of Standards and the latter by the Carnegie Institute of Technology; SS denotes samples prepared at the University of Lund by Dr. Stig Sunner; and USBM-P1 denotes the sample of rhombic sulfur prepared in this Laboratory. The fifth column lists the values of $-\Delta U_c°$ for reaction I, all referred to a common value of 115 for n. A small correction for reaction with the soft glass ampoule material (see discussion in a later section) has been applied to the values of this investigation for 1-pentanethiol, 3-thiapentane, 2-methyl-2-propanethiol and thiacyclopentane. The value of this investigation for thiacyclobutane is based only on the data of the B series of combustion experiments, for which Vycor and Pyrex were used as ampoule material instead of soft glass. The sixth column lists the values of $-\Delta U_c°$ for the combustion to carbon dioxide, water and rhombic sulfur, according to the equation

$$C_aH_bO_cS_d(\text{s or l}) + (a + b/4 - c/2)O_2(g) = aCO_2(g) + b/2H_2O(l) + dS(\text{rh}) \quad \text{(II)}$$

For the calculation of the values of this investigation in column 6, 142.81 kcal. mole^{-1} was used for $-\Delta U_c°$ for the combustion of rhombic sulfur according to the equation

$$dS(\text{rh}) + 3d/2O_2(g) + (nd + d)H_2O(l) = d(H_2SO_4 \cdot nH_2O)(l) \quad \text{(III)}$$

with d equal to 1 and n equal to 115. This value is the average of those for three series of combustion experiments with mixtures of rhombic sulfur and oil, 142.83 for series A, 142.84 for series B, and 142.75 kcal. mole^{-1} for a third series not reported here. The seventh column lists the values of $-\Delta H_c°$ for reaction II. The last two columns list the values of $\Delta H°$ for the formation of the compound in the liquid or solid state, and in the gaseous state, from graphite, hydrogen gas and rhombic sulfur. Values of the heat of vaporization obtained in this Laboratory, either by direct calorimetric

determinations or from vapor-pressure measurements, were used to compute the values of $\Delta H_f°$ for the gas from those for the liquid or solid. The uncertainties given in columns 5, 8 and 9 are uncertainty intervals equal to twice the final "overall" standard deviation.[16]

The results of Franklin and Lumpkin[17] for 2-methyl-2-propanethiol were obtained from two combustion experiments with a "static" illium bomb and a Parr calorimeter. Because of the uncertainties inherent in their method, the agreement of their value for $\Delta H_f°$ with that of this investigation is as good as is to be expected. Sunner's values for 1-pentanethiol, thianthrene and two series for rhombic sulfur are from unpublished work.[18] His values for thiacyclopentane, thiacyclobutane and one series for rhombic sulfur are corrections of the values given in ref. 4b for 20° to refer to the reactions at 25°. Sunner used the value of Craig and Vinal[19] for the heat capacity of $H_2SO_4 \cdot 115H_2O$ for the calculation of the corrections.[18] It is noteworthy that in the case of three of the compounds, 1-pentanethiol, thianthrene and rhombic sulfur USBM-P1, portions of the same sample were used by Sunner and by this Laboratory. However, a strict comparison cannot be made because the methods of (a) calibration and (b) application of corrections for the reduction to standard states that were used by Sunner and by this Laboratory differed considerably. The agreement is good enough to make it appear unlikely that there are any large systematic errors in the methods used in either laboratory.

Discussion of the Method

Calibration and the Method of Comparative Measurements.—When compounds that contain elements other than carbon, hydrogen and oxygen undergo combustion in a bomb calorimeter, the final state of the system is different chemically from that obtained in calibration experiments with benzoic acid. Therefore, the simple application of comparative measurements, in which the combustion and calibration experiments are performed under as nearly identical conditions as possible, is not feasible. Any systematic errors related to the final state of the system are different in the combustion and calibration experiments and do not necessarily cancel. However, it is often possible to plan experiments in such a way that two combustion experiments that have nearly identical final states are compared, and any errors related to the final states are nearly canceled.

For the combustion of an organic sulfur compound in a rotating bomb, it is desirable to add 10 ml. of water to the bomb. The question arises as to whether to perform the calibration experiments with benzoic acid with 10 ml. of water in the bomb or to follow the recommendations of the standardizing laboratory and use approximately 1 ml. of water in the bomb. Ideally, corrections can be applied if the conditions of the calibration experiments differ from the standard ones, and the same value of the energy equivalent should be obtained from calibration experiments with different amounts of water in the bomb. However, the experiments described in the next section suggest that such a result may not be obtained in practice. It may be argued that the calibration experiments should be conducted in a bomb to which the extra water has been added because errors associated with the use of the extra water will tend to cancel. However, the extent to which the errors will cancel depends upon the similarity of the experimental conditions and/or the ability to correct for different conditions. In the case under consideration, if both the calibration experiments and the combustion experiments with organic sulfur compounds are performed with 10 ml. of water in the bomb, the initial states will be comparable, but the final state of the calibration experiments will have water in equilibrium with the bomb gases, and the final state of the combustion experiments will have sulfuric acid solution in equilibrium with the bomb gases. As the final states are not comparable, errors associated with the use of the extra water may not cancel.

If the only experiments to be performed are the calibration experiments and the combustion experiments with the organic sulfur compound, the calibration should possibly be carried out in a bomb to which 10 ml. of water has been added, as partial cancellation of errors would probably yield more accurate results than if the bomb were calibrated under standard conditions. However, for the combustion calorimetry of organic sulfur compounds, there is another way of planning the experiments that will lead to a more complete cancellation of systematic errors. According to this method, the calibration experiments with benzoic acid are performed under conditions that are not significantly different from those used by the standardizing laboratory. Then two sets of combustion experiments are performed. The first of these is the usual combustion of the compound (eq. I). The second is the combustion of a mixture of rhombic sulfur and a hydrocarbon oil, the heat of formation of which is accurately known (eq. IV, in which for simplicity, the empirical formula of the oil is taken to be CH_2).

$$a\mathrm{CH_2(l)} + d\mathrm{S(rh)} + (3a/2 + 3d/2)\mathrm{O_2(g)} + (nd + d - a)\mathrm{H_2O(l)} = a\mathrm{CO_2(g)} + d(\mathrm{H_2SO_4}\cdot n\mathrm{H_2O})\mathrm{(l)} \quad \text{(IV)}$$

The heat of combustion experiments to determine the heat of formation of the oil should be performed under the same standard conditions that are used for the calibration experiments. In the experiments with mixtures of sulfur and oil (eq. IV), the amounts of sulfur and oil used and the amount of water added to the bomb are chosen to make the final state of the system nearly identical with that obtained in the experiments with the organic sulfur compound (eq. I). In theory, the two final states can be made identical except for a difference in the amount of oxygen that is consumed. Any

(16) F. D. Rossini and W. E. Deming, *J. Wash. Acad. Sci.*, **29**, 416 (1939).

(17) J. L. Franklin and H. E. Lumpkin, *J. Am. Chem. Soc.*, **74**, 1023 (1952).

(18) Personal communication.

(19) N. Craig and G. W. Vinal, *J. Research Natl. Bur. Standards*, **24**, 475 (1940).

systematic errors in the two sets of combustion experiments should be nearly the same, and will cancel when ΔU_c° of reaction IV is subtracted from ΔU_c° of reaction I to give ΔU_c° of reaction V.

$$C_aH_bO_cS_d(l \text{ or } s) + (b/4 - a/2 - c/2)O_2(g) = aCH_2(l) + dS(rh) + (b/2 - a)H_2O(l) \quad (V)$$

The heat of formation of the compound is readily obtained from the value of ΔU_c° of reaction V. In practice, it is more convenient to subtract ΔU_c° for the combustion of the oil according to reaction VI from ΔU_c° of reaction IV to obtain ΔU_c° of reaction III.

$$aCH_2(l) + 3a/2O_2(g) = aCO_2(g) + aH_2O(l) \quad (VI)$$

$$dS(rh) + 3d/2O_2(g) + (nd + d)H_2O(l) = d(H_2SO_4 \cdot nH_2O)(l) \quad (III)$$

Subtraction of ΔU_c° of reaction III from ΔU_c° of reaction I then gives ΔU_c° of the combustion of the compound to carbon dioxide, water and rhombic sulfur, from which the heat of formation is also readily obtained.

$$C_aH_bO_cS_d(s \text{ or } l) + (a + b/4 - c/2)O_2(g) = aCO_2(g) + b/2H_2O(l) + dS(rh) \quad (II)$$

The increase in temperature of the calorimeter in the two sets of measurements (reactions I and IV) may differ, and calibration for the two different increases in temperature may be necessary. Experimentally, it is found that the energy equivalent of the calorimeter differs very little for increases in temperature of 1.7 and 2.5°. Moreover the values of ΔU_c° for reaction III, the combustion of rhombic sulfur, are found not to differ significantly when the experiments with mixtures of sulfur and oil are designed to make the final states nearly identical with those of combustion experiments for compounds in which the carbon–sulfur ratio, a/d, varies between 4 and 6 and the hydrogen–sulfur ratio, b/d, varies between 4 and 10. Therefore, in practice, the experiments with mixtures of sulfur and oil, reaction IV, need not be repeated for each compound.

Rotation Energy.—The bomb is rotated both in the calibration and the combustion experiments. Therefore, the energy effect associated with rotation of the bomb is included in the energy equivalent of the calorimeter, $C_{eff.}$ (calor.), and does not need to be determined separately. The only requirement is that there be no significant variation in the rotation energy in different experiments. This requirement is more likely to be met if the rotation energy itself is small. Calorimetric measurements of the rotation energy showed that it was small, of the order of 0.2 cal. for the 15 end-over-end rotations of the bomb that occurred in each calibration and each combustion experiment. A variation of 50% in rotation energy, therefore, could be tolerated though such a large variation is very unlikely.

Equilibrium between Liquid and Gas Phases.—With 10 ml. of water in the bomb, necessary for proper mixing and satisfactory definition of states, complete equilibrium with respect to the solution of the bomb gases in the aqueous phase may not be obtained. No direct experimental determinations of the degree of saturation of the aqueous phase with the bomb gases have been made. However, to ascertain whether the extent of non-equilibrium, if present, is thermally significant, a series of calibration experiments with benzoic acid was carried out in which, in alternate experiments, 1 and 10 ml. of water were added to the bomb. The energy equivalent of the calorimeter, $C_{eff.}$ (calor.), was computed from the results of each of the two sets of experiments. The treatment of Hubbard, Scott and Waddington[12] was used to apply the corrections necessary because the calibration experiments with 10 ml. of water were not done under the same conditions as those of the standardizing laboratory. Theoretically, if equilibrium is attained, the two sets of experiments should give the same value for the energy equivalent, provided the corrections that are applied are adequate. The results of the experiments are summarized below. The uncertainty assigned is the standard deviation from the mean.

Condition	No. of expts.	$C_{eff.}$ (calor.), cal. deg.$^{-1}$
10 ml. of water	6	3916.7 ± 0.35
1 ml. of water	6	3916.2 ± 0.65

The discrepancy between the two results is of borderline significance. It is in the direction to be expected if the aqueous phase does not become completely saturated with the bomb gases, particularly carbon dioxide, in the final state of the bomb process. However, as inadequacy of the corrections, differences in the time–temperature curves, and other factors may also contribute to the discrepancy, no final conclusion can be drawn without further experimentation. Any systematic errors from failure to attain equilibrium between the liquid and gas phases are, of course, largely canceled by the comparative method that was used in this investigation.

Nature and Amount of Reaction.—The mass of compound that underwent combustion was determined by weighing the carefully dried material. However, it was necessary to study quantitatively the over-all chemistry of the combustion process so that corrections of various types could be applied and more confidence could be placed in the results obtained.

The following analyses were performed on the bomb solution after some or all of the combustion experiments: (a) hydrogen ion, by titration with standard base solution, either before or after removal of dissolved carbon dioxide, with an appropriate indicator in each case; (b) sulfate ion, by gravimetric determination as barium sulfate; (c) total nitrogen, by reduction with Devarda's alloy, distillation of the ammonia formed into standard acid solution and back-titration; (d) nitrite ion, colorimetrically by the Griess method[9]; (e) nitrate ion, as the difference between (c) and (d); (f) sulfite ion, colorimetrically with malachite green[20]; and (g) residue, by evaporation of the bomb solution and weighing the non-volatile material. The residue was also examined spectrochemically in one

(20) F. Feigl, "Qualitative Analysis by Spot Tests," 3rd Ed. Elsevier Publishing Co., Inc., New York, N. Y., 1947, p. 234. Attention is called to a typographical error: the malachite green solution should contain 10 mg. and not 10 g. of dye in 400 ml. of water.

instance. All analyses except (g) were also made of the solution in the scrubber through which the bomb gases were discharged. Various comments on the results of these analyses are given in the following paragraphs.

The chemical equivalents of hydrogen ion in the bomb solution should equal the sum of the equivalents of sulfate, nitrate and nitrite ions. When the Huffman–Ellis method[3] (static bomb) was used in this Laboratory, the amount of hydrogen ion found was only 97 ± 2% of the expected amount. With the rotating-bomb method, the amount of hydrogen ion found was 99 ± 1% of the expected amount. The rotating bomb increases the recovery of hydrogen ion, but the discrepancy may still be greater than the analytical error. Some of the acid may be consumed by corrosive attack on the metal parts of the bomb or by reaction with the glass ampoule.

A number of analyses for sulfate ion gave values 100.5 ± 0.5% of theoretical. The analytical method that was used apparently needs some refinement. Sunner[4b] reports better agreement.

The amount of nitrite ion in the bomb solution after a combustion experiment with the rotating-bomb method is less than after a combustion experiment with the Huffman–Ellis method.

For the rotating-bomb method, with 10 ml. of water in the bomb, the amount of total nitrogen in the solutions from the scrubber through which the bomb gases were discharged was very small, and only traces of nitrite ion were detected in these solutions. For the Huffman–Ellis method, on the other hand, the amount of nitrite ion from the bomb gases was significant if the hydrogen–sulfur ratio, b/d, of the sample that underwent combustion was less than 12. As nitrate and nitrite ion in the scrubber solutions probably come from oxides of nitrogen in the bomb gases, in the Huffman–Ellis method thermochemical corrections with their attendant uncertainty must be made for these oxides of nitrogen in the gas phase. These corrections and the uncertainties associated with them are eliminated in the rotating-bomb method.

The completeness of the oxidation of the sulfur to sulfuric acid is important because the heats of oxidation of sulfur dioxide and sulfurous acid to sulfuric acid are about 76 and 65 cal. per millimole, respectively, and the formation of more than 0.001 millimole of sulfur in the +4 oxidation state will cause a significant error in the calorimetric determination. Analyses for sulfite ion never showed a significant amount of sulfur in the +4 oxidation state for combustion experiments in which air was left in the bomb.

Several milligrams of non-volatile residue was obtained when the bomb solutions were evaporated. This residue presumably resulted from action of the hot combustion gases on the bomb parts and contents. Samples of the soft glass used for ampoules and of the residue from combustion experiments in an illium bomb (preliminary experiments before a platinum-lined bomb was available) were analyzed spectrochemically. The residue contained the elements present in the glass and also the metals present in the bomb, including a small amount of platinum, of which the crucible was made.

In the Huffman–Ellis method, addition of a small amount of water to the bomb solution sometimes causes it to turn blue. The blue color presumably arises from a complex of sulfuric acid with an oxide of nitrogen. The blue color was never observed in experiments with the rotating-bomb method, and it is believed that, with 10 ml. of water added to the bomb, the final solution is dilute enough to hydrolyze any complex that might be formed.

Correction for Reaction of Soft Glass Ampoules.—Ampoules of soft glass were originally selected to contain the samples of liquid organic sulfur compounds because they are customarily used to contain samples of organic liquids in combustion calorimetry, and the techniques for their use are well established. However, several observations now suggest that there is some chemical reaction of the soft glass with the products of combustion of organic sulfur compounds and that a significant energy effect is associated with the reaction. The glass beads to which the ampoules melt down are usually dark brown. The occurrence in the residue from the bomb solution of the elements present in the glass indicates that some of the glass is converted to water-soluble materials. In the A series of combustion experiments for thiacyclobutane, in which soft-glass ampoules were used, the average value of $\Delta U_c^\circ/M$ differed from that of the B series, in which Pyrex and Vycor ampoules were used, by 2.5 cal. g.$^{-1}$, which is equivalent to 2.1 cal. per combustion experiment. In combustion experiments on 3-methylthiophene,[21] a series in which soft-glass ampoules were used gave results that differed by 2.3 cal. per combustion experiment from a series in which Pyrex and Vycor ampoules were used. In both cases the observed differences were only slightly greater than the sum of the precision uncertainties of the two series. However, the differences were in the right direction to be explained if the soft glass reacted with the products of combustion with liberation of heat, and the more chemically resistant Pyrex and Vycor did not react. (The Pyrex ampoules melted down to colorless beads, and the Vycor ampoules shattered but did not fuse.) If the soft glass does react as suggested, the heat effect of the reaction may differ from compound to compound and from experiment to experiment with the same compound, and it is not possible to apply a rigorous correction for it. Soft glass therefore appears to be unsatisfactory as an ampoule material for organic sulfur compounds, and its use has been discontinued in this Laboratory.

It seemed desirable to apply corrections to the data that had already been obtained with the use of soft glass ampoules, even though, for the reasons just given, the corrections would necessarily be somewhat arbitrary. On the basis of the results for 3-methylthiophene, a correction of 2.3 cal. per combustion experiment was applied to the results for 1-pentanethiol, 3-thiapentane, 2-methyl-2-propanethiol and thiacyclopentane. This correction

(21) J. P. McCullough, S. Sunner, H. L. Finke, W. N. Hubbard, M. E. Gross, R. E. Pennington, J. F. Messerly, W. O. Good and G. Waddington, *J. Am. Chem. Soc.*, **75**, 5075 (1953).

was equivalent to corrections of 0.40, 0.31, 0.27 and 0.25 kcal. mole^{-1}, respectively, to $\Delta U_c°$ for the four compounds. For purposes of calculation of the uncertainty interval, an uncertainty of ± 1 cal. per combustion experiment was assigned to the correction.

Summary.—Experience with the rotating-bomb method for the combustion calorimetry of organic sulfur compounds shows that it is an improvement over the Huffman–Ellis method in several respects. (a) The aqueous solution in the final state is essentially homogeneous. (b) Analytically determined amounts of hydrogen ion in the final solution that are closer to the theoretical amounts suggest that the chemistry of the bomb process is more nearly in accord with the assumptions made as to its over-all nature. (c) The greater dilution of the final solution in the rotating-bomb method decreases the possibility of error from the formation of a complex of sulfuric acid with an oxide of nitrogen. (d) The oxides of nitrogen in the final gaseous phase are reduced to insignificant amounts in the rotating-bomb method.

Acknowledgment.—The authors wish to express their gratitude to Dr. Stig Sunner of the University of Lund, Sweden, for supplying the sample of thianthrene, for making his data available to this Laboratory prior to publication, and for coöperating in many other ways.

REDUCTION TO STANDARD STATES (AT 25°) OF BOMB CALORIMETRIC DATA FOR COMPOUNDS OF CARBON, HYDROGEN, OXYGEN AND SULFUR[1]

BY WARD N. HUBBARD, DONALD W. SCOTT AND GUY WADDINGTON

Contribution No. 38 from the Thermodynamics Laboratory, Petroleum Experiment Station, Bureau of Mines, Bartlesville, Okla.

Received June 6, 1953

The Washburn corrections, *i. e.*, corrections for the reduction of bomb calorimetric data to standard states, are extended to apply to compounds that contain sulfur in addition to carbon, hydrogen and oxygen. A critical selection is made of the values of the numerical constants that are required for these corrections at 25°. The corrections are presented in a form which is (a) general enough to cover a wide range of experimental conditions, (b) readily adaptable to revision whenever better values of any of the numerical constants become available and (c) suitable for extension to include compounds of carbon, hydrogen, oxygen and elements other than sulfur.

In 1933, in a paper entitled "Standard States for Bomb Calorimetry," Washburn[2] emphasized that the energy evolved when the combustion of a substance takes place in a bomb calorimeter may differ significantly from the decrease in internal energy for the combustion reaction under standard conditions. He treated in detail the corrections that must be applied to bomb calorimetric data in order that investigators may obtain values of the standard change of internal energy. Washburn's treatment (a), applied to the combustion of compounds that contain only carbon, hydrogen and oxygen and (b), referred these combustion reactions to a temperature of 20°. In high-precision combustion calorimetry, it has become standard practice to apply the corrections proposed by Washburn. They are usually referred to as the "Washburn corrections" or collectively as the "Washburn reduction."

Several developments have occurred in the field of combustion calorimetry since publication of Washburn's paper two decades ago. First, great improvements have been made in techniques for determining heats of combustion of compounds that contain elements other than carbon, hydrogen and oxygen (in particular, sulfur and the halogens). For these classes of compounds, to which Washburn's treatment does not apply, data are being obtained, or are likely to be obtained in the near future, that must be reduced to standard states if full advantage is to be taken of their accuracy. Second, there is an increasing tendency to conduct combustion calorimetry at temperatures near 25° or at least to refer the combustion reactions to that temperature. Third, more accurate experimental values have become available for a number of the quantities that enter into the Washburn corrections.

This paper is intended to meet some of the needs that have arisen as a result of these developments. The original stimulus for the work reported herein was the necessity of applying Washburn corrections to bomb calorimetric data that are being obtained in this Laboratory for organic sulfur compounds. Therefore, the primary purpose was extension of the Washburn corrections to include organic sulfur compounds. However, a more general result was obtained, namely, a revision of the Washburn corrections that applies to 25° and takes advantage of the more accurate experimental data that have become available since 1933. Although the treatment as presented is limited to compounds that contain only sulfur in addition to carbon, hydrogen and oxygen, the method and many of the individual details are more general in nature. This treatment can therefore serve as the basis for future extensions of the Washburn corrections to other classes of organic compounds, for instance halogen compounds, whenever the need for such extensions arises.

General Considerations

Theory.—The Washburn corrections, as presented here, apply to the combustion of a sub-

(1) This investigation was part of American Petroleum Institute Research Project 48A on "The Production, Isolation and Purification of Sulfur Compounds and Measurement of their Properties," which the Bureau of Mines conducts at Bartlesville, Okla., and Laramie, Wyo.

(2) E. W. Washburn, *Bur. Standards J. Research*, **10**, 525 (1933).

stance whose general formula is $C_aH_bO_cS_d$. It is understood that some of the subscripts in this formula may be zero. For example, for a pure hydrocarbon, c and d are both zero. The calorimetric determination of the heat of combustion of this substance takes place as follows. The substance, oxygen (in excess), nitrogen and water are introduced into a combustion bomb. (The nitrogen may be merely an impurity in the oxygen, or it may be introduced deliberately to catalyze the oxidation of sulfur to the +6 oxidation state.) The substance is caused to react with the oxygen to produce carbon dioxide, water and sulfuric acid. Side reactions that produce nitric and nitrous acids may occur simultaneously. After the reaction is complete, the bomb contains carbon dioxide, water, sulfuric acid, the oxygen not consumed in the reaction, nitrogen, and possibly nitric and nitrous acids. The process just described takes place in a bomb calorimeter. The increase in temperature of the calorimeter is measured, and, by suitable calibration of the calorimeter, this increase in temperature is related to the heat liberated by the process. The heat liberated is equal to the decrease in internal energy of the contents of the bomb when they are converted from the particular state in which they exist before the combustion reaction to the particular state in which they exist after the combustion reaction, *i.e.*, the change in internal energy for the actual bomb process. In practice, by applying appropriate calorimetric corrections, this is reduced to the change in internal energy for the isothermal bomb process.

The quantity which an investigator wishes to obtain from bomb calorimetric data is not the change in internal energy for the isothermal bomb process, but the change in internal energy for an idealized combustion reaction. This is defined as the reaction, isothermally at a given temperature (25° in the present treatment), of unit quantity of substance in its standard state with an equivalent amount of pure oxygen gas and the necessary amount of pure liquid water, both of which are in their standard states, to produce the stoichiometric amounts of pure carbon dioxide and an aqueous sulfuric acid solution of a designated concentration, both of which are in their standard states. The equation of the reaction is

$$C_aH_bO_cS_d(\text{s or l}) + (a + b/4 - c/2 + 3d/2)O_2(g) + (nd - b/2 + d)H_2O(l) = aCO_2(g) + d(H_2SO_4 \cdot nH_2O) \quad (1)$$

The change in internal energy associated with this process is called the "energy of the idealized combustion reaction" and is designated $\Delta U_c°$.

The idealized combustion reaction is conveniently regarded as occurring in a series of processes, one of which is the actual bomb process and the remainder of which are imaginary. The first process starts with the substance, oxygen (in excess), nitrogen and water, all in their standard states at 25°. These are placed in the combustion bomb, and equilibrium is established at 25°, except that the substance is not allowed to mix with the other materials. Three phases result, namely, (a) pure substance, (b) a gaseous phase consisting of oxygen, nitrogen and water vapor and (c) a liquid phase consisting of water saturated with dissolved oxygen and nitrogen. The next process consists of bringing these initial contents of the bomb from their equilibrium state at 25° to their equilibrium state at the initial temperature, t_i, of the actual bomb process. The next process is the actual bomb process, in which the actual initial contents of the bomb are converted to the actual final contents of the bomb, and the temperature increases from t_i to t_f, the final temperature of the actual bomb process. Two phases result, namely, (a) a gaseous phase consisting of oxygen, carbon dioxide, nitrogen and water vapor and (b) a liquid phase consisting of an aqueous solution of sulfuric, nitric and nitrous acids saturated with dissolved oxygen, carbon dioxide and nitrogen. The next process consists of bringing these final contents of the bomb from their equilibrium state at the temperature, t_f, to their equilibrium state at 25°. In the final process, the nitric and nitrous acids are decomposed into nitrogen, oxygen and water; all of the oxygen, carbon dioxide and nitrogen are removed from the bomb, separated from each other and brought individually to their standard states at 25°; all of the water and sulfuric acid is removed from the bomb as an aqueous sulfuric acid solution under 1 atm. pressure; and this solution is adjusted to the designated concentration by the isothermal addition or removal of liquid water in its standard state at 25°. The net change in this series of processes is just the idealized combustion reaction. The sum of the changes in internal energy for all the processes is therefore the energy of the idealized combustion reaction, $\Delta U_c°$. The actual bomb process and the processes immediately preceding and following it constitute the isothermal bomb process, for which the change in internal energy is obtained calorimetrically. The changes in internal energy for the other two processes are the Washburn corrections, the addition of which to the experimentally determined change in internal energy for the isothermal bomb process gives the desired quantity, $\Delta U_c°$. The calculation of the Washburn corrections then consists of the calculation of the changes in internal energy for these other imaginary processes.

Standard States.—The standard states are defined in a manner consistent with current thermodynamic usage. The definitions are: (a) for oxygen, nitrogen and carbon dioxide, the pure substances in the ideal gas state at 1 atm. pressure, (b) for the substance, the material in a thermodynamically defined state (solid or liquid) under a pressure of 1 atm., (c) for water, the pure liquid under a pressure of 1 atm. and (d) for the aqueous sulfuric acid solution, the liquid at a defined concentration (which is selected to be approximately that obtained in the actual combustion experiment) under a pressure of 1 atm.

Manner of Presentation.—The way in which the treatment is presented in this paper was determined by several considerations. One was that all of the corrections that must be applied to the original calorimetric data should be included. Some of these corrections are calorimetric, some are thermochemical and only the rest are those usually

regarded as the Washburn corrections. However, these different kinds of corrections are not all strictly independent, and there may be ambiguity about the classification of certain of the corrections and uncertainty about the order in which they are to be applied. These difficulties are removed if all of the corrections are included in one consistent treatment. A second consideration was that the treatment should be as complete and rigorous as it is practical to make it. This consideration led to the inclusion of terms that are negligible for the experimental conditions and attainable precision that the authors consider usual in combustion calorimetry. However, these terms are included so that an investigator who uses different experimental conditions, or who obtains increased precision may determine the magnitude of these terms and decide whether or not they are negligible for his purpose. A third consideration was that all of the terms should be kept separate and not combined into a single complex expression, as was done by Washburn. Keeping the terms separate has several advantages: (a) The individual terms are more easily examined to determine whether they are significant or negligible. (b) When a more reliable experimental value for a quantity which enters the treatment becomes available, the term or terms that contain this quantity may be conveniently revised without disturbing the rest of the treatment. (c) Many of the terms of this treatment will apply, either unchanged or with slight modifications, to extensions of the Washburn corrections to other classes of organic compounds. The transfer of these terms to other extensions of the Washburn corrections will be simpler if they are kept separate.

A fourth consideration was that the treatment should be presented in a way that is adaptable for use by other investigators. The rather long calculations involved in applying all of the corrections to the original calorimetric data are conveniently carried out on a computation form. The presentation is therefore given as the items which make up such a computation form, interspersed with explanatory text. These items, 100 in number, consist of the input data (experimental values, molecular weights, physical constants, auxiliary energy quantities, etc.) and the quantities that the investigator must calculate from them to obtain the desired quantity, ΔU_c°, which is item 100. The items are so ordered that the calculation of a particular one depends only on the numerical values obtained for prior items and are so designed that the numerical operations are conveniently performed with a desk calculator. Items 1–67, which relate to the description of the initial and final states of the isothermal bomb process, items 68–80, which relate to energy factors and calorimetric data, and items 81–100, which relate to the changes in internal energy, are treated in the next three sections. As an illustration of the use of the method, and as a means of illustrating the magnitude of the various terms, a numerical example of the calculations is given. This numerical example is selected from a series of experiments carried out in this Laboratory to determine the heat of combustion of 3-methylthiophene.

Initial and Final States

Substance.—The substance is defined as all of the material that undergoes combustion, and consists of the compound whose heat of combustion is being determined and any other combustible materials added for any purpose, *e.g.*, the auxiliary material and the fuse. The first 18 items of the computation sheet list the formula (chemical or empirical), mass m, molecular weight M, number of moles n, density ρ, and volume v, of each of the materials that comprise the substance. Primes are used to distinguish different materials. In the numerical example, the compound is 3-methylthiophene, the auxiliary material is a hydrocarbon oil the empirical formula of which is $CH_{1.891}$, and the fuse is filter paper the empirical formula of which is $CH_{1.686}O_{0.843}$. Starred item numbers denote input data, and unstarred item numbers denote calculated quantities.

(1*)	Formula of cpd., $C_a'H_b'O_c'S_d'$	C_5H_6S
(2*)	m', mass of cpd.	0.85715 g.
(3*)	M', mol. wt. of cpd.	98.164 g. mole^{-1}
(4)	$n' = m'/M'$	0.00873182 mole
(5*)	ρ', density of cpd.	1.02 g. ml.$^{-1}$
(6)	$v' = m'/1000\rho'$	0.0008 l.
(7*)	Formula of auxiliary material, $C_a''H_b''O_c''S_d''$	$CH_{1.891}$
(8*)	m'', mass of auxiliary material	0.05354 g.
(9*)	M'', mol. wt. of auxiliary material	13.916 g. mole^{-1}
(10)	$n'' = m''/M''$	0.0038474 mole
(11*)	ρ'', density of auxiliary material	0.87 g. ml.$^{-1}$
(12)	$v'' = m''/1000\rho''$	0.0001 l.
(13*)	Formula of fuse, $C_a'''H_b'''O_c'''S_d'''$	$CH_{1.686}O_{0.843}$
(14*)	m''', mass of fuse	0.00410 g.
(15*)	M''', mol. wt. of fuse	27.197 g. mole^{-1}
(16)	$n''' = m'''/M'''$	0.0001508 mole
(17*)	ρ''', density of fuse	1.5 g. ml.$^{-1}$
(18)	$v''' = m'''/1000\rho'''$	0.0000 l.

In the numerical example, c', c'', d'' and d''' are zero.

Items 19–25 list the subscripts, a, b, c and d, of the empirical formula $C_aH_bO_cS_d$, and the mass, m(sub.), molecular weight, M(sub.), and the number of moles, n(sub.), of the total substance that undergoes combustion. The subscripts a, b, c and d are defined so that n(sub.) is always unity.

(19)	$a = n'a' + n''a'' + n'''a'''$	0.0476573
(20)	$b = n'b' + n''b'' + n'''b'''$	0.0599206
(21)	$c = n'c' + n''c'' + n'''c'''$	0.0001271
(22)	$d = n'd' + n''d'' + n'''d'''$	0.0087318
(23)	m(sub.) $= m' + m'' + m'''$	0.91479 g.
(24)	M(sub.) $= 12.010a + 1.008b + 16.000c + 32.066d$	0.91479 g. mole^{-1}
(25)	n(sub.) $= m$(sub.)$/M$(sub.)	1.00000 mole

O_2, N_2 and H_2O in the Initial State.—Items 26–36 deal with the amounts of O_2, N_2 and H_2O in the bomb, and the distribution of these compounds between the gaseous and liquid phases, in the initial state of the isothermal bomb process. Except for stoichiometry, the N_2 is treated as though it were O_2. This approximation is justified because (a) N_2 and O_2 have similar physical properties, (b) the mole fraction of N_2 in the bomb gases is small (less than 0.03 in current practice) and (c) the errors from treating N_2 as O_2 in the initial state are nearly compensated by similar errors from so

treating it in the final state, since N_2 is present in nearly the same amount and condition in both states.

In the equations to follow, superscripts i and f are used to designate the initial and final states, respectively, of the *isothermal* bomb process. (Subscripts i and f are reserved to designate the initial and final states of the *actual* bomb process.) The material to which a symbol applies and the state of that material are given parenthetically after the symbol. The abbreviations used include the chemical formulas of single compounds and the following other abbreviations: sub., total substance; gas., gaseous mixture of O_2, N_2 and H_2O vapor (and CO_2 in the final state); soln., aqueous solution of H_2SO_4, HNO_3 and HNO_2; vap., vapor; liq., liquid; diss., dissolved; and tot., total.

The next three items list the volume of the bomb, v (bomb), the volume of H_2O added to the bomb, $v^i(H_2O\ tot.)$, and the initial pressure at 25°, $p^i(gas.)$. The volume of the bomb is defined as the internal volume, exclusive of the volume occupied by the crucible, electrodes and other non-combustible accessories. In the numerical example, 10.03 ml. of water is introduced into the bomb, the volume of which is 347.1 ml., and the bomb, which contains air at atmospheric pressure, is charged to a total pressure of 30.00 atm. (at 25°).

(26*)	v(bomb)	0.3471 l.
(27*)	$v^i(H_2O\ tot.)$	0.01003 l.
(28*)	$P^i(gas.)$	30.00 atm.

The density at 25°, 997 g. $l.^{-1}$, and molecular weight, 18.016 g. $mole^{-1}$, of H_2O are used to calculate the mass and number of moles of total H_2O in the bomb.

(29)	$m^i(H_2O\ tot.) = 997v^i(H_2O\ tot.)$	10.00 g.
(30)	$n^i(H_2O\ tot.) = m^i(H_2O\ tot.)/18.016$	0.5551 mole

The volume occupied by the gaseous phase is obtained by subtracting the volume of liquid H_2O and of substance from the volume of the bomb. The volume of liquid H_2O differs from $v^i(H_2O\ tot.)$ only by the amount vaporized into the gaseous phase, an amount which is insignificant in this calculation.

(31) $v^i(gas.) = v(bomb) - v^i(H_2O\ tot.) - v' - v'' - v'''$ 0.3362 l.

The concentration of saturated H_2O vapor in gases at various pressures, C_W, may be represented by the equation given by Washburn [eq. 105 of ref. 2], $C_W = C_O + \alpha P$. The term, C_O, which is the concentration of saturated H_2O vapor in the absence of other gases, is 0.02304 g. $l.^{-1}$ at 25°.[3] P is the pressure of other gas, which, for the pressure range of interest here, does not differ significantly from the total pressure. The constant α is determined by the nature of the gas phase. Unfortunately experimental data are still unavailable for the evaluation of α for O_2, and it is necessary to assume, as Washburn did, that α is the same for O_2 as for N_2 or air. However, the data used by Washburn for the concentration of H_2O vapor in N_2 and air[4] have been superseded by more recently determined data.[5] The value of α selected here 0.000105 g. $l.^{-1}$ $atm.^{-1}$, is based on the smoothed data of Deaton and Frost[5b] for air at 400 lb. $in.^{-2}$ gage (28.1 atm. absolute). The number of moles, $n^i(H_2O\ vap.)$, of water in the gaseous phase is calculated from the equation

(32) $n^i(H_2O\ vap.) = [0.02304 + 0.000105P^i(gas.)]v^i(gas.)/18.016$ 0.000489 mole

The number of moles, $n^i(H_2O\ liq.)$, of liquid water is obtained by difference.

(33) $n^i(H_2O\ liq.) = n^i(H_2O\ tot.) - n^i(H_2O\ vap.)$ 0.5546 mole

The equation of state at 25°, $Pv = n(24.465)(1 - 0.00061P)$, fits the PvT data of O_2[6] exactly for $P = 30$ atm. and to a sufficiently good approximation over the range $P = 20$ to $P = 40$ atm. This equation applies to the gaseous phase, since N_2 is treated as though it were O_2 and the concentration of H_2O vapor is too small to affect the PvT behavior significantly. It is used to calculate the number of moles, $n^i(gas.)$, of the gaseous mixture.

(34) $n^i(gas.) = P^i(gas.)v^i(gas.)/\{24.465[1 - 0.00061P^i(gas.)]\}$ 0.4199 mole

The solubility of O_2 in aqueous H_2SO_4 solutions at 25° will be discussed in the next subsection. The limiting value for pure H_2O, 0.0000228 mole per mole of H_2O per atm. O_2 partial pressure, is used to calculate the number of moles of $O_2 + N_2$ dissolved in the liquid H_2O.

(35) $n^i[(O_2 + N_2)\ diss.] = 0.0000228n^i(H_2O\ liq.)[P^i(gas.) - 0.03]$ 0.000379 mole

The quantity, 0.03, in item 35 is the approximate partial pressure of H_2O vapor (in atm.) in the gaseous mixture.

The total number of moles of $O_2 + N_2$ is calculated next.

(36) $n^i[(O_2 + N_2)\ tot.] = n^i(gas.) - n^i(H_2O\ vap.) + n^i[(O_2 + N_2)\ diss.]$ 0.4198 mole

O_2, CO_2, N_2, H_2O, H_2SO_4, HNO_3 and HNO_2 in the Final State.—Items 37–67 deal with the compounds present in the bomb in the final state of the isothermal bomb process, and the distribution of these between the gaseous and aqueous phases. The substance has reacted with O_2 according to the net equation

$$C_aH_bO_cS_d + (a + b/4 - c/2 + 3d/2)O_2 = aCO_2 + (b/2 - d)H_2O + dH_2SO_4$$

Side reactions may have occurred according to the net equations

$$^1/_2N_2 + {}^5/_4O_2 + {}^1/_2H_2O = HNO_3$$

and

$$^1/_2N_2 + {}^3/_4O_2 + {}^1/_2H_2O = HNO_2$$

The extent of these side reactions is determined experimentally by chemical analysis of the final bomb

(3) N. S. Osborne, H. F. Stimson and D. C. Ginnings, *J. Research Natl. Bur. Standards*, **23**, 261 (1939).

(4) (a) E. P. Bartlett, *J. Am. Chem. Soc.*, **49**, 65 (1927); (b) F. Pollitzer and E. Strebel, *Z. physik. Chem.*, **110**, 768 (1924).

(5) (a) A. W. Saddington and N. W. Krase, *J. Am. Chem. Soc.*, **56**, 353 (1934); (b) W. M. Deaton and E. M. Frost, Jr., *Am. Gas Assoc., Proc. Natural Gas Sect.*, 143 (1941).

(6) J. A. Beattie and O. C. Bridgeman, *Proc. Am. Acad. Arts Sci.*, **63**, 229 (1928).

solution.[7] In the numerical example, it was found that 0.00069 mole of HNO_3 and 0.000005 mole of HNO_2 were formed.

(37*) $n^f(HNO_3)$ 0.00069 mole
(38*) $n^f(HNO_2)$ 0.000005 mole

The number of moles of H_2SO_4 produced in the combustion is calculated by stoichiometry

(39) $n^f(H_2SO_4) = dn(\text{sub.})$ 0.008732 mole

The number of moles of H_2O in the liquid phase is given rigorously by

$$n^i(H_2O \text{ tot.}) + (b/2 - d)n(\text{sub.}) - {}^1/_2n^f(HNO_3) - {}^1/_2n^f(HNO_2) - n^f(H_2O \text{ vap.})$$

However, the final term (which is small compared to the first two terms) is not known at this stage of calculation. If the H_2SO_4 solution in the final state is relatively dilute, the number of moles of H_2O vapor are not greatly different in the initial and final states, and it is a satisfactory approximation to substitute $n^i(H_2O \text{ vap.})$ for $n^f(H_2O \text{ vap.})$. The validity of this approximation may be verified after item 67 is calculated.

(40) $n^f(H_2O \text{ liq.}) = n^i(H_2O \text{ tot.}) + (b/2 - d)n(\text{sub.}) - {}^1/_2n^f(HNO_3) - {}^1/_2n^f(HNO_2) - n^i(H_2O \text{ vap.})$ 0.5755 mole

The mass of solution is obtained by summing the masses of the constituents.

(41) $m^f(\text{soln.}) = 18.016n^f(H_2O \text{ liq.}) + 98.1n^f(H_2SO_4) + 63n^f(HNO_3) + 47n^f(HNO_2)$ 11.27 g.

The weight per cent. of H_2SO_4 and of the combined nitrogen acids are calculated next.

(42) wt. % $(H_2SO_4) = 9808n^f(H_2SO_4)/m^f(\text{soln.})$ 7.60%
(43) wt. % $(HNO_3 + HNO_2) = [6302n^f(HNO_3) + 4702n^f(HNO_2)]/m^f(\text{soln.})$ 0.39%

Density data for H_2SO_4 and HNO_3 solutions individually[8] may be represented, for the concentration ranges of interest here, by $\rho = 0.9970 + 0.0066$ wt. % (H_2SO_4) and $\rho = 0.9970 + 0.0054$ wt. % (HNO_3) g. ml.$^{-1}$. In the calculation of the density and volume of the aqueous solution, two approximations are made: (a) that H_2SO_4 and HNO_3 increase the density of H_2O additively according to weight per cent., and (b) that the small amount of HNO_2 may be treated as though it were HNO_3. The second approximation will be made repeatedly throughout this subsection.

(44) $\rho^f(\text{soln.}) = 0.9970 + 0.0066$ wt. % $(H_2SO_4) + 0.0054$ wt. % $(HNO_3 + HNO_2)$ 1.049 g. ml.$^{-1}$
(45) $v^f(\text{soln.}) = m^f(\text{soln.})/1000\rho^f(\text{soln.})$ 0.01074 l.

The normality of H_2SO_4 and of the combined nitrogen acids, and the molar ratio of H_2O to H_2SO_4 are calculated in the next three items.

(46) $N(H_2SO_4) = 2n^f(H_2SO_4)/v^f(\text{soln.})$ 1.626 N
(47) $N(HNO_3 + HNO_2) = [n^f(HNO_3) + n^f(HNO_2)]/v^f(\text{soln.})$ 0.065 N
(48) $n^f(H_2O \text{ liq.})/n^f(H_2SO_4)$ 65.91

(7) The corrections for iron wire discussed by Washburn are omitted from this treatment, as the iron wire method of firing has been superseded by better methods that do not require these special corrections.

(8) "International Critical Tables," Vol. III, McGraw-Hill Book Co., Inc., New York, N. Y., 1928, pp. 56–59.

The volume of the gaseous mixture is obtained by difference.

(49) $v^f(\text{gas.}) = v(\text{bomb}) - v^f(\text{soln.})$ 0.3364 l.

The number of moles of CO_2 produced in the combustion is calculated from stoichiometry.

(50) $n^f(CO_2 \text{ tot.}) = an(\text{sub.})$ 0.047657 mole

The solubility of CO_2 in aqueous H_2SO_4 solution is read from a smooth curve through a large scale plot of the data of Markham and Kobe,[9] Kobe and Williams,[10] Geffcken[11] and Sumner.[12] The table of smoothed values given below will permit investigators to plot this solubility curve for their own use. The data of Geffcken show that HNO_3, on a normality basis, *increases* the solubility of CO_2 in aqueous solutions approximately half as much as H_2SO_4 *decreases* it. The independent variable is therefore selected to be $N(H_2SO_4) - {}^1/_2N(HNO_3 + HNO_2)$. An extrapolation to negative values of this variable is included to cover cases in which nitrogen acids are present and H_2SO_4 is not. The solubility constant, $K(CO_2)$, is defined as the number of moles of CO_2 dissolved in 1 l. of solution at unit fugacity of CO_2 gas.

$N(H_2SO_4) - {}^1/_2N(HNO_3 + HNO_2)$	$K(CO_2) \times 10^4$	$N(H_2SO_4) - {}^1/_2N(HNO_3 + HNO_2)$	$K(CO_2) \times 10^4$
−0.5	356.5	2.0	297.0
0.0	340.5	2.5	290.8
0.5	326.9	3.0	285.0
1.0	314.5	3.5	279.2
1.5	304.5	4.0	274.2

(51) $K(CO_2)$ 0.0303 mole l.$^{-1}$ atm.$^{-1}$

In the computation of the number of moles of CO_2 dissolved in the aqueous phase, it is necessary to take account of (a) the fugacity of the CO_2 gas in the presence of the O_2 gas and (b) the total pressure on the aqueous phase. It is convenient to treat the CO_2 and O_2 as ideal gases and then use a fictitious solubility constant, $K^*(CO_2)$, that includes corrections for fugacity and total pressure.[13] The fictitious solubility constant is obtained by multiplication of the actual solubility constant by a factor, $D(CO_2)$. Values of $D(CO_2)$ are tabulated below as a function of the mole fraction of CO_2, $x(CO_2)$, and the final pressure, $P^f(\text{gas.})$. At this stage of the computation, only approximate estimates of $x(CO_2)$ and $P^f(\text{gas.})$ are required; the estimated values may be checked after accurate values have been calculated in items 63 and 65.

	$P^f(\text{gas.})$, atm.		
$x(CO_2)$	20	30	40
0.0	0.914	0.873	0.834
0.1	.900	.854	.810
0.2	.887	.836	.787

(9) A. E. Markham and K. A. Kobe, *J. Am. Chem. Soc.*, **63**, 1165 (1941).

(10) K. A. Kobe and J. S Williams, *Ind. Eng. Chem., Anal. Ed.*, **7**, 37 (1935).

(11) G. Geffcken, *Z. physik. Chem.*, **49**, 257 (1904).

(12) S. Sunner, Dissertation, "Studies in Combustion Calorimetry Applied to Organo-Sulfur Compounds," Carl Bloms Boktryckeri, Lund, Sweden, 1949.

(13) The equation of state of item 65 was used in the computation of the fugacity of CO_2 gas in the presence of O_2 gas. A value of 33 ml. for the partial molal volume of CO_2 in aqueous solution was used in the computation of the effect of total pressure.

In the numerical example, the estimated values are 0.12 for $x(CO_2)$ and 28 atm. for P^f(gas.).

(52) $D(CO_2)$ 0.859

(53) $K^*(CO_2) = D(CO_2)K(CO_2)$ 0.0260 mole l.$^{-1}$ atm.$^{-1}$

(54) $n^f(CO_2\ \text{diss.}) = \dfrac{24.465K^*(CO_2)v^f(\text{soln.})/v^f(\text{gas.})}{1 + 24.465K^*(CO_2)v^f(\text{soln.})/v^f(\text{gas.})} n^f(CO_2\ \text{tot.})$ 0.000949 mole

(55) $n^f(CO_2\ \text{gas}) = n^f(CO_2\ \text{tot.}) - n^f(CO_2\ \text{diss.})$ 0.046708 mole

The number of moles of $O_2 + N_2$ in the final state is calculated next.

(56) $n^f[(O_2 + N_2)\ \text{tot.}] = n^i[(O_2 + N_2)\ \text{tot.}] - (a + b/4 - c/2 + 3d/2)n(\text{sub.}) - 7/4n^f(HNO_3) - 5/4n^f(HNO_2)$ 0.3429 mole

The solubility of O_2 in aqueous H_2SO_4 solution is read from a large scale plot of the data of Geffcken.[11] Smoothed values are given below. As HNO_3 decreases the solubility of O_2 approximately half as much as H_2SO_4, on a normality basis, the independent variable is selected to be $N(H_2SO_4) + {}^1/_2N(HNO_3 + HNO_2)$. The solubility constant, $K(O_2)$, is defined as the number of moles of O_2 dissolved in 1 l. of solution per atm. O_2 partial pressure.

$N(H_2SO_4) + {}^1/_2N(HNO_3 + HNO_2)$	$K(O_2) \times 10^4$	$N(H_2SO_4) + {}^1/_2N(HNO_3 + HNO_2)$	$K(O_2) \times 10^4$
0.0	12.60	2.5	9.85
0.5	11.81	3.0	9.39
1.0	11.26	3.5	8.95
1.5	10.77	4.0	8.61
2.0	10.31		

(57) $K(O_2)$ 0.00106 mole l.$^{-1}$ atm.$^{-1}$

The solubility of $O_2 + N_2$ in the aqueous solution is handled in much the same way as that of CO_2. However, as the solubility of $O_2 + N_2$ is much smaller, it is unnecessary to use fugacity instead of pressure or to consider the effect of pressure on the aqueous phase. The values of $D(O_2)$ tabulated below merely correct for the deviation of the partial pressure of $O_2 + N_2$ from that calculated from the ideal gas law.

$x(CO_2)$	P^f(gas.), atm. 20	30	40
0.0	0.988	0.982	0.976
.1	.989	.9835	.978
.2	.990	.985	.980

(58) $D(O_2)$ 0.985

(59) $K^*(O_2) = D(O_2)K(O_2)$ 0.00104 mole l.$^{-1}$ atm.$^{-1}$

(60) $n^f[(O_2 + N_2)\ \text{diss.}] = \dfrac{24.465K^*(O_2)v^f(\text{soln.})/v^f(\text{gas.})}{1 + 24.465K^*(O_2)v^f(\text{soln.})/v^f(\text{gas.})} n^f[(O_2 + N_2)\ \text{tot.}]$ 0.000278 mole

(61) $n^f[(O_2 + N_2)\ \text{gas}] = n^f[(O_2 + N_2)\ \text{tot.}] - n^f[(O_2 + N_2)\ \text{diss.}]$ 0.3426 mole

The number of moles of gaseous mixture is calculated next. As in item 40, $n^i(H_2O\ \text{vap.})$ is used as an approximation for $n^f(H_2O\ \text{vap.})$.

(62) $n^f(\text{gas.}) = n^f[(O_2 + N_2)\ \text{gas}] + n^f(CO_2\ \text{gas}) + n^i(H_2O\ \text{vap.})$ 0.3898 mole

Item 63 lists the mole fraction of CO_2 in the gaseous mixture, $x(CO_2)$.

(63) $x(CO_2) = n^f(CO_2\ \text{gas})/n^f(\text{gas.})$ 0.1198

Washburn gives an equation for μ in the equation of state, $Pv = nRT(1 - \mu P)$, for O_2–CO_2 mixtures as a function of $x(CO_2)$ [eq. 28 of ref. 2]. The equation applies strictly at 20°, but may be used at 25° without significant loss of accuracy.

(64) $\mu^f(\text{gas.}) = 0.00061\{1 + 3.21x(CO_2)[1 + 1.33x(CO_2)]\}$ 0.00088 atm.$^{-1}$

The pressure of the final gaseous mixture is calculated from the equation of state.

(65) $P^f(\text{gas.}) = \dfrac{1}{[0.040875v^f(\text{gas.})/n^f(\text{gas.})] + \mu^f(\text{gas.})}$ 27.66 atm.

The ratio, g, of the vapor pressure of water over the solution of H_2SO_4 and $HNO_3 + HNO_2$ to that over pure H_2O is obtained by interpolation from a large scale plot. Such a plot may be constructed from the values of g in the following table, which is based on data from a number of sources.[14]

wt. % (HNO_3 + HNO_2),	wt %, (H_2SO_4) 0	2	4	6	8	10	12	14	16	18
0.0	1.0000	0.9905	0.9812	0.9720	0.9618	0.9522	0.9416	0.9290	0.9147	0.8983
0.4	.9973	.9878	.9785	.9693	.9591	.9495	.9389	.9263	.9120	.8956
0.8	.9947	.9852	.9759	.9662	.9565	.9469	.9363	.9237	.9094	.8930
1.2	.9920	.9825	.9732	.9640	.9538	.9442	.9336	.9210	.9067	.8903

(66) g 0.961

The value of Wiebe and Gaddy[15] for the concentration of saturated water vapor in CO_2 at 25 atm. and 25° leads to a value of 0.00048 g. l.$^{-1}$ atm.$^{-1}$ for α in the equation, $C_W = C_O + \alpha P$. The value of α previously selected for O_2 is 0.000105 g. l.$^{-1}$ atm.$^{-1}$. Assuming that α for O_2–CO_2 mixtures varies linearly with the mole fraction of CO_2, one may write

$$C_W = 0.02304 + [0.000105 + 0.00037x(CO_2)]P \text{ g. l.}^{-1}$$

This relationship is used to calculate the number of moles of H_2O vapor in the gaseous phase.

(67) $n^f(H_2O\ \text{vap.}) = \dfrac{g\{0.02304 + [0.000105 + 0.00037x(CO_2)]P^f(\text{gas.})\}v^f(\text{gas.})}{18.016}$ 0.000488 mole

Energy Factors and Calorimetric Data

The description of the initial and final states of the isothermal bomb process is complete with item 67. Before the calculation of the actual corrections, it is convenient to tabulate values of certain quantities which are unique for the particular experiment or the particular substance and therefore cannot be expressed in a general form. These quantities are tabulated in items 68–80.

(14) (a) C. H. Greenewalt, *Ind. Eng. Chem.*, **17**, 522 (1925); (b) E. M. Collins, THIS JOURNAL, **37**, 1191 (1933); (c) S. Sharkman and A. R. Gordon, *J. Am. Chem. Soc.*, **61**, 2370 (1939); (d) ref. 3, Vol III, p. 304.

(15) R. Wiebe and V. L. Gaddy, *J. Am. Chem. Soc.*, **63**, 475 (1941).

The first of these are values of $(\partial U/\partial P)_T$ for the materials which constitute the substance. As discussed by Washburn (ref. 2, pp. 542–543), it is a satisfactory approximation to take $(\partial U/\partial P)_T$ equal to $-T(\partial v/\partial T)_P$. In the numerical example, the values of $(\partial v/\partial T)_P$ are 1.013×10^{-6}, 8.50×10^{-7} and *ca.* 10^{-6} l. g.$^{-1}$ deg.$^{-1}$ for 3-methylthiophene, the auxiliary oil, and the fuse, respectively.

(68*) $(\partial U/\partial P)_{T'} = -7221(\partial v/\partial T)_{P'}$ -0.00731 cal. g.$^{-1}$ atm.$^{-1}$

$(\partial U/\partial P)_{T''} = -7221(\partial v/\partial T)_{P''}$ -0.00614 cal. g.$^{-1}$ atm.$^{-1}$

$(\partial U/\partial P)_{T'''} = -7221(\partial v/\partial T)_{P'''}$ -0.007 cal. g.$^{-1}$ atm.$^{-1}$

The value of $(\partial U/\partial P)_T$ for the final solution is also required. It is read from a large scale plot of this quantity as a function of wt. % (H_2SO_4). Such a plot may be made from the following table, which is based on density data for H_2SO_4 solutions[8] and the approximate equality of $(\partial U/\partial P)_T$ and $-T(\partial v/\partial T)_P$.

wt. % (H_2SO_4)	$(\partial U/\partial P)_{T^f(\text{soln.})}$ $\times 10^5$, cal. g.$^{-1}$ atm.$^{-1}$	wt. % (H_2SO_4)	$(\partial U/\partial P)_{T^f(\text{soln.})}$ $\times 10^5$, cal. g.$^{-1}$ atm.$^{-1}$
0	−186	10	−281
2	−213	12	−292
4	−235	14	−302
6	−254	16	−312
8	−269	18	−321

(69) $(\partial U/\partial P)_{T^f(\text{soln.})}$ -0.00266 cal. g.$^{-1}$ atm.$^{-1}$

Values are also required for the change in internal energy for diluting (or concentrating) the $HNO_3 + HNO_2$ to a concentration of 0.1 *N* and the H_2SO_4 to an even concentration close to that obtained in the actual experiment. In the numerical example, the even concentration is selected to be $H_2SO_4 \cdot 70H_2O$. The quantity, $\Delta U_{\text{diln.}}$ ($HNO_3 + HNO_2$), is read directly from a plot, and the quantity, $\Delta U_{\text{diln.}}$ (H_2SO_4), is obtained as the difference between ΔH° of formation of H_2SO_4 at the even concentration and that at the concentration of the final solution. The required values of ΔH°_f for H_2SO_4 are read from a large scale plot of that quantity as a function of $n(H_2O)/n(H_2SO_4)$. Numerical values from which the two plots may be constructed are given below. These are based on data from the tables of selected values.[16]

wt. % ($HNO_3 + HNO_2$)	$\Delta U_{\text{diln.}}$($HNO_3 + HNO_2$), cal. mole^{-1}	$\frac{n(H_2O)}{n(H_2SO_4)}$	ΔH°_f(H_2SO_4), cal. mole^{-1}
0.0	+102	25	−211190
.1	+ 46	30	−211280
.2	+ 31	40	−211380
.3	+ 21	50	−211440
.4	+ 13	60	−211475
.5	+ 7	70	−211506
.6	+ 2	80	−211534
.8	− 6	90	−211562
1.0	− 12	100	−211590
1.5	− 23	115	−211629
2.0	− 29	130	−211665
2.5	− 34	150	−211711
3.0	− 37		
3.5	− 39		

(70) $\Delta U_{\text{diln.}}$($HNO_3 + HNO_2$) +14 cal. mole^{-1}

(71) $\Delta U_{\text{diln.}}$(H_2SO_4) −12 cal. mole^{-1}

(16) "Selected Values of Chemical Thermodynamic Properties," Series 1, Tables 14-7 and 18-6, Natl. Bur. Standards Circular 500 Washington, D. C., 1952.

The next two items list the energy of the idealized combustion reaction, ΔU_c°, for the auxiliary material and for the fuse. These quantities must have been determined in previous series of experiments.

(72*) ΔU_c°(auxiliary material) −152850 cal. mole^{-1}

(73*) ΔU_c°(fuse) −106710 cal. mole^{-1}

The next three items deal with the energy equivalent of the calorimetric system. This is conveniently divided into two parts, one the energy equivalent of the whole system minus the contents of the bomb, $C_{\text{eff.}}$ (calor.),[17] which is the same in the initial and final states, and the other the energy equivalent of the contents of the bomb, $C_{\text{eff.}}$(cont.), which is different in the initial and final states. The value of $C_{\text{eff.}}$ (calor.) must have been determined experimentally, either by electrical calibration or by combustion of a standard substance such as benzoic acid.

(74*) $C_{\text{eff.}}$(calor.) 3909.44 cal. deg.$^{-1}$

The values of $C_{\text{eff.}}$(cont.) are obtained by summing the heat capacity of all the contents of the bomb. The gaseous phase may be considered to be at constant volume, as the change in volume from thermal expansion of the bomb and of the condensed phases and from vaporization of H_2O is negligible. Similarly the condensed phases may be considered to be at constant pressure, as the change of pressure with temperature is too small to be significant. The effective heat capacity of the two-phase system, liquid H_2O or aqueous solution plus H_2O vapor, may be represented by two terms, one proportional to the total mass, and the second a "vaporization correction" proportional to the amount of H_2O vapor at 25°.[18] Thus for the initial state

$$C_{\text{eff.}}(H_2O \text{ tot.}) = Am^i(H_2O \text{ tot.}) + Bn^i(H_2O \text{ vap.})$$

and for the final state

$$C_{\text{eff.}}(\text{soln.} + H_2O \text{ vap.}) = A[m^f(\text{soln.}) + 18n^f(H_2O \text{ vap.})] + Bn^f(H_2O \text{ vap.})$$

The following values of A as a function of the concentration of the solution are based on heat capacity data for H_2SO_4[19] and HNO_3[20] solutions. As HNO_3, on a wt. % basis, lowers the heat capacity about 1.6 times as much as H_2SO_4, the independent variable is selected to be wt. % (H_2SO_4) + 1.6 wt. % ($HNO_3 + HNO_2$).

(17) The symbols S and E which have been used in the past to denote the energy equivalent are more commonly used to denote entropy and energy. To avoid confusion, a new symbol, $C_{\text{eff.}}$, meaning the effective heat capacity, is adopted here for the energy equivalent. By definition, the energy equivalent of a bomb calorimetric system is the amount of energy that must be added to it, *under the conditions of the combustion experiment*, to raise its temperature from t to t', divided by $(t' - t)$. In a combustion experiment, the pressure in the bomb changes in going from the initial to the final state, and therefore the elastic strain on the bomb proper and the compression of the crucible and other internal parts also changes. The provision "under the conditions of the combustion experiment" means that any energy effects associated with these changes in the bomb and internal parts are included in the definition of the energy equivalent.

(18) H. J. Hoge, *J. Research Natl. Bur. Standards*, **36**, 111 (1946).

(19) M. Randall and M. D. Taylor, THIS JOURNAL, **45**, 959 (1941). Note that the values of c_p listed in Tables 2 and 3 of ref. 19 are per g. of H_2O and not per g. of solution.

(20) F. D. Rossini, *Bur. Standards J. Research*, **7**, 47 (1931).

wt. % (H_2SO_4) + 1.6 wt. % (HNO_3 + HNO_2)	A, cal. $g.^{-1}$ $deg.^{-1}$	wt. % (H_2SO_4) + 1.6 wt. % (HNO_3 + HNO_2)	A, cal. $g.^{-1}$ $deg.^{-1}$
0	0.997	10	0.914
2	.979	12	.898
4	.961	14	.883
6	.945	16	.869
8	.929	18	.854

The variation of B with the concentration of the solution is not significant, and the value, 550 cal. $mole^{-1}$ $deg.^{-1}$, may be used for all concentrations.

In the numerical example, the crucible and other parts made of platinum weighed 30.05 g., and the glass ampoule to contain the 3-methylthiophene sample weighed 0.047 g. The applicable heat capacity values are: for 3-methylthiophene, 0.367; for the auxiliary oil, 0.53; and for the fuse, *ca.* 0.4 cal. $deg.^{-1}$ $g.^{-1}$.

(75) $C_{eff.}{}^{i}(cont.) =$
$5.056n^{i}[(O_2 + N_2)\ tot.] + 0.997m^{i}(H_2O\ tot.) +$
$550n^{i}(H_2O\ vap.) + m'c_p' + m''c_p'' + m'''c_p''' +$
$0.0325m(Pt) + 0.17m(glass) + \ldots\ldots$
13.69 cal. $deg.^{-1}$

(76) $C_{eff.}{}^{f}(cont.) =$
$5.056n^{f}[(O_2 + N_2)\ tot.] + 7.251n^{f}(CO_2\ tot.) +$
$A[m^{f}(soln.) + 18n^{f}(H_2O\ vap.)] + 550n^{f}(H_2O\ vap.) +$
$0.0325m(Pt) + 0.17m(glass) + \ldots\ldots$
13.79 cal. $deg.^{-1}$

The foregoing equations apply strictly at 25° and a pressure of 30 atm., and approximately at any temperature near room temperature and any pressure in the usual range of bomb-calorimetric practice. Errors from their use are minimized if the combustion experiment is conducted at temperatures near 25°, and furthermore, since the expression for $C_{eff.}{}^{i}(cont.)$ is somewhat more reliable than that for $C_{eff.}{}^{f}(cont.)$, it is advantageous to have the final temperature, t_f, close to 25°.

The electrical energy supplied to ignite the sample, $\Delta U_{ign.}$, is listed next.

(77) $\Delta U_{ign.}$ 1.35 cal.

The next three items list the initial and final temperatures of the actual bomb process, t_i and t_f, and the quantity $\Delta t_{cor.}$, which is the correction that must be applied to the change in temperature of the calorimeter to correct for the heat of stirring and the heat exchanged between the calorimeter and its environment.[21]

(21) The term, $\Delta t_{cor.}$, is best understood in relation to the calorimetric experiment. In the calorimetric experiment, the time of experimental observations is divided into three periods. In the "fore period," the temperature of the calorimeter, t, is observed as a function of time, T. (In this footnote, T is used to denote time and not Kelvin temperature.) At the end of the fore period, $T = T_i$ and $t = t_i$. The "reaction period" begins at T_i. During the reaction period, the sample is ignited, the rapid increase of temperature is observed, and enough time is allowed to elapse so that the rate of change of temperature is again uniform. The "after period" begins at T_f, at which time the temperature is t_f. In the after period, the observation of the temperature as a function of time is continued. From the observations in the fore and after periods, the rates of change of temperature at T_i and T_f, $(dt/dT)_i$ and $(dt/dT)_f$, are determined.

The changes of internal energy equivalent to the heat of stirring and the heat exchanged between the calorimeter and its environment are designated by $\Delta U_{stir.}$ and $\Delta U_{ex.}$. By definition

$$\Delta t_{cor.} = [\Delta U_{stir.} + \Delta U_{ex.}]/[C_{eff.}(calor.) + C_{eff.}{}^{f}(cont.)] \quad (I)$$

For the determination of the small correction term, $\Delta t_{cor.}$, the difference in $C_{eff.}$ (cont.) in the initial and final states is not significant, and $C_{eff.}{}^{i}$ (cont.) could have been used in eq. I instead of $C_{eff.}{}^{f}$ (cont.).

If the rate at which heat of stirring is supplied to the calorimeter is constant, and if the rate of heat exchange between the calorimeter and environment is proportional to the temperature difference (Newton's law), then at T_i and T_f

$$(dt/dT)_i = z + \alpha(t_{env.} - t_i) \quad (II)$$

and

$$(dt/dT)_f = z + \alpha(t_{env.} - t_f) \quad (III)$$

The first term on the right is the constant rate of temperature change from stirring, and the second is the rate of temperature change from heat exchange.

There are at least three methods in common use for calculating $\Delta t_{cor.}$ In the first, the temperature of the environment, $t_{env.}$, is measured, and z and α are evaluated by simultaneous solution of eq. II and III. The values of z and α are then substituted into the relation

$$\Delta t_{cor.} = \int_{T_i}^{T_f} [z + \alpha(t_{env.} - t)]dT. \quad (IV)$$

The second method does not require the determinaton of $t_{env.}$ A "convergence temperature," t_c, is defined by $t_c = z/\alpha + t_{env.}$ Physically, t_c is the limiting value the calorimeter temperature would approach after an indefinitely long period of time. Equations II, III and IV may be rewritten as

$$(dt/dT)_i = \alpha(t_c - t_i) \quad (V)$$
$$(dt/dT)_f = \alpha(t_c - t_f) \quad (VI)$$

and

$$\Delta t_{cor.} = \alpha \int_{T_i}^{T_f} (t_c - t)\, dT \quad (VII)$$

The values of α and t_c are obtained by simultaneous solution of eq. V and VI and are then substituted into eq. VII.

In the third method, which is the one used in this Laboratory, a "mid-time," T_m, is defined by the relationship

$$\int_{T_i}^{T_m} (t_i - t)\, dT = -\int_{T_m}^{T_f} (t_f - t)\, dT \quad (VIII)$$

Separation of the integral of eq. IV into two parts, the addition and subtraction of t_i in the first integrand and the addition and subtraction of t_f in the second yields

$$\Delta t_{cor.} = \int_{T_i}^{T_m} [z + \alpha(t_{env.} - t_i + t_i - t)]\, dT + \int_{T_m}^{T_f} [z + \alpha(t_{env.} - t_f + t_f - t)]\, dT \quad (IX)$$

By use of eq. VIII, this may be reduced to

$$\Delta t_{cor.} = [z + \alpha(t_{env.} - t_i)](T_m - T_i) + [z + \alpha(t_{env.} - t_f)](T_f - T_m) = (dt/dT)_i(T_m - T_i) + (dt/dT)_f(T_f - T_m) \quad (X)$$

The value of T_m is obtained from the relationship derivable from eq. VIII

$$T_m = T_f - [1/(t_f - t_i)] \int_{T_i}^{T_f} (t - t_i)\, dT \quad (XI)$$

Substitution into eq. X then yields the value of $\Delta t_{cor.}$

(78*) t_i 23.00239°
(79*) t_f 25.00842°
(80*) $\Delta t_{cor.}$ 0.00631°

Changes in Internal Energy

In this section, the idealized combustion reaction is considered as occurring in a series of steps, and the change of internal energy of each is calculated. The symbol, $\Delta U_{operation}$ (material), is used to denote the change of internal energy when the indicated operation is performed on the indicated material. The operations are abbreviated as follows: vaporization, vap.; dilution, dil.; solution, sol.; mixing, mix.; and decomposition, dec. The symbol $\Delta U(material)]_{P'}^{P''}$ is used to denote the change in internal energy of the indicated material when the pressure changes from P' to P''. When used without a superscript, ΔU applies either to a mole or to

a gram of material as convenience dictates. (The units of ΔU are always evident from the necessity that the equations be dimensionally consistent.) When used with a superscript i or f, ΔU applies to the actual amount of material involved in the combustion experiment.

Step 1.—$n^i(H_2O$ vap.) moles of liquid H_2O in its standard state at 25° is decompressed from 1 atm. to its saturation pressure at 25°, $P_{sat.}(H_2O)$, vaporized, and then decompressed in the vapor state to a negligibly small pressure. The change in internal energy is

$$n^i(H_2O \text{ vap.})\{\Delta U(H_2O \text{ liq.})]_1^{P_{sat.}(H_2O)} + \Delta U_{vap.}(H_2O) + \Delta U(H_2O \text{ vap.})]_{P_{sat.}(H_2O)}^{0}\}$$

The two decompression terms are negligibly small,[22] and only the vaporization term need be considered in the computation form. The data of ref. 3 give $\Delta H_{vap.}(H_2O) = 10{,}514$ cal. mole^{-1}, from which it follows that $\Delta U_{vap.}(H_2O) = 9922$ cal. mole^{-1}.

(81) $\Delta U_{vap.}^i(H_2O) = 9922n^i(H_2O \text{ vap.})$ +4.85 cal.

Step 2.—$(a + b/4 - c/2 + 3d/2)n$(sub.) moles of O_2 in the ideal gas state at 25° is decompressed from 1 atm. to a negligibly small pressure.

Step 3.—The O_2 gas from step 2 is mixed with $n^i(H_2O$ vap.) moles of H_2O vapor from step 1 and $n^i[(O_2 + N_2)$ tot.] $- (a + b/4 - c/2 + 3d/2)$ n(sub.) moles of excess O_2 and N_2 gas initially at a negligibly small pressure at 25°.

Step 4.—$n^i(H_2O$ liq.) moles of liquid H_2O and n(sub.) moles of the substance in their respective standard states are placed in the bomb at 25°. Steps 2, 3 and 4 do not involve any change in internal energy.

Step 5.—The liquid water is compressed to a pressure of P^i(gas.). For the pressure range involved, $(\partial U/\partial P)_T$ may be assumed to be constant. The change in internal energy is $n^i(H_2O$ liq.)$(\partial U/\partial P)_T(H_2O$ liq.)$[P^i$(gas.) $- 1]$. The value of $(\partial U/\partial P)_T(H_2O$ liq.) is -0.00186 cal. g.$^{-1}$ atm.$^{-1}$ (see table immediately preceding item 69) or -0.0335 cal. mole^{-1} atm.$^{-1}$.

(82) $\Delta U^i(H_2O \text{ liq.})]_1^{P^i(gas.)} = -0.0335n^i(H_2O \text{ liq.})[P^i(gas.) - 1]$ −0.54 cal.

Step 6.—The substance is similarly compressed.

(83) $\Delta U^i(sub.)]_1^{P^i(gas.)} = [m'(\partial U/\partial P)_T' + m''(\partial U/\partial P)_T'' + m'''(\partial U/\partial P)_T'''][P^i(gas.) - 1]$ −0.19 cal.

If the compound is enclosed in a sealed ampoule which it does not fill, the energy of compression of the compound must be replaced by the energy of compression of the ampoule in item 83. As the latter is difficult to estimate, it is desirable to enclose a volatile compound in a completely filled, thin walled ampoule so that the pressure in the bomb is transmitted to the compound. Such a procedure was followed in the numerical example.

Step 7.—$n^i[(O_2 + N_2)$ diss.] moles of O_2 and N_2 gas from the mixture of step 3 are dissolved in the liquid H_2O. The change in internal energy is $\Delta U_{soln.}(O_2 + N_2)$ $n^i[(O_2 + N_2)$ diss.]. The values of $\Delta U_{soln.}(O_2 + N_2)$ for aqueous H_2SO_4 solutions will be discussed under step 15; the limiting value for pure H_2O is -3200 cal. mole^{-1}.

(84) $\Delta U_{soln.}^i(O_2 + N_2) = -3200n^i[(O_2 + N_2)$ diss.] −1.21 cal.

Step 8.—n^i(gas.) moles of the mixture of O_2 gas, N_2 gas and H_2O vapor is compressed into the remaining space of the bomb to the pressure, P^i(gas.). If the effect of the small concentration of H_2O vapor is neglected and the N_2 is treated as though it were O_2, the change in internal energy may be represented by $\Delta U(O_2$ gas$)]_0^{P^i(gas.)}n^i$(gas.). The calorimetric data of Rossini and Frandsen[23] for O_2 at 28°, when corrected to 25° by use of a temperature coefficient[24] of -0.4% deg.$^{-1}$ for $(\partial U/\partial P)_T$ give $\Delta U(O_2$ gas$)]_0^P = -1.574P$ cal. mole^{-1}.

(85) $\Delta U^i(gas.)]_0^{P^i(gas.)} = -1.574P^i(gas.)n^i(gas.)$ −19.83 cal.

Step 9.—The bomb is placed in the calorimetric system at 25°. This step, for which there is no change in internal energy, brings the system to the initial state of the isothermal bomb process.

In the foregoing, it has been assumed that all of the substance is liquid or solid in the initial state, and that it does not interact in any way with the other materials in the bomb. This assumption may not be strictly true for relatively non-volatile materials that are not sealed in ampoules but are exposed directly to the bomb gases. For such materials there are energy effects associated with volatilization of a small amount of the material, with the solution of O_2, N_2 and H_2O in liquids, and with the adsorption of these on solids. The corrections for these effects are difficult to assess in practice. Therefore in precision calorimetry, the experiments must be designed in such a way that these effects are negligibly small.

Step 10.—The temperature of the system is changed from 25° to t_i. The equivalent change in internal energy is $[C_{eff.}(calor.) + C_{eff.}^i(cont.)](t_i - 25)$.

Step 11.—The actual bomb reaction is caused to occur, and the temperature of the system increases from t_i to t_f. The equivalent change in internal energy is the sum of the electrical energy supplied to ignite the sample, the stirring energy, and the energy exchanged between the calorimeter and its environment, $\Delta U_{ign.} + \Delta U_{stir.} + \Delta U_{ex.} = \Delta U_{ign.} + [C_{eff.}(calor.) + C_{eff.}^f(cont.)]\Delta t_{cor.}$

Step 12.—The temperature of the system is changed from t_f to 25°. This step brings the system to the final state of the isothermal bomb process. The equivalent change in internal energy is $[C_{eff.}(calor.) + C_{eff.}^f(cont.)](25 - t_f)$.

The change of internal energy for the isothermal bomb process, $\Delta U_{I.B.P.}$, is the sum of the changes of internal energy for steps 10, 11 and 12.

(86) $\Delta U_{I.B.P.} = C_{eff.}(calor.)(t_i - t_f + \Delta t_{cor.}) + C_{eff.}^i(cont.)(t_i - 25) + C_{eff.}^f(cont.)(25 - t_f + \Delta t_{cor.}) + \Delta U_{ign.}$ −7843.81 cal.

(22) In the numerical example, the decompression terms are 0.000016 and 0.0024 cal.

(23) F. D. Rossini and M. Frandsen, *Bur. Standards J. Research*, **9**, 733 (1932).

(24) E. W. Washburn, *ibid.*, **9**, 521 (1932).

Step 13.—The liquid and gas phases are removed from the bomb and calorimeter at 25° and are confined separately at a pressure of P^f(gas.). No change of internal energy is associated with this step.

Step 14.—The dissolved CO_2 is allowed to escape from the liquid phase and expand to a negligibly small pressure, and is then brought to its standard state at 25°. The change in internal energy is $-\Delta U_{soln.}(CO_2)n^f(CO_2$ diss.). For pure H_2O as solvent, the "selected value" for $\Delta H_{soln.}(CO_2)$ is -4640 cal. mole^{-1} [25]; the corresponding value of $\Delta U_{soln.}(CO_2)$ is -4050 cal. mole^{-1}. The solubility of CO_2 in H_2SO_4 solutions has been studied as a function of temperature by Geffcken[11](0–4 N) and Sunner[12](0–1.2 N). Values of the heat of solution were computed from these solubility data, reduced to 25° by use of the temperature coefficient given by Harned and Davis,[26] and converted to values of the change of internal energy. The equation, $\Delta U_{soln.}(CO_2) = -4050 + 240\ N(H_2SO_4)$ cal. mole^{-1}, was selected to represent the values so obtained. This equation is consistent with the "selected value" for pure H_2O as solvent, and fits the values for H_2SO_4 solutions with an average deviation of 110 cal. mole^{-1}.

(87) $\Delta U_{soln.}{}^f(CO_2) = [4050 - 240N(H_2SO_4)]n^f(CO_2$ diss.) $+3.47$ cal.

Step 15.—The dissolved O_2 and N_2 are allowed to escape from the liquid phase and expand to a negligibly small pressure. The change in internal energy is $-\Delta U_{soln.}(O_2)\ n^f[(O_2 + N_2)$diss.]. For pure H_2O as solvent, the "selected value"[27] for $\Delta H_{soln.}(O_2)$ is -3800 cal. mole^{-1}; the corresponding value for $\Delta U_{soln.}(O_2)$ is -3200 cal. mole^{-1}. The data of Geffcken[11] on the solubility of O_2 in H_2SO_4 solutions at 15 and 25° lead to values of $\Delta U_{soln.}(O_2)$ at 20° which may be represented by the equation, $\Delta U_{soln.}(O_2) = -2770 + 280\ N(H_2SO_4)$. The assumption that the difference between 20 and 25° is independent of the H_2SO_4 concentration gives the following equation for 25°: $\Delta U_{soln.}(O_2) = -3200 + 280\ N(H_2SO_4)$.

(88) $\Delta U_{soln.}{}^f(O_2 + N_2) = [3200 - 280N(H_2SO_4)]n^f[(O_2 + N_2)$ diss.] $+0.76$ cal.

Step 16.—The liquid phase is decompressed to a final pressure of 1 atm.

(89) $\Delta U^f(\text{soln.})\Big]_{P^f(\text{gas.})}^{1} = (\partial U^f/\partial P)_{T^f(\text{soln.})} m^f(\text{soln.})[1 - P^f(\text{gas.})]$ $+0.80$ cal.

Step 17.—The $HNO_3 + HNO_2$ are removed from the solution and dissolved in the amount of H_2O (in its standard state) required to give a 0.1 N solution.

(90) $\Delta U_{diln.}{}^f(HNO_3 + HNO_2) = \Delta U_{diln.}(HNO_3 + HNO_2)[n^f(HNO_3) + n^f(HNO_2)]$ $+0.01$ cal.

Step 18.—Water (in its standard state) is added to or removed from the solution to bring the concentration of H_2SO_4 to the selected even concentration.

(91) $\Delta U_{diln.}{}^f(H_2SO_4) = n^f(H_2SO_4)\Delta U_{diln.}(H_2SO_4)$ -0.10 cal.

Step 19.—The HNO_3 and HNO_2 are decomposed according to the reactions: HNO_3(aq. 0.1 N) = $^1/_2H_2O(l) + {}^1/_2N_2(g) + {}^5/_4O_2(g)$ and HNO_2 (aq. 0.1 N) = $^1/_2H_2O(l) + {}^1/_2N_2(g) + {}^3/_4O_2(g)$. The O_2 and N_2 are allowed to expand to a negligibly small pressure. The water used to make the solution in step 17 and that formed in the decomposition reactions is brought to its standard state. The values of ΔU for the reactions are calculated from the "selected values" of the heats of formation of HNO_3, HNO_2 and H_2O[28] to be 14074 and -6600 cal. mole^{-1}.

(92) $\Delta U_{dec.}{}^f(HNO_3 + HNO_2) = 14074n^f(HNO_3) - 6600n^f(HNO_2)$ $+9.68$ cal.

Step 20.—The gaseous phase containing O_2, N_2, CO_2 and H_2O vapor is expanded to a negligibly small pressure. The change in internal energy is $\Delta U(\text{gas.})\Big]_{P^f(\text{gas.})}^{0} n^f(\text{gas.})$. The calorimetric data of Rossini and Frandsen[23] for the change in internal energy for the compression of O_2–CO_2 mixtures, when reduced to 25°, may be represented by

$$\Delta U\Big]_0^P = -1.574\{1 + 1.69x(CO_2)[1 + x(CO_2)]\}P \text{ cal. mole}^{-1}$$

(93) $\Delta U^f(\text{gas.})\Big]_{P^f(\text{gas.})}^{0} = 1.574\{1 + 1.69x(CO_2)[1 + x(CO_2)]\}P^f(\text{gas.})n^f(\text{gas.})$ $+20.82$ cal.

Step 21.—The O_2, N_2, CO_2 and H_2O vapor are separated from each other, and the CO_2 is brought to its standard state. There is no change in internal energy in this step.

Step 22.—The H_2O vapor is compressed to its saturation pressure, $P_{sat.}(H_2O)$, condensed to liquid, and further compressed to a final pressure of 1 atm. The changes in internal energy are

$$n^f(H_2O \text{ vap.})\{\Delta U(H_2O \text{ vap.})\Big]_0^{P_{sat.}(H_2O)} - \Delta U_{vap.}(H_2O) + \Delta U(H_2O \text{ liq.})\Big]_{P_{sat.}(H_2O)}^{1}\}$$

As in step 1, only the vaporization term is significant.

(94) $\Delta U_{vap.}{}^f(H_2O) = -9922n^f(H_2O$ vap.) -4.84 cal.

In the foregoing series of 22 steps, the calorimeter, the bomb, the N_2, the excess O_2 and the excess H_2O are all returned to their original state. The net change is simply the idealized combustion reaction. The energy of the idealized combustion reaction, for the actual amount of substance involved in the combustion experiment, $n\Delta U_c°$(sub.), is therefore just the sum of the changes in internal energy for all of the steps.

(95) $n\Delta U_c°$(sub.), sum of items 81–94 incl. -7830.13 cal.

The previous item applies to the total substance. Corrections for the auxiliary material and fuse are applied in the next three items to obtain the value for the compound alone.

(96) $n''\Delta U_c°$(auxiliary material) -588.08 cal.

(97) $n'''\Delta U_c°$(fuse) -16.09 cal.

(98) $n'\Delta U_c°$(compound) = $n\Delta U_c°$(sub.)$-n''\Delta U_c°$(auxiliary material) $- n'''\Delta U_c°$(fuse) -7225.96 cal.

(25) Reference 16, Series 1, Table 23-2.

(26) H. S. Harned and R. Davis, Jr., *J. Am. Chem. Soc.*, **65**, 2030 (1943).

(27) Reference 16, Series 1, Table 1-1.

(28) Reference 16, Series 1, Tables 18-5, 18-6 and 2a-1.

The quantity in item 98 is converted to units of cal. $g.^{-1}$ and kcal. $mole^{-1}$ in the final two items.

$$(99)\quad \frac{\Delta U_c^\circ}{M}(\text{compound}) = \frac{n'\Delta U_c^\circ(\text{compound})}{m'}$$

-8430.2 cal. $g.^{-1}$

$$(100)\quad \Delta U_c^\circ(\text{compound}) = \frac{n'\Delta U_c^\circ(\text{compound})}{1000n'}$$

-827.54 kcal. $mole^{-1}$

Comments

In the foregoing presentation, the treatment has been given in a very general form. In its application to particular calorimetric experiments, certain simplifications will always be possible. For example, since it is a customary procedure to always charge the bomb to a certain predetermined pressure, P^i(gas.) will be the same for all experiments and can be introduced as a constant in items 28, 32, 34, 82, 83 and 85 of the computation form. It will seldom be necessary to make the complete calculation for all the experiments of a series. If the calculation is made for the two experiments with the most widely differing experimental conditions, it will be evident which of the energy terms (items 81–94 incl.) change significantly with the experimental conditions and which are essentially the same in all experiments. Then it will only be necessary to calculate for each experiment those energy terms that change significantly from experiment to experiment.

The calibration of bomb calorimeters is usually carried out by the combustion of benzoic acid. The standard samples of benzoic acid issued by the National Bureau of Standards are certified in terms of an energy quantity, ΔU_B. In the notation of this paper, ΔU_B is $[\Delta U_{\text{I.B.P.}} + \Delta U_{\text{dec.}}{}^{f}(HNO_3 + HNO_2) + \Delta U_{\text{diln.}}{}^{f}(HNO_3 + HNO_2) - n'''\Delta U_c^\circ(\text{fuse})]$. If the conditions of the calibration experiment meet the specifications of the certificate with respect to the O_2 pressure, the ratio of the mass of sample to the volume of the bomb, and the ratio of the mass of H_2O placed in the bomb to the volume of the bomb, then the certified value of ΔU_B may be used directly to compute $C_{\text{eff.}}$(calor.). If the conditions differ from those specified in the certificate, it is necessary to compute ΔU_c° for the benzoic acid and then reverse the calculations for the new conditions to obtain $C_{\text{eff.}}$(calor.) from the value of ΔU_c°.

The extension of the present treatment to make it applicable to compounds of carbon, hydrogen, oxygen and nitrogen will be particularly straightforward. For this class of compounds, N_2 is a product of the combustion reaction, and there is more N_2 present in the final state than in the initial state. For this situation it will no longer be valid to treat the N_2 as though it were O_2. The necessary modification of the present treatment will then be the introduction of the appropriate terms for treating the N_2 separately from the O_2.

CATION EXCHANGE PROPERTIES OF BENTONITE[1a]

BY W. H. SLABAUGH[1b]

Department of Chemistry, Kansas State College, Manhattan, Kansas

Received June 15, 1953

Equilibrium constants based upon the law of mass action and enthalpy changes during the process of ion exchange of aliphatic amine hydrochlorides with sodium bentonite have been experimentally determined. From these data free energy and entropy changes have been calculated.

Introduction

It has been adequately shown by many workers, including Hauser[2a] and Jordan,[2b] that amines react chemically with bentonite to form organo-clay complexes. These complexes are the result of ion-exchange processes wherein the attractions between the cationic groups of the amine and the anionic sites on the clay are primarily coulombic. In addition there is a significant amount of van der Waals type adsorption which causes the hydrocarbon chain of the higher amines to become adsorbed onto the surface of the clay lamina. The resultant orientation should manifest itself as a significant entropy change.

In this study, a specially prepared sodium bentonite was treated with aliphatic, straight chain amines. The enthalpy and the equilibrium constant for these exchanges were measured, and the free energy and entropy changes were calculated from these data.

Materials and Experimental Procedure

A sample of typical Wyoming bentonite, supplied by the Baroid Sales Division of the National Lead Company, was dispersed in water at 2% solids. After three months of aging at room temperature, the non-clay sediment was separated; the supernatant clay suspension was passed through an Amberlite IR-120 column which had been converted to the sodium form by NaCl treatment. This bentonite suspension, at approximately 1% solids, was essentially a sodium bentonite, its original content of exchangeable Ca^{++} and Mg^{++} being reduced to less than 1 meq./100 g. clay. The prepared clay, which was very similar to that prepared by Williams and co-workers,[3] had a base-exchange capacity of 92 meq./100 g. clay, compared to an original BEC of 82 meq./100 g. clay as determined by the ammonium acetate method.

The enthalpy of ion exchange was measured in a microcalorimeter which permitted the addition of the exchanging

(1) (a) Presented at the 124th National Meeting of the American Chemical Society, Chicago, September, 1953. (b) Department of Chemistry, Oregon State College, Corvallis, Oregon.

(2) (a) E. A. Hauser in Jerome Alexander, "Colloid Chemistry," Vol. VII, Reinhold Publ. Corp., New York, N. Y., 1950, pp. 431–32; U. S. Patents 2,531,427 and 2,531,812. (b) John W. Jordan, B. J. Hook and C. M. Finlayson, THIS JOURNAL, **54**, 1196 (1950).

(3) F. J. Williams, M. Neznayko and D. J. Weintritt, *ibid.*, **57**, 6 (1953).

reagent in small amounts. The calorimeter, which uses a 57 junction Cu-constantan thermocouple and gives a response of 2.2 cm. scale reading per calorie, has been fully described previously.[4] Data for the calculation of the equilibrium constants were obtained by micro-Kjeldahl analysis for the amine, and by flame spectrophotometry for the sodium.

The exchanging reagents were prepared from commercially available straight chain amines. Lower amines up to butylamine were purchased from the Matheson Company, and all the higher amines were distilled grade fatty amines kindly supplied by Armour and Company. From these amines the amine hydrochlorides were prepared by adding sufficient HCl to reach a neutral point predicted by a potentiometric titration. The *p*H of the exchanging reagents thus made varied from 3.8 to 5.0.

Experimental Results and Discussion

A. The Cation-exchange Equilibrium Constant.—The formulation of suitable mathematical equations to describe the equilibria between soluble, exchanging ions and adsorbed, exchanged ions has been attacked in various manners. Boyd and coworkers[5] examined heterogeneous ion exchange on the basis of Langmuir's adsorption mechanism and on the mass action principle. Boyd, and later Coleman[6] were successful in applying mass action arguments to ion exchange of inorganic ions on organic exchangers. Kressman[7] obtained data from exchange reactions between quaternary ammonium salts and organic exchangers which fit the mass action relationship.

Similarly, in the present work the exchange reaction between sodium bentonite and organic amine hydrochlorides is assumed to be a metathetical reaction

$$\text{Na-Bentonite} + RNH_3^+ \longrightarrow Na^- + RNH_3\text{-Bentonite} \quad (1)$$

from which a thermodynamic equilibrium constant is defined as

$$K = \frac{\gamma \cdot C_{RNH_3^+} \times a_{Na^+}}{\gamma \cdot C_{Na^+} \times a_{RNH_3^+}} \quad (2)$$

Here, $\gamma \cdot C_{RNH_3^+}$ and $\gamma \cdot C_{Na^+}$ are the activities of RNH_3^+ and Na^+, respectively, which are exchanged on the clay. The activities of Na^+ and RNH_3^+ in the aqueous phase are expressed by the terms a_{Na^+} and $a_{RNH_3^+}$.

Data for equation 2 were obtained by analyzing reaction mixtures at various concentrations of amine. Amine hydrochloride solutions were added up to a 500% excess over that amount which is equivalent to the base-exchange capacity and sufficient water was added to give a total solids content of 0.98% (dried at 105°). After shaking by hand for a few minutes and allowing the mixture to stand overnight, the reaction systems were centrifuged and portions of the supernatant liquids were analyzed for Na^+ and RNH_3^+. In order to make certain that the equilibrium point had been reached, a similar series of determinations was made on reaction systems which started with a suspension of amine-bentonite to which various amounts of NaCl solution were added. The amine-bentonite was made by adding the amine to hydrogen-bentonite which was prepared by passing the clay suspension through an Amberlite IR-120 column which was in the acid form. Results of these two types of experiments indicated that chemical equilibrium was reached under the above conditions.

The amount of Na associated with the bentonite (C_{Na^+}) was calculated from the difference between the amount of Na^+ on the original clay and the amount released in successive additions of the amine hydrochloride. The amount of RNH_3^+ associated with the bentonite may be determined experimentally, or it may be calculated in either of two manners. The first method of calculating $C_{RNH_3^+}$ is shown in Table I. The amount of $CH_3NH_3^+$ added distributes itself between the liquid phase and the exchanger. On the exchanger, the amine ion further distributes itself between the cationic exchange sites (where it releases an equivalent amount of sodium ion) and the adsorption sites. Thus, if no absorption occurs, the amount of $C_{CH_3NH_3^+}$ is the difference between the amount of $CH_3NH_3^+$ added and the amount of $CH_3NH_3^+$ remaining in the aqueous phase. Actually for the lower amines, particularly at the lower levels of RNH_3^+ concentration, there was very little if any measurable amount of the amine ion that was adsorbed on the exchanger; in other words, in these cases there was essentially a process of stoichiometric exchange as indicated by equation 1. The inconsistencies between initial and final amine ion concentrations in Table I reflect the analytical errors that are cited later.

TABLE I

EXPERIMENTAL DATA FOR THE REACTION:
Na-Bentonite + $CH_3NH_3^+ \rightarrow Na^+ + CH_3NH_3^-$

Bentonite at 25°; concn. are in mmoles/l. of clay suspension.

Sample	Initial		Final concn.				
	Na^+	$CH_3NH_3^+$	Na^+	$CH_3NH_3^+$	C_{Na^+}	$C_{CH_3NH_3^+}$	K
1	6.63	0	6.63	0	9.10	0	...
2	6.63	1.77	7.93	0.93	7.80	0.84	0.91
3	6.63	3.54	8.87	2.20	6.86	1.34	.78
4	6.63	5.31	9.68	3.45	6.05	1.86	.86
5	6.63	7.10	9.91	4.12	5.82	2.98	.89
6	6.63	10.8	10.33	7.75	5.40	3.05	.77
7	6.63	14.2	10.60	10.28	5.13	3.90	.77
8	6.63	17.7	10.96	13.18	4.77	4.52	.77
9	6.63	35.2	11.58	28.95	4.15	6.20	.60
10	6.63	53.1	11.95	45.1	3.78	8.0	.56
							0.77

The second method of calculating $C_{RNH_3^+}$ is based upon the quantity of sodium ion which is released by clay exchanger when it is treated with RNH_3^+. This method was used with the higher amines when adsorption occurred in addition to chemical exchange. It is assumed here that RNH_3^+ can cause the release of Na^+ only when it exchanges with the Na-exchanger system. An example will show how this method was used: In a particular case with the reaction Na-Bentonite + $C_{14}H_{29}NH_3^+$, 6.8 mmoles of RNH_3^+ was added. There was a release of 5.6 mmoles of Na^+ and 0.3 mmole of RNH_3^+ remained in solution. The remaining 0.9 mmole of RNH_3^+ was adsorbed. In this case $C_{RNH_3^+} = 5.6$. These concentrations,

(4) W. H. Slabaugh, *J. Am. Chem. Soc.*, **74**, 4462 (1952).

(5) G. E. Boyd, J. Schubert and A. W. Adamson, *ibid.*, **69**, 2818 (1947).

(6) N. T. Coleman, *Soil Sci.*, **74**, 115 (1952).

(7) R. R. E. Kressman and J. A. Kitchener, *J. Chem. Soc.*, 1190 (1949).

as well as those expressed elsewhere in this paper, are in terms of millimoles per liter of bentonite suspension. This method not only gives the value $C_{RNH_3^+}$ but supplies the quantities of amine ion that were adsorbed by the exchanger. These latter data are summarized in Table II. There is a noticeable trend toward more adsorption at higher levels of RNH_3^+ concentrations and with the higher amines. The equilibrium constants were calculated on the basis of the quantities actually exchanged, that is, the values for $C_{RNH_3^+}$ used in calculations based upon equation 2 do not include the quantities shown in Table II.

TABLE II

QUANTITIES OF AMINE IONS ADSORBED ON THE CLAY EXCHANGER

Concentrations are in mmoles per liter of bentonite suspension. Sample numbers are identical to those in Table I.

R group: Samples	CH_3	C_4H_9	C_8H_{17}	$C_{10}H_{21}$	$C_{14}H_{29}$	$C_{18}H_{37}$
2	0	0	0	0	0	0
3	0	0	0	0	0.1	0
4	0	0	...	0.18	.41	0.40
5	...	0	0.10	0.49	.92	1.00
6	0	0	.20	2.9	3.2	3.4
7	0.02	0.14	.70	3.5	5.5	5.9
8	0	0.55	.97	3.9	6.6	9.1
9	0.35	3.2	...	3.6	6.8	25
10	0.20	3.3	...	3.5	6.7	...

There was experimental support of the assumption that moles of Na^+ released = moles of RNH_3^+-bentonite formed. The accuracy of the data in this phase of the work is 4% at 0.0018 to 0.018 molar concentrations.

In order to use equation 2, it was necessary to evaluate either the activities of Na^+ and RNH_3^+ or the ratio of their respective activity coefficients. Sufficient discussion of this problem has been given by Boyd, *et al.*[5] Whitlow and Felsing[8] have determined the activity coefficients for CH_3NH_2·HCl at 25 and 0°, and have noted a negligible temperature coefficient. Comparing these values to γ_{NaCl} from Glasstone[9] up to 0.05 molar systems, the maximum concentration encountered in the present work, the ratio $\gamma_{NaCl}/\gamma_{CH_3NH_2\cdot HCl}$ is very nearly unity. Thus in place of their activities, the molar concentrations for Na^+ and $CH_3NH_3^+$ were used in equation 2, assuming that the mean ionic activity coefficients were not seriously influenced by the presence of other electrolytes. Lacking activity coefficients for the higher amine hydrochlorides it was assumed that the ratio of the activity coefficients such as $\gamma_{Na^+}/\gamma_{RNH_3^+}$ did not deviate far from unity. This is a rather tenuous assumption, particularly for the higher amines, but it is fairly well supported by the consistency of the data which was analyzed for each group of reactions. When $\log C_{RNH_3^+}/C_{Na^+}$ was plotted against $\log [Na^+]/[RNH_3^+]$, the adherence of the data to a straight line with a slope of -1 was indicative of the consistency of the value for the equilibrium constant. Although the ionic strengths of these systems vary almost sevenfold, the constancy of the K values probably indicates that the ratio of the activity coefficients of the ionic species concerned does not deviate seriously from constancy.

From the data of other reaction systems similar to that in Table I, values of K were calculated. Table III summarizes these K values for all Na-Bentonite–amine reactions investigated. Those values in parentheses were rejected in the calculation of the means.

TABLE III

SUMMARY OF K VALUES AT 25° FOR THE REACTIONS:

Na-Bentonite + RNH_3^+ → Na^+ + RNH_3-Bentonite

R group: Sample	CH_3 K	C_4H_9 K	C_8H_{17} K	$C_{10}H_{21}$ K	$C_{14}H_{29}$ K	$C_{18}H_{37}$ K
1	...	...				
2	0.91	1.35				
3	.78	1.36	7.0	28		
4	.86	2.20	4.3	30	72	84
5	.94	2.72	9.4	23	62	81
6	.77	2.24	8.9	33	62	92
7	.77	1.53		18	67	122
8	.77	1.46	5.0	(9.0)	64	112
9	.60			(7.2)	68	122
10	.56				52	
Mean K	0.77	1.83	6.9	26	64	102

Direct calorimetric measurements of ΔH at 25° were made by making at least six successive measurements on each system. Table IV shows both observed data and calculations of ΔH as based upon these measurements. Because it was impossible to distinguish between the enthalpies of exchange and of adsorption, the values in Table IV include the total enthalpy of the reaction between Na-Bentonite and the amine hydrochloride.

TABLE IV

CALORIMETRIC DETERMINATION OF THE HEAT OF EXCHANGE FOR THE REACTION:

Na-Bentonite + $C_4H_9NH_3^+$ → Na^+ + $C_4H_9NH_3$-Bentonite

K = 1.8 at 25°. To each step was added 0.145 mM in $C_4H_9NH_3^+$ beyond the amine concn. in the preceding step.

Step	$C_4H_9NH_3^+$ reacting, mmoles	Heat of reaction (obsd.), cal.	H, cal./mole
1	0.106	...	...
2	.100	0.212	−212
3	.097	.268	−276
4	.093	.219	−236
5	.089	.244	−252
		Mean	−244 ± 10

In order to calculate the molar ΔH values it was necessary to apply the equilibrium constant for the corresponding reaction. Thus if the equilibrium constant for the reaction between Na-Bentonite and $C_4H_9NH_3^+$ is 1.8, then each mole of $C_4H_9NH_3^+$ added to a mole of Na-Bentonite accounts for only 0.57 mole of actual exchange. Or, from equation 2

$$\frac{(X)(X)}{(1-X)(1-X)} = 0.57, \quad X = 0.57 \text{ and } \% \text{ completion} = 0.57/1.00 = 57\%$$

In this particular run the calorimeter calibration was equal to 0.80 cm. deflection of the galvanometer for 0.36 cal. In step 2, Table IV, the deflection

(8) E. P. Whitlow and W. A. Felsing, *J. Am. Chem. Soc.*, **66**, 2028 (1944).

(9) S. Glasstone, "Thermodynamics for Chemists," D. Van Nostrand Co., Inc., New York, N. Y., 1947, p. 402.

was 0.54 which represented the reaction of 0.100 mmole of $C_4H_9NH_3^+$ with sodium bentonite. This is equivalent to 212 cal. per mole of $C_4H_9NH_3^+$ which has reacted. The percentage of reaction was calculated from the mean value of the equilibrium constant K as derived in Table III.

It is admitted that a probable discrepancy exists here. ΔH values were calculated on the basis of ionic exchange only, while experimentally the heats of the total reaction (including exchange and adsorption) were observed. In view of the fact that at low levels of amine concentration very little adsorption occurred, the ΔH values are viewed as dependable within experimental error. In several of the calorimetric measurements at higher amine concentrations after the sharp but slight rise in temperature produced by the addition of the reagent a very slight but noticeable endothermic process was observed. Because this phenomenon occurred most commonly with the higher amines it was tentatively attributed to the heat of adsorption of the amine ion by the bentonite. However, more precise measurements will be required before this idea can be concluded.

Using the mean K values in Table III, the free energies of these exchange reactions were calculated by using the equation

$$\Delta F = -RT \ln K$$

Now having both ΔF and ΔH values, the calculations of the corresponding entropies were made from the relation

$$\Delta S = (\Delta H - \Delta F)/T$$

A summary of these calculations is given in Table V. Based upon a 4% probable error in determining the values used in calculating K from equation 2, the resulting ΔS values have a range of $\pm 16\%$ error. The range of error in the calorimetric values was of approximately the same magnitude.

X-Ray diffraction studies by Jordan[2] and others have given structural proof that the hydrocarbon chain of the exchanged amine lies flat upon the clay lamina surface. Thus, when an amine ion exchanges with the sodium ion on the clay, at least four factors are concerned:

1. Dissociation of the sodium ion from the clay going into true solution.
2. The amine ion leaves the solution phase and becomes associated with the colloidal clay particle.
3. The amine ion becomes oriented about the exchange site, its ionic charge balanced by the charge on the clay lamina.
4. The hydrocarbon chain of the amine is adsorbed onto the clay laminar surface accompanied by the removal of the water which was previously adsorbed on this surface. That is, the hydrophilic laminar surfaces are transformed into hydrophobic surfaces.

Since significant energies may be involved with each of these factors, the entropies in Table V can be attributed to the total process only. It would be of great interest to be able to associate portions of the total entropy to each of the above factors.

TABLE V

THERMODYNAMIC DATA FOR THE REACTIONS:

Na-Bentonite + RNH_3^+ $\rightleftharpoons$ Na^+ + RNH_3-Bentonite

RNH_3^+	Equilibrium constant K	Free energy F, cal.	Enthalpy of exchange H, cal.	Entropy S, e.u.
$CH_3NH_3^+$	0.77 ± 0.12^a	150	150	0.0
$C_4H_9NH_3^+$	1.8 ± 0.5	− 350	− 240	.4
$C_8H_{17}NH_3^+$	6.9 ± 2.0	−1140	− 900	.8
$C_{10}H_{21}NH_3^+$	26 ± 5.3	−1920	−1780	.5
$C_{14}H_{29}NH_3^+$	64 ± 5.9	−2450	−2500	− .2
$C_{18}H_{37}NH_3^+$	102 ± 5.3	−2740	...	...

[a] Standard deviations.

Acknowledgment.—The assistance of Dr. W. G. Schrenk in making the spectrophotometric determinations for this study is appreciated.

ACTIVITY COEFFICIENTS OF PIPERIDINE IN AQUEOUS SALT SOLUTIONS[1]

By F. A. Long and R. L. Bergen, Jr.

Contribution from Department of Chemistry, Cornell University, Ithaca, N. Y.

Received June 30, 1953

The activity coefficients of piperidine in aqueous salt solutions have been determined at 25° by measuring the distribution of the non-electrolyte between salt solutions and benzene. Data are given for 12 salts. The salt effects range from pronounced salting out with sodium sulfate to salting in with salts of large anions or cations. The observed salt order is the typical one expected for a basic non-electrolyte in that, relative to the salt order for non-polar non-electrolytes, the positions of sodium and potassium ions are inverted, lithium ion salts in more than normally and there is a greater sensitivity to changes of anion than of cation. The data are compared with those of other acidic and basic non-electrolytes of similar size and a qualitative explanation of the observed trends for acidic and basic non-electrolytes is given in terms of interactions between the non-electrolytes and water of hydration of the ions.

The effects of salts on the activity coefficients of non-electrolytes in aqueous solution show a decided variability and it has recently been pointed out that there are two rather different aspects to the problem.[2] One aspect is a distinctly specific character of the salt effects which enters even with the simplest non-polar non-electrolytes. For different salts the effects, *i.e.*, the salt order, can range from pronounced salting out to pronounced salting in. It has been shown that these specific effects on non-polar non-electrolytes correlate well with properties of the salt solutions themselves[3] and in this sense one can speak of the salt order shown with non-polar molecules as the "normal" one.

The other aspect, which enters with polar non-electrolytes, is a pronounced dependence of the specificities, *i.e.*, of the salt order, on the particular character of the non-electrolyte. With acidic non-electrolytes the activity coefficient is more sensitive to changes of salt cation than to the anion. Salts of lithium and hydrogen ions cause markedly greater salting out than is found with non-polar molecules. Finally, the magnitude of these changes appears to depend on the acid strength of the non-electrolyte as measured by its ionization constant. For example, un-ionized phthalic acid is salted out considerably more by lithium chloride than by sodium chloride[2,4] whereas with benzene and other non-polar non-electrolytes the opposite is observed.[2,3]

With basic non-electrolytes the effects are opposite to those for the acidic species. The degree of salting out is influenced relatively more by the anions than by cations and in particular lithium chloride causes markedly less salting out than with non-polar molecules. Thus ammonia is actually salted in by lithium chloride and the order of the cations potassium and sodium is inverted from that found with non-polar molecules so that potassium ion causes greater salting out than sodium ion.[2,5] However, in contrast to the situation with acidic species, not enough data are available for basic non-electrolytes of similar size to see if the changes parallel the base strength of the non-electrolytes.

In order to obtain data for a comparatively strong base, we have determined the influence of salts on the activity coefficient of piperidine (pK_B = 2.9) in aqueous solution. Piperidine has a molar volume at 20° of 99 ml. per mole, so that the observed salt effects can be fairly simply compared to those for aniline and other simple benzene derivatives of similar molar volume. The experimental procedure that has been used is measurement of the distribution of piperidine between benzene and aqueous salt solutions.

Experimental

In dilute solutions the activity coefficient of a non-electrolyte, referred to its infinitely dilute solution in water, can be expressed as[2]

$$\log f_i = k_s C_s + k_i C_i \qquad (1)$$

where f_i is the molar activity coefficient, C_s and C_i are molar (or normal) concentrations of salt and of non-electrolyte, k_s is the salting out parameter and k_i is the "self-interaction" parameter. By working with sufficiently dilute solutions of non-electrolyte, the self-interaction term, $k_i C_i$, can be made negligible. Then for two distribution experiments one involving pure water and the other involving a salt solution, if the concentration of non-electrolyte in the non-aqueous reference phase is the same

$$\log \frac{f_i}{f_i^0} = \log \frac{C_i^0}{C_i} = k_s C_s \qquad (2)$$

where the superscript zero refers to solution in pure water. Hence from the two experiments k_s can be determined by measuring C_i^0 and C_i and C_s for salt solution. In practice one does not attempt to keep the concentration in the reference phase, C_i^R, constant. Instead one determines the distribution coefficient, $K_D = C_i^R/C_i^0$, as a function of non-electrolyte concentration and uses this to determine the appropriate C_i^0 for a particular distribution experiment with a salt solution.

For the present case benzene was used as the reference phase. Concentrations of piperidine in the aqueous phase were maintained in the range of from 0.02 to 0.04 *M* and ionization of the base was repressed by making all experiments in the presence of 0.12 *M* piperidinium chloride. (In other words the reference phase for the activity coefficient of the piperidine is actually 0.12 *M* piperidinium chloride rather than pure water.)

The distribution constant for piperidine between benzene and salt-free solutions was measured at four values of C_{Bz}, the concentration in the benzene phase. The distribution coefficient, $K_D = C_{Bz}/C_{H_2O}$, is linear with C_{Bz} and the value of K_D varies only slightly with concentration, ranging from 1.27 at C_{Bz} = 0.017 *M* to 1.22 at C_{Bz} = 0.064 *M*. The agreement of these results at C_{Bz} = 0.017 *M* with those of Hantzsch and Seboldt[6] at the same concentration is excellent.

For all distribution experiments, samples were equilibrated 24 hours at 25 ± 0.01° with shaking. Aliquots were then taken of both the benzene and aqueous phases and the piperidine concentrations determined by titration with hydrochloric acid and sodium carbonate. For experiments

(1) Presented at the 123rd meeting of the American Chemical Society, Los Angeles, California, March, 1953.

(2) F. A. Long and W. F. McDevit, *Chem. Revs.*, **51**, 119 (1952).

(3) W. F. McDevit and F. A. Long, *J. Am. Chem. Soc.*, **74**, 1773 (1952).

(4) A. C. D. Rivett and E. I. Rosenblum, *Trans. Faraday Soc.*, **9**, 297 (1914).

(5) H. M. Dawson and J. McCrae, *J. Chem. Soc.*, **79**, 493 (1901).

(6) A. Hantzsch and F. Seboldt, *Z. physik. Chem.*, **30**, 259 (1899).

with salt solutions the value of log f_i was then determined by use of the distribution coefficient for salt-free solutions along with eq. 2, making the assumption that f_i^0 is unity. Experimentally it was found that all of the data with salt solutions obeyed the empirical Setschenow equation[7]

$$\log f_i = \log (C_i^0/C_i) = KC_s$$

up to the highest salt concentration studied (1.5 N). Hence the parameter k_s could easily be determined from plots of log f_i *vs.* C_s. (For dilute solutions of both salt and non-electrolyte where eq. 1 is applicable and where the term k_iC_i can be neglected the parameters k_s and K are clearly identical. However, the Setschenow equation frequently holds both for more concentrated salt solutions and for situations where the term k_iC_i is not negligible.)

The benzene used was redistilled, thiophene free. The piperidine was reagent grade with a boiling point of 105–106°. All salts were reagent grade. The majority were used without further purification but the sodium benzenesulfonate, sodium benzoate, tetraethylammonium bromide and tetramethylammonium chloride were recrystallized from methanol. All salt solutions were made up by weight with the exception of sodium perchlorate whose concentration was determined by density measurement.

Results and Discussion

The activity coefficients of piperidine were determined as a function of salt concentration for twelve salts: sodium sulfate, potassium chloride, sodium chloride, rubidium chloride, lithium chloride, sodium bromide, sodium iodide, sodium perchlorate, sodium benzoate, sodium benzenesulfonate, tetramethylammonium chloride and tetraethylammonium bromide. In all cases studies were made with at least four salt concentrations generally ranging from 0.2 to 1.5 N. Table I gives typical data for two salts and indicates the method of calculation. The first two columns give the salts and their concentration in the aqueous phase, in equivalents per liter. The third and fourth columns of the table give equilibrium concentrations of piperidine in the two layers and since the ionization is essentially completely repressed these can be taken as concentrations of un-ionized piperidine. (Because slightly different total amounts of piperidine were used in the different experiments, the sums of the concentrations of the third and fourth columns vary slightly.) The fifth column gives the values of piperidine concentration for a salt-free solution in equilibrium with the stated value of C_{Bz}; these values of $C_{H_2O}^0$ were calculated using the previously determined distribution coefficient for piperidine between benzene and salt-free solutions. The value of log f_i is then given by eq. 2 under the assumption that f_i^0 is unity.

TABLE I

TYPICAL SALT EFFECTS FOR PIPERIDINE DISTRIBUTION, 25°

Salt	C_s, eq./l.	$C_{H_2O} \times 10^3$	$C_{Bz} \times 10^3$	$C_{H_2O}^0 \times 10^3$	log f_i
Na_2SO_4	0.25	30.9	42.8	34.7	0.050
	0.50	28.3	45.7	36.9	.114
	1.00	23.7	50.0	40.3	.230
	1.50	20.0	54.7	44.5	.347
$(C_2H_5)_4NBr$	0.25	35.5	42.9	34.6	− .012
	.50	36.0	42.4	34.2	− .023
	.75	35.8	41.3	33.0	− .035
	.875	36.1	41.0	32.8	− .042

Figure 1 gives plots of log f_i *vs.* C_s for all the salts studied and also lists the observed values of k_s. Experimental points are given in two cases to illustrate the linear character of the plots. In a general sense the results of Fig. 1 are similar to those observed for other non-electrolytes.[2] The values of k_s vary considerably with salt. Salts of small and highly charged ions cause salting out whereas salts of large anions or cations cause salting in. As would be expected from the well known theories of Debye[8] and Kirkwood,[9] the polar piperidine molecule (μ = 1.2 Debye units) is salted out rather less than the non-polar benzene molecule which is of comparable size.

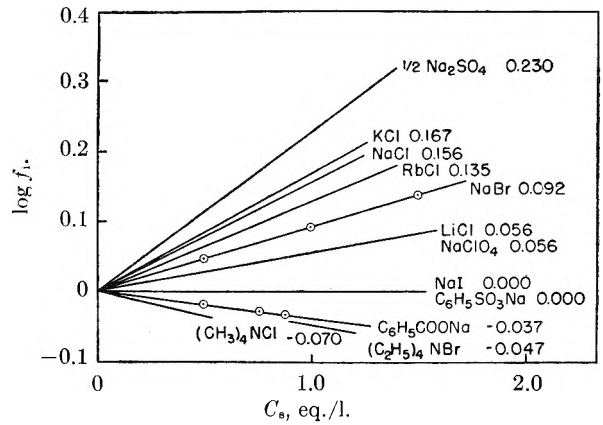

Fig. 1.—Salt effects for piperidine at 25°. Values of k_s are given after the formulas of the salts.

In a more detailed sense the salt order for piperidine is considerably different from that found for non-polar molecules and shows the characteristics expected for basic non-electrolytes. There is increased sensitivity to changes in anion as shown by the wide spread in k_s values for the halides: sodium chloride, sodium bromide and sodium iodide. There is an inversion in the salting out order of sodium and potassium ions similar to that found for ammonia.[5] Finally lithium ion "salts in" relatively more than it does with non-polar molecules; in fact k_s for lithium chloride is less than half that for rubidium chloride, whereas with non-polar molecules the k_s values for these are very similar and with acidic non-electrolytes the k_s value for lithium is much higher than for rubidium.[2]

In agreement with the expectation that these acidic and basic effects will increase with the acid or base strength of the non-electrolyte, the basic effects with piperidine are much greater than for the weaker base aniline[2,10] (pK_B = 9.4) which has a similar size and dipole moment. Although aniline shows some basic effects in that the salting out is more sensitive to anions than for the non-polar benzene,[2] it does not show the inversion of the sodium, potassium order, nor is the added salting in by lithium ion as great as with piperidine.

An over-all picture of the different effects of cations with acidic and basic non-electrolytes is given in Fig. 2 for several benzene derivatives of roughly

(7) J. Setschenow, *Ann. chim. phys.*, [6] **25**, 226 (1891).

(8) P. Debye and J. McAulay, *Physik. Z.*, [2] **26**, 22 (1925); P. Debye, *Z. physik. Chem.*, **130**, 56 (1927).

(9) J. G. Kirkwood, "Proteins, Amino Acids and Peptides," edited by E. J. Cohn and J. T. Edsall, Reinhold Publ. Corp., New York, N. Y., 1943, Chap. 12.

(10) S. Glasstone, J. Bridgeman and W. R. P. Dodgson, *J. Chem. Soc.*, 635 (1927).

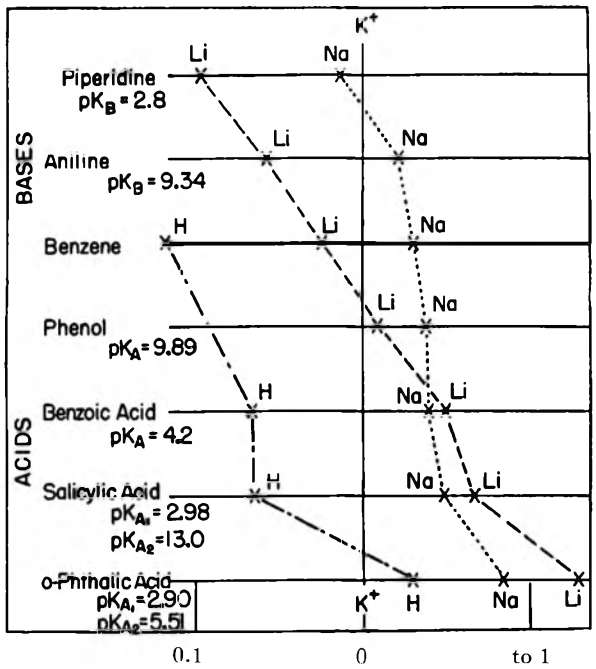

Fig. 2.—Salt effects of cations, relative to potassium ion, on acidic and basic benzene derivatives.

similar molar volumes. This figures gives the effects of the three cations, hydrogen, lithium and sodium, *relative* to that of potassium ion. The trends with acidic and basic character and the rough parallelism with ionization constants are apparent. A similar plot[2] for anions, *i.e.*, showing the effects of such ions as iodide, bromide, nitrate and sulfate relative to chloride, shows the trend toward increased sensitivity to anions as one goes from acidic to basic non-electrolytes.

A qualitative explanation for these effects has been advanced by Long and McDevit.[2] Briefly it is proposed that there are interactions between the non-electrolyte and water molecules in the hydration sphere of the ions and that the interactions are largest for the most highly hydrated ions, *i.e.*, the smaller, more highly charged ions. With cations, the hydrogens of the water molecules are assumed to be oriented outward, away from the central ion. The proposal then is that there will be attraction between these hydrogens and basic non-electrolytes resulting in enhanced salting in and repulsion between the hydrogens and the acidic non-electrolytes leading to increased salting out. With anions it is assumed that the oxygens of the waters of hydration are oriented outwards leading to attraction with acidic and repulsion with basic non-electrolytes. This explanation is in accord with the dependence of the salt order on the acid or basic strength of the non-electrolyte and with the larger effects shown by the highly hydrated ions such as lithium, hydrogen and sulfate. However, it should be emphasized that there is every reason to expect still other specific effects depending on the particular structure of the non-electrolyte.

POLAROGRAPHY OF PICOLINIC AND ISONICOTINIC ACID AND THEIR AMIDES

BY H. H. G. JELLINEK AND J. R. URWIN

Chemistry Department, University of Adelaide, Adelaide, South Australia

Received June 30, 1953

The polarography of picolinic acid, isonicotinic acid and their amides has been studied over a range of *p*H values. In all cases the wave heights decrease rapidly when certain *p*H values are reached. In contrast to the acids, which show only one type of wave each, the amides have two different types of waves. The dependence of the wave heights on *p*H is discussed in terms of a recombination reaction taking place in the electrode interface.

A study of the acid hydrolysis of picolinamide, isonicotinamide and nicotinamide was made previously.[1] The analysis of reaction mixtures containing amide in the presence of its acid was carried out polarographically.

In the present paper, the polarography of pyridine carboxylic acids and their amides has been studied in greater detail. It presents a number of very interesting features, which can now be understood on the basis of theories advanced by Wiesner and Brdicka,[2] Koutecky and Brdicka[3] and Delahay.[4]

The polarography of picolinic and isonicotinic acid was previously studied by Tompkins and Schmidt.[5] However, their data are insufficient just in the range of *p*H values, where a sharp decrease in wave heights takes place. These acids and their amides have been examined here over a range of *p*H values from 1 to 12, and care has been taken to obtain sufficient data of the wave heights as a function of *p*H. The polarography of pyridine, quinoline and its derivatives was investigated more recently by Shchennikova and Korshunov.[5]

Experimental

(a) **Apparatus.**—The polarograph was a "manual" instrument, constructed on the same lines as the "manual" instrument described by Kolthoff and Lingane.[6] An H-type cell was used consisting of a saturated calomel electrode in one compartment and a dropping mercury electrode in the

(1) H. H. G. Jellinek and A. Gordon, THIS JOURNAL, **53**, 996 (1949); H. H. G. Jellinek and J. R. Urwin, *ibid.*, **57**, 900 (1953).

(2) R. Brdicka and K. Wiesner, *Collection Czech. Chem. Communs.*, **12**, 138 (1947).

(3) J. Koutecky and R. Brdicka, *ibid.*, **12**, 337 (1947).

(4) P. Delahay, *J. Am. Chem. Soc.*, **73**, 4944 (1951).

(5) (a) P. C. Tompkins and C. L. A. Schmidt, *Univ. Calif. Publ. in Physiology*, **8**, No. 16, 229 (1943); (b) M. K. Shchennikova and I. A. Korshunov, *J. Phys. Chem., U.S.S.R.*, **22**, 503 (1948).

(6) I. M. Kolthoff and J. J. Lingane, "Polarography," Interscience Publishers, Inc., New York, N. Y., 1946.

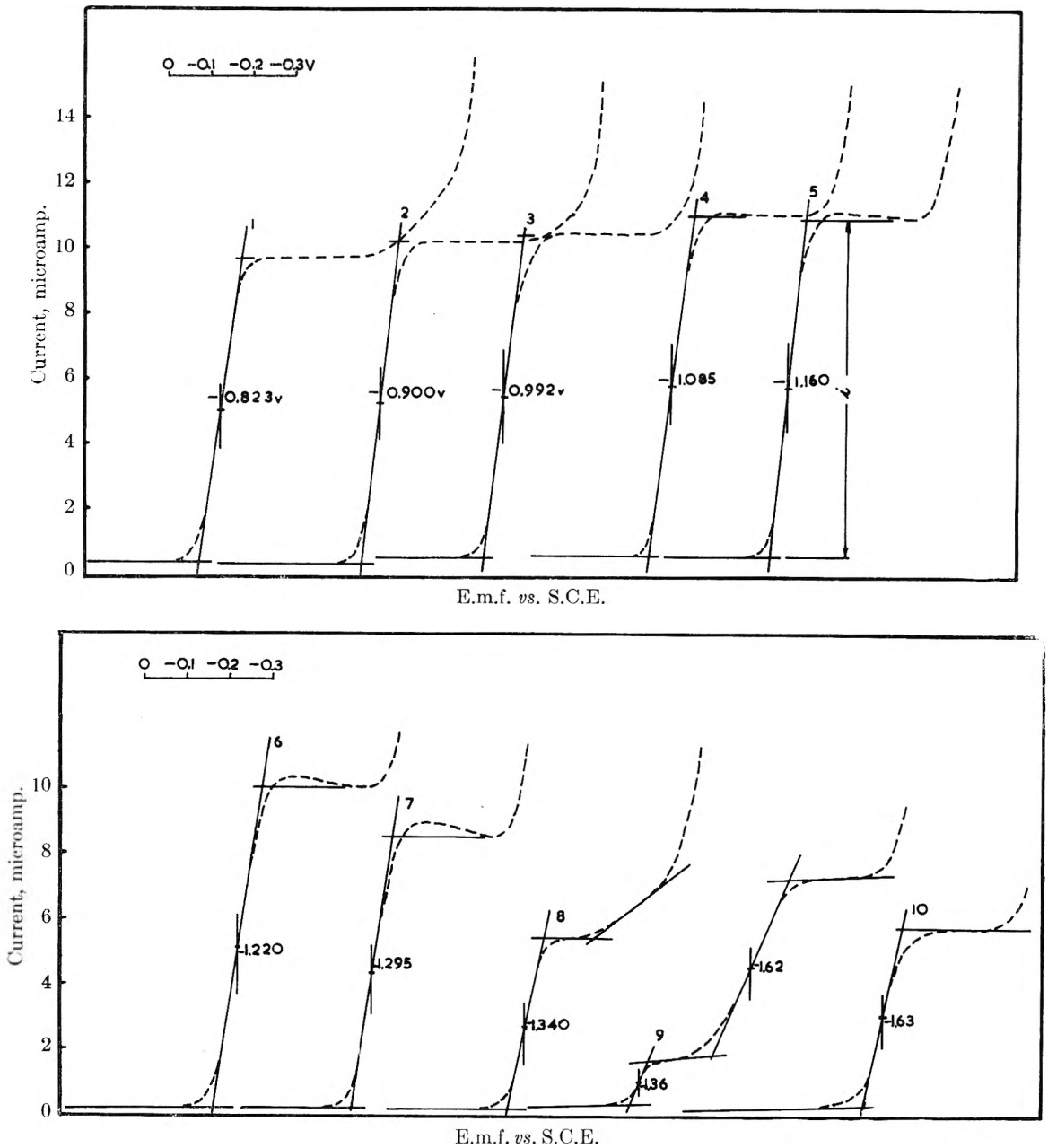

Fig. 1.—Polarographic waves of 1×10^{-3} *M* picolinamide at various *p*H values: 1 to 10, *p*H: 2.5, 3.45, 4.40, 5.48, 6.36, 7.12, 8.17, 8.93, 9.54 and 11.68, respectively. Ground solutions: 1 to 5, citric acid–phosphate buffer; 6 to 9, sodium barbiturate–HCl; 10, phosphate–caustic soda. Half-wave potentials in volts *vs.* S.C.E.

other, separated by an agar bridge, saturated with potassium chloride. The current measuring circuit consisted of a sensitive galvanometer with a long period (Guthrie type H.S.G. 1; undamped 27 seconds, maximum sensitivity 4×10^{-4} amp.; internal resistance 3,500 ohms).

Capillaries had internal diameters of 0.03 and 0.05 mm., the drop time was 4 to 6 seconds and the height of the mercury 72 and 64 cm., respectively. The height of the waves was evaluated by drawing straight lines through the residual, limiting currents and along the slope of the wave (see Fig. 1). The vertical distance of the two intersection points was taken as the height of the wave. When a maximum appeared, the value was taken as the height of the minimum. The oscillations were usually small, about 2% of the total wave height.

(b) Materials.—All materials were of Analar grade, except picolinic and isonicotinic acids and their amides.

Picolinic acid was prepared by oxidation of α-picoline with potassium permanganate according to Singer and McElvain.[7] The picolinic acid obtained in this way was recrystallized several times from an alcohol ether mixture and finally dried over phosphorus pentoxide (m.p. 136°).

Picolinamide was prepared from picolinic acid according to Camps.[8] The amide was recrystallized from an alcohol-benzene mixture and dried over phosphorus pentoxide (m.p. 106.5°).

Isonicotinic acid was obtained from B.D.H. and was recrystallized several times from an alcohol–benzene mixture. Isonicotinamide was obtained from the acid by the same method as that used for picolinamide (m.p. 156°).

Experimental Results

(a) **Picolinic and Isonicotinic Acids.**—Table I shows wave heights expressed as $i_d^x = i_d/m^{2/3}t^{1/6}$ (where i_d is in microamp., m in mg. and t in seconds) and corresponding half wave potentials in volts *ver-*

(7) Singer and McElvain, *Org. Syntheses*, **20**, 79 (1940).

(8) R. Camps, *Archiv. Pharm.*, **360**, 240 (1902).

TABLE I

Solution	Picolinic acid pH	Picolinic acid i_d^x, μ amp.	Picolinic acid $E_{1/2}$ vs. S.C.E., v.	Isonicotinic acid pH	Isonicotinic acid i_d^x, μ amp. I	Isonicotinic acid i_d^x, μ amp. II	Isonicotinic acid $E_{1/2}$ vs. S.C.E., v. I	Isonicotinic acid $E_{1/2}$ vs. S.C.E., v. II
McIlvaine's buffer solutions—0.2 *M* Na_2HPO_4 and 0.1 *M* citric acid	2.25	5.10	−0.930	2.24	4.60	0.41	−0.855	−1.01
	3.44	4.79	−1.004	3.46	4.70	0.24	−0.925	−1.035
	4.50	4.90	−1.077	4.45	4.95		−0.995	
	5.46	4.61	−1.160	5.45	5.20		−1.070	
	6.46	4.61	−1.260	6.43	4.95		−1.150	
	7.38	4.67	−1.340	7.38	4.28		−1.236	
	7.84	4.61	−1.382	7.83	3.61		−1.279	
0.1 *M* sodium barbitone + 0.1 *N* HCl Michaelis 1930	8.20	3.20	−1.392	8.10	3.18		−1.300	
	8.60	2.32	−1.415	8.48	2.56		−1.327	
	8.84	1.61	−1.437	8.83	2.045		−1.357	
	9.25	1.11	−1.462	9.17	1.375		−1.388	
	9.60	0.84	−1.46	9.30	0.905		−1.40	
0.1 *M* Na_2CO_3 + 0.1 *N* HCl	10.30	0.26	−1.50	10.20	0.185		−1.44	
0.01 *N* HCl	1.90	4.97	−0.908	2.0	4.12	0.6	−0.837	−1.105
M/20 Pot. hydrogen phthalate + 0.1 *N* HCl	2.80	4.63	−0.970	2.6	4.49		−0.901	
	3.75	4.84	−1.040	4.0	4.85		−0.987	
	4.10	4.93	−1.064	...	...		...	
M/20 Pot. hyd. phthalate + 0.1 *N* NaOH	5.04	4.88	−1.137	...	...		...	
0.1 *M* Phosphate + 0.1 *N* NaOH	9.6	0.503	−1.49	...	...		...	
	10.9	Small	−1.6	...	...		...	
	11.6	...	...	11.1	Small		−1.45	
0.1 *M* Phosphate + 0.1 *N* HCl	6.55	4.63	−1.280	...	...		...	
	7.46	4.63	−1.340	...	...		...	
NaOH	13	...	...	12.5	...		...	
M/20 Borax + 0.1 *N* HCl	...	...	...	8.8	2.03		−1.376	

sus the saturated calomel electrode (S.C.E.) for different *p*H values and various buffered and unbuffered mixtures. The half-wave potentials are corrected for the voltage drop across resistances in the circuit. The cell resistance was less than 1000 Ω and no correction was made. It can be seen that the wave heights decrease rapidly in the region of *p*H values from 8 to 9 for picolinic acid and from about 7 to 9 for isonicotinic acid.

Any difference between the i_d^x values found by Tompkins and Schmidt and our values is probably due to different methods of evaluation. The half-wave potentials for either substance increase with increasing *p*H values and agree quite satisfactorily with those found by Tompkins and Schmidt.[5] They can be expressed up to *p*H 9 by the equation

$$E_{1/2} = -0.081pH - 0.741 \text{ v.}$$

The half-wave potentials for isonicotinic acid can be expressed similarly

$$E_{1/2} = -0.080pH - 0.651 \text{ v.}$$

The relationship between wave height and concentration of either picolinic or isonicotinic acid was found to be linear for constant *p*H values.

(b) **Picolinamide and Isonicotinamide.**—The amides show some characteristic differences from the corresponding acids.

Table II shows i_d^x values and corresponding half-wave potentials at various *p*H values in a number of ground solutions.

Table II shows that up to about *p*H 9, the waves for picolinamide show very similar characteristics to those obtained for picolinic acid. However, a second wave appears with a more negative half wave potential at about *p*H 9. The wave heights for this second wave increase as the *p*H is further increased, becoming constant when the *p*H values reach about 9 to 10. The half-wave potentials are independent of *p*H for this second wave. The first wave disappears completely when *p*H values of about 11 are reached. The second wave was used for the analysis of reaction mixtures containing picolinic acid and its amide, when investigating the hydrolysis of picolinamide.[1]

Unlike picolinamide, the wave heights as a function of *p*H do not decrease to zero with increasing *p*H in the case of isonicotinamide, but become constant, when a *p*H value of about 9 is reached. Apparently two waves are also involved in the case of isonicotinamide, but their half-wave potentials are so similar that a separation of the two waves does not take place. At a *p*H of about 9, the first wave has disappeared completely and the second wave, characteristic of the amide, is left.

It was observed by Tompkins and Schmidt,[9] in the case of nicotinamide, that a discontinuity appeared in the half-wave potentials as the *p*H increased. However, these authors did not seem to realize that two different kinds of waves are involved. The first wave is common to the acid and amide, whereas the second is only shown by the amide. Representative polarographic waves of picolinamide and isonicotinic acid over a range of *p*H values, selected from the available experimental data are shown in Figs. 1 and 2.

(9) Reference 5a, p. 247.

TABLE II

i_d^x = wave height/$m^{2/3}t^{1/6}$

	Picolinamide					Isonicotinamide		
	pH	i_d^x, μ amp.		$E_{1/2}$ vs S.C.E. v.		pH	i_d^x μ amp.	$E_{1/2}$ vs. S.C.E., v.
McIlvaine's buffer solutions—0.2 *M* Na_2HPO_4 and 0.1 *M* citric acid	2.50	6.57		−0.818		2.25	6.68	−0.730
	3.45	6.93		−0.895		3.46	6.98	−0.812
	4.40	6.93		−0.988		4.46	7.10	−0.902
	5.43	7.30		−1.080		5.46	6.68	−0.992
	6.36	7.25		−1.155		6.44	5.98	−1.066
	6.40	7.13		−1.153		7.40	4.80	−1.134
	7.07	6.98		−1.220		7.84	4.17	−1.167
	7.20	7.16		−1.218		...	..	...
	7.42	7.08		−1.238		...	..	...
	7.55	6.70		−1.258		...	..	...
	7.68	6.40		−1.276		...	..	...
	7.92	6.20		−1.290		...	..	...
	8.13	5.77		−1.305		...	..	...
0.1 *M* Sodium Barbitone + 0.1 *N* HCl ref. Michaelis 1930	7.12	6.83		−1.215		8.13	3.92	−1.186
	8.17	5.80		−1.295		8.52	3.57	−1.206
	8.58	5.06		−1.311		8.88	3.38	−1.222
	8.93[a]	3.65[b]		−1.337[b]		9.26	3.38	−1.245
	9.17[a]	2.34[b]		−1.342[b]		...	..	..
	9.54	0.935	3.64	−1.360	−1.620	...	..	...
0.1 *M* Na_2CO_3 + 0.1 *N* HCl	...	...		...		10.22	3.49	−1.282
	...	...		...		10.98	3.34	−1.300
M/20 Pot. hydrogen phthalate + 0.1 *N* HCl	2.85	6.88		−0.848		...	..	...
	4.12	7.34		−0.978		...	..	...
M/20 Pot. hydrogen phthalate + 0.1 *N* NaOH	5.08	7.50		−1.063		...	..	...
	6.58	7.10		−1.197		...	..	..
0.1 *M* Na_2HPO_4 + 0.1 *N* HCl	8.26[a]	3.24	2.17	−1.317	−1.613	...	..	...
0.1 *M* Na_2HPO_4 + 0.1 *N* NaOH	9.78	0.68	3.38	−1.36	−1.617	10.1	3.43	−1.32
	11.04	...	3.38	...	−1.617	11.6	3.43	−1.33
	11.68	...	3.42	...	−1.627	...	..	...
NaOH	...	...		...		12.4	3.12	−1.36

[a] 2nd wave appears, poorly defined. [b] Values uncertain.

The half-wave potentials as a function of *p*H for the first waves of picolinamide can be expressed by the equation

$$E_{1/2} = -0.087pH - 0.597 \text{ v.}$$

The half-wave potentials for isonicotinamide can be expressed by

$$E_{1/2} = -0.083pH - 0.526 \text{ v.}$$

The relationship between wave height and concentration of amide for constant *p*H values was found to be linear.

It was pointed out above that the concentration of the amide can be determined in the presence of its acid polarographically,[1] if the *p*H of the ground solution is high enough (*ca.* *p*H 11.5). The relationship between wave height and concentration at such a *p*H value is linear. Figure 3 gives a typical series of polarograms for picolinamide at definite stages of the hydrolysis. The hydrolysis was carried out in 0.1 *N* HCl at 130°. The solution was diluted five times with phosphate buffer. A ground solution of *p*H 11.5 was thus obtained.

Discussion

The wave heights as a function of *p*H for picolinic acid show the characteristics of a current composed of a diffusion component and a component due to a recombination reaction. Such cases have been discussed in a simplified way by Wiesner and Brdicka.[2] A strict derivation was given by Koutecky and Brdicka[3] and a somewhat simpler one by Delahay.[4] A paper by Knobloch on catalytic evolution of hydrogen due to nicotinamide is also of interest in this connection.[10]

As the picolinic acid and its amide give similar current *versus* *p*H curves, the reaction current cannot be due to the undissociated carboxyl group, but must be due to a reaction of the nitrogen in the ring with a proton. Thus the reaction taking place in the interface is

$$B + H^+ \underset{k_2}{\overset{k_1}{\rightleftharpoons}} BH^+$$

where

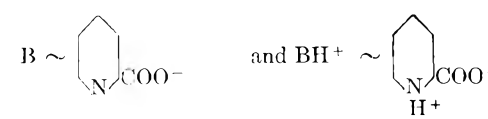

The species ultimately discharged at the electrode is BH^+ in this particular case. B can also stand for the respective amide. The rate constants k_1 and k_2 are interrelated by the dissociation constant $K = k_2/k_1$.

Investigations of the absorption spectra of picolinic acid as a function of *p*H gave a value for the

(10) E. Knobloch, *Collection Czech. Chem. Communs.*, **12**, 407 (1947).

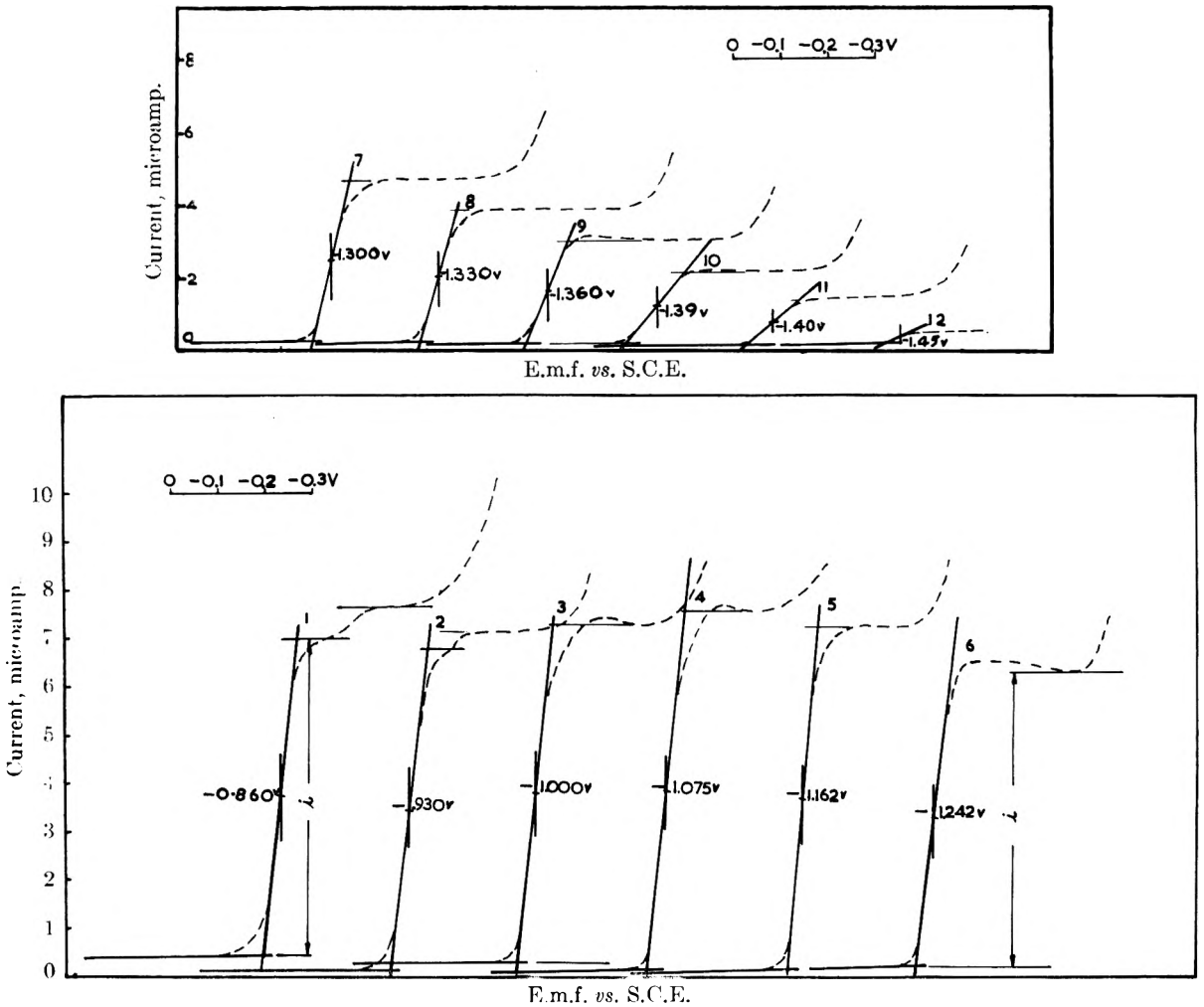

Fig. 2.—Polarographic waves of 1×10^{-3} *M* isonicotinic acid at various *p*H values: 1 to 12, *p*H: 1.90, 3.46, 4.45, 5.45, 6.43, 7.38, 8.10, 8.48, 8.83, 9.17, 9.3 and 10.2, respectively. Ground solutions: 1 to 6, citric acid–phosphate; 7 to 11, sodium barbiturate–HCl; 12, sodium carbonate–HCl. Half-wave potentials in volts *vs.* S.C.E.

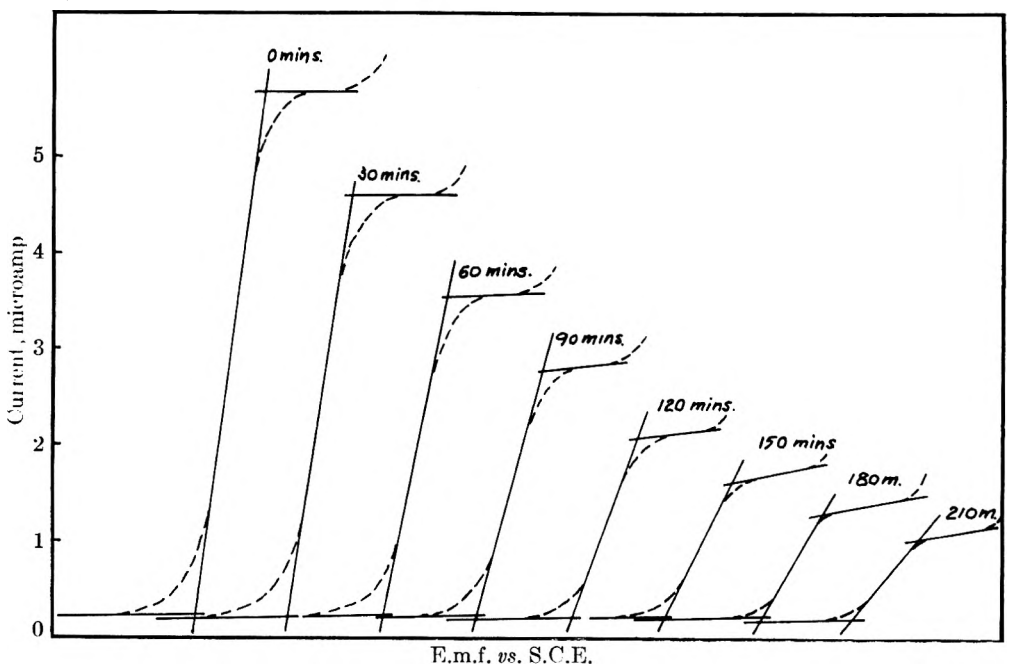

Fig. 3.—Polarographic waves for different stages of hydrolysis of picolinamide in 0.1 *N* HCl at 130°; reaction mixtures diluted five times with phosphate buffer; final *p*H 11.5.

dissociation constant $K = 10^{-1.6}$ where $K = ([B]\cdot[H^+]/[BH^+])$.

Koutecky and Brdicka[3] have derived an expression relating the rate constant of recombination k_1, the dissociation constant K and the ratio i/i_∞ at definite pH values. i is here the wave height at any pH, and i_∞ the wave height at a low pH, where the current is completely diffusion controlled (100% BH^+). For $K \gg [H^+]$, this expression reads as

$$Y_1 = \frac{k_1[H^+]^2 t_1}{K} \qquad (1)$$

where

$$f(Y_1) = \frac{6}{7\sqrt{\pi}Y_1^{7/6}} \int_0^{Y_1} F(Y)\,dY = \frac{i}{i_\infty} \qquad (2)$$

Ruetschi and Trumpler[11] have pointed out that a writing error is inherent in formula (2) as given by Koutecky and Brdicka.[3] Equation 2 above is the form as presented by the Swiss authors. A table of corresponding Y_1 and $f(Y_1)$ values was given by the Czech authors.[3]

Equation 1 also can be written in logarithmic form

$$\log k_1 = 2(p\mathrm{H} + {}^1/_2 \log Y_1) - pK - \log t_1 \qquad (3)$$

t_1 is the mercury drop time.

The theoretical and experimental curves for i/i_∞ as function of pH are shown in Fig. 4. The theoretical curve was obtained by calculating k_1 for $i/i_\infty = 0.5$, $t_1 = 4.6$ seconds, $k_1 = 10^{14.3}$ sec.$^{-1}$ (mole/l.)$^{-1}$. The theoretical curve shows deviations from the experimental one in the same directions as found by Koutecky and Brdicka for phenylglyoxylic acid[3]) and by Ruetschi and Trumpler for p-phenylazobenzoic acid.[11]

The respective rate constants for picolinamide, isonicotinic acid and its amide were calculated in the same way as the rate constants for picolinic acid. The dissociation constants for these compounds were obtained from spectroscopical measurements. The results are summarized in Table III.

TABLE III

RATE CONSTANTS CALCULATED ACCORDING TO THE THEORY OF KOUTECKY AND BRDICKA[3]

	$p\mathrm{H}_{1/2}$	pK	$\log t_1$	$\log k_1$
Picolinic acid	8.5	1.6	0.66	14.3
Picolinic amide	8.9	2.1	.66	14.6
Isonicotinic acid	8.4	1.7	.66	14.0
Isonicotinic amide	7.0	3.6	.66	9.8

The waves appearing at higher pH values, in the case of the amides, are of quite a different nature to those at lower pH values. It is clear that these waves do not belong to the dissociation equilibrium considered above; otherwise, the height of these waves should have the same value as that belonging to the first wave at low pH values. That this is not the case emerges clearly from the waves belonging to isonicotinamide.

It appears that the second wave has probably the same height over the whole range of pH values. Moreover, whereas the half wave potentials of the first waves are a function of pH, this does not seem to be the case for the second wave. The second wave of picolinamide has much more negative half wave potentials than the corresponding waves for isonicotinamide. This is the reason why these waves appear only at high pH values in the case of picolinamide. As the pH decreases, the potential for the discharge of hydrogen becomes more positive and thus the second amide waves are completely masked. The reason why there are no second waves appearing for picolinic and isonicotinic acids is probably that the half wave potentials are more negative than the potentials for the discharge of hydrogen. Thus, the introduction of amido groups facilitates the type of reduction corresponding to the second waves. The number of electrons involved in this reduction can be calculated from the Ilkovic equation and amounts for picolinamide and isonicotinamide to 2.36. (Diffusion coefficient 5.8×10^{-6} cm.^{2} sec.$^{-1}$, this is the value for pyridine.)

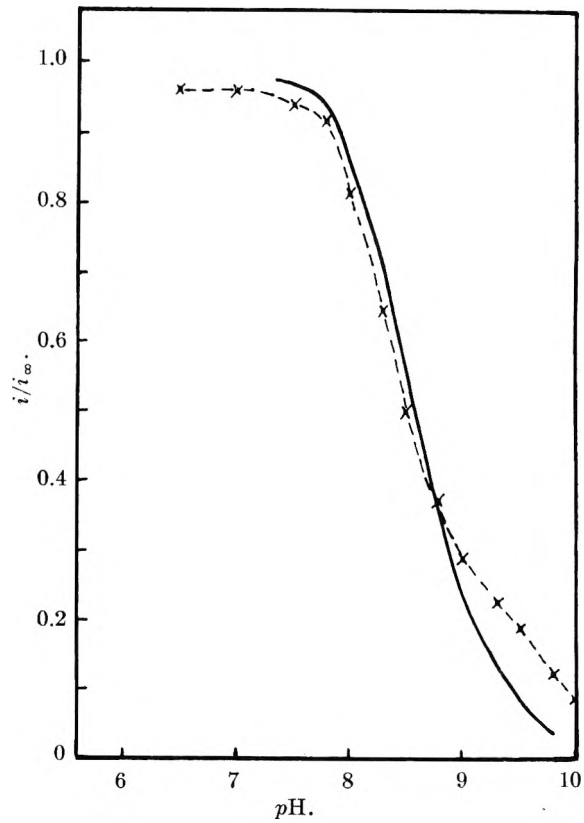

Fig. 4.—i/i_∞ as a function of pH for picolinic acid: ---x---, experimental; ——, theoretical curve according to equation 3 ($t_1 = 4.6$ sec., $K = 10^{-1.6}$, $p\mathrm{H}_{1/2}$ 8.5).

There is an indication of another small wave in the case of isonicotinic acid at lower pH values (see Fig. 2). It is not unlikely that this wave is due to the species B.

Although Tompkins and Schmidt[5,9] advance some suggestions as to the electrode reactions involved in the various reductions, the present authors prefer to refrain from any speculations in this respect.

It is the authors' pleasure to thank Mr. W. G. Jones, Division of Industrial Chemistry, C.S.I.R.O., for the construction of the H-type polarographic cell.

(11) P. Ruetschi and G. Trumpler, *Helv. Chim. Acta*, **35**, 1957 (1952).

BOND REFRACTIONS FOR TIN, SILICON, LEAD, GERMANIUM AND MERCURY COMPOUNDS

BY A. I. VOGEL, W. T. CRESSWELL AND J. LEICESTER

Department of Chemistry, Woolwich Polytechnic, London, S.E. 18, England

Received July 1, 1953

Analysis of the refraction data in the literature for liquid tin, silicon, lead, germanium and mercury compounds, using the fundamental bond refractions of Vogel (1948) has yielded a system of bond refractions for these five elements. These replace and extend *inter alia* the bond refractions for tin compounds of West and Rochow (1952) and for silicon compounds of Warrick (1946), which were based upon the older constants computed by Denbigh (1940).

Denbigh[1] deduced the fundamental bond refractions (D-line) for (C–H) and (C–C) as 1.69 and 1.25, respectively, from the literature data upon liquid hydrocarbons: these values were used as the basis for calculating the refractions of other bonds from data given in "International Critical Tables" and Landolt–Börnstein "Tabellen." More trustworthy figures for these fundamental bond refractions (1.676 and 1.296, respectively) were first given by the senior author in 1948[2]: these were computed from the mean CH_2 differences derived from new measurements upon a series of highly purified alkyl chlorides, bromides and iodides[3] and *n*-aliphatic hydrocarbons.[4] (An independent confirmation of our constants was provided by Vickery and Denbigh[5] who deduced (C–H) 1.674 and (C–C) 1.296 from the molar refractions of 196 alkanes as the result of an exhaustive mathematical analysis.) By utilizing our own experimental data, a new series of bond refractions was proposed.[6–8] To facilitate the calculations of the molecular refractions of compounds containing alkyl groups, a table of constants for alkyl groups has been provided.[9]

West and Rochow[10] have recently published a series of tin bond refractions based upon Denbigh's 1940 values.[1] It seems rather surprising that our tables of bond constants, published in 1948 and 1950, were overlooked by the American authors. In view of the importance of the subject, we have recalculated the bond refractions for tin compounds from the molecular refractions given by West and Rochow with the aid of our own values for (C–H) and (C–C) and for alkyl groups. Our results are collected in Table I; the American authors' values are given in parentheses.

West and Rochow (ref. 10) give two values for the refraction of the (Sn–C) bond; the so-called "primary" 4.09 deduced from 19 compounds and the so-called "secondary" 4.24 deduced from 12 compounds. We find that only one value 4.16 for (Sn–C) is necessary and have used the molecular refractions for all the 40 tin tetraalkyls in arriving at this constant; the slightly higher standard deviation (0.091) can be appreciably reduced by omitting the data for certain compounds (as, indeed, was done by West and Rochow), but we do not consider that this apparently artificial rejection of literature data is scientifically sound. The present authors find it difficult to agree that it is possible to derive true values for "Sn–C (secondary)" from the 12 compounds used by the American authors; the only compounds containing secondary carbon *directly* attached to tin are triethyl-*i*-propyltin (MR_D 59.98; *cf.* triethyl-*n*-propyltin 59.79) and *dl*-amyltin (MR_D 110.66; *cf.* tetra-*n*-amyltin 110.64). Compounds with *i*-butyl and *i*-amyl groups, which were employed in their calculations, do not contain secondary carbon directly attached to the metal. The tin bond refractions given in Table I permit the calculation of MR_D for the 90 compounds (collected by West and Rochow) with an average percentage error of 0.41%.

TABLE I

TIN BOND REFRACTIONS

Bond	Refraction	No. of cpd. used	Standard dev.
(Sn–C)	4.16 (4.09, primary; 4.24, secondary)	40	0.091
($Sn–C_{ar}$)	3.78 (3.54)	3	.12
(Sn–Cl)	8.91 (8.81)	11	.37
(Sn–Br)	12.00 (12.02)	14	.51
(Sn–I)	17.92 (17.95)	15	.54
(Sn–Sn)	10.77 (10.96)	3	.52
(Sn–O)	3.84 (3.84)	4	.27

Recently West, Webster and Wilkinson[11] have examined three tertiary alkyl tin compounds and find values of 4.87, 4.52 and 4.89, respectively, for the "Sn–C tert." bond. We prefer, in agreement with Vickery and Denbigh,[5] to retain only one value for the Sn–C bond since it is of greater general utility and also in order to keep the number of constants required for the calculation of molecular refractions to a minimum. The slight exaltation may be characteristic of the *t*-alkyl grouping.

All our detailed results for tin compounds are collected in Table II. In our calculations of the tertiary compounds, we have deduced the contributions of the tertiary alkyl groups from our own data for *t*-butyl and *t*-amyl chloride, respectively.[3]

Bond refractions for silicon compounds have been determined by Warrick[12] on the basis of Denbigh's

(1) K. G. Denbigh, *Trans. Faraday Soc.*, **36**, 936 (1940).
(2) Vogel, *J. Chem. Soc.*, 607 (1948).
(3) Vogel, *ibid.*, 636 (1943).
(4) Vogel, *ibid.*, 133 (1946).
(5) Vickery and Denbigh, *Trans. Faraday Soc.*, **45**, 61 (1949).
(6) Cresswell, Jeffery, Leicester and Vogel, *Research*, **1**, 719 (1948).
(7) Vogel, Cresswell, Jeffery and Leicester, *Chemistry and Industry*, 358 (1950).
(8) Vogel, Cresswell, Jeffery and Leicester, *J. Chem. Soc.*, 531 (1952).
(9) Vogel, Cresswell, Jeffery and Leicester, *ibid.*, 518 (1952).
(10) R. West and E. G. Rochow, *J. Am. Chem. Soc.*, **74**, 2490 (1952).
(11) R. West, M. H. Webster and G. Wilkinson, *ibid.*, **74**, 5794 (1952).
(12) Warrick, *ibid.*, **68**, 2455 (1946); compare Sauer, *ibid.*, 954 (1946).

constants (1940). We have recalculated the literature data on organosilicon compounds, using our own constants and the results are collected in Tables III and VII.

TABLE II

MOLECULAR REFRACTIONS OF TIN COMPOUNDS

	Temp., °C.	MR_D Found	MR_D Calcd.	Error, %	Ref.
Section A. Tin tetraalkyls					
$(CH_3)_4Sn$	25	36.43	36.64	+0.6	a
$(CH_3)_3Sn(n\text{-}C_4H_9)$	20	50.76	50.57	− .4	a
$(CH_3)_3Sn(i\text{-}C_4H_9)$	21.5	50.72	50.60	− .2	a
$(CH_3)_3Sn(i\text{-}C_5H_{11})$	21	55.53	55.26	− .5	a
$(CH_3)_2Sn(i\text{-}C_4H_9)_2$	20.1	64.85	64.57	− .4	a
$(CH_3)_2Sn(CH_2)_5$	23.1	48.39	48.42	+ .1	a
$(CH_3)Sn(C_2H_5)_3$	20	50.27	50.57	+ .6	a
$(CH_3)Sn(n\text{-}C_4H_9)_3$	20	78.85	78.44	− .5	a
$(CH_3)Sn(i\text{-}C_5H_{11})_3$	15	92.08	92.51	+ .5	a
$(C_2H_5)_4Sn$	25	54.94	55.22	− .5	a
$(C_2H_5)_3Sn(n\text{-}C_3H_7)$	20.6	59.77	59.89	+ .2	a
$(C_2H_5)_3Sn(i\text{-}C_3H_7)$	12	59.98	59.90	− .1	a
$(C_2H_5)_3Sn(i\text{-}C_4H_9)$	20.3	64.77	64.54	− .4	a
$(C_2H_5)_3Sn(n\text{-}C_5H_{11})$	20	69.16	69.17	.0	a
$(C_2H_5)_3Sn(i\text{-}C_5H_{11})$	20.1	69.36	69.20	− .2	a
$(C_2H_5)_2Sn(i\text{-}C_4H_9)_2$	20.4	74.10	73.86	− .3	a
$(C_2H_5)_2Sn(CH_2)_5$	19.9	57.87	57.71	− .3	a
$(C_2H_5)_2Sn(i\text{-}C_5H_{11})_2$	19.0	83.42	83.18	− .3	a
$(C_2H_5)Sn(n\text{-}C_3H_7)_3$	21.8	69.32	69.23	− .1	a
$(C_2H_5)Sn(n\text{-}C_4H_9)_3$	20	83.05	83.09	.0	a
$(C_2H_5)Sn(i\text{-}C_4H_9)_3$	21.0	83.15	83.18	.0	a
$(C_2H_5)Sn(n\text{-}C_3H_7)(i\text{-}C_5H_{11})_2$	21.9	87.57	87.85	+ .3	a
$(n\text{-}C_3H_7)_4Sn$	20.2	73.99	73.90	− .1	a
$(n\text{-}C_3H_7)_3Sn(n\text{-}C_4H_9)$	20	78.55	78.52	.0	a
$(n\text{-}C_3H_7)_3Sn(i\text{-}C_4H_9)$	24.1	78.86	78.55	− .4	a
$(n\text{-}C_3H_7)Sn(n\text{-}C_5H_{11})_3$	20	101.56	101.74	+ .2	a
$(n\text{-}C_4H_9)_4Sn$	20	92.11	92.38	+ .3	a
$(i\text{-}C_4H_9)_4Sn$	23.0	92.60	92.50	− .1	a
$(n\text{-}C_4H_9)_3Sn(i\text{-}C_5H_{11})$	20	97.07	97.07	.0	a
$(i\text{-}C_4H_9)_3Sn(i\text{-}C_5H_{11})$	26.8	97.61	97.16	− .5	a
$(n\text{-}C_4H_9)_3Sn(n\text{-}C_6H_{13})$	17	102.73	101.65	−1.0	a
$(n\text{-}C_5H_{11})_4Sn$	20	110.64	111.02	+0.3	a
$(i\text{-}C_5H_{11})_4Sn$	19.6	111.32	111.14	− .2	a
$(d,l\text{-}C_5H_{11})_4Sn$	20	110.66	110.02	− .6	a
$(i\text{-}C_5H_{11})_3Sn(n\text{-}C_7H_{15})$	20	119.88	120.41	+ .4	a
$(n\text{-}C_6H_{13})_4Sn$	20	128.83	129.46	+ .5	a
$(n\text{-}C_7H_{15})_4Sn$	20	147.48	148.22	+ .5	a
$(n\text{-}C_8H_{17})_4Sn$	20	165.75	166.58	+ .5	a
$(C_2H_5)_3Sn(CH_2)_5Sn(C_2H_5)_3$	20	113.00	113.08	+ .1	a
$(C_2H_5)_3Sn(CH_2)_{10}Sn(C_2H_5)_3$	20.7	136.20	136.30	+ .1	a
$(CH_3)_2Sn(t\text{-}C_4H_9)_2$	25	65.97	65.01	−1.5	b
$(CH_3)_2Sn(t\text{-}C_5H_{11})_2$	25	74.54	74.07	−0.6	b
$(n\text{-}C_4H_9)_2Sn(t\text{-}C_4H_9)_2$	25	93.82	92.88	−1.0	b
Section B. Tin–chlorine compounds					
$SnCl_4$	25.0	35.22	35.62	+1.1	a
$(C_2H_5)_3SnCl$	23.3	50.14	50.33	+0.4	a
$(C_2H_5)_2(n\text{-}C_3H_7)SnCl$	15.7	54.77	55.00	+ .4	a
$(C_2H_5)_2(i\text{-}C_5H_{11})SnCl$	19.9	63.94	64.31	+ .7	a
$(n\text{-}C_3H_7)_3SnCl$	28.0	64.75	64.34	− .6	a
$(n\text{-}C_4H_9)_3SnCl$	25	78.41	78.20	− .3	a
$(i\text{-}C_4H_9)_3SnCl$	24.8	78.97	78.29	− .9	a
$(i\text{-}C_5H_{11})_3SnCl$	34.2	92.55	92.27	− .3	a
$(cis\text{-}ClCH{=}CH)_3SnCl$	20	62.59	63.48	+1.5	a
$(cis\text{-}ClCH{=}CH)_2SnCl_2$	20	53.93	54.19	+0.5	a
$(trans\text{-}ClCH{=}CH)SnCl_3$	20	43.61	44.91	+3.0	a
Section C. Tin–bromine compounds					
$SnBr_4$	35.0	48.73	48.00	−1.5	a
$(C_2H_5)_3SnBr$	20	53.22	53.42	+0.4	a
$(C_2H_5)_2(n\text{-}C_3H_7)SnBr$	21	57.46	58.09	+1.1	a
$(C_2H_5)_2(i\text{-}C_4H_9)SnBr$	20.4	62.74	62.74	0.0	a
$(C_2H_5)_2(n\text{-}C_5H_{11})SnBr$	22.3	68.12	67.37	−1.1	a
$(C_2H_5)_2(i\text{-}C_5H_{11})SnBr$	17.0	66.61	67.40	+1.2	a
$(C_2H_5)_2(Br(CH_2)_5)SnBr$	20.3	75.39	75.08	−0.4	a
$(C_2H_5)(i\text{-}C_4H_9)_2SnBr$	19.5	72.41	72.06	−0.5	a
$(C_2H_5)(i\text{-}C_5H_{11})_2SnBr$	20.0	80.56	81.38	+1.0	a
$(n\text{-}C_3H_7)_3SnBr$	25.2	68.35	67.43	−1.3	a
$(n\text{-}C_4H_9)_3SnBr$	20	81.41	81.29	−0.1	a
$(i\text{-}C_4H_9)_3SnBr$	20	81.09	81.38	+ .4	a
$(n\text{-}C_5H_{11})_3SnBr$	20	94.99	95.27	+ .3	a
$(i\text{-}C_5H_{11})_3SnBr$	20.7	95.72	95.36	− .4	a
Section D. Tin–iodine compounds					
$(CH_3)_2SnI_2$	39.3	53.88	54.12	+0.5	a
$(CH_3)_3SnI$	28	45.11	45.40	+ .6	a
$(CH_3)_2(n\text{-}C_4H_9)SnI$	20	59.31	59.34	.0	a
$(CH_3)_2(i\text{-}C_4H_9)SnI$	20	59.33	59.37	+ .1	a
$(CH_3)_2(n\text{-}C_5H_{11})SnI$	18	63.69	64.00	+ .5	a
$(CH_3)_2(i\text{-}C_5H_{11})SnI$	21	64.01	64.03	.0	a
$(C_2H_5)_3SnI$	17.5	59.37	59.34	− .1	a
$(C_2H_5)_2(n\text{-}C_3H_7)SnI$	20	63.09	64.01	+1.5	a
$(C_2H_5)_2(n\text{-}C_4H_9)SnI$	20	69.31	68.63	−1.0	a
$(n\text{-}C_3H_7)_3SnI$	30.4	73.32	73.35	0.0	a
$(n\text{-}C_3H_7)_2(n\text{-}C_4H_9)SnI$	20	77.13	77.97	+1.1	a
$(i\text{-}C_4H_9)_3SnI$	22.2	88.47	87.30	−0.2	a
$(n\text{-}C_4H_9)_2(i\text{-}C_5H_{11})SnI$	20	92.36	91.90	− .5	a
$(n\text{-}C_4H_9)_2(n\text{-}C_6H_{13})SnI$	18	97.14	96.48	− .7	a
$(i\text{-}C_5H_{11})_3SnI$	26.5	100.92	101.28	+ .4	a
$(n\text{-}C_8H_{17})_3SnI$	20	134.32	142.86	+6.4	a
Section E. Distannanes					
$[(C_2H_5)_3Sn]_2$	17.8	93.28	93.62	+0.4	a
$[(C_2H_5)_2(n\text{-}C_3H_7)Sn]_2$	15.3	102.56	102.95	+0.4	a
$[(C_2H_5)_2(i\text{-}C_4H_9)Sn]_2$	19.8	118.17	122.25	−5.0	a
$[(n\text{-}C_3H_7)_3Sn]_2$	19.5	122.36	121.63	−0.6	a
$[(i\text{-}C_4H_9)_3Sn]_2$	59	150.91	149.53	−0.9	a
Section F. Aryltin compounds					
$(C_2H_5)_3Sn(o\text{-}HOC_6H_4)$	25	71.10	71.23	+0.2	a
$(C_6H_5)SnCl_3$	23	55.15	55.00	− .3	a
$(C_6H_5)SnBr_3$	23	64.28	64.29	.0	a
Section G. Tin–oxygen compounds					
$(C_2H_5)_3Sn(OC_2H_5)$	23.3	56.02	56.45	+0.8	a
$(n\text{-}C_4H_9)_3Sn(OH)$	25	75.25	74.96	− .4	a
$(n\text{-}C_4H_9)_2Sn(OOCCH_3)_2$	25	76.50	76.19	− .4	a
$(n\text{-}C_4H_9)_2Sn(OOCC_{11}H_{23})_2$	25	168.29	168.33	.0	a

(a) R. West and E. G. Rochow, *J. Am. Chem. Soc.*, **74**, 2490 (1952). (b) R. West, M. H. Webster and G. Wilkinson, *ibid.*, **74**, 5794 (1952).

TABLE III

MOLECULAR REFRACTIONS OF SILICON COMPOUNDS

	Temp., °C.	MR_D Calcd.	MR_D Found	Error, %	Ref.
Section A. Silicon Tetraalkyls					
$(CH_3)_4Si$	18.7	30.02	30.11	+0.3	c
$(C_2H_5)_4Si$	25.1	48.38	48.69	+ .6	c
$(CH_3)_3Si(C_2H_5)$	20.2	34.90	34.75	− .4	c
	20	34.73	34.75	+ .1	c
$(CH_3)_2Si(C_2H_5)_2$	24.8	39.40	39.40	.0	c
$(CH_3)_3Si(C_{10}H_{21})$	20	72.04	71.92	− .2	c
$(CH_3)_3Si(n\text{-}C_3H_7)$	25.2	39.49	39.42	− .2	c
$(CH_3)_2Si{=}(CH_2)_5$	20.1	42.04	42.02	.0	c
$(CH_3CHCl)Si(CH_3)_3$	20	39.82	39.59	− .6	c
$(ClCH_2)Si(CH_3)_3$	20	35.17	34.96	− .6	c
$(ICH_2)Si(CH_3)_3$	20	43.02	43.06	+ .1	c
$(CH_3)_3Si(n\text{-}C_4H_9)$	24.8	44.26	44.04	− .5	d
$(CH_3)_2Si(C_2H_5)(n\text{-}C_3H_7)$	25.2	44.10	44.07	− .1	d
$(CH_3)_3Si(i\text{-}C_5H_{11})$	24.9	48.92	48.73	− .4	d
$(CH_3)_2Si(C_2H_5)(i\text{-}C_4H_9)$	25.4	48.76	48.72	− .1	d
$(CH_3)_2Si(n\text{-}C_3H_7)_2$	25.8	48.84	48.74	− .2	d
$(C_2H_5)_3Si(n\text{-}C_3H_7)$	25.2	53.11	53.36	+ .5	d
$(C_2H_5)_3Si(n\text{-}C_4H_9)$	25.4	57.77	58.08	+ .5	d
$(C_2H_5)_3Si(i\text{-}C_4H_9)$	25.5	57.78	58.01	+ .4	d
$(C_2H_5)_3Si(i\text{-}C_5H_{11})$	25.7	62.45	62.67	+ .4	d
Section B. Aryl–silicon compounds					
$(C_6H_5)Si(CH_3)_3$	24.7	50.10	50.02	−0.2	c
$(C_6H_5)SiCl_3$	20.2	48.94	48.78	− .3	c
$(C_6H_5)(C_2H_5)Si(OC_2H_5)_2$	20	65.46	65.59	+ .2	c
$(C_6H_5)_2Si(OC_2H_5)_2$	20	80.30	80.86	+ .5	c
$(C_6H_5)_2Si(OCH_2CH_2Cl)_2$	20.0	90.54	90.58	.0	c
$(C_6H_5)Si(OCH_3)_3$	20.0	52.30	52.47	+ .3	e
$(C_6H_5)Si(OC_2H_5)_3$	20.0	66.53	66.41	− .2	e
$(C_6H_5)Si(O\text{-}n\text{-}C_3H_7)_3$	20.0	80.43	80.42	.0	e
$(C_6H_5)Si(O\text{-}i\text{-}C_3H_7)_3$	20.0	80.68	80.45	− .3	e
$(C_6H_5)Si(O\text{-}n\text{-}C_4H_9)_3$	20.0	94.27	94.28	.0	e
$(C_6H_5)Si(O\text{-}i\text{-}C_4H_9)_3$	20.0	94.48	94.37	− .1	e
$(C_6H_5)Si(CH_3)_2(C_2H_5)$	25.3	54.67	54.66	.0	e
$(C_6H_5)Si(C_2H_5)_3$	25.1	63.79	63.95	+ .2	e

TABLE III (*Continued*)

	Temp., °C.	MR_D Calcd.	MR_D Found	Error, %	Ref.
Section C. Silicon–hydrogen compounds					
$HSiCl_2(CH_3)$	20	24.82	24.92	+0.4	c
$(CH_3SiHO)_4$ cyclic tetramer	20.0	57.10	57.21	+ .2	c
$(CH_3SiHO)_5$ cyclic pentamer	20.0	71.54	71.50	− .1	c
$(CH_3SiHO)_6$ cyclic hexamer	20.0	85.82	85.79	.0	c
$HSi(CH_3)[(CH_3)_2SiO]_2$	20.0	63.14	63.07	− .1	c
$[(CH_3)_2SiOSiH(CH_3)]_2O$	20.0	77.42	77.37	− .1	c
$[(CH_3)_2SiOSi(CH_3)HO]_2$-SiH$(CH_3)$	20.0	91.77	91.68	− .1	c
$HSi(OCH_2CH_2Cl)_3$	20.0	56.63	56.72	+ .2	c
$HSiCl_2(C_2H_5)$	20	29.56	29.57	.0	f
$HSiCl_2(n\text{-}C_4H_9)$	20	38.54	38.86	+ .8	f
Section D. Silicon–oxygen compounds					
$Si(OCH_3)_4$	22.0	33.32	33.38	+0.2	c
	20.0	33.49	33.38	− .3	c
$Si(OC_2H_5)_4$	15.0	52.05	51.96	− .2	c
$Si(O\text{-}n\text{-}C_3H_7)_4$	22.7	70.25	70.64	+ .6	c
$(CH_3)_3Si(OC_2H_5)$	20	35.67	35.57	− .3	c
$(CH_3)_2Si(OC_2H_5)_2$	20	41.05	41.04	.0	c
$(CH_3)Si(OC_2H_5)_3$	20	46.97	46.49	−1.0	c
$(CH_3)_2Si(O\text{-}n\text{-}C_4H_9)_2$	25	59.45	59.62	+0.3	c
$(CH_3)Si(O\text{-}n\text{-}C_4H_9)_3$	20	74.19	74.36	+0.2	c
$[Si(O\text{-}n\text{-}C_3H_7)_3]_2O$	22.6	107.68	109.56	+1.8	c
$[(n\text{-}C_4H_9O)(CH_3)_2Si]_2O$	20	78.17	78.27	+0.1	c
$[(CH_3)_2SiO]_4$ cyclic tetramer	25	74.60	74.63	0	c
$[(CH_3)_2SiO]_5$ cyclic pentamer	25	93.40	93.29	− .1	c
$[(CH_3)_2SiO]_6$ cyclic hexamer	25	112.08	111.94	− .1	c
$[(CH_3)_2SiO]_7$ cyclic heptamer	25	130.48	130.61	+ .1	c
$[(CH_3)_3Si]_2O$ dimer	25	48.89	48.76	− .3	c
$[(CH_3)_3SiO]_2Si(CH_3)_2$ trimer	25	67.48	67.42	− .1	c
$[(CH_3)_2SiOSi(CH_3)_2]_2O$ tetramer	25	86.15	86.09	− .1	c
$[(CH_3)_2SiOSi(CH_3)_2O]_2$-$Si(CH_3)_2$ pentamer	25	104.70	105.06	− .3	e
Hexamer	25	123.56	123.41	− .1	c
Heptamer	25	142.98	142.05	− .6	c
Octamer	25	160.88	160.71	− .1	c
$ClCH_2Si(CH_3)_2OSi(CH_3)_2$	20.0	53.62	53.62	.0	c
	20	53.90	53.62	− .5	c
$ClCH_2Si(CH_3)_2OSi(CH_3)_2$-$CH_2Cl$	20.0	58.18	58.47	+ .5	c
	20	58.58	58.47	− .2	c
$Si(OCH_2CH_2Cl)_4$	20.0	71.07	71.40	+ .5	c
$(CH_3)Si(OCH_2CH_2Cl)_3$	20.0	60.92	61.07	+ .2	c
$(CH_3)Si[OSi(CH_3)_3]_3$	20.0	86.23	86.09	− .2	d
$(CH_3)_3Si(O\text{-}n\text{-}C_4H_9)$	20.0	44.85	44.86	.0	d
$[(n\text{-}C_4H_9O)(CH_3)_2SiO]_3$-$(n\text{-}C_4H_9)$	20.0	96.82	96.93	+ .1	d
$Si(OCH_3)_4$	20	33.15	33.38	+ .7	e
$Si(OC_2H_5)_4$	20	52.00	51.96	− .1	e
$Si(O\text{-}n\text{-}C_3H_7)_4$	20	70.56	70.64	+ .1	e
$Si(O\text{-}n\text{-}C_4H_9)_4$	20	89.05	89.12	+ .1	e
$Si(O\text{-}i\text{-}C_3H_7)_4$	20	70.81	70.68	− .2	e
$[(CH_3O)_3Si]_2O$	20	53.34	53.67	+ .6	e
$[(C_2H_5O)_3Si]_2O$	20	81.65	81.56	− .1	e
$[(n\text{-}C_3H_7O)_3Si]_2O$	20	109.46	109.57	+ .1	e
$[(i\text{-}C_3H_7O)_3Si]_2O$	20	109.82	109.63	− .2	e
$[(n\text{-}C_4H_9O)_3Si]_2O$	20	137.26	137.29	.0	e
$[(CH_3O)_3SiO]_2Si(OCH_3)_2$	20	73.50	73.96	+ .6	e
$(\beta\text{-}C_6H_{11})Si(OCH_3)_3$	20	50.97	51.18	+ .4	e
$(\beta\text{-}C_6H_{11})Si(OC_2H_5)_3$	20	65.10	65.12	.0	e
$(\beta\text{-}C_6H_{11})Si(O\text{-}n\text{-}C_3H_7)_3$	20	79.10	79.13	.0	e
$(\beta\text{-}C_6H_{11})Si(O\text{-}i\text{-}C_3H_7)_3$	20	79.24	79.16	− .1	e
$(\beta\text{-}C_6H_{11})Si(O\text{-}n\text{-}C_4H_9)_3$	20	92.80	92.99	+ .2	e
Section E. Silicon–chlorine compounds					
$SiCl_4$	22.9	28.71	28.45	−0.9	c
$(C_6H_5CH_2)SiCl_3$	20.1	53.76	53.28	−0.9	c
$(C_2H_5)SiCl_3$	19.8	33.85	33.51	−1.0	c
$(CH_2)_5{=}SiCl_2$	20.2	40.83	41.22	+1.0	c
$(n\text{-}C_3H_7)SiCl_3$	20.3	38.42	38.18	−0.6	d
$(n\text{-}C_4H_9)SiCl_3$	20.2	43.18	42.80	− .9	d
$(n\text{-}C_3H_7)(C_2H_5)SiCl_2$	19.9	42.89	43.25	+ .8	d
$(i\text{-}C_4H_9)(C_2H_5)SiCl_2$	20.0	47.71	47.90	+ .4	d
$(CH_3)_3SiCl$	20	29.90	29.69	− .7	g
$(C_2H_5)_3SiCl$	20	43.36	43.63	+ .6	g
Section F. Silicon–bromine compounds					
$SiBr_4$	23.5	40.74	40.32	−1.0	c
$(C_2H_5)_3SiBr$	20	46.55	46.60	+0.1	g
$(ClCH_2CH_2)(C_2H_5)_2SiBr$	20	51.37	51.46	+0.2	g
Section G. Silicon–fluorine compounds					
$(C_2H_5)_3SiF$	25	38.09	38.23	+0.4	c
$(n\text{-}C_3H_7)_3SiF$	25	51.58	52.24	+1.3	c
$(n\text{-}C_4H_9)_3SiF$	25	66.70	66.10	−0.9	c
$(n\text{-}C_6H_{11})_3SiF$	25	80.28	80.08	−0.2	h
Section H. Silicon–sulfur compounds					
$Si(SCH_3)_4$	35	62.12	63.02	+1.4	c
$Si(SC_2H_5)_4$	25	82.10	81.60	−0.6	c
$Si(S\text{-}n\text{-}C_3H_7)_4$	25	100.25	100.28	0	c
$Si(S\text{-}n\text{-}C_4H_9)_4$	25	119.13	118.76	− .3	c
Section I. Silicon–silicon compounds					
$(CH_3)_3SiSi(CH_3)_3$	24.4	51.39	51.05	−0.7	c
Si_2Cl_6	14.5	48.71	48.57	− .3	c
$Si_2Cl_5(OC_2H_5)$	14.5	54.41	54.45	+ .1	c
$Si_2Cl_4(OC_2H_5)_2$	14.5	59.94	60.33	+ .7	c
$Si_2Cl_3(OC_2H_5)_3$	14.5	66.28	66.20	− .1	c
$Si_2(OC_2H_5)_6$	14.5	83.65	83.85	+ .2	c
Si_2Cl_6	14.5	68.81	68.69	− .2	c
Section J. Silicon–nitrogen compounds					
$[(CH_3)_3Si]_2NH$	20	51.38	51.24	−0.2	c
$(CH_3)_3SiNHCH_3$	20	33.12	33.08	−0.1	c
$(C_2H_5)_2ClSiN(C_2H_5)_2$	20	56.79	56.06	−1.3	c
$(C_2H_5)_2Si[N(C_2H_5)_2]_2$	20	72.38	71.40	−1.4	c
$Si(NCO)_4$	20.0	37.29	36.96	−0.9	c
$Si(OCH_3)(NCO)_3$	20.0	36.33	36.06	− .7	c
$Si(OCH_3)_2(NCO)_2$	20.0	35.07	35.17	+ .3	c
$Si(OCH_3)_3(NCO)$	20.0	33.95	34.27	+ .9	c
$Cl_3Si(NCO)$	25	31.11	30.58	−1.7	c
$Cl_2Si(NCO)_2$	25	33.34	32.71	−1.9	c
$ClSi(NCO)_3$	25	35.31	34.83	−1.4	c
$[(CH_3)_2SiNH]_3$ cyclic trimer	20	63.36	63.40	+0.1	i
$[(C_2H_5)_2SiNH]_3$ cyclic trimer	20	90.52	91.29	+0.9	i
$[(C_2H_5)_2SiNH]_4$ cyclic tetramer	20	119.87	121.72	+1.5	i
$(C_2H_5)(CH_3)_2SiNH$	20	59.48	60.54	+1.8	i
$[(CH_3)_2SiNH]_2Si(CH_3)_2$	20	72.13	72.40	+0.4	i
$(CH_3)_3Si(NCO)$	20.0	31.92	31.82	− .3	j
$(CH_3)_2Si(NCO)_2$	20.0	33.60	33.54	− .2	j
$(CH_3)Si(NCO)_3$	20.0	35.39	35.24	− .4	j
$(n\text{-}C_4H_9)Si(NCO)_3$	20.0	48.53	49.18	+1.3	j
$(C_2H_5)_2Si(NH_2)(CH_2CH_2Cl)$	20	47.02	47.06	+0.1	g

(c) E. L. Warrick, *J. Am. Chem. Soc.*, **68**, 2455 (1946).
(d) W. O. Sauer, *ibid.*, **68**, 954 (1946).
(e) Smith, *Svensk. Kem. Tidskr.*, **61**, 213 (61) (1949).
(f) C. A. MacKenzie, A. P. Mills and J. M. Scott, *J. Am. Chem. Soc.*, **72**, 2032 (1950).
(g) D. L. Bailey, L. H. Sommer and F. C. Whitmore, *ibid.*, **70**, 435 (1948).
(h) J. A. Gierut, F. J. Sowa and J. A. Nieuwland, *ibid.*, **58**, 897 (1936).
(i) S. D. Brewer and C. P. Haber, *ibid.*, **70**, 3888 (1948).
(j) G. S. Forbes and H. H. Anderson, *ibid.*, **70**, 1222 (1948).

The subsequent tables incorporate the results of our calculations for lead, germanium and mercury compounds. It may be pointed out that we regard the experimental data of Fajans and Cook and of Johnson and Fritz upon the tetraalkylgermanes

TABLE IV

MOLECULAR REFRACTIONS OF LEAD COMPOUNDS

	Temp., °C.	MR_D Calcd.	MR_D Found	Error, %	Ref.
$(CH_3)_4Pb$	20.0	40.18	41.04	+2.0	k
$(C_2H_5)_4Pb$	20.0	59.45	59.62	+0.3	k
$(n\text{-}C_3H_7)_4Pb$	20.0	78.60	78.30	−0.4	k
$(i\text{-}C_3H_7)_4Pb$	20.0	79.87	78.34	−1.9	k
$(n\text{-}C_4H_9)_4Pb$	20.0	97.11	96.78	−0.4	k
$(n\text{-}C_5H_{11})_4Pb$	20.0	115.39	115.42	0.0	k
$(d,l\text{-}C_5H_{11})_4Pb$	20.0	116.25	114.42	−1.6	k
$(i\text{-}C_5H_{11})_4Pb$	20.0	116.13	115.54	−0.5	k
$(CH_3)_3Pb(C_2H_5)$	20.0	45.07	45.68	+1.3	k
$(CH_3)_3Pb(n\text{-}C_3H_7)$	20.0	49.95	50.35	+0.8	k
$(CH_3)Pb(C_2H_5)_3$	20.0	54.70	54.98	+ .5	k
$(CH_3)_3Pb(n\text{-}C_4H_9)$	20.0	54.63	54.97	+ .6	k
$(CH_3)_2Pb(C_2H_5)(n\text{-}C_3H_7)$	20.0	54.66	55.00	+ .6	k
$(CH_3)_2Pb(n\text{-}C_3H_7)_2$	20.0	59.28	59.67	+ .6	k
$(CH_3)Pb(C_2H_5)_2(n\text{-}C_3H_7)$	20.0	59.34	59.66	+ .5	k
$(C_2H_5)_3Pb(n\text{-}C_3H_7)$	20.0	64.19	64.29	+ .2	k

TABLE IV (*Continued*)

	Temp., °C.	MR_D Calcd.	MR_D Found	Error, %	Ref.
$(CH_3)Pb(n\text{-}C_3H_7)_3$	20.0	68.93	68.98	+ .1	k
$(CH_3)_2Pb(n\text{-}C_4H_9)_2$	20.0	68.52	68.91	+ .6	k
$(C_2H_5)_2Pb(n\text{-}C_3H_7)_2$	20.0	69.04	68.96	− .1	k
$(C_2H_5)Pb(n\text{-}C_3H_7)_3$	20.0	73.77	73.63	− .2	k
$(CH_3)_2Pb(n\text{-}C_5H_{11})_2$	20.0	77.63	78.23	+ .8	k
$(C_2H_5)_2Pb(n\text{-}C_4H_9)_2$	20.0	77.75	78.20	+ .6	k
$(C_2H_5)_2Pb(n\text{-}C_5H_{11})_2$	20.0	87.05	87.52	+ .5	k
$(n\text{-}C_3H_7)_2Pb(n\text{-}C_4H_9)_2$	20.0	87.49	87.54	+ .1	k
$(n\text{-}C_4H_9)_2Pb(i\text{-}C_4H_9)_2$	20.0	96.96	96.84	+ .1	k
$(n\text{-}C_3H_7)_2Pb(n\text{-}C_5H_{11})_2$	20.0	97.07	96.86	− .2	k
$(i\text{-}C_4H_9)_2Pb(n\text{-}C_5H_{11})_2$	20.0	105.91	106.16	+ .2	k
$(n\text{-}C_4H_9)_2Pb(n\text{-}C_5H_{11})_2$	20.0	106.01	106.10	+ .1	k
$(n\text{-}C_4H_9)_2Pb(i\text{-}C_5H_{11})_2$	20.0	106.20	106.16	.0	k
$(n\text{-}C_4H_9)_2Pb(d,l\text{-}C_5H_{11})_2$	20.0	106.56	105.60	− .9	k
$(n\text{-}C_5H_{11})_2Pb(d,l\text{-}C_5H_{11})_2$	20.0	114.88	114.92	.0	k
$(n\text{-}C_5H_{11})_2Pb(i\text{-}C_5H_{11})_2$	20.0	115.43	115.48	.0	k

(k) Jones, Evans, Gulwell and Griffiths, *J. Chem. Soc.*, 39 (1935).

TABLE V

MOLECULAR REFRACTIONS OF GERMANIUM COMPOUNDS

	Temp., °C.	MR_D Found	MR_D Calcd.	Error, %	Ref.
$Ge(CH_3)_4$	25	32.30	32.22	−0.2	l
$Ge(C_2H_5)_4$	25	50.43	50.80	+ .7	l
$Ge(C_2H_5)_4$	24.5	50.41	50.80	+ .8	m
$Ge(n\text{-}C_3H_7)_4$	25	69.43	69.48	+ .1	l
$Ge(n\text{-}C_3H_7)_4$	20	69.00	69.48	+ .7	m
$Ge(n\text{-}C_4H_9)_4$	25	87.89	87.96	+ .1	l
$Ge(n\text{-}C_5H_{11})_4$	25	106.75	106.60	− .1	l
$Ge(i\text{-}C_5H_{11})_4$	20	106.32	106.74	+ .4	m
$Ge(n\text{-}C_6H_{13})_4$	25	125.13	125.04	− .1	l
$Ge(OCH_3)_4$	25	35.74	36.06	+0.9	n
$Ge(OC_2H_5)_4$	25	54.91	54.64	− .5	n
$Ge(O\text{-}n\text{-}C_3H_7)_4$	25	73.45	73.32	− .2	n
$Ge(O\text{-}n\text{-}C_4H_9)_4$	25	91.86	91.80	− .2	n
$Ge(O\text{-}n\text{-}C_5H_{11})_4$	25	110.35	110.44	+ .1	n
$Ge(O\text{-}n\text{-}C_6H_{13})_4$	25	129.21	128.88	− .3	n
$[(C_2H_5)_3Ge]_2O$	20	80.31	81.15	+1.0	o
$[(C_2H_5)_2GeO]_4$	20	120.44	121.40	+0.8	o
$[(n\text{-}C_3H_7)_3Ge]_2O$	20	108.1	109.1	+ .9	p
$[(n\text{-}C_4H_9)_3Ge]_2O$	20	135.7	136.8	+ .8	p
$(HCOO)Ge(C_2H_5)_3$	20	46.6	47.0	+ .9	o
$(HCOO)_2Ge(C_2H_5)_2$	20	43.0	43.3	+ .7	o
$(HCOO)Ge(n\text{-}C_3H_7)_3$	20	60.7	61.0	+ .5	q
$(HCOO)Ge(n\text{-}C_4H_9)_3$	20	74.4	74.9	+ .7	r
$(CH_3COO)Ge(C_2H_5)_3$	20	51.2	51.6	+ .8	o
$(CH_3COO)Ge(n\text{-}C_3H_7)_3$	20	65.0	65.5	+ .8	q
$(CH_3COO)Ge(n\text{-}C_4H_9)_3$	20	79.3	79.5	+ .3	r
$(CH_3COO)_2Ge(C_2H_5)_2$	20	52.0	52.2	+ .4	o
$(C_2H_5CCO)Ge(n\text{-}C_3H_7)_3$	20	69.7	70.3	+ .9	q
$(n\text{-}C_6H_{13})Ge(n\text{-}C_4H_9)_3$	20	102.2	102.7	+ .5	r
$GeCl_4$	20	31.54	30.4	−3.4	s
$(CH_3)_2GeCl_2$	29	31.70	31.3	−1.2	t
$(n\text{-}C_3H_7)_3GeCl$	20	59.5	59.7	+0.3	p
$(n\text{-}C_4H_9)_3GeCl$	20	73.3	73.5	+0.3	r
$GeBr_4$	25	44.53	44.4	−0.2	u
$(CH_3)_3GeBr$	18	35.73	35.2	−1.4	t
$(n\text{-}C_3H_7)_3GeBr$	20	62.7	63.2	+0.8	p
$(n\text{-}C_4H_9)_3GeBr$	20	77.1	77.1	...	r
$(n\text{-}C_3H_7)_3GeI$	20	68.7	68.7	...	p
$(n\text{-}C_4H_9)_3GeI$	20	82.6	82.6	...	r
$(n\text{-}C_3H_7)_3GeF$	20	53.6	53.4	−0.4	p
$(n\text{-}C_4H_9)_3GeF$	20	67.0	67.2	+0.3	r
$(C_2H_5)_3Ge(NCO)$	25	47.25	47.51	+0.6	v
$(C_2H_5)_2Ge(NCO)_2$	25	44.39	44.22	−0.4	v
$(C_2H_5)Ge(NCO)_3$	25	41.70	40.93	−1.8	v
$Ge(NCO)_4$	25	38.77	37.64	−2.9	v
$(n\text{-}C_4H_9)_3Ge(NCO)$	20	75.0	75.4	+0.5	r
$Ge(SCH_3)_4$	25	65.29	66.54	+1.9	t
$Ge(SC_2H_5)_4$	25	84.91	85.12	+0.2	t
$Ge(S\text{-}n\text{-}C_3H_7)_4$	25	103.64	103.80	+ .2	t
$Ge(S\text{-}i\text{-}C_3H_7)_4$	25	104.13	103.84	− .3	t
$Ge(S\text{-}n\text{-}C_4H_9)_4$	25	122.38	122.28	− .1	t
$Ge(S\text{-}i\text{-}C_4H_9)_4$	25	122.28	122.40	+ .1	t
$Ge(S\text{-}s\text{-}C_4H_9)_4$	25	122.94	121.60	−1.1	t

(l) K. Fajans and B. Cook, Symposium on Organometallic Compounds, Chicago Meeting of the Am. Chem. Soc., April 1948; Cook, thesis, Ann Arbor, University of Michigan, 1948; Fajans, *Chem. Eng. News*, **27**, 900 (1949).

(m) Krause and Grosse, "Die Chemie der Metall-organischen Verbindungen," Springer, Berlin, 1937.

(n) O. H. Johnson and H. E. Fritz, *J. Am. Chem. Soc.*, **75**, 718 (1953).

(o) H. H. Anderson, *ibid.*, **72**, 2089 (1950).

(p) H. H. Anderson, *ibid.*, **73**, 5440 (1951).

(q) H. H. Anderson, *ibid.*, **73**, 5798 (1951).

(r) H. H. Anderson, *ibid.*, **73**, 5800 (1951).

(s) Laubengayer and Tabern, THIS JOURNAL, **30**, 1047 (1926).

(t) O. H. Johnson, *Chem. Revs.*, **48**, 259 (1951).

(u) L. M. Dennis and F. E. Hance, *J. Am. Chem. Soc.*, **44**, 299 (1922).

(v) H. H. Anderson, *ibid.*, **71**, 1799 (1949).

and the tetraalkyloxygermanes, respectively, as the most trustworthy and have utilized these in the computations of the (Ge–C) and (Ge–O) refractions.

TABLE VI

MOLECULAR REFRACTIONS OF MERCURY COMPOUNDS

	Temp., °C.	MR_D Calcd.	MR_D Found	Error, %	Ref.
$(CH_3)_2Hg$	20.0	23.72	24.43	+3.0	k
$(C_2H_5)_2Hg$	20.0	33.26	33.72	+1.4	k
$(n\text{-}C_3H_7)_2Hg$	20.0	42.93	43.06	+0.3	k
$(i\text{-}C_3H_7)_2Hg$	20.0	43.98	43.08	−2.0	k
$(n\text{-}C_4H_9)_2Hg$	20.0	52.57	52.30	−0.5	k
$(i\text{-}C_4H_9)_2Hg$	20.0	52.06	52.36	+0.6	k
$(s\text{-}C_4H_9)_2Hg$	20.0	53.48	51.96	−2.8	k
$(n\text{-}C_5H_{11})_2Hg$	20.0	61.57	61.62	+0.1	k
$(i\text{-}C_5H_{11})_2Hg$	20.0	61.37	61.68	+0.5	k
$(d,l\text{-}C_5H_{11})_2Hg$	20.0	60.51	61.12	+1.0	k
$(n\text{-}C_6H_{13})_2Hg$	20.0	70.67	70.84	+0.2	k

The bond refractions for silicon, germanium, lead and mercury, deduced from the above results for "MR_D found" are given in Table VII.

TABLE VII

BOND REFRACTIONS

Bond	Refraction	No. of cpd. used	Standard dev.
	Silicon		
(Si–C)	2.52	19	0.043
($Si–C_{ar}$)	2.93	13	.14
(Si–F)	1.7	4	.46
(Si–Cl)	7.11	10	.16
(Si–Br)	10.08	3	.08
(Si–Si)	5.89	7	.22
(Si–O)	1.80	46	.056
(Si–H)	3.17	10	.15
(Si–S)	6.14	4	.14
(Si–N)	2.16	21	.29
	Germanium		
(Ge–C)	3.05	6	0.038
(Ge–Cl)	7.6	4	.22
(Ge–Br)	11.1	4	.35
(Ge–I)	16.7	2	...
(Ge–F)	1.3	2	...
(Ge–O)	2.47	6	0.057
(Ge–S)	7.02	7	.18
(Ge–N)	2.33	5	.28
	Lead		
(Pb–C)	5.26	32	0.14
	Mercury		
(Hg–C)	7.21	11	0.32

The authors thank Imperial Chemical Industries for a grant.

THE SATURATION IN THE NEGATIVE JOSHI EFFECT WITH RESPECT TO THE LIGHT INTENSITY AS THE CONSEQUENCE OF THE NEGATIVE SPACE CHARGE RESPONSIBLE FOR THE *EFFECT*

BY S. R. MOHANTY

Chemical Laboratories, Banaras Hindu University, India

Received July 2, 1953

The tendency to saturation in the negative Joshi effect $-\Delta i$ with respect to the light intensity I is the consequence of decrease in the quantum efficiency of the photoelectronic emission process due to increase in the negative space charge density. This last remains constant when the area of the electrode surface irradiated S_L, at a given I, is varied; the space charge sheath is, however, enlarged in extent proportional to S_L. The observed linear increase in $-\Delta i$ with S_L follows. The change in $d(-\Delta i)/dS_L$ with variation in (the nature of) the electrode surface shows conclusively that the latter is of primary significance for the occurrence of the Joshi effect.

The author and Kamath have shown earlier[1] that the negative Joshi effect $-\Delta i$ increases with ν the effective mean frequency of the irradiating light and I the intensity. Whilst, however, the variation of $-\Delta i$ with ν at constant I is sensibly linear,[2] with I of a given ν the initial rapid rise slows down at large values of I, due presumably to saturation.[1] It was of interest therefore, to study the dependence of $-\Delta i$ in oxygen on the electrode surface area irradiated S_L, ν and I of the irradiating light remaining constant. The results show that *ceteris paribus* $-\Delta i$ is a linear function of S_L. The change in the slope of the line with variation in (the nature of) the electrode surface shows conclusively that the latter is of primary significance for the occurrence of the Joshi effect.

Experimental

The discharge was produced in carefully purified oxygen contained in the annular space of an Indian soft soda glass Siemens tube at 225 mm. (31°). The tube had the following dimensions: outer diam. of the inner tube, 8.0 mm.; inner diam. of the outer tube, 17.1 mm.; mean thickness of wall, 1.0 mm.; length of the discharge column, 27.0 cm. The H.T. electrode consisted of a moderately strong solution of sodium chloride inside the inner tube, and a helix of fine copper wire (the distance between consecutive turns being uniform and sufficiently large to permit irradiation of the enclosed gas) wound tightly on the outer tube, excluding the extremities, the L.T. The ozonizer was enclosed in a rectangular light-tight box which was provided, on one side, with a movable shutter operated by a rack and pinion arrangement. The shutter incorporated a device which completely cut off light from the non-irradiated portion of the discharge column. The source of light (3700–7800 Å.) consisted of a 200-watt incandescent tungsten filament (in glass) lamp placed at a distance of 25 cm. from the Siemens tube(s). The heat radiations from the lamp were cut off with a cm.-thick water filter. The gas was excited at various applied potentials V (4–5.5 kv., r.m.s.) of 50 cycles frequency, and the discharge current i was observed with a sensitive mirror galvanometer actuated by a Cambridge vacuum thermocouple ("Vacuo-junction"), in dark (i_D) and when different lengths (2–22 cm.) of the discharge column were irradiated (i_L). The mean intensity of light on the ozonizer, as determined with a thermopile and galvanometer, was kept constant by regulating the lamp current. S_L was calculated from a knowledge of the outer and inner diameters of the inner and outer tubes, respectively. In Fig. 1 are plotted values for $-\%\Delta i$ ($= -\Delta i \times 100/i_D$; $-\Delta i = i_D - i_L$), at constant V, against the corresponding S_L.

In another series of experiments (Fig. 2), the electrodes of the Siemens tube were coated, over half their length, with a 2.5 M aqueous solution of BDH "Analar" KCl. The tube was vacuum dried, and filled with oxygen at the original pressure, *viz.*, 225 mm. (25°). It was excited, excluding the extremities, at 4.00 and 5.34 kv., and $-\Delta i$ observations made as before.

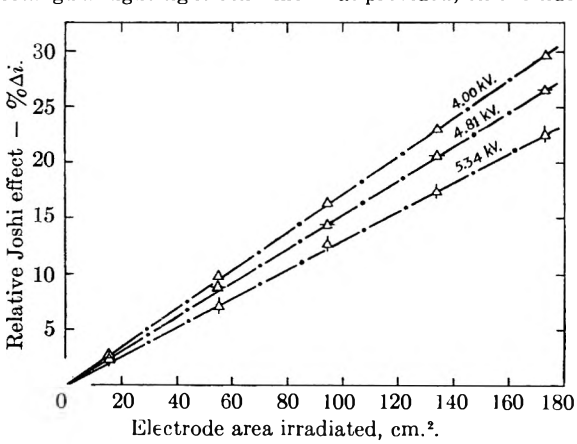

Fig. 1.—Variation with electrode surface area irradiated of the negative Joshi effect in oxygen: Siemens tube; p_{O_2}, 225 mm.; temp., 23°; 50 cycles; "Vacuo-junction" detection; 3700–7800 Å.

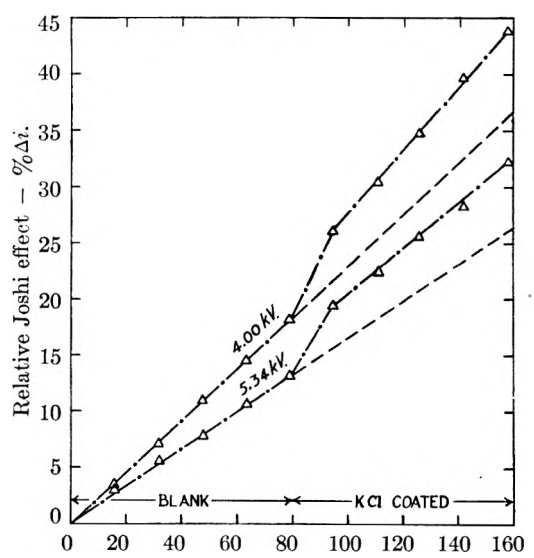

Fig. 2.—Surface dependence of the negative Joshi effect in oxygen: Siemens tube; p_{O_2}, 225 mm.; temp., 26°; 50 cycles; "Vacuo-junction" detection; 3700–7800 Å.

Discussion

It will be seen from Fig. 1 that an increase in the electrode surface area irradiated S_L increases

(1) S. R. Mohanty and G. S. Kamath, *J. Indian Chem. Soc.*, **25**, 467 (1948).

(2) S. R. Mohanty, *Indian J. Phys.*, communicated.

linearly the relative $-\%\Delta i$ (and the net $-\Delta i$) at constant applied V. Thus, $-\%\Delta i$ at 4.81 kv. is 2.7 for 15.8 cm.^{2} irradiated and increases to 26.5 for 173 cm.^{2}; the corresponding values of $-\Delta i$ are, respectively, 0.3 and 2.99. Since irradiation of the electrode surface results in simultaneous irradiation of the enclosed gas, and since with increase in S_L the volume of the gas irradiated increases proportionately, it is not possible to decide with any degree of certainty, from the above results alone, whether the Joshi effect is of gas bulk or electrode surface in origin. The fact that *ceteris paribus* a change in the slope of the $-\Delta i$–S_L line results from variation in the nature of the electrode surface, from blank to KCl coated (Fig. 2), shows conclusively, however, that the electrode surface is the seat of the $\pm\Delta i$ phenomenon.[3,4] In accordance with this, it is observed that when equal areas of the two different portions are excited separately, at a given V, and irradiated, $-\Delta i_{coated} > -\Delta i_{blank}$. Irradiation of the gas phase is thus only incidental, but not fundamental for the production of the Joshi effect; its avoidance in Siemens tubes is not easily possible, especially in view of the small electrode separation necessitated by comparatively large pressures (of the order of a few hundreds of mm.) essential for the occurrence of appreciable $-\Delta i$.[5-7] Using flat ended discharge tubes with external electrodes, on the other hand, Harries and von Engel[8,9] have shown oscillographically that whilst irradiation of the electrodes produces $-\Delta i$, this last does not occur when only the gas bulk is irradiated. Essentially similar are the observations of the author, Prasada Rao and Ramaiah,[10] and of Setty, Kulkarni and Srivastava[11] from measurements of the discharge current in "sleeve" tubes.

From the linearity of the $-\Delta i$–S_L graph, and its origin from that of the axes

$$-\Delta i = mS_L$$

The maximum Joshi effect characteristic of the system is obtained when $S_L = S_e$, the total electrode area. The slope m depends upon the various electrical parameters, gas pressure and temperature, the nature of the electrode surface, etc. It is of interest to record that an estimate of the influence of any of these variables on the Joshi effect can be had from the change in the magnitude of m caused by that variable.

According to Joshi,[4,12-14] $-\Delta i$ is the consequence of a space charge of slow moving negative ions formed from capture, by the electronegative gas particles in the discharge, of electrons released under light from an adsorption-like ionic + molecular layer on the electrodes. The space charge density which governs $-\Delta i$ is determined by the primary emission, and the probability of electron attachment.[15] Vacuum photoelectric emission[16] is strictly proportional to the light intensity I. Such a relationship does not hold, however, under conditions productive of the Joshi effect, since with progressive increase in I on a constant area of the electrode surface, the space accumulation of the negative ions in the neighborhood of the photoactive surface, brings into existence a retarding electrostatic field which inhibits the primary emission. This inhibition is more pronounced the larger the space charge density and the attendant field, *i.e.*, the larger the I and the emission. The quantum efficiency of the process, and the rate of increase in the space charge density, fall off as I is increased. The observed progressive diminution in $d(-\Delta i)/dI$ with I follows. On increasing the emitting surface, *i.e.*, the electrode area irradiated, on the other hand, I remaining constant, the space charge density (and the retarding field) is not altered, but the space charge is proportionately increased in extent, leading to the observed linear variation in $-\Delta i$ with S_L.

The comparatively large $-\Delta i$ for KCl coated surfaces is attributable to strong adsorption on KCl,[17] a consequence of the high surface tension[18] (2050 dynes/cm.) of the salt.

Acknowledgments.—Grateful thanks of the author are due to Prof. S. S. Joshi, Professor of Physical Chemistry, Banaras Hindu University, for his kind interest in the work.

(3) S. S. Joshi, *Proc. Indian Sci. Cong.*, Presidential Address, Chem. Sec. (1943).

(4) S. S. Joshi, *Current Sci.*, **16**, 19 (1947).

(5) S. R. Mohanty and G. S. Kamath, *J. Indian Chem. Soc.*, **25**, 405 (1948).

(6) S. R. Mohanty, *ibid.*, **26**, 553 (1949).

(7) D. V. R. Rao and B. K. Sarma, THIS JOURNAL, **53**, 753 (1949).

(8) W. L. Harries and A. von Engel, *J. Chem. Phys.*, **19**, 514 (1951).

(9) W. L. Harries and A. von Engel, *Proc. Phys. Soc. (London)*, **B64**, 916 (1951).

(10) S. R. Mohanty, T. D. Prasada Rao and R. Ramaiah, unpublished results.

(11) P. S. V. Setty, K. Kulkarni and C. M. Srivastava, *Indian J. Phys.*, **26**, 455 (1952).

(12) S. S. Joshi, *Current Sci.*, **15**, 281 (1946).

(13) S. S. Joshi, *Proc. Indian Sci. Cong.*, Part III, Phys. Sec., Abst. 26 (1946).

(14) S. S. Joshi, *ibid.*, Part III, Phys. Sec., Abst. 25 (1947).

(15) L. B. Loeb, "Fundamental Processes of Electrical Discharge in Gases," John Wiley and Sons, Inc., New York, N. Y., 1939, pp. 258-304.

(16) A. L. Hughes and L. A. DuBridge, "Photoelectric Phenomena," McGraw-Hill Book Co., Inc., New York, N. Y., 1932, pp. 28-32.

(17) J. W. McBain, "The Sorption of Gases and Vapours by Solids," George Routledge and Sons, Ltd., London, 1932, p. 252.

(18) J. E. Lennard-Jones and B. M. Dent, *Proc. Roy. Soc. (London)* **A121**, 258 (1928).

THE ADSORPTION OF COPPER SULFATE ON COPPER AND SILVER[1]

BY LAWRENCE R. SCHARFSTEIN AND CECIL V. KING

Department of Chemistry, New York University, New York, N. Y.

Received July 6, 1953

The amount of copper(II) sulfate removed from solutions in water and methanol, on percolation through columns of finely divided copper and silver, has been measured. The nature of the adsorption isotherms obtained is discussed. At low concentrations in aqueous solution, the adsorption on copper falls off rapidly, as if a null point would be found at about 10^{-6} *M*. The adsorption in all cases is equivalent to less than a monatomic layer, but is greater than necessary to charge the electrical double layer, if this is considered in the simple Helmholtz sense.

Introduction

The precise measurement of adsorption of metal salts on metals is difficult, because so little is adsorbed. It is necessary to bring a very large surface area into equilibrium with a small amount of solution if the latter is to decrease appreciably in concentration. Very dilute solutions are sometimes used if a suitable analytical method is available, since the per cent. change in concentration is greater. However, it is advantageous to cover a wide concentration range in order to find the type of adsorption isotherm obeyed, and whether an upper limit is approached.

The use of radioactive tracers for such measurements looks inviting, but presents additional problems. Metals exchange with their own ions to an extent equivalent to many atomic layers, and it is not certain how much of this is due to statistical fluctuations at the surface, how much to local cell action, and how much to internal diffusion. No one has attempted to distinguish between adsorption and exchange in such cases. Adsorption studies have been limited to the case of less noble ions on more noble metals, or on passive metals.

In order to obtain more information about adsorption on metal surfaces by a simple, direct experimental method, it was decided to make measurements of the retention of copper sulfate from solution, on the surface of copper and silver. To obtain the advantage of large surface area and small solution volume, the method of percolation through a column of finely divided metal was chosen. If equilibrium were attained rapidly as the liquid seeps through the (initially dry) column, the first effluent should be free of the metal salt, and increase to the initial concentration should be very sharp. This is not quite true in practice, but the total amount of retention can be found by analyzing a few ml. of effluent rather than the much larger volume which would be required to bathe the entire metal sample.

The main disadvantage of this method is that it is time-consuming; the metal must be washed thoroughly and dried in the column for each experiment. With corrodable metals air must be excluded.

Experimental

The Metals.—Electrolytic copper, in the form of a granular powder, was employed.[2] The manufacturer stated that it was prepared by ejection of molten metal through a fine nozzle, with rapid cooling in an inert fluid. The particles were approximately spherical, and varied in diameter from 0.003 to 0.1 mm., with over 50% between 0.01 and 0.08 mm. Measurement of 20 particles from each of 7 samplings gave an estimated area of 180 cm.²/g. Spectroscopic analysis[3] showed 0.005% Fe, 0.003% Ni, 0.002% each of Ag and Pb, 0.001% each of Zn and Sn, with smaller amounts of Mg and Si. The copper was washed with alcohol and ether, and in the columns it was washed with acidified copper sulfate solution to remove exchangeable base metals, until a negative test for iron was obtained.

The silver was a sample previously prepared and used in this Laboratory.[4,5] It consisted of uniform crystals about $9 \times 9 \times 14\ \mu$, and had an estimated area of 500 cm.²/g.

The Columns.—Most of the work reported with copper was done with a column about 3 cm. in diameter, filled with 536 g. of copper, to a height of 41 cm. The bottom of the glass tube was melted down to a short, thick-walled capillary tube, and the copper was retained by a 14-mg. plug of glass wool. Side arms at the top of the tube permitted passage of nitrogen and hydrogen. A similar smaller column was used for preliminary experiments. The silver column was 1 cm. in diameter and contained 96 g. of silver.

Operation of the Columns.—The solutions dripped onto the metal from a Teflon plug buret, which could be adjusted very easily to the desired rate of delivery. The flow rate was ordinarily one or a few drops per minute; the solution spread over and down through the metal without flooding at any point. About 33 ml. of solution was required to wet the copper in the large column; the first effluent appeared after 2 to 6 hours. Ordinarily 3 to 25 ml. was collected, in portions, for analysis; the first effluent was copper-free, and the rise to full strength took place in 3 to 5 ml. of solution.

Before use in each experiment the copper, after thorough washing with water, was dried in a stream of nitrogen passed in at the capillary tip, while the column was warmed in a tube furnace. Hydrogen was then passed in for 2 hours at 350°, and the metal was cooled in nitrogen. With nitrogen still flowing, the buret was attached. All solutions were previously deaerated, and nitrogen was passed through the top of the buret, through the top of the column, and around the tip of the column until effluent appeared.

The silver was heated in hydrogen to 150°, which would reduce sulfide if present, and it was not considered necessary to protect with nitrogen during runs.

Analysis of Solutions.—Most of the analyses were done with a Lumetron photoelectric colorimeter, some with a colorimeter which used a smaller solution cell. The effluents were collected in weighing bottles and diluted with water and reagents as required, by weight. Volume concentrations were obtained by estimating densities as closely as possible. The copper ammonia complex was used for concentrations above 10^{-3} *M*. For more dilute solutions, a copper test proposed by Clarke and Jones, and further described by Kolthoff,[6] was developed into a quantitative procedure, as follows.

To the solution to be analyzed were added one drop of 0.5 *M* sulfuric acid, 0.2 ml. of 0.1% dimethylglyoxime in ethanol and one ml. of saturated potassium periodate solution; the whole was diluted (by weight) to approximately 10 ml. The mixture could now be kept until a convenient time for analysis, since no color appears in acid solution. On adding 5 mg. of solid sodium bicarbonate a red-violet color develops (absorption maximum at 525 mμ), reaches full intensity in about 3 minutes, and starts to fade several

(1) From the Ph.D. thesis submitted by Lawrence R. Scharfstein in the Graduate School of New York University, May, 1953.

(2) From Belmont Smelting and Refining Works, Inc.

(3) Courtesy of the Chemistry Department, Columbia University.

(4) C. V. King and F. S. Lang, *J. Electrochem. Soc.*, **99**, 295 (1952).

(5) C. V. King and R. K. Schochet, THIS JOURNAL, **57**, 895 (1953).

(6) I. M. Kolthoff, *J. Am. Chem. Soc.*, **52**, 2-22 (1930).

minutes later. With a suitable filter in the colorimeter, Beer's law was shown to be obeyed in the range 4×10^{-6} to 1.2×10^{-4} M copper sulfate. Addition of methanol up to 20% by volume did not affect the absorption. It was shown that solutions analyzed with the ammonia complex could be diluted and analyzed with dimethylglyoxime with the same results, within the usual precision of about 3%.

Since water from copper stills may contain as much as 5×10^{-6} M copper ion, water with a much lower copper content was obtained and used for the most dilute solutions.

While part of the copper ion in the column effluent has been reduced to the cuprous state, this need not be considered in the analysis, since it is reoxidized during preparation of the solutions for the colorimeter.

Preliminary Experiments.—The first runs were made, in the smaller column, with (analytical grade) copper sulfate dissolved in pure water; the *p*H varies in the range 4 to 6, depending on the concentration.[7] While the amounts of copper ion retained seemed reasonable, the *p*H of the effluent remains lower than the original after equilibrium has been established in the column. For example, 4.68×10^{-3} M copper sulfate went into the column at *p*H 5.1; about 2 ml. of effluent was deficient in copper ion, and after another 16 ml. was collected the *p*H was still 3.6 to 3.7.

All the older work indicates that cuprous oxide will be formed on the copper under these conditions; an excellent treatment of the system is given by Pourbaix.[8] The question of stability of cuprous oxide, however, depends mainly on a knowledge of the equilibrium constant of the reaction

$$Cu^{++} + Cu \rightleftarrows 2Cu^{+}; \quad K = a_{Cu^{+2}}/a_{Cu^{+}}^{2}$$

The accepted value of K[9,10] has been 10^{-6}, measured with acidified solutions. More recently El Wakkad[11] has found the value 10^{-5} for unacidified solutions. El Wakkad measured the *p*H of equilibrated solutions, and found that the amounts of cuprous and hydroxyl ions could not exceed the solubility product constant.

Because of the possibility of cuprous oxide formation, it was decided to employ acidified solutions in further runs. It was found that if the *p*H were adjusted to any value from 3.5 to 2.5 by addition of sulfuric acid, there was no change on passing through the column, and the amount of copper retained was independent of *p*H. When sulfuric acid, *p*H 3.5, was passed through, the effluent contained no more copper than the water used.

During the experiments, the results were checked repeatedly by returning to two reference concentrations, namely, 2.1×10^{-2} and 6.7×10^{-3} M. It was found that if the column were left open to the air, or in contact with air-containing solutions, new measurements at these concentrations showed an increased adsorption of a few per cent. In the course of two years the adsorption capacity of each of the two columns was nearly doubled. This is attributed to the repeated formation and removal of an oxide film; it has been shown by Rhodin[12] that oxidation of a very smooth copper surface, followed by reduction in hydrogen, leads to an increase in area, as measured by nitrogen adsorption.

Results

The measurements on copper reported below were obtained with the column in almost daily use and filled with deaerated copper sulfate solution when idle. In this way good checks were found on returning to the reference solutions. Table I gives results at such concentrations that reduction to copper(I) ion is negligible. The methanol solutions were made by dissolving $CuSO_4 \cdot 5H_2O$ in anhydrous methanol, and were not acidified.

At lower concentrations reduction to cuprous ion becomes appreciable, and after equilibrium is established in the column, the total copper concentration of the effluent is greater than that of the initial solution. The analytical method was not good enough to fix the final concentration reliably, and this had to be calculated. Measurements in more dilute solutions are given in Table II; under "moles ads.," min. and max. refer to the amounts of adsorbed copper ion based on calculations of the final concentration employing the two values of K mentioned above. As will be seen later the difference in values is unimportant; in fact, if no correction were made, the conclusions would be no different.

TABLE I

ADSORPTION OF COPPER SULFATE ON COPPER

Temp. 20–27°; 536 g. copper; *p*H 3.0 in first 5 solutions, 3.5 in others

	C_{CuSO_4}, $M \times 10^2$	No. of expt.	Moles ads./g. Cu $\times 10^8$	Av. dev., %
Water	4.01	3	8.2	4.5
	2.10	7	6.2	3.3
	1.73	2	6.1	3.7
	1.30	3	5.4	3.4
	1.12	2	5.5	4.4
	0.672	4	5.1	0.8
	.421	2	4.4	2.5
	.290	3	3.4	5.7
Methanol	2.30	2	8.5	4.3
	1.42	2	8.0	3.8
	1.00	1	5.4	...
	1.00	2	6.3[a]	4.3

[a] At 0° with ice jacket around column.

TABLE II

ADSORPTION FROM AQUEOUS SOLUTION

Temp. 20–27°, 536 g. copper, *p*H 3.5

C_{CuSO_4}, M	No. of expt.	Moles ads./g. Cu $\times 10^{10}$ Min.	Max.	Av. dev., %
7.52×10^{-4}	3	180	190	4.3
1.30×10^{-4}	2	48	52	10
7.71×10^{-5}	2	33	36	7.3
3.41×10^{-5}	3	17	19	2.1
1.45×10^{-5}	2	5.2	6.2	12
7.31×10^{-6}	2	2.5	3.0	5.3
5.25×10^{-6}	3	1.3	1.6	7.2

Adsorption on Silver.—From aqueous solutions the adsorption on silver was similar, in moles per gram, to the adsorption on copper. Much more copper salt was retained from methanol, and most of the experiments were done with solutions of $CuSO_4 \cdot 5H_2O$ in methanol. Addition of the same amount of sulfuric acid that was used in the aqueous solutions had little or no effect, so the solutions reported were not acidified. It was found that in successive runs the retention of copper decreased; for example, from 2.27×10^{-3} M solution the adsorption per g. silver in four runs was 44, 37, 31, 30×10^{-8} mole. A small amount of copper was so firmly retained that it could not be washed out with water or methanol; it was displaced by passing silver nitrate solution through the column, and about 10^{-8} g. atom was recovered in this way in each of three runs. Thereafter, the column was washed with water, with silver nitrate and again with water before drying and heating in hydrogen; agreement was then found in successive runs.

(7) C. W. Davies, *J. Chem. Soc.*, **140**, 2093 (1938).

(8) M. J. N. Pourbaix, "Thermodynamics of Dilute Aqueous Solutions," Edward Arnold and Co., London, 1949, Chap. VI.

(9) F. Fenwick, *J. Am. Chem. Soc.*, **48**, 860 (1926).

(10) E. Heinerth, *Z. Elektrochem.*, **37**, 61 (1931).

(11) S. E. S. El Wakkad, *J. Chem. Soc.*, 3563 (1950).

(12) T. N. Rhodin, *J. Am. Chem. Soc.*, **72**, 4343 (1950).

Table III summarizes these experiments. More dilute solutions were not used because the amount of copper-free effluent would be so large; at the lowest concentration over 50 ml. had to be collected to reach the initial concentration.

TABLE III

ADSORPTION OF COPPER SULFATE AND METHANOL SOLUTIONS

Temp. 20–27°, 96 g. silver, two runs each concentration.

C_{CuSO_4}, M	Moles ads./g. Ag $\times 10^8$	Av. dev. %
1.99×10^{-2}	69	6.1
1.07×10^{-2}	59	8.6
4.80×10^{-3}	53	9.4
2.29×10^{-3}	43	2.8
8.92×10^{-4}	36	8.5
6.33×10^{-4}	31	13
1.17×10^{-2}	63[a]	5.0
3.07×10^{-3}	50[b]	8.0
1.69×10^{-2}	4.0[b]	...

[a] At 0°. [b] From aqueous solution, *p*H 3.5.

Discussion

The data of Tables I and III show fair agreement with Freundlich isotherms; *i.e.*, the points fall reasonably close to straight lines on log-log plots. The data of Table II deviate widely from such a plot. It can be seen in Table II that the amount of adsorption falls off rapidly at low concentrations; actually, the volume of copper-deficient effluent went through a maximum at 3.4×10^{-5} M, and the decrease at lower concentrations was not entirely due to the increased total copper content of the equilibrium solution. Possibly copper(I) ion is adsorbed to a smaller extent than copper(II), but it is probable that no adsorption at all would occur at approximately 10^{-6} M total copper ion. This situation has been found in the silver–silver ion system at 10^{-5} M,[13] and is in accord with the theory of electrode potentials.

If the data of Table I are plotted as reciprocal of amount adsorbed *vs.* reciprocal of concentration (Langmuir isotherm), there is again reasonable agreement with a straight line, but no assurance that results at still higher concentrations would not deviate from this line. Extrapolation to $1/c = 0$ gives about 7.8×10^{-8} g. atoms copper ion per g. copper as a limiting value.

The true surface area of the copper cannot be estimated accurately, but an approximation can be made. The roughness factor probably lies between 3 and 5. Some of the surface must have been inaccessible to solution; on dismantling the columns, the pellets were found to be partly sintered or cemented together. A reasonable estimate of the effective area should be from 500 to 750 cm.^{2}/g. This would give 1.0 to 1.6×10^{-10} g. atoms/cm.^{2} as the maximum adsorption.

The amount of adsorption is then always far less than the equivalent of a monolayer, which would be near 25×10^{-10} g. atoms/cm.^{2} (based on the reticular density of (100) planes in the copper crystal). On the other hand, the amount of adsorbed copper(II) ion necessary to charge the electrical double layer, if considered in the simple Helmholtz sense, would be only 1×10^{-11} g. atoms/cm.^{2} per 0.1 volt. The potential difference at the interface probably does not exceed 0.2 volt.

The results of the adsorption from methanol on silver (Table III) do not lie on a straight line when plotted as reciprocals, but a rough extrapolation to $1/c = 0$ leads to a saturation value of about 8×10^{-7} mole per g. silver. Taking the area as 500 cm.^{2}/g., the maximum adsorption is 16×10^{-10} mole/cm.^{2}, a value not much smaller than was found for silver salts on silver from aqueous solutions.[5]

Rudberg and v. Euler[14] found little difference in the amount of silver nitrate adsorbed on silver from water and from 96% alcohol. There is no great difference in the amount of copper sulfate adsorbed on copper from water or from methanol, as seen in Table I. The adsorption on silver is some 12 to 15 times as great from methanol, and at least part of the copper is very firmly bound, as evidenced by the difficulty in removing it. It was thought possible that some exchange took place, but silver ion could not be detected in the effluent solution.

The few experiments at 0° do not indicate a much greater temperature effect than the experimental error. Rudberg and v. Euler found little effect of temperature with silver nitrate on gold, but King and Schochet[5] found that much larger amounts might be adsorbed on silver at 0°.

(13) M. Proskurnin and A. Frumkin, *Z. physik. Chem.*, **A155**, 29 (1931).

(14) E. G. Rudberg and H. v. Euler, *Z. Physik*, **13**, 275 (1923).

EQUILIBRIUM STUDIES OF SOME MONOVALENT IONS ON DOWEX 50

BY OSCAR D. BONNER AND WILLIAM H. PAYNE[1,2]

Department of Chemistry of the University of South Carolina, Columbia, S. C.

Received July 17, 1953

Equilibrium studies involving lithium, hydrogen, sodium, ammonium, potassium and silver ions on a Dowex 50 resin of approximately 8% divinylbenzene content have been made while maintaining a constant ionic strength of approximately 0.1 *M*. A quantitative relationship between the selectivity and maximum water uptake of the resin is shown.

Introduction

One of the principal limitations in any attempt to explain the ion-exchange process is a lack of data on characterized resins. The resin used for these exchange reactions was therefore characterized as to capacity in the dry hydrogen form (5.10 meq. per gram) and as to maximum water uptake in the various ionic forms.

Equilibrium studies of the silver–sodium, silver–hydrogen and sodium–hydrogen exchanges on several Dowex 50 resins have been reported previously.[3,4] Eight additional exchange reactions on approximately 8% DVB Dowex 50 involving six monovalent ions are now completed. These data make possible the establishment of quantitative selectivity scale for these ions on this resin. It appears, however, that a completely satisfactory theoretical interpretation of these results is not possible at this time. Perhaps future studies of the osmotic properties of concentrated solutions of electrolytes in water or in mixed solvents will furnish the information necessary for such an interpretation.

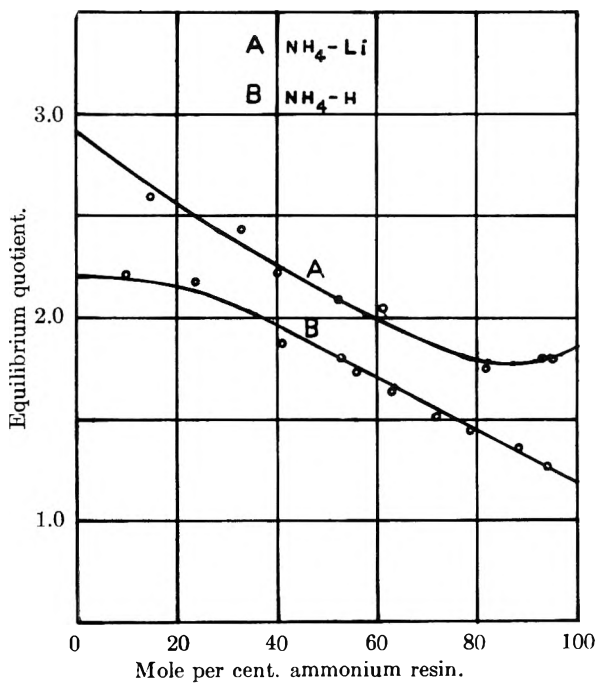

Fig. 1.

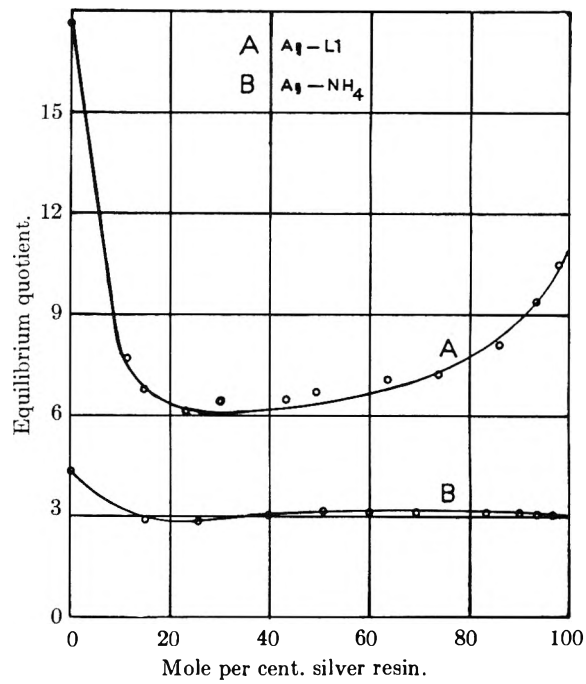

Fig. 2.

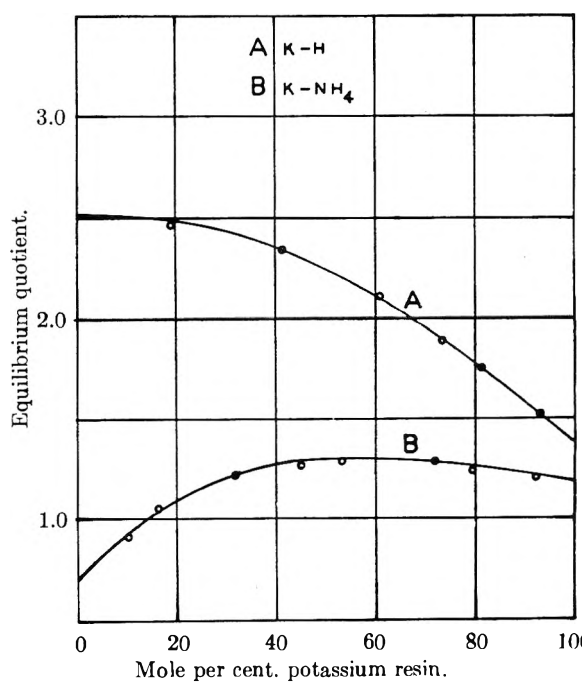

Fig. 3.

(1) Part of the work described herein was included in a thesis submitted by William H. Payne to the University of South Carolina in partial fulfillment of the requirements for the degree of Master of Science.

(2) These results were developed under a project sponsored by the United States Atomic Energy Commission.

(3) O. D. Bonner, W. J. Argersinger and A. W. Davidson, *J. Am. Chem. Soc.*, **74**, 1044 (1952).

(4) O. D. Bonner and Vickers Rhett, THIS JOURNAL, **57**, 254 (1953).

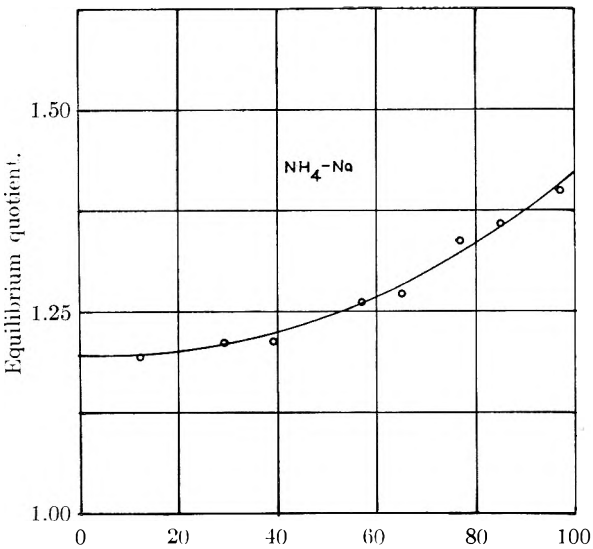

Fig. 4

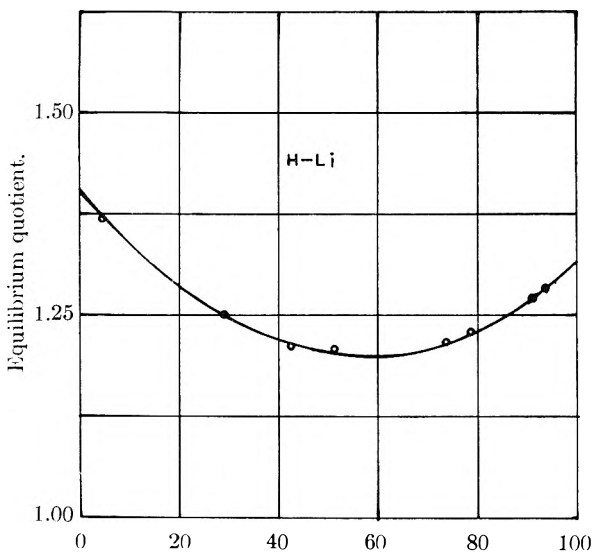

Fig. 5.

Experimental and Results

The methods of equilibration, separation and analysis used in this work were identical with those reported previously.[4] Hydrogen, ammonium and silver ion concentrations were determined volumetrically, and lithium, sodium and potassium ion concentrations were determined spectrophotometrically with a Beckman DU flame photometer except when radioactive methods of analysis were used. The aqueous solution concentration was approximately constant at about 0.1M, and the samples were maintained at a temperature of 25 ± 0.5° during the equilibration period.

The results of these exchanges are presented graphically in Figs. 1–5. The complexities of ion-exchange equilibria are illustrated by the slopes of equilibrium quotient–resin composition curves. No explanation is at present forthcoming for the different types of behavior which are exhibited.

TABLE I

TABLE OF EQUILIBRIUM CONSTANTS

Exchange system	K_{exp}	K_{calcd}	
Ammonium–hydrogen	1.76	1.72[b]	1.85[c]
Hydrogen–lithium	1.26	1.23[d]	1.32[e]
Ammonium–lithium	2.17	2.22[f]	2.45[g]
Ammonium–sodium	1.26	1.18[h]	1.23[i]
Potassium–ammonium	1.17	1.19[j]	
Silver–lithium	7.74		
Silver–ammonium	3.16		
Potassium–hydrogen	2.09		
Silver–hydrogen[a]	5.84		
Silver–sodium[a]	3.89		
Sodium–hydrogen[a]	1.49		

[a] Previously reported.[4] [b] From NH_4–Li and H–Li exchanges. [c] From Ag–NH_4 and Ag–H exchanges. [d] From NH_4–Li and NH_4–H exchanges. [e] From Ag–Li and Ag–H exchanges. [f] From H–Li and NH_4–H exchanges. [g] From Ag–Li and Ag–NH_4 exchanges. [h] From NH_4–H and Na–H exchanges. [i] From Ag–NH_4 and Ag–Na exchanges. [j] From K–H and NH_4–H exchanges.

It is of interest to note that for these exchanges there was no reversal of selectivity such as occurred in the sodium–hydrogen exchange[4] on 16% DVB resin. It appears, however, that such a reversal might occur on a higher cross-linked resin in the ammonium–hydrogen or ammonium–lithium systems.

The true thermodynamic equilibrium constants, calculated[3] from the equation $\log K = \int_0^1 \log k \, dN$ are given in Table I. In these calculations it is assumed that the activity coefficients of these uni-univalent electrolytes in 0.1M aqueous solution are approximately equal. Hence k is merely the equilibrium quotient at any resin composition. The reasonable agreement of the experimental equilibrium constants with those calculated from other exchanges appears to justify the application of the mass action law to ion-exchange equilibria.

It may also be observed that there is a relationship between the affinity of the resin for each of these ions, relative to the affinity for the lithium ion taken as unity, and the maximum water uptake of the resin in that ionic form. This semi-logarithmic relationship is shown in Fig. 6. This relative affin-

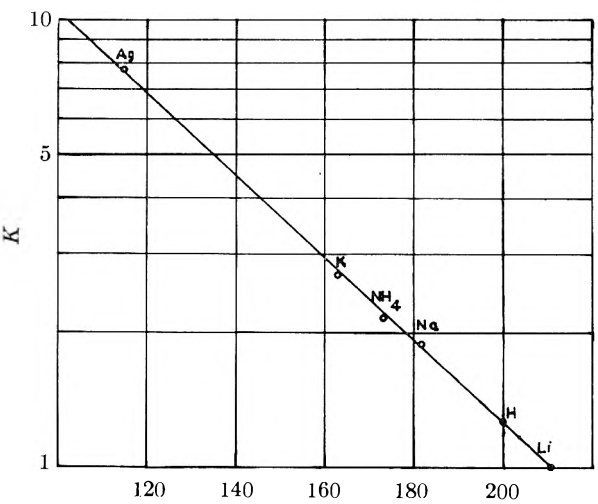

Fig. 6.

ity of the resin for these ions in effect establishes a quantitative selectivity scale for these monovalent ions on a resin of this cross-linkage. The selectivity will, of course, be different for resins of varying divinylbenzene content. It has been shown,[4] however, for the sodium–hydrogen system, that the selectivity may be calculated when the maximum water uptake is known, and it is expected that similar calculations will be possible for other systems.

STUDIES IN MOLECULAR ORBITAL THEORY OF VALENCE. III. MULTIPLE BONDS INVOLVING d-ORBITALS[1]

By H. H. Jaffé

Venereal Disease Experimental Laboratory, U. S. Public Health Service, School of Public Health, University of North Carolina, Chapel Hill, North Carolina

Received August 6, 1953

Multiple bonding involving both valence and penultimate electron shell d-orbitals has long been postulated. This paper discusses the construction of molecular orbitals for such multiple bonds from combination of $d\pi$- and hybrid $dp\pi$-orbitals with $p\pi$- and $d\pi$-orbitals, and from $d\delta$- with $d\delta$-orbitals, and illustrates the resulting MO's graphically. The symmetry and directional properties of d-orbitals are used to discuss conjugation by such multiple bonds of several radicals attached to a central atom in several geometric arrangements. Square planar and octahedral central atoms are found to permit conjugation of four and six radicals, respectively. Tetrahedral central atoms on the other hand are seen to permit conjugation only at the expense of appreciable multiple bonding energy. Hence it is concluded that unequal radicals will enter into effective competition for the d-orbitals of the central atom. This conclusion explains the apparently contradictory findings in attempts to demonstrate conjugation in compounds such as sulfones. Finally it is concluded that multiple bonding involving valence shell d-orbitals can be important only if the central atom carries a positive charge in the single bonded structures.

Introduction

Double bonds involving d-orbitals have long been postulated.[2,3] In the complex compounds and ions of the transition metals, double bonded structures involving the partially filled d-orbitals of the penultimate electron shell[4] have been suggested.[2,3] Furthermore, expansion of the valence shell beyond the octet, with formation of multiple bonds, has been proposed for the oxy-compounds and halides of sulfur, oxygen and silicon.[2] For the complexes of platinum(II) chlorides with the trihalides and trialkyls of phosphorus, Chatt has recently postulated double bonds formed by use of penultimate d-orbitals of platinum and *n*d-orbitals[4] of phosphorus.[5] Resonance with structures having double bonds involving d-orbitals also occurs in aromatic metalloörganic compounds,[6] and probably in heterocyclic compounds of sulfur.[7,8]

Originally double bonds using d-orbitals were proposed in order to explain abnormally short bond distances,[2,3] and further evidence for the existence of bonds involving $(n-1)$d-orbitals[4] is plentiful.[5,9] However, the existence of double bonds involving *n*d-orbitals has been subject to controversy.[10,11]

Kimball has derived, from group theory, the number of d-orbitals of correct symmetry for multiple bond formation for most common states of hybridization.[12] However, he has considered neither the directional properties of the orbitals involved, nor the possibilities of conjugation of several groups. Multiple bonding and conjugation have been considered on the basis of non-localized molecular orbitals for a few specific compounds[11,13,14]; however, such arguments are difficult to generalize, since they depend strongly on the symmetry properties of the specific compounds involved.

The present paper is concerned with an examination of the symmetry and directional properties of d-orbitals, and their relation to multiple bond formation and conjugation. The discussion will be based on molecular orbital (MO) theory. In the framework of this theory a multiple bond is described as arising from the superposition of a single bond (σ-bond) having local cylindrical symmetry around the bond axis, and one or more π-bonds arising from the interaction of π-orbitals of the bonded atoms. The π-bonding MO's are characterized by nodal planes which contain the σ-bond axis. In almost all cases previously treated by MO theory the

(1) Presented before the Division of Physical and Inorganic Chemistry, at the 122nd Meeting of the American Chemical Society, Atlantic City, N. J., September, 1952. For paper II of this series see *J. Chem. Phys.*, **21**, 1618 (1953).

(2) L. Pauling, "The Nature of the Chemical Bond," 2nd ed., Cornell University Press, Ithaca, N. Y., 1944, Chapter VII.

(3) Y. K. Syrkin and M. E. Dyatkina, "Structure of Molecules and the Chemical Bond," translated and revised by M. A. Partridge and D. O. Jordan, Interscience Publishers, Inc., New York, 1950, Chapter 14.

(4) For convenience we shall denote the orbitals of the valence shell by *ns*, *np*, *nd* and the d-orbitals of the penultimate electron shell by $(n-1)$d.

(5) J. Chatt and A. A. Williams, *J. Chem. Soc.*, 3061 (1951); J. Chatt and R. G. Wilkins, *ibid.*, 273 (1952).

(6) A detailed investigation of the importance of such resonance in metalloörganic compounds will be the subject of a later paper.

(7) H. C. Longuet-Higgins, *Trans. Faraday Soc.*, **45**, 173 (1949).

(8) V. Schomaker and L. Pauling, *J. Am. Chem. Soc.*, **61**, 1769 (1939).

(9) See *e.g.*, H. H. Coerver, P. A. McCusker and C. Curran, Abstracts 121st ACS Meeting, Buffalo, N. Y., March 1952, p. 7N; E. O. Brimm and M. A. Lynch, Jr., *ibid.*, p. 38N; J. Owen and R. W. H. Stevens, *Nature*, **171**, 836 (1953).

(10) E.g., A. F. Wells, *J. Chem. Soc.*, **55** (1949) and references cited there.

(11) For sulfur–oxygen bonds, *cf.* also W. Moffitt, *Proc. Roy. Soc. (London)*, **A200**, 409 (1950).

(12) G. E. Kimball, *J. Chem. Phys.*, **8**, 188 (1940).

(13) H. P. Koch and W. Moffitt, *Trans. Faraday Soc.*, **47**, 7 (1951).

(14) M. Wolfsberg and L. Helmholz, *J. Chem. Phys.*, **20**, 837 (1952).

π-orbitals were p-orbitals, which have cylindrical symmetry around an axis normal to the nodal plane, and hence all directions parallel to this plane are equivalent.

An extension of this description of multiple bonds to those formed from d-orbitals requires a knowledge of the symmetry and directional properties of these orbitals. These properties may be inferred from the equations[15]

$$\begin{aligned} d_1 &= (5/4)^{1/2} f(r)\,(3\cos^2\theta - 1) = d_z \\ d_2 &= (15)^{1/2} f(r)\sin\theta\cos\theta\cos\phi = d_{x+z} \\ d_3 &= (15)^{1/2} f(r)\sin\theta\cos\theta\sin\phi = d_{y+z} \\ d_4 &= (15/4)^{1/2} f(r)\sin^2\theta\sin 2\phi = d_{x+y} \\ d_5 &= (15/4)^{1/2} f(r)\sin^2\theta\cos 2\phi = d_{xy} \end{aligned} \qquad (1)$$

The $f(r)$ in these equations are the radial parts of the orbitals, which will not be considered further except in numerical evaluation of overlap integrals. θ and ϕ are the usual polar angles.

The angular dependence of these orbitals is well known.[16] It can be seen from equation 1 that the orbitals d_2 to d_5, are equivalent except for orientation with respect to each other. The vectors of maximum intensity of these orbitals define three mutually normal planes, one of which contains two orbitals which form angles of 45° between their maximum intensity vectors. The orbital d_z will not concern us much, since it has a form which makes it useful in multiple bonding only in special cases.

The Molecular Orbitals

The Isolated Multiple Bond.—We shall now consider a multiple bond between two atoms M and A. M is the central atom of a molecule, and is bonded to a number of atoms by a skeleton of σ-bonds. Although not necessarily orthogonal to the multiple bonding MO's, the σ-bonding MO's may be assumed to have sufficiently low energy that interaction between the two types of MO's can be neglected in the first approximation. We will further make the assumptions: (1) multiple bonding need be considered only between M and a single atom A; (2) M has five d-orbitals, and A has two p-orbitals available for such bonding. If MA is taken as the z-axis, orbitals d_{x+z} and d_{y+z} of M have the same symmetry as orbitals p_x and p_y of A, respectively, and the interaction of these orbitals leads to bonding MO's.[17] Such MO's are shown in Fig. 1,[18] where it is seen that overlap is more efficient if the σ-bond MA lies not only in the common nodal plane of a given pair of orbitals, but also in the plane defined by the vectors of maximum intensity of the d-orbitals. Hence, the directional properties of the d-orbitals are important, and for this reason we propose to call bonding by such MO's dπ-bonding, to distinguish it from π-bonding by p-orbitals, where the directional properties of the p-orbitals are of no importance.

In case the central atom M is not utilizing its valence shell p_x- or p_y-orbital in the formation of the σ-bond skeleton, such p-orbitals may be hybridized with the orbitals d_2 or d_3 to form orbitals of the form

$$X = \sin\beta\, p_x + \cos\beta\, d_2 \qquad (2)$$

Such hybrid orbitals of M may also interact with the p-orbitals of A and lead to MO's of the type shown in Fig. 2. In general the hybrid dp-orbitals will give rise to stronger dπ-bonding than either pure p- or d-orbitals.

If the atom A also has dπ-orbitals available for bonding, further possibilities need be considered. Thus orbitals d_2 and d_3 of M can interact with the corresponding orbitals of A, leading to dπ-bonding orbitals of the type shown in Fig. 3. The d-orbitals of A also may be hybridized with p-orbitals, and hence various MO's analogous to those of Fig. 2, but formed from a dp-hybrid orbital and a d-orbital or from two dp-hybrid orbitals are possible. Further, orbitals d_4 and d_5 of M also interact with the corresponding orbitals of A; the resulting MO's, which have two nodal planes containing the σ-bond, are illustrated in Fig. 4. Bonding from such orbitals will be referred to as δ-bonding, to indicate the symmetry properties of the MO. Although in δ-

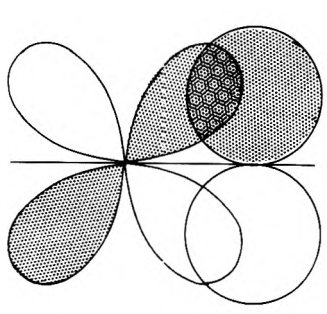

Fig. 1.—dπ-Bonding MO formed from a d- and a p-orbital.

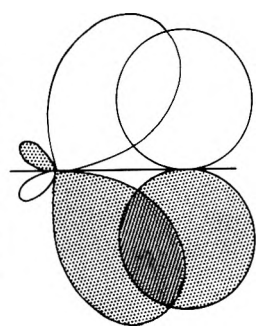

Fig. 2.—dπ-Bonding MO formed from a dp hybrid orbital and a p-orbital.

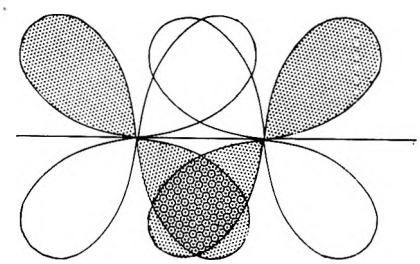

Fig. 3.—dπ-Bonding MO formed from two d-orbitals.

(15) L. Pauling, *J. Am. Chem. Soc.*, **53**, 1367 (1931).

(16) J. C. Slater, "Quantum Theory of Matter," McGraw-Hill Book Co., Inc. New York, N. Y., 1951, p. 119.

(17) This statement assumes that orbitals d_{x+z} and d_{y+z} are not involved in σ-bonding. This assumption is undoubtedly a good approximation if we are dealing with nd orbitals and is strictly valid for $(n-1)$d-orbitals in molecules with the central atom in dsp^2 or d^2sp^3 hybridization. In dealing with $(n-1)$d-orbitals in molecules where the central atom is in different states of hybridization, the partial involvement of the orbitals d_{x+z} and d_{y+z} in σ-bonding makes them less available for multiple bonding, and must be considered specifically for each type of hybridization. I am grateful to one of the referees for pointing out this fact.

(18) All orbitals are drawn to scale. The shaded areas correspond to negative values of the wave function, the unshaded areas to positive values. Since the figures in this paper represent only the angular part of the wave functions, too much significance should not be attached to the relative magnitudes of the overlapping areas; the overlap integrals, which represent the magnitude of the overlap quantitatively, depend strongly on the radial factor of the wave function, and on the effective nuclear charges and bond distances involved, and hence vary greatly from compound to compound. A few typical overlap integrals are tabulated in a later section of this paper. The orbitals are drawn assuming A to be a single atom; the extension to polyatomic groups A involves no complications.

bonding the directional properties of the d-orbitals do not appear as favorable as in dπ-bonding, the overlap of four instead of two lobes of the orbitals is a compensating factor. The relative importance of the two types of bonding may be inferred from the respective overlap integrals (*cf.* below).

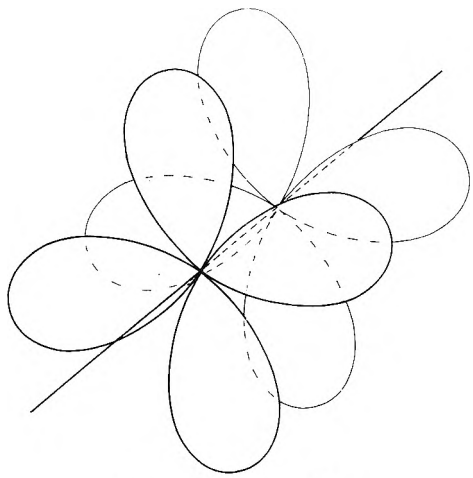

Fig. 4.—δ-Bonding MO.

The maximum order of multiple bonds formed by dπ- and δ-bonding is as follows: The use of two d-orbitals of M and two p-orbitals of A may lead to two dπ-bonds, so that MA may be triple, or partially triple, bonded. Further, use of d-orbitals of both M and A can give rise to a σ-, two dπ- and two δ-bonds. However, it may be anticipated that such strong multiple bonding will rarely be encountered. Thus if M and A are different elements, their orbitals will usually enter the MO's with different weights, and each bonding MO will give rise only to a fractional bond. Only if the energies of all interacting atomic orbitals are equal, and all are singly filled, can the bonding properties of the MO's be fully utilized.

Central Atoms in dsp^2 and d^2sp^3 Hybridization.—Having derived the MO's which can lead to an isolated multiple bond along a σ-bond MA, we shall now examine the possibilities of formation of more than one multiple bond around a single atom M, and of the conjugation of several groups bonded to M. The results of such a discussion depend strongly on the geometry of the σ-bond skeleton and the hybridization of M. The discussion is simplest if all the σ-bonds of the molecule are at right angles, and hence we shall deal first with square planar and octahedral molecules (M in dsp^2 or d^2sp^3 states of hybridization, respectively).

Assume an octahedral molecule MA_6, with orbitals d_2, d_3 and d_4 of M, and two p-orbitals of each A available for multiple bonding. Each of the d-orbitals can interact with one p-orbital from each of four A's to form a MO of the type shown in Fig. 5.[19]

(19) Combination of these five atomic orbitals of course gives rise to five MO's. The figures throughout this paper represent only the MO of lowest energy. In the case under discussion this is the only bonding MO, the next three being non-bonding, and the last anti-bonding. Therefore, the conclusions are essentially independent—except for electronic repulsion terms—of the number of electrons to be assigned to this set of MO's, as long as there are at least 2, and no more than 8, such electrons.

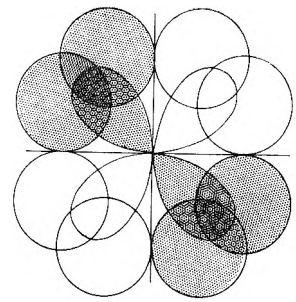

Fig. 5.—Conjugating dπ-bonding MO.

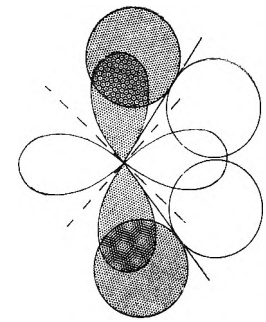

Fig. 6.—The orbital wa_1 (*cf.* text).

Hence three such MO's are formed in mutually normal planes, and each MO leads to conjugation of four of the six A's. Accordingly, each MA bond may have partial triple bond character. This conclusion is equally valid whether the A's are single atoms or radicals, such as —C≡N, as long as each has two π-orbitals available. If the A's are not all equal, the MO's constructed remain unchanged, except that the atomic orbitals of the different A's enter the MO's with different coefficients. Use of pd-hybrid orbitals (*cf.* Fig. 2) is not possible since the p-orbitals of M are used in σ-bonding. In the case under discussion the multiple bonding MO's are orthogonal to the σ-bonding MO's, and hence no interaction with these orbitals occurs.

If the A's have d-orbitals instead of p-orbitals (or both) available for bonding, the MO's of Fig. 5 are replaced by analogous orbitals made up of individual sections resembling Fig. 3. The MO's of Fig. 5 can further interact with d_3-orbitals of the A's above and below their plane, leading to appreciable δ-bonding, and thus may conjugate all six A's.

The above discussion can readily be extended to square planar molecules of the type MA_4 (M hybridized dsp^2). One MO identical to the one shown in Fig. 5 can be constructed in the plane of the molecule, and two others normal to this plane involve only two A's each (but two further A's by δ-bonding if the d-orbitals are available in the A's). Since the p-orbital of M normal to the plane of the molecule is not utilized in σ-bonding, it is available for multiple bonding in these compounds. If all four A's are equal, this p-orbital gives rise to a conventional π MO by overlap with the p-orbitals of the four A's. However, in compounds MA_2B_2, where A has a greater tendency for the multiple bonding than B, the availability of this p-orbital permits an interpretation of the *trans* effect.[5,20] In *trans*-MA_2B_2, the A's are bonded by a dπ-orbital in the plane of the molecule, a dπ-orbital normal to this plane, and a π-orbital. In *cis*-MA_2B_2, however, one can construct the same dπ-orbital in the molecular plane, and two dπ-orbitals normal to the plane. One of these involves a d-orbital of M, the other a dp-hybrid orbital. Since it is possible to adjust the degree of hybridization of this hybrid orbital (by adjustment of the parameter β of equation 2), the double bonding may utilize the optimum amount of p-character; the remainder of the p-character is assigned to an orbital not involved in bonding, or in weaker multiple bonding with the

(20) I. I. Chernyaev, *Ann. inst. platine*, **5**, 118 (1927).

B's. Consequently the bonding MO's in the *cis*-compound have lower energy than the corresponding MO's in the *trans*-compound, and the *cis*-compound is more stable.

It has long been accepted that one of the main factors determining the strengths of chemical bonds is the magnitude of the overlap integrals of the orbitals which interact to form the bonding MO. The MO's leading to $d\pi$- and δ-bonding around dsp^2- and d^2sp^3-hybridized central atoms involve as efficient overlap as the corresponding MO's derived above for isolated multiple bonds. Hence it may be concluded that in square planar and in octahedral molecules each potentially double bonding atom or group A contributes equally to the conjugation in the molecule, independent of the number of A's present.

Tetrahedral Central Atoms.—A discussion of multiple bonds involving d-orbitals formed by a tetrahedral central atom (M hybridized sp^3 or $sp^{3-x}d^x$) is considerably more difficult for several reasons: (1) Since the bond angles are in the neighborhood of 109°, a d-orbital of M appropriately oriented for maximum interaction with a π-orbital of one atom A will not be so oriented with respect to any other A atom. Hence (2) the appropriate orientation of d-orbitals of M for maximum interaction with several atoms A will depend strongly on the number n of such atoms. (3) Since the interaction with n atoms is possible only for orientation of d-orbitals not leading to maximum interaction with any one A, the degree of interaction will also greatly depend on n. (4) The d-orbitals of M are not orthogonal to the σ-bonding orbitals, and hence interaction of single bonding and multiple bonding orbitals may be important. This last factor is the more important the larger n.

In the following paragraphs the compounds MA_2B_2 and MA_4 (where A but not B has orbitals available for multiple bonding) will be discussed separately. The case of MAB_3 corresponds to the isolated multiple bond discussed above, and requires no further comment.

Compounds of the type MA_2B_2 have been discussed, for the special case of sulfones, by Moffitt,[11] who constructed two multiple bonding MO's, (xb_1)[21] and (va_2) by his notation. Using the internal and external bisectors of the angle AMA as x- and y-axis, respectively, these orbitals correspond to interaction of orbitals d_{x+y} and d_{y+z} of M with p_z of the A's. To the extent that the d-orbitals of M are involved in σ-bonding (expressed by x in $sp^{3-x}d^x$ hybridization), p-orbitals are released and may contribute to multiple bonding. Interaction of the p_z-orbital of M with p_z-orbitals of A's lowers the energy of (xb_1) in which it can participate, but simultaneously renders (va_2) more nearly non-bonding, and hence does not appreciably affect the general argument.

However, Moffitt's statement that A orbitals, described as (wa_1), (*i.e.*, the p-orbitals of A in the xy-plane not involved in σ-bonding) cannot be involved in multiple bonding[11] is incorrect. Although their nodes do not coincide with those of the orbital d_{x+y} of M, they interact strongly with this orbital. The MO formed by this interaction is shown in Fig. 6. The orbital (wb_2) slightly interacts with both orbitals d_{x+y} and d_{xy}; however, overlap integrals for this interaction must be very small, and hence (wb_2) may be considered as non-bonding orbital on the A atoms, in agreement with Moffitt.

Since the orbitals (xb_1), (va_2) and (wa_1) involve interaction of d-orbitals of M with p-orbitals of the A's, it is possible to compare directly group overlap integrals, and hence arrive at conclusions concerning the relative importance of the various orbitals. Table I expresses these group overlap integrals in terms of the maximum overlap integral of a $d\pi$- and a $p\pi$-orbital in the situation described as an isolated double bond. The group overlap integrals for the compound MA_2B_2 (M hybridized sp^2d) with valence angles 90° is included for comparison. The orbital (wa_1) is seen to be more important than either (xb_1) or (va_2), and all of the integrals for the tetrahedral compounds are somewhat smaller than the maximum value for MA double bonding in the square and octahedral compounds.

Koch and Moffitt[13] have considered the conjugation of π-orbitals of the two R groups in the xz-plane of sulfones (R_2SO_2) with the orbitals discussed in the last section (xb_1 and va_2). Unfortunately, the orbitals were constructed from considerations involving symmetry classifications of the sulfones by group theory only, without special consideration of the form of the atomic orbitals involved in their formation. This origin of the MO's in Figs. 1–3 of reference 13 explains that these orbitals have nodal planes only in the direction of the twofold axis of symmetry of the sulfone molecule. Inspection of the MO's shown in this paper indicates that MO's built up from d-orbitals require two nodal planes, and therefore that Koch and Moffitt's orbitals (other than the one of symmetry a_2) must have nodal planes normal to the twofold axis. These nodal planes are omitted from their Fig 3 and this omission raises doubt as to the extent of the possible "b_1- and a_1-overlap," since inclusion of such nodal planes must lead to an extensive cancellation of overlap. Further, the orbital (wa_1) permits no conjugation.

The case of compounds of the type MA_4 has been treated by Wolfsberg and Helmholz[14] for the anions MO_4^{-n}, with M = Mn, Cr and Cl. The MO's which they derived include five which may be called $d\pi$-bonding. In MnO_4^- these orbitals appear as the least strongly bonding MO's, however, in $CrO_4^=$ two of them (1e in the notation of reference 14) are the most stable orbitals of the molecule. It is of particular interest that in the case of the molecule MA_4 interaction between σ-bonding and multiple bonding MO's appears to be very important, and separation of the σ-bonding and $d\pi$-bonding MO's of the class T_2 is impossible. Also, there is appreciable mixing of the p- and d-orbitals of the central atom, so that multiple bonding by p- and d-orbitals cannot be readily distinguished.

Overlap Integrals

The strength of a chemical bond appears to be closely related to the overlap integrals (OI) which

(21) There appears to be a mistake in the assignment of the symmetry symbols of Table V of reference 11: the symbols b_1 and b_2 appear to be reversed, either in the text or in the table.

are associated with the corresponding MO[22]; hence a knowledge of the magnitude of the OI's associated with the MO's discussed in the preceding sections was considered of interest, since it might assist in an estimation of the importance of this type binding. Relative OI's have been tabulated in Table I for several of the more important orbitals. Formulas and tables of the OI's have been reported recently for a variety of values of the

TABLE I

RELATIVE OVERLAP INTEGRALS FOR VARIOUS TYPES OF MOLECULES

Compound	Configuration	Orbitals	Overlap integral[a]
MA_2B_2	Tetrahedral	xb_1[b]	$(2/3)^{1/2}S$
		va_2[b]	$(4/(3)^{1/2}S$
		wa_1[b]	$4/3S$
	Square or octahedral		$(2)^{1/2}S$
MA_4	Tetrahedral	E or T_2[c]	$2(2/3)^{1/2}S$
	Square or octahedral		$2S$

[a] The overlap integrals are given in terms of the corresponding integral $S(Md\pi, A\pi)$ for the isolated MA bond. [b] The notation is that of reference 11. [c] The notation is that of reference 14.

parameters ρ and τ, which depend on the effective nuclear charges and interatomic distances.[23] Numerical values for a number of important cases are given in Table II. The integrals in this table are of similar order of magnitude as the $2p\pi C$-$2p\pi C$ OI ($S \sim 0.27$), which gives rise to the familiar carbon–carbon double bonds of organic chemistry: in some cases the OI's of Table II are even appreciably larger than the carbon–carbon integrals.

TABLE II

NUMERICAL VALUES FOR SOME TYPICAL OVERLAP INTEGRALS

Compound	Bond A–B[a]	μ_A[b]	μ_B[b]	R[c]	S[d]	S[e]
SiF_4	F–Si	2.61	0.77	1.54	0.20	
$SiCl_4$	Cl–Si	2.036	0.35	2.00	.15	
SiO_4^{4-}	O–Si	2.03	0.55	1.62	.20	
$PO_4^{=}$	O–P	2.04	0.76	1.55	.28	
R_3PO	O–P	2.04	0.49	1.55	.16	
	C–P	1.625	0.49	1.87	.22	
$SO_4^{=}$	O–S	2.06	0.93	1.50	.32	
R_2SO_2	O–S	2.06	0.80	1.50	.29	
	C–S	1.625	0.80	1.81	.33	
ClO_4^-	O–Cl	2.09	1.09	1.49	.35	
$Fe(CN)_6^{4-}$	C–Fe	1.625	1.85	1.89	.20	
$Fe(CN)_6^{3-}$	C–Fe	1.625	1.97	1.88	.17	
$Ni(CN)_4^{=}$	C–Ni	1.625	2.40	1.88	.11	
	C–Ni	1.625	0.675[f]	1.88	.20[f]	
$Pt(II)$–PR_3	P–Pt	0.400	1.80	2.41	.06	0.13
$Pt(II)$–PCl_3	P–Pt	0.500	1.80	2.41	.11	.15
$Pt(II)$–PF_3	P–Pt	0.96	1.80	2.41	.30	.16

[a] Assignments A and B are made in accordance with R. S. Mulliken, C. A. Rieke, D. Orloff and H. Orloff, *J. Chem. Phys.*, **17**, 1248 (1949). [b] $\mu = Z_{eff}/n_{eff}$, *cf.* reference under footnote *a*. [c] From references 2 and 24. [d] $S(A\pi, B\pi)$. [e] $S(Ad\delta, Bd\delta)$. [f] These values refer to Ni 3p-orbitals, which may be hybridized with 3d-orbitals. S from reference in footnote *a*.

(22) R. S. Mulliken, *J. Am. Chem. Soc.*, **72**, 4403 (1950); *Record Chem. Progr. Kresge-Hooker Sci. Lib.*, **13**, 67 (1952).

(23) H. H. Jaffé, *J. Chem. Phys.*, **21**, 258 (1953). Table III in this reference contains an error; all values in this table should be multiplied by 0.9736. The author is grateful to Dr. D. P. Craig for calling attention to a discrepancy from his data, which led to the discovery of this error.

The computation of the OI's of Table II requires some comment. They are based on nodeless Slater atomic orbitals. Bond distances were taken mostly from Pauling,[2,24] or estimated from covalent radii.[25] Difficulties were encountered in the evaluation of the effective nuclear charge needed for the calculation of the parameters ρ and τ. The effective nuclear charges for a 3d-electron of the elements of the last short period of the periodic system vanish if they are calculated for the neutral atoms according to Slater's rules.[26] The fact that the central atoms in many of the compounds considered carry a formal positive charge somewhat increases the effective nuclear charges (Z_{eff}) for all the elements except silicon. However, the bonds in the compounds under consideration all are appreciably polar. The polar character of the bonds increases the formal positive charges on these atoms. Z_{eff} was calculated by taking account of the charges due to the ionic character of the σ-bonds which were evaluated following Pauling.[24] No correction for the amount of neutralization of these charges due to multiple bonding was made since quantitative information is lacking. However, such neutralization occurs by placing d-electrons near the central atom, and since electrons do not greatly shield other electrons in the same shell, the correction would not greatly effect the OI's.

The OI's for the interaction of platinum with phosphorus bound to groups of moderate electronegativity appear to be rather small. But it should be noted that these integrals are extremely sensitive to the exact values of Z_{eff} and the interatomic distances, and it appears likely that they are appreciably underestimated.

Discussion

In the preceding sections we have seen that $d\pi$-bonding MO's can be constructed and are associated with overlap integrals of sufficient magnitude to lead to appreciable bonding. One further condition must be fulfilled in order to make bonding by these MO's important: the contributing atomic orbitals must have sufficiently similar energies. It has been primarily the energy consideration which has led to the belief that expansion of valence shells is unlikely. The arguments are based on the fact that in general, 3s- and 3p-orbitals have appreciably lower energy than 3d-orbitals. However, in almost every compound where formation of multiple bonds by expansion of the valence shell is postulated, the central atom carries a formal positive charge in single bonded structures and is surrounded by atoms or groups appreciably more electronegative than itself. The positive charge of such central atoms greatly increases their electron affinity, and hence lowers the energy of nd-orbitals. The operation of this effect is well illustrated in Moffitt's calculation of the energy of the orbitals of sulfur in sulfones.[11] It was seen above that the forma. positive charge also leads to the appreciable overlap integrals of Table II. Thus the formation of multiple bonds utilizing nd-orbitals hinges on the positive charges of the atoms, and atoms without such

(24) L. Pauling, THIS JOURNAL, **66**, 361 (1952).

(25) Reference 2, Chapter V.

(26) J. C. Slater, *Phys. Rev.*, **36**, 57 (1930).

charge can be expected not to form $d\pi$-bonds. On the other hand formal positive charge and appreciable overlap integral appear to be sufficient conditions for $d\pi$-bonding. These conditions are fulfilled for ClO_4^- for which Wolfsberg and Helmholz[14] concluded that the 3d-orbitals were not appreciably involved in bonding. It seems likely that their conclusion was based on a choice of an unreasonably high energy for the 3d-orbitals of chlorine.

The use of sulfur 3d-orbitals in thiophene has been postulated by Schomaker and Pauling,[8] and by Longuet-Higgins.[7] Since the sulfur atom in thiophene is neutral in the first approximation, we might expect, in the light of the above discussion, little if any use of 3d-orbitals. Resonance structures with a positive sulfur (structures II and III of reference 8), however, appear to make an appreciable contribution to the ground state, and hence Schomaker and Pauling's estimate of 10% contribution by structures involving d-orbitals does not appear unreasonable.

The results of Longuet-Higgins,[7] on the other hand, suggest a much greater involvement of these orbitals. Unfortunately his orbitals ϕ_f and ϕ_g are not independent. Independent linear combinations analogous to ϕ_f and ϕ_g can be formed. However, if they are to satisfy the desired symmetry relations, they must be orthogonal, and hence S_{fg} vanishes. Longuet-Higgins' analogy between thiophene and benzene breaks down at this point. His conclusion that S_{fg}, S_{af}, and H_{ff} must each be very similar to the corresponding primed quantities is not essential for the subsequent agreements; the combined effect of the three primed and unprimed quantities is all that need be equal in the observed similarity of thiophene and benzene.

Much experimental evidence exists both for and against the existence of multiple bonds using nd-orbitals. Almost the only direct evidence consists in the bond lengths in the halides and the anions of the oxygen acids of Si, P, S and Cl.[2] Most other evidence depends in various ways on the demonstration of conjugation, or the lack thereof, of unsaturated organic radicals with such multiple bonds. The interpretation of such evidence has usually involved analogy with conjugation by π-bonds, and such arguments by analogy are, at least, partly invalidated by the special character of $d\pi$-bonds. The following considerations will show why such arguments by analogy break down.

(1) For conjugation to be observed, several double bonded groups must surround the central atom. In a planar organic molecule, each such group makes an independent contribution to the π-bonding conjugating MO. However, around a tetrahedral central atom M, introduction of a second $d\pi$-bonded group reduces the double bond character of the already existing $d\pi$-bond.

(2) Two unlike groups will enter into competition, with the result that the stronger $d\pi$-bonding group will approach maximum bonding at the expense of the weaker bonding group. Hence conjugation will appear greatly reduced.

(3) Most organic radicals are planar, but not linear, and hence have only a single π-orbital available for $d\pi$-bonding. Conjugation will then greatly depend on the relative orientation of these planes. Such orientation will be determined only partly by the energy gained from attainment of maximum conjugation, and largely by steric considerations and vibrational motion.

The above arguments indicate why interpretation of experimental evidence on conjugation has not led to unequivocal decisions concerning $d\pi$-bonding involving nd-orbitals. The concept of a competition for the double bonding MO's particularly explains the apparently inconsistent result that the presence or absence, or at least the degree, of conjugation appears to be a sensitive function of the electronic repelling power of the organic radicals in sulfones.[13] In the light of this discussion it must be concluded that such $d\pi$-bonding occurs frequently; the evidence to the contrary may be interpreted as being due to unfavorable competition or steric orientation.

Little doubt exists that $d\pi$-bonding involving $(n-1)$d-orbitals is important. In square planar and octahedral complexes such as the cyanides and nitroso compounds, the ideal conditions for such bonding are fulfilled. The situation in tetrahedral carbonyls also appears favorable compared to $d\pi$-bonding involving nd-orbitals.

STANDARD POTENTIALS OF SILVER–SILVER CHLORIDE CELLS IN SOME ETHANOL– AND ISOPROPYL ALCOHOL–WATER SOLUTIONS AT 25°

BY HERBERT S. HARNED AND DONALD S. ALLEN

Contribution No. 1184 from the Department of Chemistry of Yale University, New Haven, Conn.

Received August 19, 1953

From measurements of the electromotive forces of suitable cells, the standard potentials of the silver–silver chloride electrode in water–isopropyl alcohol solutions of 20 weight % isopropyl alcohol and in water–ethanol solutions of 30, 40 and 50 weight % of ethanol at 25° have been evaluated.

The standard potential of the cell

$$H_2 \,|\, HCl(m), \text{ solvent } (X), \text{ water } (Y) \,|\, AgCl\text{–}Ag$$

has been determined with high accuracy in a number of water–organic solvent solutions. Some of these results at 25° and as functions of temperature have been tabulated by Harned and Owen,[1] and include values determined in water–methanol, water–ethanol, water–isopropyl alcohol, water–glycerol and water–dioxane mixtures. More recently, measurements of equal accuracy have been obtained with ethylene glycol–water solutions containing 5 to 50% ethylene glycol by weight[2] and with *d*-fructose–water solutions containing 15 and 10% of the sugar.[3] The present communication contains results with ethanol–water and isopropyl alcohol–water solutions which supplement the data obtained by Harned and Calmon,[4] Patterson and Felsing[5] and Moore and Felsing.[6]

Experimental Results and Extrapolations

The experimental electromotive forces in absolute volts at one atmosphere hydrogen pressure and at the molalities designed are tabulated in Table I.

TABLE I

ELECTROMOTIVE FORCES OF THE CELLS: $H_2|HCl(m), S(X), H_2O(Y)|AgCl\text{–}Ag$

X = weight % of alcohol

m	E	$\gamma_\pm$	m	E	$\gamma_\pm$
(1) Isopropyl alcohol–water. X = 20			(2) Ethanol–water. X = 30		
0.005705	0.47655	0.90	0.005124	0.47694	0.899
.005899	.47518	.89	.009768	.44533	.868
.012338	.43955	.87	.016212	.42121	.840
.016786	.42472	.85	.018574	.41455	.832
.022987	.40963	.83	.029336	.39307	.812
.027627	.40066	.82	.029737	.37228	.808
.027900	.40076	.82	.045850	.37198	.772
			.053154	.36518	.761
(3) Ethanol–water. X = 40			(4) Ethanol–water X = 50		
0.006306	0.46180	0.865	0.006027	0.45659	0.836
.013185	.46625	.835	.011901	.42414	.814
.019214	.40838	.811	.021062	.39746	.774
.021231	.40382	.804	.028877	.38272	.751
.022995	.39999	.800	.051775	.35609	.704
.041587	.37323	.758	.070456	.34199	.681

As a check, two standard methods of extrapolation were carried out. The first method employed the function $E^{\circ\prime}$,[7] defined by

$$E^{\circ\prime} = E + 2k \log m - \frac{2kS_{(f)}\sqrt{c}}{1 + A'\sqrt{c}} - 2k \log (1 + 0.002M_{xy}m) = E^\circ - f(m) \quad (1)$$

in which k equals $2.3026RT/NF$, $S_{(f)}$ is the limiting slope of the Debye and Hückel theory, A' the parameter of the mean distance of approach of the ions and M_{xy} the mean molecular weight. The intercept of the plot of $E^{\circ\prime}$ *versus* m yields the standard potential of the cell E°. The second method, first used by Hitchcock,[8] is carried out by plotting the simpler function

$$E^{\circ\prime\prime} = E + 2k \log m - 2kS_{(f)}\sqrt{c} = E^\circ - f(m) \quad (2)$$

which omits the term $(1 + A'\sqrt{c})$ in equation 1, against the molality.

In Table II, the properties of the solvents and the theoretical functions employed in the calculations are recorded. Values of the fundamental physical constants recommended by Birge[9] were used in computing the values of $S_{(f)}$ and A' given in the table. The value of 4.3 Å. was employed for the computation of the mean distance of approach parameter of theory, A'. This value is in agreement with that found by Harned and Thomas[10] for 10 and 20% methanol–water solutions, by Crockford, Knight and Staton[2] for ethylene glycol–water solutions and by Harned and Ehlers[11] for pure water. The densities and vapor pressures given in the table were measured by us. Values of the dielectric constants were obtained by Akerlof.[12]

TABLE II

PROPERTIES OF SOLVENTS AT 25°

X = weight % alcohol

X	30[a]	40[a]	50[a]	20[b]
d_0	0.9507	0.9315	0.9098	0.9669
D	61.1	55.0	49.0	64.1
p(mm.)	44.0	47.3	49.7	36.5
$S_{(f)}$	0.7428	0.8683	1.033	0.6902
A'	1.603	1.688	1.788	1.564
M_{xy}	22.03	23.82	25.90	20.95

[a] Ethanol. [b] Isopropyl.

(1) H. S. Harned and B. B. Owen, "The Physical Chemistry of Electrolytic Solutions," second edition, Reinhold Publ. Corp., New York, N. Y., 1943, Table (11-3-2) p. 336, Table (15-7-1) p. 519, and Table 11-3-3A, p. 546.

(2) S. B. Knight, J. F. Masi and D. Roesel, *J. Am. Chem. Soc.*, **68**, 661 (1946); H. D. Crockford, S. B. Knight and H. A. Staton, *ibid.*, **72**, 2164 (1950).

(3) H. D. Crockford and A. A. Sakhnovsky, *ibid.*, **73**, 4177 (1951).

(4) H. S. Harned and C. Calmon, *ibid.*, **61**, 1491 (1939).

(5) A. Patterson and W. A. Felsing, *ibid.*, **64**, 1478 (1942).

(6) R. L. Moore and W. A. Felsing, *ibid.*, **69**, 1076 (1947).

(7) Reference 1, p. 332.

(8) D. I. Hitchcock, *J. Am. Chem. Soc.*, **60**, 2076 (1928).

(9) R. T. Birge, *Rev. Mod. Phys.*, **13**, 233 (1941); ref. 1, p. 586.

(10) H. S. Harned and H. C. Thomas, *ibid.*, **57**, 1666 (1935).

(11) H. S. Harned and R. W. Ehlers, *ibid.*, **55**, 2179 (1933).

(12) G. Akerlof, *ibid.*, **54**, 4125 (1932); also ref. 1, p. 118.

In carrying out the extrapolations according to equations 1 and 2, c was replaced by md_0. For low concentrations this substitution is a close approximation and in the limit it becomes exact. Large scale graphs of the functions in equations 1 and 2 were made so that the intercept could be read to the fifth decimal place. In all cases the extrapolated values of the ethyl alcohol mixtures by the two methods checked within the expected limits of the precision of the method. The maximum deviation was ±0.06 mv. The results with isopropyl alcohol were of an accuracy of the order of ±0.2 mv. As to be expected, the graphs of equation 2 had a considerable slope whereas those of equation 1 approach the limit nearly horizontally.

Standard Potentials and Activity Coefficients

The values of the standard potentials of the cell, E°_m obtained by the method described above are on the molality scale. These are recorded in Table III along with the value in pure water of Harned and Ehlers[11] and the values of Harned and Calmon[4] as indicated in the table. The standard potentials, E°_c, on the molar concentration scale, and E°_N, on the mole fraction scales, also included in the table, were computed by the equations

$$E^\circ_c = E^\circ_m + 0.1183 \log d_0 \qquad (3)$$

$$E^\circ_N = E^\circ_m + 0.1183 \log (1000/M_{xy}) \qquad (4)$$

TABLE III

STANDARD POTENTIALS AT 25° OF THE CELLS: $H_2|HCl(m), S(X), H_2O|(Y)AgCl–Ag$

Mixture	X	E°_m	E°_c	E°_N
Ethanol–H_2O	0[a]	0.22246	0.22158	0.01603
Ethanol–H_2O	10[b]	.21449	.21347	.01123
Ethanol–H_2O	20[b]	.20743	.20568	.00763
Ethanol–H_2O	30	.20033	.19773	.00424
Ethanol–H_2O	40	.19454	.19089	.00239
Ethanol–H_2O	50	.18588	.18103	−.00189
Isopropyl alcohol–H_2O	10[b]	.2137	.2127	.01095
Isopropyl alcohol–H_2O	20	.2060	.2043	.0073

[a] From Harned and Ehlers.[11] [b] From Harned and Calmon.[4]

where d_0 the density of the solvent medium and

$$M_{xy} = \frac{100}{X_1/M_1 + X_2/M_2} \qquad (5)$$

In this equation M_1 and M_2 are the molecular weights of the solvents and X_1 and X_2 are the weights of each solvent in 100 g. of solution. Values of the activity coefficients calculated by the equation

$$-\log \gamma_\pm = \frac{E - E^\circ}{0.1183} + \log m \qquad (6)$$

are given in Table I.

New Schedule

BACK ISSUE PRICES

AMERICAN CHEMICAL SOCIETY JOURNALS

Effective January 1, 1953

Single copies or complete volumes of nearly all the ACS journals listed below may be purchased at these prices.

Journal	Current Year		Back Years			
	Member	Non-Member	Member	Non-Member	Foreign Postage	Canadian Postage
AGRICULTURAL AND FOOD CHEMISTRY	$0.40	$0.50	...	...	$0.15	$0.05
ANALYTICAL CHEMISTRY	.40	.50	$0.60	$0.75	.15	.05
Analytical Edition (I&EC)						
Volumes 1–4	...	...	1.60	2.00	.15	.05
Volumes 5–8	...	...	1.00	1.25	.15	.05
Volumes 9 et seq.	...	...	.60	.75	.15	.05
CHEMICAL ABSTRACTS, Volumes 11–44						
Numbers 1–22	...	...	1.00	1.25	.15	.05
Numbers 23 and 24	...	...	2.40	3.00*	.45	.15
CHEMICAL ABSTRACTS, Vol. 45 et seq.						
Numbers 1–22	1.00**	2.00	1.60**	2.00	.15	.05
Number 23 (Author Index)	6.00**	12.00	9.60**	12.00	free	free
Number 24 (Subject, Patent, Formula Indexes, complete)	12.00**	24.00	19.20**	24.00	free	free
CHEMICAL AND ENGINEERING NEWS	.15	.15	.15	.15	.05	free
INDUSTRIAL AND ENGINEERING CHEMISTRY	.60	.75	.80	1.00	.15	.05
Industrial Edition (I&EC)	...	...	.80	1.00	.15	.05
JOURNAL OF THE AMERICAN CHEMICAL SOCIETY, Vols. 32–73	...	...	1.00	1.25	.15	.05
JOURNAL OF THE AMERICAN CHEMICAL SOCIETY, Vol. 74 et seq.	.50	.75	.80	1.00	.15	.05
JOURNAL OF PHYSICAL CHEMISTRY	1.00	1.25	1.20	1.50	.15	.05

RATES FOR VOLUMES OF BACK NUMBERS

	Member	Non-Member	Foreign Postage	Canadian Postage
ANALYTICAL CHEMISTRY (formerly Analytical Edition)	$6.00	$7.50	$0.75	$0.25
CHEMICAL ABSTRACTS				
Volumes 11–44	20.00	25.00	2.40	.80
Volume 45 et seq.	50.80**	63.50	2.40	.80
CHEMICAL AND ENGINEERING NEWS (Volumes 1–24)	2.80	3.50	2.25	.75
CHEMICAL AND ENGINEERING NEWS (Vol. 25 et seq.)	5.60	7.00	2.25	.75
INDUSTRIAL AND ENGINEERING CHEMISTRY	8.80	11.00	2.25	.75
JOURNAL OF THE AMERICAN CHEMICAL SOCIETY (Vol. 32 et seq.)	12.00	15.00	1.50	.50
JOURNAL OF PHYSICAL CHEMISTRY (Vol. 56 et seq.)	10.00	12.50	1.20	.40

(Prior Volumes—Order from Walter Johnson, 125 East 23rd Street, New York 10, N. Y.)

* Each part, when divided.

** The member discount for Volume 45 et seq. applies only if purchase is for personal use and not for resale.

AMERICAN CHEMICAL SOCIETY

Back Issue Department

1155 Sixteenth St., N.W. • Washington 6, D. C.